REPUBLIC OF TÜRKİYE
YILDIZ TECHNICAL UNIVERSITY
GRADUATE SCHOOL OF SCIENCE AND ENGINEERING

NOVEL ANALYTICAL STRATEGIES FOR THE DETERMINATION OF ENDOCRINE DISRUPTIVE COMPOUNDS IN ANTARCTIC SAMPLES, REMOVAL OF CADMIUM FROM WASTEWATER AND BIOSYNTHESIS OF GOLD NANOPARTICLES

Buse Tuğba ZAMAN

DOCTOR OF PHILOSOPHY THESIS

Department of Chemistry

Analytical Chemistry Program

Supervisor

Prof. Dr. Sezgin BAKIRDERE

Co-Supervisor

Assoc. Prof. Dr. Emine Gülhan BAKIRDERE

February, 2024

REPUBLIC OF TÜRKİYE

YILDIZ TECHNICAL UNIVERSITY

GRADUATE SCHOOL OF SCIENCE AND ENGINEERING

NOVEL ANALYTICAL STRATEGIES FOR THE DETERMINATION OF ENDOCRINE DISRUPTIVE COMPOUNDS IN ANTARCTIC SAMPLES, REMOVAL OF CADMIUM FROM WASTEWATER AND BIOSYNTHESIS OF GOLD NANOPARTICLES

A thesis submitted by Buse Tuğba ZAMAN in partial fulfillment of the requirements for the degree of DOCTOR OF PHILOSOPHY is approved by the committee on 28.02.2024 in Department of Analytical Chemistry, Chemistry Program.

Prof. Dr. Sezgin BAKIRDERE Yıldız Technical University Supervisor	Assoc. Prof. Dr. Emine Gülhan BAKIRDERE Yıldız Technical University Co- supervisor

Approved By the Examining Committee

Prof. Dr. Sezgin BAKIRDERE, Supervisor
Yildiz Technical University _____

Prof. Dr. Yücel ŞAHİN, Member
Yildiz Technical University _____

Prof. Dr. Yusuf DİLGİN, Member
Çanakkale 18 March University _____

Assoc. Prof. Dr. Şule DİNÇ ZOR, Member
Yildiz Technical University _____

Sondan DURUKANOĞLU FEYİZ, Member
Kadir Has University _____

I hereby declare that I have obtained the required legal permissions during data collection and exploitation procedures, that I have made the in-text citations and cited the references properly, that I haven't falsified and/or fabricated research data and results of the study and that I have abided by the principles of the scientific research and ethics during my Thesis Study under the title of New Solid and Liquid Phase Microextraction Strategies for Trace Analyte Determinations in Atomic Spectroscopy supervised by my supervisor, Prof. Dr. Sezgin BAKIRDERE and my co-advisor Assoc. Prof. Dr. Emine Gülhan BAKIRDERE. In the case of a discovery of false statement, I am to acknowledge any legal consequence.

Buse Tuğba ZAMAN

Signature

A part of this thesis was supported by the Scientific and Technological Research Council of Turkey (TUBITAK) Grant No: 119Z846. The thesis was funded Council of High Education (CoHE) 100/2000 priority fields (100/2000 YÖK Doktora Bursu).

Dedicated to my grandparents, Gülsüm and Osman

ACKNOWLEDGEMENTS

"*C'est le temps que tu as perdu pour to rose qui fait ta rose si importante" – Antoine de Saint-Exupéry*

First and foremost, I would like to thank my PhD supervisor, Prof. Dr. Sezgin BAKIRDERE. His constant support, guidance, and encouragement have been invaluable throughout the entire process. From the initial stages of my undergraduate thesis to the final submission of my doctorate thesis, his unwavering presence and wealth of wisdom have been instrumental in shaping my academic growth. His exceptional academic expertise, coupled with his commitment to support early career researchers truly make you a role model in the often competitive realm of academia. His guidance and encouragement through all these years have been invaluable.

I'd also like to express my thanks to my patient and supportive co-advisor Assoc. Prof. Dr. Emine Gülhan BAKIRDERE, who has supported me throughout my PhD journey. I am extremely grateful for her friendly chats and her personal support in my academic endeavours.

I would also like to express my gratitude to my PhD thesis committee members: Prof. Dr. Yücel ŞAHİN, Prof. Dr. Yusuf DİLGİN. Thank you for your time and effort, leading me with your valuable feedback and thought-provoking questions during my thesis monitoring committee meetings. Your insights have greatly enriched the quality of my thesis.

Furthermore, I cannot envision a better senior than Dr. Çağdaş BÜYÜKPINAR and Dr. Dotse Selali CHORMEY. Their countless feedback and guidance have played a pivotal role in refining my academic writing and sharpening my arguments. They were not just instructors for me, they were my elders whose support and tolerance I will always feel. Their unwavering passion for science is truly inspiring, and I aspire to follow in their footsteps one day.

I would like to thank Dr. Arda ATAKOL and Dr. Melike ATAKOL for their dedicated support and guidance. They continuously provided encouragement and were always willing and enthusiastic to assist in any way they could.

I would like to express my deepest gratitude to all Bakırdere Research Group members. It was always a pleasure to work with such a lovely and engaging people. I would like to thank my colleagues Sezin ERARPAT BODUR and Süleyman BODUR for their contributions and helps throughout my scientific researches. My beloved academic sister, Dr. Gamze DALGIÇ BOZYİĞİT, has always been more than a real sister, and her contribution to my scientific/academic life has always been more than a help by spending her valuable time for me, even prior to herself. While working diligently on my thesis, the small breaks organized by my precious friends Ayça Girgin, Berfin METİN, Cansu DEMİR, Esra DORU, İrem Zehra KUBLAY, Meltem ŞAYLAN, Miray ÖNER, Nazime Ebrar KARLIDAĞ, and Tülay BORAHAN KUSTANTO, became my favorite moments after long working days. These refreshing moments motivated me and inspired me to persevere. I am also grateful to my lab mates Dr. Ayşegül ERGENLER, Bedrihan KARTOĞLU, Dr. Elif Seda KOÇOĞLU, Ümmügülsüm POLAT KORKUNÇ, Sude OFLU, and Yağmur KILINÇ, for their help in my PhD experiments. I would like to express my sincere gratitude to my beloved little brothers and sisters, the *"Az Takipçililer"* – Efe Sinan AYDIN, Hilal AKBIYIK, Nagehan Kübra ZEYTİNCİ and Selim GÜRSOY. Their support, help and love have been invaluable throughout my PhD process. They were not only lab mates who helped me with experimental work, but with their deep love and admirable respect, they always tried to make me happy and supported me to see that lab as a family.

My dearest friend Nursu Aylin KASA, words cannot express how much your unwavering belief in me has meant. You have been my biggest cheerleader throughout this journey, and I cannot thank you enough for your love and support. Additonally, I am deeply thankful to my friend Dr. Sabriye SEL for her love and support during this process.

A part of this thesis was supported by Scientific and Technological Research Council of Türkiye (TÜBİTAK) by the grant number of 1119Z846 'Antarctica 1001' project. In addition, I owe a special thanks to Council of High Education (CoHE) 100/2000 priority fields (100/2000 YÖK Doktora Bursu) for funding me during my PhD education.

At last but not least, I owe a tremendous debt of gratitude to my family. Their tireless work and unwavering commitment to provide for me and my sister while

always emphasizing the value of education have made a profound impact on my journey.

As I bring my above five-year-long PhD journey to a close, I can genuinely say that I am immensely proud of my accomplishments. This transformative journey has not only shaped me as a researcher but also as an individual, imparting the invaluable lesson that perseverance yields fruitful rewards in the long run. The unwavering commitment and determination displayed by those around me have profoundly influenced my character.

Buse Tuğba ZAMAN

TABLE OF CONTENTS

LIST OF SYMBOLS **xi**
LIST OF ABBREVIATIONS **xi**
LIST OF FIGURES **xviii**
LIST OF TABLES **xxi**
ABSTRACT **xxiii**
ÖZET **xxvi**
1 INTRODUCTION **1**
1.1 Literature Review……..1
1.2 Objective of the Thesis……..4
1.3 Hypothesis……5
2 GENERAL INFORMATION **7**
2.1 Antarctica…….. 7
2.2 Pollutants……... 8
2.2.1 Organic Pollutants.....10
2.2.2 Inorganic Pollutants 16
2.3 Sample Preparation……..20
2.3.1 Liquid Phase Microextraction Strategies 23
2.3.2 Solid Phase Microextraction Strategies 33
2.4 Instrumental Detection Techniques……36
2.4.1 Spectroscopic Methods 37
2.4.2 Chromatographic Methods.....42
2.5 Quantification of Analytes…….. 48
2.5.1 Standard Addition and Matrix-Matching Calibration Strategies 49
2.6 Method Validation……...50
2.7 Treatment Strategies of Water Sources……... 51
2.7.1 Chemical Based Removal Procedures 53
2.7.2 Adsorption Based Removal Methods 54
2.7.3 Equilibrium Isotherm Models 59
2.8 Nanotechnology……...60
2.8.1 Synthesis of Gold Nanoparticles.....62
3 MATERIALS AND METHODS **66**
3.1 Chemicals and Reagents……..66

3.2 Instruments……..... 68

3.3 Simultaneous Determination of Endocrine Disruptor Compounds and Pesticides in GC-MS System……...70

3.3.1 Spraying Apparatus.....70

3.3.2 Spray Assisted Droplet Formation based Liquid Phase Microextraction Procedure…….....70

3.3.3 Preparation of Real Sample Used in Spiked Recovery Experiments. 71

3.3.4 Preparation of Real Samples Collected from Antarctic Region 72

3.4 Magnetic $CuFe_2O_4$ Nanoparticle Assisted Batch Type Adsorption Based Removal Strategy…… 73

3.4.1 Magnetic $CuFe_2O_4$ Nanoparticle Synthesis Procedure 73

3.4.2 Magnetic $CuFe_2O_4$ Nanoparticle Assisted Batch Type Adsorption Based Removal Procedure 73

3.4.3 Preparation of Synthetic Wastewater Samples 74

3.4.4 Evaluation of Removal Efficiency of the Magnetic $CuFe_2O_4$ Nanoparticle Assisted Batch Type Adsorption Based Removal Strategy .75

3.4.5 Langmuir Isotherm Model 76

3.5 Synthesis of Gold Nanoparticles and Their Toxicological Assessment…….. 77

3.5.1 Synthesis of Gold Nanoparticles.....77

3.5.2 Test organisms and experiments to examine the lethal doses.....78

3.5.3 Cell Viability Tests 79

4 RESULTS AND DISCUSSION 81

4.1 Simultaneous Determination of Endocrine Disruptor Compounds and Pesticides in GC-MS System……...81

4.1.1 Chromatographic Elution of the Endocrine Disruptor Compounds and Pesticides.....81

4.1.2 Analytical Figures of Merit.....88

4.1.3 Determination of Proper Liquid Phase Microextraction Method for Simultaneous Preconcentration of the Analytes 92

4.1.4 Optimization Studies.....94

4.1.5 Validation of the SADF-LPME Method.....105

4.2 Removal of Cadmium Ions From Wastewater by Using $CuFe_2O_4$ Nanoparticle Assisted Batch Type Surface Adsorption Procedure Based Treatment Strategy…… 130

4.2.1 Characterization of Magnetic $CuFe_2O_4$ Nanoparticles.....130

4.2.2 Optimization of the $CuFe_2O_4$ Nanoparticle Assisted Batch Type Surface Adsorption Based Treatment Procedure 132

4.2.3 Evaluation of Removal Efficiency of the Developed Method 139

4.3 Development of Biogenic Gold Nanoparticles (GNP) Synthesis and its Cytotoxic and Genotoxic Assessment……... 144

4.3.1 Optimization Studies…..……..145

4.3.2 Characterization Studies 147

4.3.3 Evaluation of Toxicological Profile of GNPs 151

5 CONCLUSION **158**

REFERENCES **160**

PUBLICATIONS FROM THE THESIS **193**

LIST OF SYMBOLS

As	Arsenic
B	Boron
Cd	Cadmium
Cr	Chromium
R^2	Coefficient of Determination
Cu	Copper
°C	Degree Celsius
y	Dependent Variable
D_2	Deuterium
K_F	Distribution Coefficient
C_e	Equilibrium Adsorbate Concentration
q_e	Equilibrium Adsorption Capacity
A_e	Equilibrium Adsorption Level
A_i	Equilibrium Adsorption Level
Au	Gold
g	Gram
x	Independent Variable
C_i	Initial Adsorbate Concentration
n	Intercept
Fe	Iron
K_L	Langmuir Constant
Pb	Lead
L	Liter
Mn	Manganese
m	Mass
m/z	Mass of Ion to Ion Charge Ratio
q_m	Maximum adsorption capacity
Hg	Mercury
µg	Microgram

µL	Microliter
µm	Micrometer
µM	Micromolar, µmol/L

LIST OF ABBREVIATIONS

%RE	Percent Removal Efficiency
%RSD	Percent Relative Standard Deviation
0-D	Zero-Dimensional
1,2-DCE	1,2-dichloroethane
1-D	One-Dimensional
2-D	Two-Dimensional
AAS	Atomic Absorption Spectrometry
AC	Alternating Current
ACN	Acetonitrile
ACT	Acetone
ADI	Acceptable Daily Intake
AOP	Advanced Oxidation Process
ARfD	Acute Reference Dose
AU	Arbitrary Unit
AuNP	Gold Nanoparticle
BET	Brunauer-Emmett-Teller
BOD	Biological Oxygen Demand
BS-DLLME	Binary Solvent Dispersive Liquid-Liquid Microextraction
CE	Catechin Equivalents
CF	Continous Flow
CHL	Chloroform
CI	Chemical Ionization
CM	Carbamate
CNM	Carbonaceous Nanomaterial
CNT	Carbon Nanotubes
COD	Chemical Oxygen Demand
COP	Covalent Organic Polymers
CRM	Certified Reference Material
CT	Computed Tomography

D-μ-SPE	Dispersive Micro-Solid Phase Extraction
DD	Drop-to-Drop
DDT	Dichloro-Diphenyl-Trichloroethane
DES	Deep Eutectic Solvents
DI	Direct Immersion
GDI	Genetical Damage Index
DLLME	Dispersive Liquid-Liquid Microextraction
DM	Dried Sample
DMEM	Dulbecco's Modified Eagle Medium
DMSO	Dimethyl Sulfoxide
DSPE	Dispersive Solid Phase Extraction
ECD	Electron Capture Detector
EDC	Endocrine Disruptive Compound
EDL	Electric Double Layer
EI	Electron Ionization
EP	Emerging Pollutant
EPA	Environmental Protection Agency
EtOH	Ethanol
EU	European Union
FAAS	Flame Atomic Absorption Spectrometry
FAO	Food and Agriculture Organization
FBS	Fetal Bovine Serum
FID	Flame Ionization Detector
FT-IR	Fourier Transform-Infrared Spectroscopy
GAE	Gallic Acid Equivalents
GAP	Good Agricultural Practices
GC	Gas Chromatography
GC-FID	Gas Chromatography-Flame Ionization Detector
GC-HRMS	Gas Chromatography-High Resolution Mass Spectrometry
GC-MS	Gas Chromatography-Mass Spectrometry
GC-MS/MS	Gas Chromatography-Tandem Mass Spectrometry
GLC	Gas-Liquid Chromatography

GNP	Gold Nanoparticle
GO	Graphene Oxide
HCB	Hexachlobenzene
HCH	Hexachlorocycloexane
HCL	Hollow Cathode Lamp
HCT116	Human Colorectal Carcinoma Cell
HF-LPME	Hollow Fiber-Liquid Phase Microextraction
HPLC-MS/MS	High Performance Liquid Chromatography- Tandem Mass Spectrometry
HPLC-UV	High Performance Liquid Chromatography-Ultraviolet Spectroscopy
HS	Headspace
HUVEC	Human Umbilical Vein Endothelial Cells
IARC	International Agency for Research on Cancer
ICP-MS	Inductively Coupled Plasma-Mass Spectrometry
ICP-OES	Inductively Coupled Plasma-Orbital Emission Spectrometry
IDMS	Isotope Dilution Mass Spectrometry
IPA	Isopropyl Alcohol
IR	Infrared
LC	Liquid Chromatography
LC-MS	Liquid Chromatography-Mass Spectrometry
LC-MS/MS	Liquid Chromatography-Tandem Mass Spectrometry
LDR	Linear Dynamic Range
LLE	Liquid-Liquid Extraction
LLL	Liquid-Liquid-Liquid
LMPA	Low Melting Point Agarose
LOD	Limits of Detection
LOQ	Limits of Quantification
LPME	Liquid Phase Microextraction
m-D-μ-SPE	Magnetic Dispersive Micro-Solid Phase Extraction
MeOH	Methanol
MIP	Molecular Imprinted Polymer
MNP	Magnetic Nanoparticle
MOP	Microporous Organic Polymer

MRL	Minimum Residue Level
MS	Mass Spectrometry
MSPD	Matrix Solid Phase Dispersion
MSPE	Magnetic Solid Phase Extraction
m-SPME	Magnetic Solid Phase Microextraction
MSRL	Mass Spectrometer Resource Library
MTT	3-(4,5-Dimethylthiazol-2-yl)-2,5-Diphenyltetrazolium Bromide
MWCNT	Multi-Walled Carbon Nanotubes
NIST	National Institute of Science and Technology
NM	Nanomaterial
NMPA	Normal Melting Point Agarose
OCP	Organochlorine Pesticide
ODS	Octadecyl Groups
OECD	Organization for Economic Co-operation and Development
OPP	Organophosphate Pesticide
PAC	Polyaluminum Chloride
PAM	Polyacrylamide
PBS	Phosphate Buffered Saline
PCB	Polychlorinated Biphenyls
PDT	Photodynamic Therapy
PE	Polyelectrolytes
PEEK	Polyetheretherketone
PFS	Polyferric Sulfate
PMT	Photomultiplier Tube
POP	Persistent Organic Pollutant
PPy	Polypyrrole
PTFE	Polytetrafluoroethylene
PTT	Photo-Thermal Therapy
RF	Radio Frequency
rGO	Reduced Graphene Oxide
RT	Radiation Therapy
RT	Retention Time

SADF-LPME	Spray Assisted Droplet Formation based Liquid Phase Microextraction
SBSE	Stir-Bar Sorptive Extraction
SD	Standard Deviation
SDME	Single Drop Microextraction
SEM	Scanning Electron Microscopy
SFC	Supercritical Fluid
SFOD	Solidified Floating Organic Droplet
SIM	Selected Ion Monitoring
SLM	Supported Liquid Membrane
SPE	Solid Phase Extraction
SPME	Solid Phase Microextraction
SPR	Surface Plasmon Resonance
SRM	Standard Reference Material
SS	Switchable Solvent
SS-LPME	Switchable Solvent-Liquid Phase Microextraction
SV	Stripping Voltammetry
SWCNT	Single-Walled Carbon Nanotubes
TCD	Thermal Conductivity Detector
TEM	Transmission Electron Microscope
TFC	Total Flavonoid Compounds
TGA	Thermal Gravimetric Analysis
TKN	Total Kjeldahl Nitrogen
TPC	Total Phenolic Compounds
TSS	Total Suspended Solids
UN	United Nations
UV-VIS	Ultraviolet-Visible
WW	Wastewater
WWTP	Wastewater Treatment Plant
XRD	X-ray Diffraction
ZP	Zeta Potential

LIST OF FIGURES

Figure 2.1 EP sources and their pathways in the environmental sources **9**

Figure 2.2 Functions and places of some prominent endocrine organs in the human body **14**

Figure 2.3 A mnemonic technique to recall the principles of green analytical chemistry **22**

Figure 2.4 Different practical modes of SDME procedure **25**

Figure 2.5 A schematic display of two-phase and three-phase HF-LPME **28**

Figure 2.6 An illustrative scheme of DLLME procedure **31**

Figure 2.7 An illustrative scheme of BS-DLLME procedure **32**

Figure 2.8 An illustrative scheme of the SADF-LPME method **33**

Figure 2.9 An illustrative scheme of D- μ-SPE procedure **35**

Figure 2.10 An illustration of FAAS system **40**

Figure 2.11 A diagram of a hollow cathode lamp **41**

Figure 2.12 An instructive schematic illustration of the various constituents of a GC-MS system **48**

Figure 2.13 A simple schematic display of the chemical precipitation process **53**

Figure 2.14 An illustrative depiction of the coagulation-flocculation treatment process **54**

Figure 2.15 Adsorption process used for water treatment **55**

Figure 2.16 Implementation fields of nanotechnology **60**

Figure 2.17 Noble metal nanoparticles and some of their usage areas 61

Figure 3.1 Spray apparatus used to create droplets in the study **70**

Figure 3.2 Schematic display of the biogenic GNP synthesis procedure **78**

Figure 3.3 96-well plates with formazon crystals 80

Figure 4.1 Total ion chromatography obtained for 50 mg kg^{-1} mix standard solution containing all the pesticide and endocrine disruptor determined in the study **84**

Figure 4.2 Extracted ion chromatogram of diazinon's five prominent mass fragments (*m/z*: 179, 137, 152, 199, 304) **87**

Figure 4.3 Identification of diazinone via NIST compound database based on compound's mass spectrum similarity to library spectrum **88**

Figure 4.4 The results of the extraction methods applied to determine the appropriate extraction method **93**

Figure 4.5 Determination of optimum solution pH (Group 1) **95**

Figure 4.6 Determination of optimum solution pH (Group 2) **95**

Figure 4.7 Determination of the optimum volume of buffer solution (Group 1) **97**

Figure 4.8 Determination of the optimum volume of buffer solution (Group 2) **97**

Figure 4.9 Determination of the appropriate solvent/solvent mixture (Group 1)..... **99**

Figure 4.10 Determination of the appropriate solvent/solvent mixture (Group 2) **100**

Figure 4.11 Determination of the optimum solvent mixture volume ratio (Group 1) **101**

Figure 4.12 Determination of the optimum solvent mixture volume ratio (Group 2) **102**

Figure 4.13 Determination of the optimum volume of extraction solvent mixture by spraying repetition (Group 1)..... **104**

Figure 4.14 Determination of the optimum volume of extraction solvent mixture by spraying repetition (Group 2)..... **104**

Figure 4.15 The selected ion chromatograms were acquired utilizing the diazinon analyte from a seaweed sample collected from Horseshoe Island, along with a 5000 ng/g mixed reference solution of the same material. (m/z: 179) **129**

Figure 4.16 FE-SEM images obtained for $CuFe_2O_4$ nanoparticles at different magnification (a) 5 µm (b) 1 µm **130**

Figure 4.17 Powder XRD pattern obtained for $CuFe_2O_4$ nanoparticles **131**

Figure 4.18 The linear regression of $CuFe_2O_4$ nanoparticles obtained by multi-point BET..... **131**

Figure 4.19 A plot of %RE against different buffer solutions, n=3 for the error bars (*Experimental conditions: 40 mL 4.0 mg L^{-1} Cd^{2+} aqueous standard solution;2.0 mL of buffer solution; 50 mg $CuFe_2O_4$ nanoparticle; 60 s contact period with the aid of vortex mixing*) **134**

Figure 4.20 Fractions of Cd(II) depending on the pH 134

Figure 4.21 A plot of %RE values against different volumes of buffer solution, n=3 for the error bars (*Experimental conditions: 40 mL 4.0 mg L^{-1} Cd^{2+} aqueous standard solution;0.50 M borate-HCl buffer solution; 50 mg $CuFe_2O_4$ nanoparticle; 60 s contact period with the aid of vortex mixing*) **136**

Figure 4.22 A plot of %RE values against different amounts of magnetic $CuFe_2O_4$ nanoparticle, n=3 for the error bars (*Experimental conditions: 40 mL 4.0 mg L^{-1} Cd^{2+} aqueous standard solution;2.0 mL of 0.50 M borate-HCl buffer solution; 60 s contact period with the aid of vortex mixing*) **137**

Figure 4.23 A plot of %RE values against different mixing types, n=3 for the error bars (*Experimental conditions: 40 mL 4.0 mg L^{-1} Cd^{2+} aqueous standard solution;2.0 mL of 0.50 M borate-HCl buffer solution; 100 mg $CuFe_2O_4$ nanoparticle; 60 s contact period with the aid of mixing*) **138**

Figure 4.24 A plot of %RE values against different vortex periods, n=3 for the error bars (*Experimental conditions: 40 mL 4.0 mg* L^{-1} Cd^{2+} *aqueous standard solution; 2.0 mL of 0.50 M borate buffer solution; 100 mg* $CuFe_2O_4$ *nanoparticle; contact period with the aid of vortex mixing*) **139**

Figure 4.25 Calibration plot indicates the linear working range of the FAAS system for cadmium(II) ions in synthetic wastewater samples **140**

Figure 4.26 A plot of Langmuir isotherm for cadmium adsorption on $CuFe_2O_4$ nanoparticles under optimum conditions in synthetic wastewater..... **144**

Figure 4.27 The absorption spectrums giving SPR band for GNPs in different macro-algae extract contains **146**

Figure 4.28 The absorption spectrums giving SPR band for GNPs at different temperatures..... **147**

Figure 4.29 The UV-Vis spectrum of synthesized biogenic GNPs..... **148**

Figure 4.30 TEM images of the biogenic GNPs **149**

Figure 4.31 TEM images of the biogenic GNPs **150**

Figure 4.32 Distribution graph of zeta potential obtained for GNPs..... **151**

Figure 4.33 Representative image of Daphnia magna used as a model organism in the study..... **152**

Figure 4.34 ANOVA statistical results for HCT116 (leftside) and HUVEC (rightside) Cell lines at MTT Cell Viability tests **156**

Figure 4.35 MTT test results obtained for both HUVEC and HCT116 cell lines for different concentrations of GNPs **156**

LIST OF TABLES

Table 2.1 The list of pesticides classified with respect to their target pests **11**

Table 2.2 Categorization of column chromatographic techniques **43**

Table 2.3 Comparison of synthesis methods by their advantages and disadvantages to each other **64**

Table 3.1 Pesticides and endocrine disruptors that were qualitatively and quantitatively determined in the study **67**

Table 3.2 Laboratory devices used in the study **69**

Table 3.3 The chemicals and their concentrations contains in synthetic wastewater samples **74**

Table 3.4 Synthetic wastewater characterization **75**

Table 3.5 Linearization of the Langmuir model **76**

Table 4.1 Temperature ramps attempted to determine suitable chromatographic conditions for separation of analytes **82**

Table 4.2 Method parameters applied in the GC-MS device used in the simultaneous determination of pesticides and endocrine disruptors **83**

Table 4.3 Chromatographic informations of the targeted analytes in the study **85**

Table 4.4 System performance values for each analyte under optimum chromatographic conditions Kontrol edilmedi **90**

Table 4.5 Experimental parameters of the extraction methods applied in order to determine the appropriate extraction method **93**

Table 4.6 Experimental parameters used in the optimization study to determine the solution pH **96**

Table 4.7 Experimental parameters used in the optimization study to determine the buffer solution volume **98**

Table 4.8 Experimental parameters used in the optimization study to determine the extraction solvent **100**

Table 4.9 Experimental parameters used in the optimization study to determine the ratio extraction solvents in the extraction mixture **102**

Table 4.10 Experimental parameters used in the optimization study to determine the spraying repetition **105**

Table 4.11 Analytical figures of merit of the SADF-LPME-GC-MS combined method for EDCs **107**

Table 4.12 Percent recovery results using matrix matching approach on seawater sample coded HS-D-26 *(n=4)* **110**

Table 4.13 Percent recovery results using matrix matching approach on seawater sample coded HS-D7 *(n=4)* **113**

Table 4.14 Percent recovery results using matrix matching approach on soil sample coded A *(n=4)* **116**

Table 4.15 Percent recovery results using matrix matching approach on soil sample coded B *(n=4)* **119**

Table 4.16 Percent recovery results using matrix matching approach on moss sample coded A *(n=4)* **123**

Table 4.17 Percent recovery results using matrix matching approach on moss sample coded B *(n=4)* **126**

Table 4.18 The percent removal efficiency results for different concentrations of cadmium **141**

Table 4.19 Linearization of the Langmuir model **142**

Table 4.20 Calculated parameter values of the Langmuir isotherm model by the linear method **143**

Table 4.21 Calculated R_L values of the Langmuir isotherm model for different initial concentrations **143**

Table 4.22 Instrumental conditions conducted in zeta measurements of GNPS **150**

Table 4.23 Behavioral respects of Daphnia magna in acute toxicity tests..... **153**

Table 4.24 The DNA damage values in neomates that were subjected to various concentrations of GNPs **154**

ABSTRACT

Novel Analytical Strategies for the Determination of Endocrine Disruptive Compounds in Antarctic Samples, Removal of Cadmium from Wastewater and Biosynthesis of Gold Nanoparticles

Buse Tuğba ZAMAN

Department of Analytical Chemistry

Doctor of Philosophy Thesis

Supervisor: Prof. Dr. Sezgin BAKIRDERE

Co-supervisor: Assoc. Prof. Dr. Emine Gülhan BAKIRDERE

Pollutants are of great concern in many disciplines, especially Environmental Engineering and Chemistry. Since classical treatment technologies do not have the capacity to effectively remove these pollutants from environmental matrices, their accurate and precise determination in environmental samples before and after treatment has been an important issue for decades in fully evaluating removal efficiency. These pollutants may contaminate wastewater, potable water, surface water, and groundwater at very low concentrations that are not readily detected by conventional analytical techniques. In recent years, both solid and liquid extraction methods have been used to obtain less time and labor-consuming procedures. This thesis is aimed at developing sensitive and innovative analytical methods for the determination of trace analytes such as endocrine disruptive compounds, pesticides, heavy metals and hormones, by employing techniques that give very accurate and precise results and removal of these analytes from wastewater samples by synthesizing nanomaterials through innovative procedures.

In the first part of the thesis, selected endocrine-disrupting chemicals (EDCs) and pesticides were concurrently determined in samples including rock, soil, water, moss, and feces obtained from the Antarctic region. A spray-assisted droplet formation-based liquid phase microextraction (SADF-LPME) method, coupled with a gas chromatography-mass spectrometry (GC-MS) system, was developed by performing extensive single-variable optimization experiments to identify the optimum parameters of each variable. The systems' analytical results were validated for the purpose of screening and monitoring twenty-nine targeted EDCs and pesticides under the optimum conditions. Recovery tests were performed to assess the accuracy and precision of the proposed method. To counteract the matrix effect of complex real samples, matrix matching calibration strategies were employed, resulting in enhanced accuracy of quantitative measurements. Furthermore, the analysis on the environmental samples obtained from the Horseshoe and Faure Islands in Antarctica was conducted to evaluate the potential contamination of endocrine-disrupting chemicals (EDCs) and pesticides.

In the second part, an innovative nanomaterial based batch type adsorption treatment procedure was developed for cadmium removal from wastewater. Magnetic $CuFe_2O_4$ nanoparticles were produced using an easy and fast co-precipitation method, and utilized as adsorbent in the treatment method. The system variables were optimized with comprehensive univariate experiments to attain the most favorable conditions for the interaction between cadmium ions and the adsorbent. The percent removal efficiency (%RE) was assessed by using synthetic wastewater samples. In addition, the Langmuir isotherm modelling was applied to the developed method in order to illustrate the adsorption mechanism.

In the last part, a biosynthesis approach for gold nanoparticles (GNP) was established using *Padina pavonica* macro-algae extract. The synthesis conditions were optimized, and the formation and efficiency of the applied conditions for the GNPs were monitored with a UV-vis spectrometer, utilizing the specific surface plasmon resonance peak of the GNPs at 542 nm. The toxicological profile of the biogenic GNPs was examined by utilizing cell viability and the comet assay tests.

Keywords: Antarctic region, gold nanoparticles, magnetic nanoparticles, microextraction, toxicological assessment.

ÖZET

Endokrin Bozucu Maddelerin Antarktik Örneklerinde Tayinleri, Kadmiyumun Atıksudan Giderimi ve Altın Nanopartiküllerin Biyosentezi için Yenilikçi Analitik Stratejiler

Buse Tuğba ZAMAN

Analitik Kimya Anabilim Dalı

Doktora Tezi

Danışman: Prof. Dr. Prof. Dr. Sezgin BAKIRDERE

Eş-Danışman: Assoc. Prof. Dr. Emine Gülhan BAKIRDERE

Kirleticiler, başta Çevre Mühendisliği ve Kimya olmak üzere birçok disiplin için endişe kaynağıdır. Klasik arıtma teknolojileri bu kirleticileri çevresel matrikslerden etkili bir şekilde uzaklaştırma kapasitesine sahip olmadığından, arıtma öncesi ve sonrası çevresel numunelerde doğru ve hassas bir şekilde belirlenmesi, uzaklaştırma verimliliğinin tam olarak değerlendirilmesinde onlarca yıldır önemli bir konu olmuştur. Bu kirleticiler, geleneksel analitik tekniklerle kolayca tespit edilemeyen çok düşük konsantrasyonlarda atık su, içme suyu, yüzey suyu ve yeraltı suyunu kirletebilir. Son yıllarda, hem katı hem de sıvı ekstraksiyon yöntemleri, daha az zaman ve emek gerektiren prosedürler elde etmek için kullanılmıştır. Bu tez, endokrin bozucu bileşikler, pestisitler, ağır metaller ve hormonlar gibi eser analitlerin belirlenmesi için çok doğru ve kesin sonuçlar veren teknikler kullanarak hassas ve yenilikçi analitik yöntemler geliştirmeyi ve bu analitlerin yenilikçi prosedürlerle sentezlenen nanomalzemeler kullanılarak atık su örneklerinden uzaklaştırılmasını amaçlamaktadır.

Tezin ilk bölümünde, Antarktika bölgesinden elde edilen kaya, toprak, su, yosun ve dışkı gibi örneklerde seçilmiş endokrin bozucu kimyasallar (EDC'ler) ve pestisitler eş zamanlı olarak tayin edilmiştir. Bir gaz kromatografisi-kütle spektrometresi (GC-MS) sistemi ile birleştirilmiş sprey destekli damlacık oluşumu tabanlı sıvı faz mikroekstraksiyon (SADF-LPME) yöntemi, her değişkenin optimum parametrelerini belirlemek için kapsamlı tek değişkenli optimizasyon deneyleri gerçekleştirilerek geliştirilmiştir. Sistemlerin analitik sonuçları, optimum koşullar altında hedeflenen yirmi dokuz EDC ve pestisitin taranması ve izlenmesi amacıyla doğrulanmıştır. Önerilen yöntemlerin doğruluğunu ve kesinliğini değerlendirmek için geri kazanım testleri yapılmıştır. Karmaşık gerçek numunelerin matriks etkisine ortadan kaldırmak için matriks eşleştirme kalibrasyon stratejileri kullanılmış ve bu da kantitatif ölçümlerin doğruluğunu artırmıştır. Ayrıca, endokrin bozucu kimyasalların (EDC'ler) ve pestisitlerin potansiyel kontaminasyonunu değerlendirmek için Antarktika'daki Horseshoe ve Faure Adaları'ndan elde edilen çevresel numuneler üzerinde analizler yapılmıştır.

İkinci bölümde, atık sulardan kadmiyum giderimi için yenilikçi bir nanomalzeme bazlı kesikli tip adsorpsiyon arıtma prosedürü geliştirilmiştir. Manyetik $CuFe_2O_4$ nanopartikülleri kolay ve hızlı bir birlikte çöktürme yöntemi kullanılarak sentezlenmiş ve arıtma yönteminde adsorban olarak kullanılmıştır. Kadmiyum iyonları ve adsorban arasındaki etkileşim için en uygun koşulları elde etmek amacıyla sistem değişkenleri kapsamlı tek değişkenli deneylerle optimize edilmiştir. Yüzde giderim verimi (%RE) sentetik atık su numuneleri kullanılarak değerlendirilmiştir. Ayrıca, adsorpsiyon mekanizmasını göstermek amacıyla Langmuir izoterm modellemesi geliştirilen yönteme uygulanmıştır.

Son bölümde, *Padina pavonica* makro-alg özütü kullanılarak altın nanopartiküller (GNP) için bir biyosentez yaklaşımı oluşturulmuştur. Sentez koşulları optimize edilmiş ve GNP'ler için uygulanan koşulların oluşumu ve etkinliği, GNP'lerin 542 nm'deki spesifik yüzey plazmon rezonans piki kullanılarak bir UV-vis spektrometresi ile izlenmiştir. Biyojenik GNP'lerin toksikolojik profili hücre canlılığı ve DNA hasar tespit testleri kullanılarak incelenmiştir.

Anahtar Kelimeler: Antarktika bölgesi, altın nanopartiküller, manyetik nanopartiküller, mikroekstraksiyon, toksikolojik değerlendirme.

1
INTRODUCTION

1.1 Literature Review

With the constant increase in human population, several activities such as the consumption of fossil fuels and deforestation have tangible impacts on the natural environment. These activities have triggered undesired phenomena such as soil erosion, global warming, air/water pollution. Environmental pollution is a longstanding crisis that continues to be a significant issue confronting humanity, being a primary source of sicknesses and fatality at extreme levels. Human activities such as industrial processing, mining, exploration and urbanization are the main causes of worldwide environmental pollution. Developed and developing/underdeveloped countries bear this responsibility collectively, nonetheless, heightened consciousness and stricter legislation in the former countries have caused greater impact for safeguarding their environment. Although the worldwide attention on environmental pollution has significantly increased and the efforts are being made to curb it, its consequences is still being experienced because of its long-term attributes [1]. The Pollution Prevention Act, established in the United States in 1990 and similar acts have been enacted in the latest decades in several countries. This protocol mandates that the Environmental Protection Agency (EPA) set up a program with the aim of reducing pollution at its source. This program intends to guide the efforts of government, industry, and the public to prevent pollution by adjusting simple and cost-effective changes in production, operation, and the consumption of raw materials. The potential of source reduction is frequently ignored due to current regulations and the industrial resources needed for full compliance, which prioritize treatment and disposal strategies for pollution prevention [2].

Water contamination arises when there is significant amount of pollutants in water reservoirs. Industrial production can result in the emission of a wide range of harmful compounds including both organic and inorganic molecules. Insufficient treatment release of these wastes into aquatic habitats result in water contamination [3]. Cadmium (Cd), arsenic (As), and chromium (Cr) are common pollutants found

in wastewater, and the industrial sector plays a key role in the release of these hazardous elements [4]. Furthermore, there is a strong correlation between water contamination and agricultural applications, specifically, the use of pesticides, nitrogen fertilizers, and organic agricultural wastes, which are major contributors to water contamination. Agricultural activities contribute to water contamination by the presence of pesticides, nitrates, sediments, phosphate, salts, and pathogens. The absence of water and sanitation services also amplifies the prevalence of diseases such as trachoma, cholera, helminthiasis trachoma and schistosomiasis [5]. Research carried out in developed nations has shown a definite correlation between cholera and polluted water. Hence, it has been suggested that applying domestic water treatment and storage methods can effectively reduce the incidence of cholera [6]. The UNESCO 2021 World Water Development Report reveals that around 829,000 individuals die per year due to diarrhea, resulting from the consumption of polluted drinking water, inadequate sanitation, and lack of hand hygiene. Shockingly, this number includes nearly 300,000 children under the age of five, which represents 5.3% of all fatalities in the demographic study [7]. Moreover, contaminated water poses several health risks, including respiratory diseases, reproductive system diseases, neurological disorders, cardiovascular problems and cancer [8]. Therefore, it is mandatory to prioritize the progress of analytical techniques for the quantification, and the application of effective strategies for the removal of these pollutants from water and wastewater systems in order to enhance the sustainability of the environment.

Gas chromatography mass spectrometry (GC-MS) is a frequently employed chromatographic technique to identify and quantify volatile organic chemicals in different sample matrices [9]–[13]. Nevertheless, the sensitivity of this analytical method is not as elevated as the advanced tandem systems such as gas chromatography-tandem mass spectrometry (GC-MS/MS). On the other hand, flame atomic absorption spectrometry (FAAS) is a frequently used technique for heavy metal determination [14]–[16]. Recently, microextraction techniques have become common requirements to concentrate and separate analytes from complex sample matrices [17]. For this purpose, different liquid [18]–[21] and solid [22]–[24] phase microextraction techniques have been introduced in the literature.

Water treatment employs a variety of techniques including biological, chemical, physical, and physicochemical routes to diminish or eradicate toxins and impurities in water sources [25]. However, conventional wastewater treatment plants (WWTP) lack the ability to completely eradicate all kinds of pollutants. Therefore, the processed wastewater (WW) and sludge produced by WWTPs may still contain various pollutants. As a result, they can contaminate soils when wastewater effluent is used for irrigation or when sludge is used as a nitrogen source for soils [26]. Thus, post-treatment methods are necessary for the removal of pollutants after classical wastewater treatment.

Nanotechnology has emerged as an important field in scientific research and has achieved substantial advancement through the creation of functional, well-engineered nanoparticles. Metallic nanoparticles have been extensively employed for numerous medical applications [27]. The nanoparticles' small size provides more efficient interaction with biomolecules. Nanomaterials have the capacity to enhance the precision and accuracy of the current *in vitro* determination methods for various diseases [28]. Gold nanoparticles (AuNPs) have been widely utilized and are popular for their significant resurgence and other extraordinary properties [27]. With respect to cellular imaging, AuNPs offer several advantages in comparison to other agents. They exhibit strong light scattering and possess significantly higher brightness compared to chemical fluorophores. AuNPs are resistant to photo-bleaching and can be readily detected even at trace concentrations [29]. Surface plasmon resonance (SPR) of gold nanoparticles have the capacity to scatter visible light and near infrared radiations in a resonant manner when their surface plasmon oscillation is excited. This property can be utilized for the transportation of substances within cells by employing gold nanoparticles as contrast agents in dark field optical microscopy [28]. Still, researches discussing the cytotoxicity and immunotoxicology of gold(I) and gold(III) complexes are limited to the evaluation of immunological response of cells to AuNPs.

Although the detrimental impacts of pollutants on the environment and human health are well-documented, their consequences, particularly at low concentrations, remain inadequately understood due to the challenges associated with precise and sensitive measurement. Consequently, the scope of protective and preventative interventions in this context is constrained. Moreover, the elimination of these

contaminants from water samples is crucial to guarantee a pristine and secure environment. Within this particular context, the primary aims of analytical chemistry encompass the advancement of methodologies that exhibit environmental sustainability, simplicity, and cost-efficiency. To establish a sustainable ecosystem, it is crucial to devise techniques that will decrease chemical usage and mitigate waste production.

1.2 Objective of the Thesis

The main objective of this thesis was to develop precise and sensitive determination and removal techniques for the identification and remediation of trace level amounts of organic and inorganic substances that contribute to the pollution of environmental resources. In one part of the thesis, easy and innovative liquid phase microextraction (LPME) method was developed to preconcentrate the analytes in order to overcome insufficient sensitivity and selectivity of the selected instrumental detection system. The developed method allowed the quantification of twenty-nine targeted organic analytes by employing the cost-effective and user-friendly gas chromatography-mass spectrometry (GC-MS) instrument, as opposed to employing other advanced instruments that are more sensitive but expensive. The proposed method was examined for its applicability and validity for environmental samples by performing recovery experiments. Furthermore, this method was successfully applied to a wide range of real samples collected from the Horseshoe and Faure Islands of Antarctica Continent.

In the second part of the thesis, the well-known inorganic pollutant, cadmium, was aimed to be removed from wastewater by applying nanomaterial assisted batch type adsorption based remediation procedure. Magnetic $CuFe_2O_4$ nanoparticles were synthesized and employed as adsorbent in the procedure. The cost effective and rapid removal strategy was developed by using a non-toxic and non-commercially available nanomaterial. Synthetic wastewater was used as test sample to assess the removal efficiency of the developed method and adsorption isotherm modeling.

For the last part of the thesis, gold nanoparticles (GNPs) were synthesized in a biogenic approach. The GNPs synthesized using macro algae extract as biological precursor was validated with different characterization tools. Subsequently, the

cytotoxic and genotoxic profiles of these nanoparticles were evaluated, and their impact on living organisms was investigated.

1.3 Hypothesis

Endocrine disruptor compounds and heavy metals are environmental pollutants that exert negative impacts on humans, plants, and aquatic ecosystems, even when they are present at very low amounts. This makes the precise identification of trace levels of these pollutants very crucial in attempts to mitigate their potential health effects and prevent environmental pollution by their removal from environmental sources. GC-MS is commonly utilized for the quantification of volatile organic analytes. Nevertheless, the sensitivity of this device is insufficient to achieve very low detection limits (parts per billion, ppb or parts per trillion, ppt) for analytes of interest. In order to enhance instrumental sensitivity to determine analytes with high accuracy and precision, innovative microextraction strategies can be integrated with the instrument. In the scope of this thesis, a liquid phase microextraction method was developed in order to enhance the detection power of the conventional GC-MS system. The system and experimental parameters that influenced the extraction efficiency to achieve high preconcentration outputs were examined by using the univariate optimization approach. Analytical features of the proposed method were assessed under the optimal experimental and instrumental conditions. The applicability and the validity of the developed method was corroborated with spiking recovery experiments. In this case, matrix matching calibration strategy was used on soil, seawater, and moss samples to eliminate intricate matrix interferences and enhance the quantitation accuracy of the analytes. This proposed microextraction technique was also applied in a wide range of environmental samples including ocean water, lake water, rock, soil, moss, seaweed, and feces collected from the Antarctic region.

Within the purview of pollution prevention, cadmium was removed from wastewater media using nanomaterial assisted batch type adsorption based remediation procedure. The prominent parameters of the method were optimized with the univariate optimization method. The adsorbent was synthesized via a novel synthesis procedure, which was simple and fast. Magnetic properties of the nanoparticle used in the study simplified and expedited its separation from the effluent. The effectiveness of the developed method was evaluated by applying the

optimum conditions to spiked synthetic wastewater samples. The adsorption process was also assessed using the Langmuir isotherm modelling.

The biogenic GNPs were prepared using a very simple and rapid synthesis method. In the synthesis process, the extract of *Padina pavonica* macro-algae, an invasive species, was used as a biological reducing agent and as well as a stabilizer. Different characterization tools were used to verify the synthesized GNPs based on their composition and morphological structure. Finally, the toxicity profile of these nanoparticles was established using the MTT cell viability test and, acute and subacute studies.

2
GENERAL INFORMATION

2.1 Antarctica

The poles, located at opposite extremities of the Earth, namely Antarctica and the Arctic, are the regions characterized by extremely low temperatures and covered with ice. The reflective white surface effectively redirects a significant portion of the sun's rays back into the atmosphere, so maintaining the Earth's temperature at a stable level. Due to their proximity to oceans, the polar areas experience regular exposure to surges, waves, and powerful winds [30]. Antarctica, or the South Pole, is the area inside the Arctic Circle, a line of latitude about 60.0° south of the Equator [31]. Antarctica's vast ice sheet (98% of the land was covered by thick ice) is the largest in the world and 80% of its fresh water [32]. There is abundant fossil evidence that today's ice-bound Antarctica supports a much more populous flora and fauna than a system that was once characterized by a few seedless plants and a few primitive insects and freshwater crustaceans [33], [34].

Antarctica, the most important part of the Earth's climate and ecosystem, is today a unique continent, the culmination of a long geological history. There are many aspects of the continent that make it scientifically and geopolitically important. Not only is it the most uninhabited continent on the planet, preserving in its cold layers the unexplored remains of millions of years, but it is also the only continent without an indigenous human population and the only continent without a dominant nation. The first studies on Antarctica were carried out centuries ago by countries such as France, Belgium, Norway, Russia and the UK, and many debates arose between them. In the 1800s, it began to be explored by sailors, especially with the discovery of land structures [35]. In the process of exploring the continent since the late 1800s, the *Antarctic Treaty*, which was signed in 1959 and entered into force in 1961, was the factor that solidified the fact that the continent did not belong to any nation. With the participation of 12 countries, this treaty not only aimed to protect the environment and ecosystem of Antarctica, but also took many measures to manage human activities in Antarctica, such as the establishment of bases and demilitarization, provided that they were limited to scientific studies [36].

Regrettably, the Antarctic ecosystem has lost its pristine nature, and similar to other isolated areas on our planet, it is being affected by both local and global human activity due to scientific research carried out on the continent [37]. While the amount of anthropogenic activities caused pollutants entering Antarctica is small, the analysis of radioactive waste found in Antarctic snow and ice from the 1950s and 1960s showed the existence of fission byproducts released. At ambient temperatures, persistent organic pollutants (POPs) can evaporate from water, soils, and vegetation into the air. Once in the atmosphere, they are not impacted by decomposition reactions and can travel long distances before being deposited again. The process of volatilization and deposition can occur multiple times, and based on the idea of cold condensation and global fractionation, highly volatile substances like hexachlobenzene (HCB), hexachlorocycloexanes (HCHs) and low-chlorinated polychlorinated biphenyls (PCBs) can disperse worldwide. In polar regions, POPs undergo condensation and deposition due to the low temperatures that inhibit evaporation. This leads to elevated levels of these pollutants in the environment and their accumulation in food chains through biomagnification. Consequently, the health of wildlife is possibly endangered, as these pollutants can act as endocrine disruptors [38]. Currently, the levels of inorganic and organic contaminant concentrations in most Antarctic organisms are generally lower than those known to have harmful impacts on similar species in temperate and Arctic areas. Nevertheless, the majority of creatures inhabiting the Southern Ocean are endemic species, possessing distinct ecophysiological traits that have developed over an extended period of evolutionary isolation. Similarly, most species in terrestrial ecosystems have reached their distributional boundaries due to the challenging Antarctic circumstances. Organisms originating from Antarctica may therefore experience higher levels of stress and increased susceptibility to the harmful impacts of long-lasting pollutants compared to organisms from other areas [39].

2.2 Pollutants

The escalating rate of industries to provide services and goods for the increasing human population has caused a great strain on potable water due to the release of pollutants from these industrial activities into water bodies [40]. The fate of these compounds in the environment depends on their distribution between water and

suspended particles, their interaction and absorption into aquatic organisms, attachment to sediments, evaporation from water, and decomposition, which can be either biological or non-biological [41]. As a result, the accumulation of these compounds leads to environmental pollution. Environmental pollution can be broadly defined as the introduction and accumulation of toxic chemicals into the Earth's biological and physical elements that adversely affect natural environmental processes. When the accumulation of these chemicals in the environment exceeds natural levels and/or exhibits harmful properties, these chemicals are then referred to as *'pollutants'* [42]. The term *'Emerging Pollutants'* (EPs) refers to substances that do not yet have legislation mandating their monitoring or public reporting in the water sources or wastewater discharges [43]. These pollutants can have detrimental effects on living species and the environment, particularly in aquatic ecosystems. Currently, the quantity of EPs that have surfaced as a result of the rise in industrial activities and economic priorities has caused great environmental concern [44]. Depicted in Figure 2.1 is the originating points and pathways of EPs in environmental sources [45].

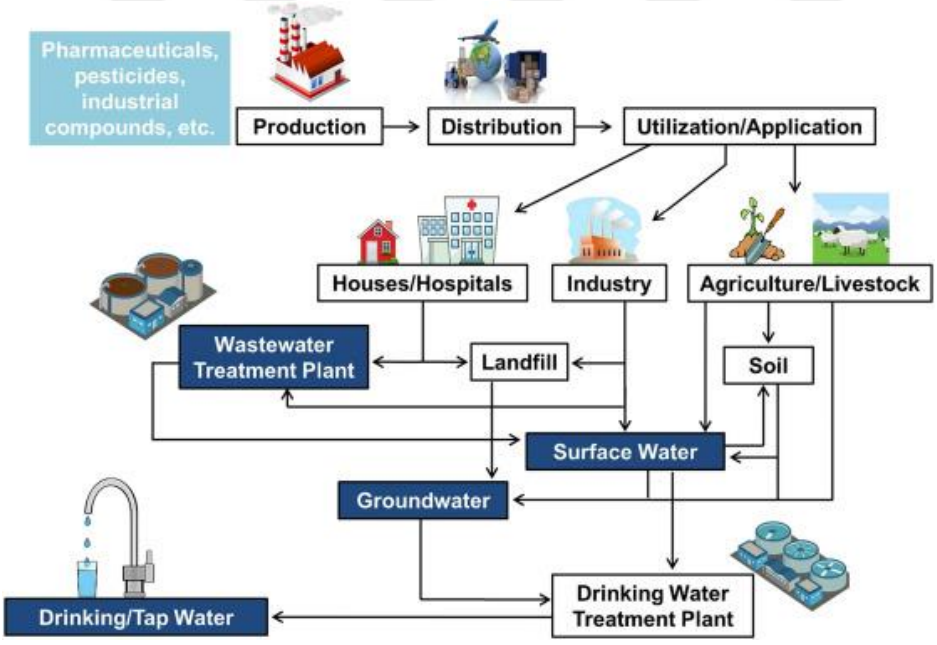


Figure 2.1 EP sources and their pathways in the environmental sources [45]

The presence of EPs in water bodies at very low concentrations generally range from a few ng to several µg per liter levels. The low concentration of pollutants presents dual challenges in terms of identification and quantification, as well as their remediation [46]. In a recent study, the levels of these harmful substances in

the human body have been reported above thresholds that lead to health problems, particularly in developing countries [47].

The European Union (EU) database classifies over 100,000 substances as pollutants. Humans are estimated to be exposed to approximately thirty thousand to seventy thousands of these contaminants daily [48]. The EU water framework directive 2000/06/CE identified 33 priority compounds or groupings of pollutants, such as metals, pesticides, phthalates, polycyclic aromatic hydrocarbons, and endocrine disruptors [49].

2.2.1 Organic Pollutants

Persistent organic pollutants (POPs) are organic compounds that have certain physical and chemical features that enable them to be widely distributed, exist in the environment for a long time, and eventually accumulate in organisms. These distinguishable properties of persistence, bioaccumulation, propensity to undergo long-range transport and toxicity are well-documented. The long-term stability exhibited by POPs is due to their resistance to degradation by environmental processes such as photolysis, chemical reactions, and biological breakdown. These substances have the tendency not to dissolve in water but lipids, which causes them to accumulate in the fatty tissues of living animals. As they move up the food chain, their quantity increases through the process of *biomagnification.* The POPs with semi-volatile characteristics are conveniently transported over long distances in the air or absorbed by particulate matter in environmental media such as air or water. Finally, POPs are considered to be detrimental due to their capacity to induce adverse effects on both humans and the environment [50].

2.2.1.1 Pesticides

A pesticide is a noxious chemical compound or an assortment of biological agents or chemical compounds that are deliberately discharged into the environment with the purpose of preventing, deterring, controlling, or eradicating populations of fungi, insects, rodents, weeds, or other undesired pests [51]. The use of pesticides for pest control has become a prevalent technique globally. This has resulted from the fact that pesticides provide improvement in food production to meet the demands of a constantly growing world population [52]. These substances are not solely limited to agricultural applications, but they are frequently utilized in

households as sprays, and powders to manage infestations of undesirable insects including mosquitoes, rats, cockroaches, ticks and fleas [51], [53]. Each year, approximately three billion kg of pesticides are used worldwide, with a mere 1% effectively employed for the purpose of controlling insect pests on specific plants [54].

Pesticides can be categorized in different ways, including by their chemical structure, mode of action, route of application, target organism, natural or synthetic origin, and organic or inorganic composition [55]. Commonly, pesticides are categorized according to their target organisms, and they are named specifically to indicate their effectiveness. In Table 2.1, the classification of pesticides based on the target pest are with their functionalities [56].

Table 2.1 The list of pesticides classified with respect to their target pests [56]

Type of pesticides	Target pests/Functions
Insecticides	Kill insects and other arthropods
Fungicides	Kill fungi (including blights, mildews, molds, and rusts)
Bactericides	Kill bacteria or acts against bacteria
Herbicides	Kill weeds and other plants that grow where they are not wanted
Acaricides	Kill mites that feed on plants and animals
Rodenticides	Control mice and other rodents
Algaecides	Control or kill growth of algae
Larvicides	Inhibits growth of larvae
Repellents	Repel pests by its taste or smell
Desiccants	Act on plants by drying their tissues
Ovicides	Inhibits the growth of eggs of insects and mites
Virucides	Acts against viruses
Molluscicides	Inhibit or kill mollusc’s i.e. snail’s usually disturbing growth of plants or crops

Table 2.2 The list of pesticides classified with respect to their target pests [56] (Continued)

Nematicides	Kill nematodes that act as parasites of plants
Avicides	Kill birds
Moth balls	Stop any damage to cloths by moth larvae molds
Lampricides	Target larvae of lampreys which are jawless fish like vertebrates in the river
Piscicides	Act against fishes
Silvicides	Acts against woody vegetation
Termiticides	Kills termites

The chemical structure classification includes subdivisions such as organophosphate pesticides (OPPs), carbamates (CMs), organochlorine pesticides (OCPs), and pyrethroids [57]. The OPPs are typically converted from phosphoric acid and thus, they include the PO_4 functional group. The OPPs are predominantly utilized in agricultural applications, mostly as insecticides and miticides. The exertion of these chemicals are mainly through oral intake and direct contact. They are used in several agricultural products such as fruit trees, vegetable crops, cotton, sugar cane, grains, and so on. Parathion methyl, diazinon, and malathion are some pesticides that are classified as OPPs. Although they have relatively low persistence in the environment, they nonetheless pose equal health hazards to humans and other living organisms [58]. The CMs are derivatives of carbamic acid, and these include pesticides such as aldicarb, carbonyl, cycloate, maneb, and metham sodium, which are used for the control of different target pests. They provide significant benefits to society by safeguarding and enhancing agricultural output as well as protecting humans and animals from ailments transmitted by insects. However, excessive exposure of both humans and animals to CMS can lead to different health problems, that range from minor diseases to extreme cases of fatality [59]. The OCPs are organic compounds that have chlorine substituents with well-known compounds such as aldrin, heptachlor, cis-chlordane, dichloro-diphenyl-trichloroethane (DDT), dieldrin, and α/β endosulfan. They are mostly employed for the purpose of

controlling and preventing disease-carrying pests and other pests found on agricultural lands. The OCPs exhibit a high degree of stability and are resistant to degradation, resulting in their prolonged persistence in the environment and posing severe risks to humans and other living organisms [60]. Pyrethroids are a type of artificial pesticides commonly used as insecticides that have negligible harm to mammals and are extensively employed in both rural and urban regions around the world. Upon entering the ecological environment, pyrethroids spread through solid, liquid, and gaseous media and may enter organisms via food chains, consequently creating some health problems [61]. Pyrethroids exist in almost a thousand individual structures, which can resemble or vary from natural pyrethrin, and they function as powerful toxins [62].

Pesticides are employed in several stages of the crop cycle or animal lifecycle in accordance with good agricultural practices (GAP). The aim of the GAP is to guarantee consumer safety by determining the quantity of pesticides used, the frequency and the growth stage of their application [63]. Pesticides are used before harvest to thwart pests, providing sufficient maturation and resulting in enhanced food quality and quantity. On the other hand, post-harvest applications are intended to protect the quality of produced crops throughout extended storage periods [64]. Regulatory authorities establish allowable thresholds for pesticide residues in commercially available agricultural products including crops, poultry, fish, and meat in order to assure public safety. The Environmental Protection Agency (EPA) and European Union (EU) use the terms "*tolerance*" and "*maximum residual limits*" *(MRL)* to depict the acceptable amounts in these products [65]. The ascertainment of these limits relies on performing risk assessments or utilizing the pesticides' toxicological profiles. The Acute Reference Dose (ARfD) quantifies the instantaneous toxicity while the Acceptable Daily Intake (ADI) of pesticides quantifies the prolonged period toxicity in the toxicological profile [63]. Risk assessment depends on real or predicted residue data, taking into account several factors including age groups, exposure types, and specific effects on the endocrine system [65]. All pesticides must undergo registration before they may be commercially applied. Prior to registration and usage, a risk assessment study is performed to establish the tolerance/MRL values. If a reasonable level of risk is identified, the pesticide should be restricted, and permitted pesticides are provided

in packages that must carry labels including specific instructions regarding the proper quantity, target products, and frequency of utilization [66].

The exposure of humans to pesticides can occur by the contact with pesticides through many routes, either directly or indirectly, leading to diverse health problems [54]. These health problems can vary from suicide attempts and mass poisoning due to contaminated food and chemical mishaps in industrial settings Furthermore, those working in the agricultural sector may face occupational exposure [67]–[69]. Additionally, several life-threatening ailments have been related to pesticide exposure with asthma, leukemia, diabetes, Parkinson's disease, cancer, and cognitive impairment as typical examples [70]–[74]. According to the World Health Organization, around 355,000 people worldwide die each year due to unintentional poisonings. These poisonings are primarily caused by excessive exposure and improper utilization of harmful pesticides [54].

2.2.1.2 Hormones and Endocrine Disruptor Compounds (EDCs)

Hormones are referred as messenger molecules produced by glands and delivered through the bloodstream to target tissues and organs. Normal functioning of living systems such as growth and development, tissue function, sleep, mood, and reproduction, as well as the other actions to respond to external and internal stimuli are all regulated by these hormones. Hormone-producing glands such as the pituitary, thymus, adrenal, thyroid, female ovaries, male testicles, and pancreas constitute the endocrine system in the human body as shown in Figure 2.2 [75].

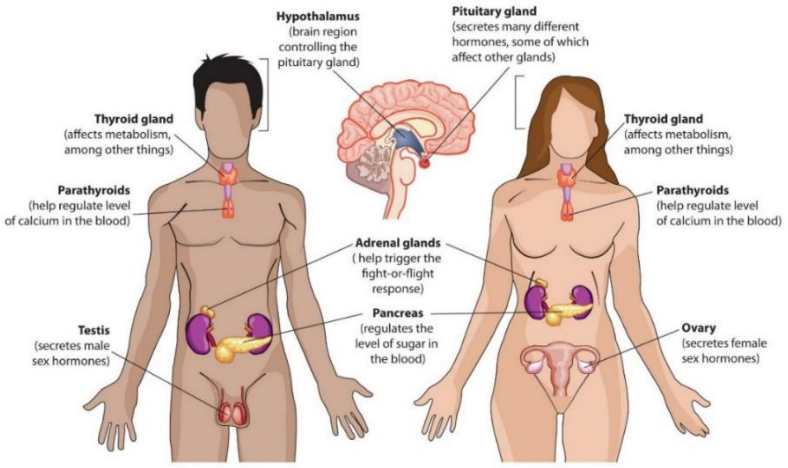


Figure 2.2 Functions and places of some prominent endocrine organs in the human body [76]

A dysfunction in the endocrine system leads to an aberrant hormonal levels that lead to diseases. Diabetes is one of the prevalent endocrine system disease, which results from insufficiency of insulin amount produced by the pancreas or when the body is resistant to the insulin. Other endocrine system-related disorders include hypothyroidism, osteoporosis, hypoglycemia, Hashimoto's thyroiditis, and thyroid cancer [77]. The regular function of the endocrine system is usually disrupted by some micro contaminants that have the capability to mimic hormones and bind receptor cites to obstruct agonist action [78]. These contaminants are commonly called endocrine disrupting compounds (EDCs) or endocrine disrupting chemicals.

EDCs was defined by the WHO in 2012 with the statement as:

"An endocrine disruptor is an exogenous substance or mixture that alters function(s) of the endocrine system and consequently causes adverse health effects in an intact organism, or its progeny, or (sub)populations" [79].

These EDCs have the tendency to accelerate or inhibit the functions of the endocrine system and cause the irreversible alterations. EDCs have been greatly linked with the delayed neurodevelopment and abnormal growth traits in children. Exposure to EDCs poses the risk of dysfunctional reproduction systems such as male infertility and spontaneous abortion or premature birth [80]. Although EDCs do not naturally exist in nature, human activities have made them ubiquitous. The main routes of human exposure are listed as through food ingestion, drinking water and gas inhalation. Developing fetus in the womb also stand the vulnerability to EDC exposure through the placenta, and nursing babies through breast milk [81]. The most susceptible members of the world to the effects of EDC exposure are children and pregnant women. Besides humans, EDCs also pose great risks to wildlife. Birds, amphibians, invertebrates, fish, reptiles, and aquatic mammals are some species affected by EDCs [82]. The pathways to wildlife exposure include the contaminated water bodies and chemical spillage in the environment. Once in the ecosystem, EDCs can be transferred from one organism to the other through the food chain. A typical example is fish-eating birds. The most common effects are birth defects and developmental disorders. The greatest concern on wildlife exposure to EDCs is the possible decline in population resulting from the damage of the reproductive system.

2.2.2 Inorganic Pollutants

Global apprehension regarding the toxicity and accumulation of heavy metals has an important influence on many organisms including animals, plants, and humans [83]. Metals including iron (Fe), zinc (Zn), and copper (Cu) show substantial biological importance, and are in this vein classified as '*essential metals'*. They tend to act as cofactors, which are essential for the operation of proteins and enzymes that participate in fundamental biological processes such as cellular respiration, cell differentiation and proliferation, and DNA synthesis. On the other hand, it is important to point out that some heavy metals, especially mercury (Hg), lead (Pb), and cadmium (Cd), are classified as *'non-essential metals'* because they do not have recognized biological functions [84]. The occurrence of toxic heavy metals, in the human body is a topic of great concern because they persist in the environment for a long period and have well documented reports on their devastating impacts on health. Exposure to heavy metals may instigate harmful effects on multiple biological systems or organs, such as the cardiovascular system, central nervous system, gastrointestinal system, kidneys, lungs, endocrine glands, liver, and bones. Absolute avoidance of hazardous metals is not practical because there are risks of exposure from unsuspecting sources such as food or drinks that contain metals, or inhaling particles in the air. In order to decrease the exposure to heavy metals, dietary therapies should be promoted for the safe metabolism or heavy metals that are consumed should be removed [85]. The persistent characteristic of heavy metals is liable for their chronic hazardous effects, because of their exhibition of resistance to degrade. Even at trace levels, heavy metals show the tendency to induce toxicity, which can result in fatality for living organisms. The process of bioaccumulation also increases the concentration of heavy metal in biota [86]. Heavy metals can find their way into the human body through different pathways, including the inhalation of polluted air, direct contact with the epidermis, and the ingestion of contaminated food and drink. Heavy metals can readily enter the biological systems of flora and fauna through the ubiquitous and easily accessible water media. The growing worries regarding water contamination brought on by heavy metals are becoming more prioritized, mostly due to the primary focus on water treatment in research [87]. The WHO has set maximum allowable thresholds for toxic heavy metals in drinking water and industrial

wastewater. Additionally, an assessment has been made on the possible health effects that could occur when these thresholds are surpassed [88].

Water pollution refers to the introduction of extraneous substances into water bodies, resulting in a decline in water quality. Water pollution pertains to the contamination of liquid bodies such as oceans and rivers. Liquid pollution is a phenomenon that takes place in various bodies of water including oceans, lakes, streams, rivers, underground water, and bays. This term refers to the contamination of liquid-containing areas. The phenomenon under consideration pertains to the discharge of hazardous compounds, disease-causing microorganisms, oxygen-demanding substances, readily-dissolvable substances, radioactive materials, and other similar agents that tend to settle on the bed of water bodies. The gradual buildup of these substances can impede the proper functioning of aquatic ecosystems. Eutrophication is a phenomenon characterized by the depletion of oxygen in a water body due to the proliferation of algae resulting from the accumulation of pollutants. As per the hydrological cycle, water in the vicinity undergoes absorption by the terrestrial surface, including the soil, and subsequently, rivers flow from the upper course to the lower course, ultimately discharging into the ocean. Under typical circumstances, microorganisms facilitate the degradation of organic pollutants, resulting in their conversion into a form that confers advantageous outcomes for aquatic organisms. In the context of inorganic pollutants, it can be observed that their dispersion is extensive and their impact on the environment in which they are released is negligible, thereby posing minimal hazards. Certain pollutants, such as lead, cadmium, mercury, arsenic (As), chromium (Cr) (particularly hexavalent chromium), nickel (Ni), barium (Ba), cobalt (Co), selenium (Se), vanadium (V), oils and grease, and pesticides, exhibit high levels of toxicity and pose a significant threat even at concentrations as low as parts per billion (ppb). Certain minerals possess beneficial properties for both human and animal health when consumed in limited quantities, exceeding threshold limits can result in toxic effects. Elements such as Zn, Cu and Fe as mentioned earlier are classified within this particular category. In the field of agriculture, specific elements such as Zn, Cu, Fe, manganese (Mn), sulphur (S) and boron (B), as well as compounds/elements such as phosphates, nitrates, urea, and potassium, are deemed beneficial when utilized in appropriate amounts. Certain chemical

compounds/elements such as cyanides, thiocyanides, phenolic compounds, fluorides, and radioactive substances have been identified as posing potential harm to both human and animal health [89].

2.2.2.1 Cadmium

Cadmium, having an atomic number of 48 and an atomic weight of 112.41 g, is classified as an element belonging to group XII of the periodic table. This metallic element, presents soft and silvery-white appearance, exhibits similar physical and chemical characteristics with zinc and mercury [90]. This element is classified as a rare metal because of its limited presence in Earth's crust, specifically 0.15 mg kg^{-1}, and similarly present at low concentrations around 1.1 x 10^{-4} mg L^{-1} in aquatic ecosystems [91]. Cadmium has a configuration of two electrons in the s orbital and ten electrons in the d orbitals. Cadmium, a highly malleable and adaptable element, tends to display a preference for the +2 oxidation state in the majority of its chemical compounds. Cadmium exhibits corrosion-resistant characteristics and is commonly used as a protective plating material. It is characterized by its insolubility in water and non-flammable nature [90]. It is employed in a wide range of industrial areas including electroplating, timber, stainless steel, Ni-Cd battery fabrication, and phosphate fertilizer production [92]. Accordingly, Cd pigments have a diverse range of hues, from yellow to deep burgundy, and exhibit exceptional opacity and durability against various atmospheric and ecological factors. Vincent Van Gogh and Claude Monet were among the pioneers utilized vivid Cd yellow, orange, and red in their art pieces [90]. The environmental stress caused by Cd results from various factors such as the combustion of fossil fuels, leachate from waste sites, runoff from agricultural land, and mining residues, specifically those from Zn and Pb mines [93].

Cadmium exhibits toxicity even at trace levels and extended exposure of human results to renal dysfunction, which is characterized by tubular proteinuria. Prolonged and excessive inhalation of dusts and fumes may lead to cadmium pneumonitis and obstructive lung disease. The condition is distinguished by thoracic discomfort, expectoration of frothy and blood-streaked phlegm, and necrosis of the pulmonary tissue lining due to an excessive amount of aqueous fluids. Cadmium has been associated with bone abnormalities, specifically osteomalacia, osteoporosis, and spontaneous fractures, as well as elevated blood

pressure and myocardial dysfunctions [89]. Cadmium has been classified as a group I human carcinogen by the International Agency for Research on Cancer (IARC) because of its cytotoxic properties that can cause apoptosis or necrosis. Occupational or environmental exposure to Cd has been associated with the development of breast, lung, urinary bladder, pancreas, prostate, and nasopharynx cancers [90]. Cadmium accumulates predominantly in the kidney, liver, and osseous tissues of the human body. The expected half-life of Cd subsequent to its introduction into a human or animal organism is between 10 and 30 years [94]. The most catastrophic event during the mid-twentieth century in Japan was the outbreak of *'Itai-itai disease'*, caused by the prolonged ingestion of cadmium contaminated rice. The condition known as *itai-itai disease* is marked by severe discomfort caused by impaired kidney function, weakened bones (osteomalacia), and low red blood cell count (anemia) [95]. The accumulation in the renal system leads to harmful effects on the kidneys and hindering the functionality of Vitamin D. Consequently, this obstructs the customary process of bone calcination and the storage of calcium and phosphorus in the bone, ultimately leading to the development of osteoporosis [94].

In accordance with the guidelines of the WHO and the Food and Agriculture Organization (FAO), the acceptable limit for Cd intake in humans is around 400 – 500 μg per week [96]. The current approximation shows that the average of the daily consumption of Cd through the food chain among the population of the United States is between 0.4 and 1263 μg/kg. On the other hand, the average dietary exposure in European countries determined to be 2.3 μg/kg body weight per week, with a range of 1.9 – 3.0 μg/kg body weight per week. The highest exposure was estimated to be 3.0 μg/kg body weight per week, with a range of 2.5 – 3.9 μg/kg body weight per week [97]. Cadmium may occur in soil at the range of 0.01 to 1 mg/kg with a worldwide average of 0.36 mg/kg. Accordingly, the typical concentration of Cd in soil water is determined to be more or less 5 μg/L, while the maximum concentration of Cd in groundwater is reported as 1 μg/L. With respect to regulation, the maximum contamination level established for Cd in the WHO Guidelines for Drinking-Water Quality is 3 μg/L [98].

2.3 Sample Preparation

The utilization of analytical instruments in the determination of target analytes at low concentrations in environmental, biological, and food samples can have some challenges due to the complex nature of these samples and interference effects from components of the sample matrices [99]. Consequently, a vast majority of analytical methods require sample preparation steps before the quantification in order to achieve three essential objectives:

(i) matrix simplification and/or substitution,

(ii) sample purification,

(iii) preconcentration of the analyte into detectable quantities [100].

The process of preparing a sample involves simplifying the composition of the sample matrix, transforming the analyte or sample into a measurable form, and enhancing the detection limits by preconcentration. The primary objective of sample preparation is to enhance the precision, accuracy, sensitivity, and durability of an analytical procedure [101]. Analytical techniques often involve various methods including sample handling, preparation, quantification, separation, and numerical assessment. Sample preparation, referred to as the limiting factor of an analytical process, is responsible for the majority of analysis time, but other processes are also crucial. [102]. Analyte loss can result in a negative discrepancy, whereas the addition of analytes to the sample or interference from the matrix might contribute to a positive discrepancy. Both types of errors may occur during this step, thus, the chosen methodology should eliminate or significantly decrease both positive and negative errors. [103]. Various aspects are considered when selecting a technique for sample preparation. The factors to consider include the kind of sample matrix, the characteristics of the target chemical (such as polarity, volatility, and solubility), the analysis technique (GC, LC, and their respective detectors), the concentration of the target analytes in the sample, the cost, and the duration of the analysis. Each approach must be evaluated in terms of its advantages and disadvantages [102], [103]. Sample preparation frequently involves dry ashing, cleaning, digesting, and derivatization, among other steps. [104]. Extraction, in the field of analytical chemistry, has become synonymous with "*sample preparation*" due to its widespread application. The advanced and modernized methods are

derived from two traditional approaches, which are broadly defined as liquid-liquid extraction (LLE) and solid-phase extraction (SPE). These two conventional methods are still widely employed for the purpose of concentrating analytes and purifying environmental samples [105]. The LLE method is the initial classical extraction technique employed in the 1950s for determining substances derived from biological and environmental sources [106], [107]. The LLE method can separate chemical substances by utilizing the solubilities of components between two liquids that are not miscible, typically an organic solvent and water [108]. Dominant factors to take into account include the solubility of the analytes in the extraction solvent and their partition coefficients in this solvent. The solvents commonly employed in LLE procedures comprise hexane, dichloromethane, chloroform, toluene, and 1-chlorobutane (n-butyl chloride) [109]. The efficiency of LLE is primarily determined by three factors:

(i) the kind of extraction solvent,

(ii) the presence of additives (such as pH modifiers that significantly impact water solubility),

(iii) the nature of impurities. The presence of interfering entities that exhibit similar features to the analytes decreases the yield of LLE.

Although LLE methods offer advantages like compatibility with large sample volumes and negligible memory influence, they nevertheless suffer from a significant drawback, namely the requirement of using substantial quantities of hazardous chemical solvents. The LLE method is characterized by numerous steps, rendering it challenging to automate and highly labor-intensive [110]. In order to overcome these concerns associated with LLE, SPE was introduced as an alternate approach. The fundamental principle of the SPE method involves the distribution of an analyte between the sample media and a sorbent material [107]. Compared to LLE, SPE has many advantages, such as not forming emulsions, demand for less solvent, quicker extraction durations, being able to work with smaller sample amounts, and being highly compatible with automation [111].

The proliferation of industrial activities commencing in the 1940s consequentially initiated environmental predicaments [112]. Regulatory institutions were established with the purpose of implementing stringent restrictions to prevent

environmental devastation and restore deteriorated areas. The framework of Green Chemistry serves to limit pollution at the source point, and this subject saw substantial breakthroughs in the 1990s. Within this period, a number of chemists started advancing creative procedures that would decrease the detrimental influence of industrial processes, as well as academic work on the safety and health of the environment and humanity [113]. In 1998, Anastas and Warner developed the twelve principles of "*Green Chemistry"* as a practical approach to minimize dangers to workers and the environment associated with industrial activities. One year later, Anastas authored an article highlighting twelve principles that serve as a model for the advancement of analytical methods and techniques. Research and development of analytical methodologies is a crucial component of green chemistry. The approach of "*green analytical chemistry*" aims to reduce or eliminate the use of potentially dangerous substances during an analytical process by implementing advanced approaches and procedures [112]. As a result, in 2013, Gałuszka et al. (2013) introduced the term "SIGNIFICANCE" as a mnemonic device for recalling the core concepts of green chemistry (Figure 2.3) [114]. The last few years have seen a decrease in the use of toxic organic solvents due to the downsizing of the SPE and LLE method. The recent advancements are equally, if not more, effective than SPE and LLE in terms of extraction efficiency, cost-effectiveness, and environmental sustainability. In recent years, more compact versions of SPE or LLE have been introduced, resulting in a reduction in the use of harmful organic solvents. Additionally, these new versions superiority, environmental friendliness, cost-effectiveness, and extraction efficiency when compared to SPE and LLE [115].

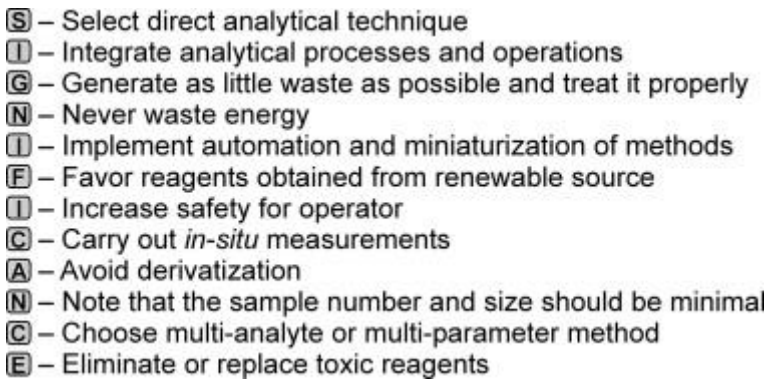


Figure 2.3 A mnemonic technique to recall the principles of green analytical chemistry [114]

The environmental impact of an analytical technique is significantly influenced by the sample preparation stage [104]. Conversely, the primary principle of green chemistry suggests bypassing the sample preparation stage in favor of direct analytical methods [114]. This approach fails to consider the need to convert samples with complex matrices into formats that can be assessed by equipment. Another factor overlooked by direct analysis is the potential deterioration in the method's sensitivity. Therefore, López-Lorente et al. (2022) established a practical structure by defining green sample preparation, drawing upon the other 10 principles. Materials and reagents that are sustainable, recyclable, and reusable are crucial for achieving these principles. Moreover, there is a reduction in energy consumption and waste, operations are optimized and automated, and operator safety is ensured [116].

2.3.1 Liquid Phase Microextraction Strategies

Solvent extraction, commonly referred to as LLE refers to the procedure of separating a solute using two immiscible liquids in contact with each other. Due to its greater affinity, a molecule experiences a phase change in this process, transitioning from one liquid state to another [111]. The most common method used for analytical sample preparations is LLE, which provides benefits such as signal amplification, enrichment, and purification. However, this strategy possesses some disadvantages, with the most notable being its detrimental impact on the environment as well as its high cost, time-consuming nature, and labor-intensive requirements [112]. Current extraction techniques generally utilize reduced amounts of solvent, fewer steps, smaller apparatus, increased sample processing capacity, diminished presence of hazardous chemicals, and decreased overall analytical costs when compared to the conventional extraction procedures [100]. Liquid phase microextraction (LPME) is regarded as a preferred approach in the scientific literature due to its adaptability as an extraction technique and the diverse range of modifications that can be used to concentrate and isolate analytes for instrumental analysis. In 1996, Jeannot and Cantwell conducted a study on the extraction of 4-methylacetophenone, while Liu and Dasgupta focused on the extraction of sodium dodecyl sulphate. Both investigations used the extraction process that made use of a little amount of chloroform in the form of a microdrop [107],[108]. Both approaches are thought to be forms of single drop microextraction

(SDME), which is considered the predecessor of LPME method. The past few decades have seen significant advancements in different LPME methods as presented below.

2.3.1.1 Single Drop Microextraction

Single drop microextraction is a variant of LPME that relies on the partitioning of analytes between an organic solvent microdrop situated at the apex of a microsyringe needle and an aqueous sample solution. The methodology integrates the processes of extraction, preconcentration, and sample introduction into a unified step [119]. In SDME, a drop of the acceptor phase (extractant) is suspended in the sample or headspace above the sample using a polytetrafluoroethylene (PTFE) rod or syringe needle, and extraction occurs under equilibrium or non-equilibrium conditions [120]. It is imperative that the solvent utilized for extraction exhibits minimal solubility in the liquid phase of the sample and possesses low volatility. The parameters that impact the SDME process are consistent with those of other solvent extraction methods. These include the type of solvent used, temperature, agitation, presence of salt, and volume of solvent [121]. The SDME method was introduced in the mid-1990s by Liu and Dasgupta for extracting sodium dodecyl sulfate utilizing a drop-in-drop approach. The study involved the immersion of 1.3 μL microdrop containing a water-immiscible organic solvent into a significantly larger flowing aqueous solution, with the aim of achieving analyte separation and enrichment [117]. The need to execute extraction and injection separately using distinct tools was a drawback of the aforementioned techniques. In order to overcome this, Jeannot and Cantwell developed the SDME procedure in 1996, which involved immersing 8.0 μL of an organic solvent held at the end of a Teflon rod in a stirred aqueous sample in a sequential manner. The retrieval of the probe from the specimen was carried out prior to the extraction of the organic layer through employment of a micro-syringe. The ultimate step involved the direct injection of the extracted sample into the inlet of a gas chromatograph (GC) [118]. The SDME method presents itself as a cost-effective and efficient microextraction technique that is environmentally friendly due to its low solvent usage. In recent years, the simplicity of operation and analyte enrichment capabilities of SDME have garnered significant attention [122]. Currently, there exist seven distinct modes of SDME that can be classified as either two-phase or three-phase modes,

based on the equilibrium co-existence of phases. The two-phase modes encompass direct immersion (DI), continuous flow (CF), drop-to-drop (DD), and bubble-in-drop (BID) techniques, whereas the three-phase mode involves headspace (HS) and liquid-liquid-liquid (LLL) microextraction. The HS and DI modes of SDME are the most frequently utilized, accounting for 41% and 38% of all described SDME procedures, respectively. This is likely attributed to their ease of use and cost-effectiveness in terms of required equipment [123]. The SDME modes are depicted in Figure 2.4 below [124]. Notwithstanding its advantages, SDME presents certain drawbacks such as the requirement for manual dexterity, the necessity of an acceptor phase possessing a surface tension of adequate magnitude to ensure the formation of a stable drop, and, in certain instances, low sensitivity. Additionally, the presence of suspended solids in aqueous samples can have an impact on the stability of the micro-drop [125].

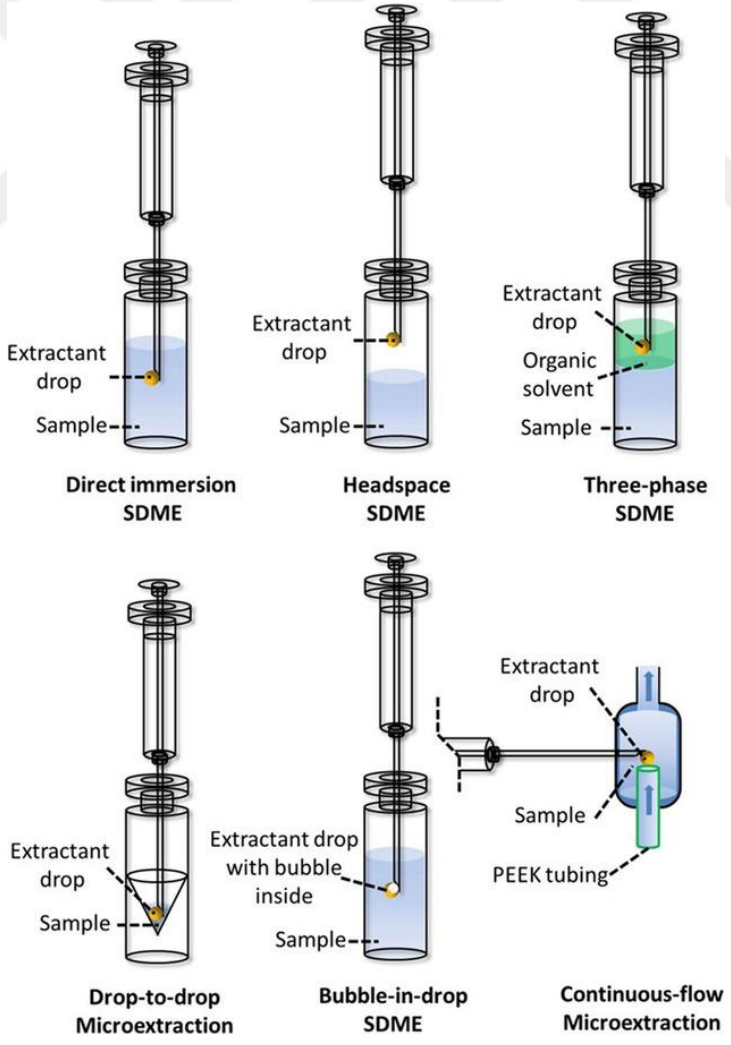


Figure 2.4 Different practical modes of SDME procedure [124]

The DI-SDME technique employs a minute quantity of organic solvent that is affixed to the apex of a micro-syringe needle. This method entails the direct retention of the droplet within an aqueous sample solution [124]. The HS-SDME technique is widely used to investigate volatile and semi-volatile chemical substances. This technique entails the placement of a minute droplet of extraction solvent on the apex of a micro-syringe [126]. In order to drastically eliminate complex matrix interferences, the single droplet is positioned for only semi-volatile or volatile compounds that migrate into the headspace from the sample. This method combines the processes of extraction, concentration, and sample introduction into a single step, which is advantageous. Furthermore, it necessitates a minimal quantity of organic solvent and cost-effective experimental and sampling equipment [127]. The single drop liquid-liquid-liquid microextraction (SD-LLLME) technique is a process that entails immersing a solitary droplet of an organic phase in a thin, planar layer [128]. This SDME methodology, characterized by its distinct thin organic layer and limited acceptor volume, demonstrates exceptional enrichment factors (EFs) that are more that hundred times higher than previous methods, all within a short timeframe of a few tens of minutes [129]. Wu et al. invented a method called static drop-to-drop solvent microextraction (DDSME) in 2006, which allows for the extraction of analytes from 7 μL of urine samples [130]. Although it is feasible to enhance the sensitivity of the DDSME by extracting a greater quantity of drug sample (more than 30 microliters), oppositely to this benefit, it was considered that the primary disadvantage of the approach is its lower selectivity. The determination of target compounds in DDSME only requires small quantities (15.0-30.0 μL) of biological samples using a rapid and straightforward sample preparation process [131]. Another feasible technique for SDME is BID-SDME, which entails infusing a predetermined quantity of air into the minuscule droplet, resulting in the formation of a bubble [132]. The surge in extraction efficiency is attributed to both the augmented surface area and the occurrence of thin film phenomena that results from the expansion of the drop's internal volume [133]. The occurrence of bubbles in micro-droplets is a bothersome consequence of organic solvent volatilization, especially when exposed to elevated ambient temperatures. Efforts have been made to mitigate the occurrence of bubble formation, but, inconsistent outcomes persist [134]. Continuous flow microextraction (CFME) was first proposed by Liu and Lee [135]. In this process,

a pump continually delivers a sample solution from the bottom of an almost immobilized organic drop on the tip of a polyetheretherketone (PEEK) tubing while extraction is ongoing [136].

2.3.1.2 Hollow-Fiber Liquid Phase Microextraction

Hollow-fiber liquid phase microextraction (HF-LPME), introduced in 1999 by Pedersen-Bjergaard and Rasmussen, is a technique that employs a permeable polypropylene hollow fiber to enhance the extraction process by confining organic solvents within the fiber's pores [137]. The approach consists of four primary components:

(i) The analytes of interest are present in an aqueous sample, which serves as the donor phase.

(ii) A porous polypropylene hollow fiber is used to trap the organic solvent.

(iii) The organic solvent is trapped within the pores of the fiber.

(iv) The interior of the fiber lumen is filled with an organic, acidic, or basic solution as the acceptor phase [138].

This method offers numerous advantages compared to other extraction methods. It is a straightforward and efficient method that utilizes hazardous organic solvents in very small quantities, minimizing consumption and it yields high enrichments [139].

The transfer of analytes from the donor phase to the acceptor phase occurs through a supported liquid membrane (SLM) located within a hollow fiber. The SLM is created by immobilizing an organic solvent that is not soluble in water within the pores of the porous fiber. The primary purpose of this device is to segregate the donor and acceptor phases with an effective separator in order to prevent their intermingling [140]. In the two-phase mode of this method, a water-immiscible organic solvent is utilized as both the solvent-liquid and acceptor phases [141]. It is common practice to use a pH-adjusted water-based solution as an acceptor in a three-phase extraction system when working with analytes that have acidic properties. It is important to note that the acceptor phase does not exhibit any indications of blending with the SLM. The objective of employing both of these

extraction procedures is to acquire diverse samples [142]. In Figure 2.5, the diagram of two-phased and three-phase HF-LPME methods are presented [143].

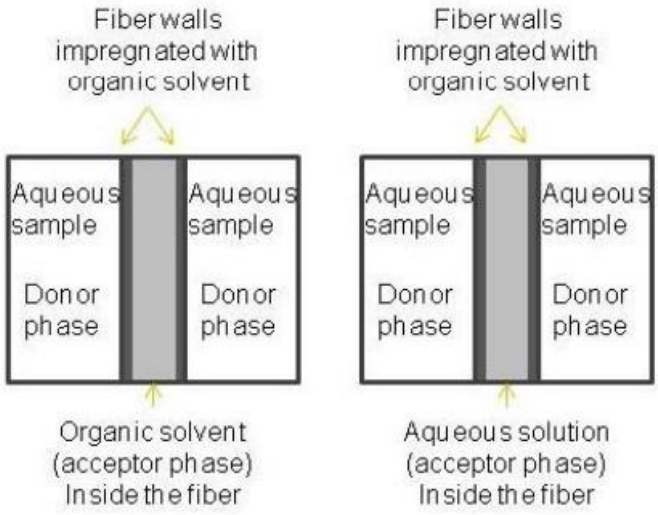


Figure 2.5 A schematic display of two-phase and three-phase HF-LPME [143]

2.3.1.3 Solidification of Floating Organic Drop Microextraction

Zanjani and colleagues (2007) introduced a novel approach that involves employing a floating organic droplet in the LPME technique [144]. In their method, an organic droplet is introduced onto the surface of the sample solution using a microsyringe and the mixture is agitated. Subsequently, the specimen is transferred to an ice bath to facilitate the solidification of the organic droplet while it is suspended in mid-air. Next, the solidified floating organic droplet (SFOD) is carefully moved to a clean vessel using a spatula or forceps. Utilizing solvents in the sub microliter range offers numerous advantages, including its superiority over traditional extraction methods. The distinctive feature of this extraction procedure lies in the utilization of solvents with freezing points ranging from 10 to 25 °C. [145]. Organic extractants including 1-undecanol, 1-dodecanol, 1-nonanoic acid, and 1-octanoic acid are suitable for this approach [146]. In order to enhance interaction and analyte extraction, a disperser solvent can be used to disperse these extractants in place of performing prolonged mixing for efficient extraction. The combination of these two different techniques, known as DLLME-SFOD, offers a remarkably high overall efficiency due to its two distinct features [145]. The issue of evaporative loss significantly impacts the accuracy and precision of extraction procedures that utilize solvents with low density. SFODME is significantly superior to those

methods as it does not encounter this kind of loss. Review papers offer comprehensive insights into the benefits and drawbacks, underlying principles, and applications of SFODME for the analysis of diverse analytes, demonstrating its widespread use among researchers [147][148].

2.3.1.4 Switchable Solvent-Liquid Phase Microextraction

Switchable solvent (SS), also known as smart solvent, was initially introduced by Jessop and his colleagues. The SS is highly advantageous in a multitude of applications, encompassing purification, catalytic processes, as well as the separation and extraction of chemicals [149], [150]. These solvents have the ability to transition their molecular bonding properties between hydrophobic and hydrophilic states. A commonly employed technique for producing solvents with adjustable hydrophilicity involves the utilization of chemicals such as secondary or tertiary amines. The hydrophilicity of a solution can be altered by constantly mixing and periodically adding dry ice to a solution containing amine and water in a 1:1 volume ratio. This process entails the protonation of the nitrogen atom possessing a lone electron on the amine. Consequently, protonation leads to the creation of a molecule that is attracted to water, resulting in a totally miscible solution. Deprotonation is achieved by inducing hydrophobicity in the switchable solvent through the elimination of carbon dioxide (CO_2) [151]. Deprotonation is commonly achieved through the application of heat or the utilization of concentrated alkali solutions [152]. The properties of the solvent arise from the ability of CO_2 to convert polarity. The mixing of water and amine with carbon dioxide gas results in the formation of ammonium carbonate, which is a water-soluble molecule. Sodium hydroxide or an inert gas can quickly transform the SS into its original separate states, rendering it an inexpensive, readily available, and secure substance. Carbon dioxide is an ideal phase change stimulus in extraction processes due to its non-toxic nature and affordability [150]. Switchable solvents have recently gained great appeal as extraction reagents in analytical separations for preconcentration of analytes from pharmaceutical, biological, and environmental materials. These solvents are known for their ecologically benign nature and intriguing physicochemical characteristics [153]. The SSs are increasingly being used in environmental sample analysis as a substitute for the more regular organic solvents to detect organic pollutants [151].

2.3.1.5 Dispersive Liquid-Liquid Microextraction

Rezaee et al. introduced the dispersive liquid-liquid microextraction (DLLME) method in 2006, which is a well-recognized and widely employed LPME technique. The DLLME process utilizes a three-solvent system, where a mixture of a hydrophobic extraction solvent (the acceptor phase) and an amphiphilic solvent (the dispenser) is rapidly injected into an aqueous donor phase, resulting in the formation of small emulsified droplets [120]. The rapid injection of the extractant-disperser mixture results in the formation of a turbid or cloudy solution. This solution consists of minuscule droplets of the extraction solvent that are evenly dispersed throughout the water sample. Dispersing the extraction solvent enhances its interaction with analytes and increases the extent of its surface area contact in the water solution. In order to facilitate the retrieval of the extraction solvent for instrumental measurement, the cloudy solution is subjected to centrifugation, resulting in the formation of a biphasic system [154], [155]. In the initial DLLME study, 1.0 mL of acetone was used to disperse 8.0 μL of tetrachloroethylene in order to extract polycyclic aromatic hydrocarbons (PAHs) from 5.0 mL of water samples. An investigation was conducted to assess the efficacy of different solvents, such as carbon disulphide and carbon tetrachloride for extraction, and methanol and acetonitrile for dispersing purposes [156]. The DLLME method is characterized by rapid mass transfer of analytes into the extractant and the achievement of extraction equilibrium, resulting in a very short and efficient extraction process [157]. In order to optimize phase separation, the most suitable extraction solvent for this method should possess a well-defined density and be incapable of mixing with water. To achieve high extraction yields, these characteristics alone are insufficient; the solvent must also possess a robust affinity for the target analyte [158]. Several DLLME extraction methods utilize chlorinated solvents, such chloroform, chlorobenzene, carbon tetrachloride, and tetrachloroethylene, as they satisfy these criteria [159]. However, chlorinated solvents are losing popularity in LPME applications because of the recent emphasis on environmentally sustainable chemistry. The characteristic quality of the DLLME method is attributed to the utilization of disperser solvents, such as acetonitrile (ACN), acetone (ACT), or methanol (MeOH), which exhibit excellent miscibility in both water and extractants [160]. An essential phase in the DLLME process involves amalgamating the

solvents utilized for dispersion and extraction into a single container. The solvent combination is rapidly injected into the sample solution using either a syringe or a micropipette. The organic extractant is visualized as a homogeneous cloudy solution following its dispersion into small droplets through rapid injection and dispersion. The extraction kinetics are significantly improved, resulting in an increased surface area of the extractant that comes into contact with the sample. Ultimately, the organic droplets that hold the analyte are swiftly isolated from the emulsion by the process of centrifugation using the extraction solution. The DLLME methodology enhances analytical sensitivity and streamlines experimental procedures when utilized in conjunction with spectroscopic and chromatographic instrumentation methods [161], [162].

A schematic illustration of the DLLME method is depicted in Figure 2.6 [163].

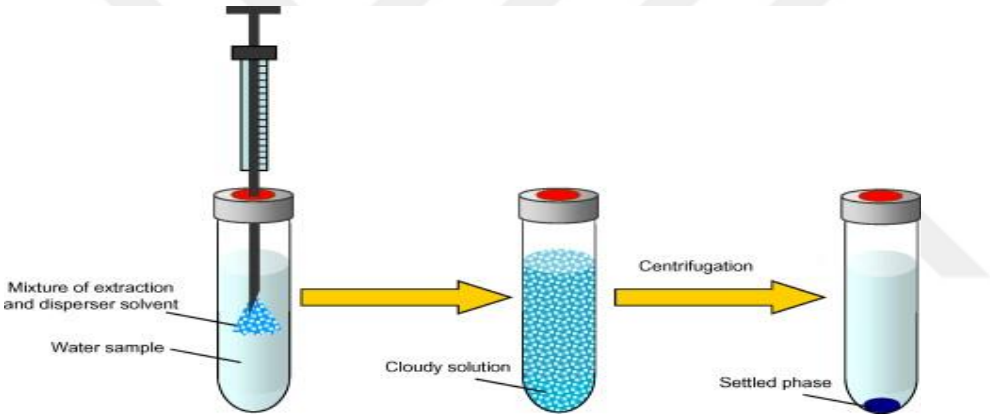


Figure 2.6 An illustrative scheme of DLLME procedure [163]

While DLLME often involves the use of very small amounts, regular applications could lead to the formation of microliters, resulting in significant volumes that could be detrimental to the environment and human health. This is mostly attributed to the fact that, in numerous instances, the amount of waste generated by the extraction process surpasses the quantity of contaminants being monitored [164]. The DLLME method enables the use of environmentally acceptable extraction solvents, resulting in an eco-friendly analytical methodology [165].

2.3.1.6 Binary Solvent Based Dispersive Liquid-Liquid Microextraction

The DLLME technique can be employed to preconcentrate analytes from different aqueous sample matrices, exhibiting favorable recovery rates and enrichment factors. Due to the varied polarity and solubility of analytes in water, determining

their concentrations using a single extraction solvent can be challenging [17]. Employing disperser solvents frequently enhances the surface area of an extractant, resulting in elevated extraction yields. There is a possibility that several substances may not react in the same way to the identical solvents during simultaneous determinations [166]. Modifying the solvents employed in the DLLME procedure can rectify this problem and typical example that employs binary solvents (BS) is BS-DLLME. This method involves two miscible extractants that are injected with a common disperser solvent, and collected as a single phase for instrumental analysis [167]. Figure 2.7 displays the procedure of the BS-DLLME method [168].

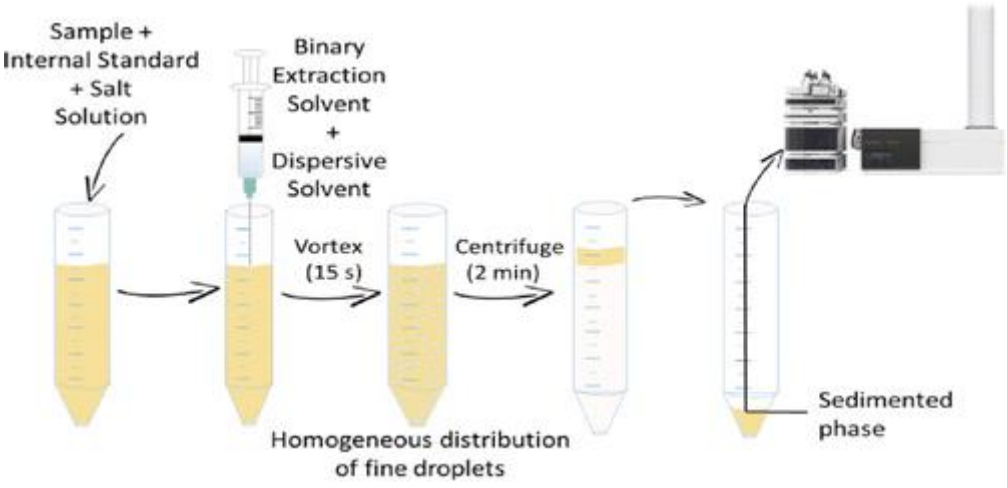


Figure 2.7 An illustrative scheme of BS-DLLME procedure [168]

2.3.1.7 Spray Assisted Droplet Formation Based Liquid Phase Microextraction

It is known that the conventional DLLME method, which has been frequently used in recent times, is performed by injecting the extraction and disperser solvent into the aqueous sample solution [169]. Although the DLLME method offers certain advantages [170], in addition to the long and difficult application process, high organic solvent consumption and the use of halogenated solvents such as chlorobenzene and carbon tetrachloride are some drawbacks [171]. To overcome these, it is necessary to develop new methods that are more environmentally friendly and can comply with the 'green chemistry' approach. Therefore, the spray assisted droplet formation based liquid phase microextraction (SADF-LPME), a new method based on the conventional DLLME method was introduced. The main difference between the SADF-LPME and the classical DLLME method is that the

extraction solvent is sent into the solution by spraying to extract the analytes without the use of a disperser solvent. The SADF-LPME method aims to achieve high separation efficiency and to support green chemistry by eliminating disperser solvent usage. The SADF-LPME method is a fast and simple procedure that involves very basic components. The key principle of SADF-LPME is to spray the extraction solvent into the sample solution containing the analytes at a constant pressure with the help of a spray tank without using a disperser solvent. A schematic procedure of the SADF-LPME procedure is depicted in Figure 2.8 [172].

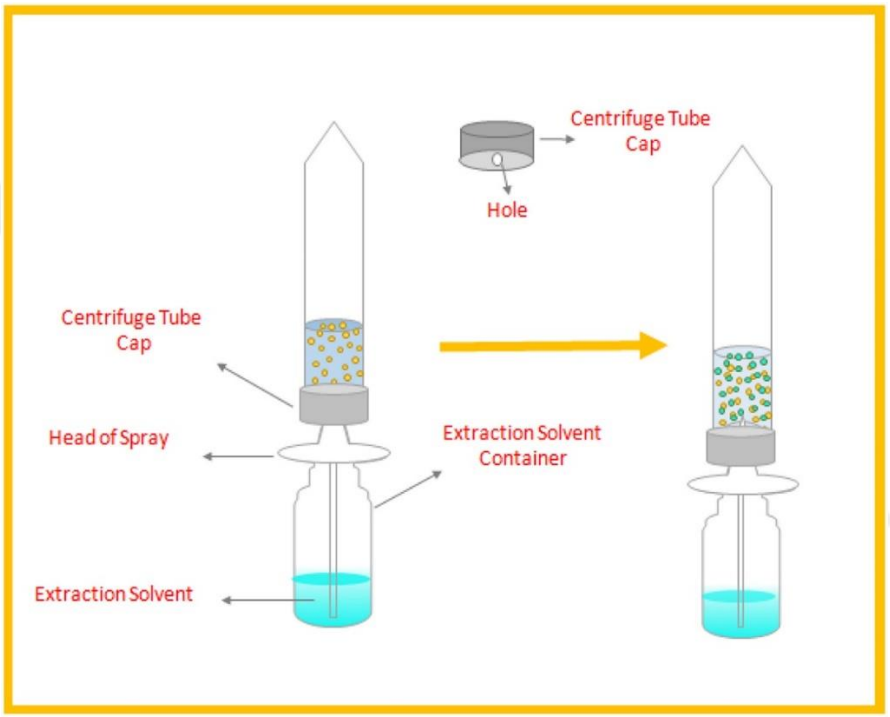


Figure 2.8 An illustrative scheme of the SADF-LPME method [172]

2.3.2 Solid Phase Microextraction Strategies

The conventional technique in solid phase extraction (SPE) involves moving the desired chemical species from a liquid sample onto the reactive areas of a sorbent material, which is typically organized in a disk, cartridge, or column. Compared to conventional extraction processes, solid-phase extraction (SPE) offers the advantage of a significant increase in analyte concentration and the ability to decrease interference from other substances in the sample [173]. An enlightening innovation introduced to the field of analytical chemistry was solid phase microextraction (SPME), a miniaturized SPE version reported by Arthur and Pawliszyn as a solvent-free methodology in the 1990s [174]. The SPME method is

a suitable approach for preparing samples in accordance with the principles of green analytical chemistry [175]. The main advantage of this strategy is its minimal reliance on solvents, if any at all. Some advantages of this technology include its potential to be reused, its simplicity in being automated, its minimal equipment needs, its quick examination time, its low cost, and its suitability for on-site application. Simultaneous sample preparation and sampling are further advantages [176]–[178]. The conventional procedure for preparing samples for SPME involves two distinct steps. Before being transferred to a separation or detection system, the analytes are initially extracted and concentrated onto the sorbent phase. The desorbed analytes are subsequently introduced into the mixture. The extraction yield of an analyte is determined by the partition coefficient, which is dependent on the volume, between the sample matrix and sorbent phase. The effectiveness of the extraction process, and consequently the overall sensitivity of the approach, are significantly influenced by the chemical properties of the sorbent material [176]. Various modifications have been made to the traditional SPE method in order to improve the enrichment factors and percentage recoveries. Different modifications to SPE have been reported in the literature including SPME [169], DSPE (dispersive solid-phase extraction) [172], MSPD (matrix solid-phase dispersion) [170], MSPE (magnetic solid phase extraction) [174], SBSE (stir-bar sorptive extraction) [171], m-SPME (magnetic solid phase microextraction) [175], D-μ-SPE (dispersive micro-solid phase extraction) [173], and m-D-μ-SPE (magnetic dispersive micro-solid phase extraction) [176]. These methods have been introduced to achieve highly satisfactory results with increased efficiency.

2.3.2.1 Magnetic Dispersive Micro-Solid Phase Extraction

An efficient and rapid technique for purifying samples was pioneered by Anastassiades and his team in 2003, known as DSPE. A modified version of the DSPE method known as D-μ-SPE was later introduced and this approach enables the extraction and concentration of several analytes including drugs, quinolones, tetracyclines, pesticides, semi-volatile chemicals, heavy metal ions, triazines, nitroaromatic hydrocarbons, and semi-volatile compounds [179]. In the D-μ-SPE process, a suitable sorbent is introduced into the sample solution and subjected to agitation for a specific duration to enhance the adsorption of the analyte. Upon centrifugation, the solid sorbent settles at the bottom of the tube, and the liquid

portion of the sample solution is carefully removed. The adsorbed analyte is extracted from the sorbent surface using a desorption solution, marking the concluding stage of the procedure. It is important to use a minimal amount of desorption solvent. Subsequently, an instrumental device is employed to assess and ascertain the analyte in the ultimate solution [180]. A schematic diagram of the D-μ-SPE procedure is given in Figure 2.9 [179].

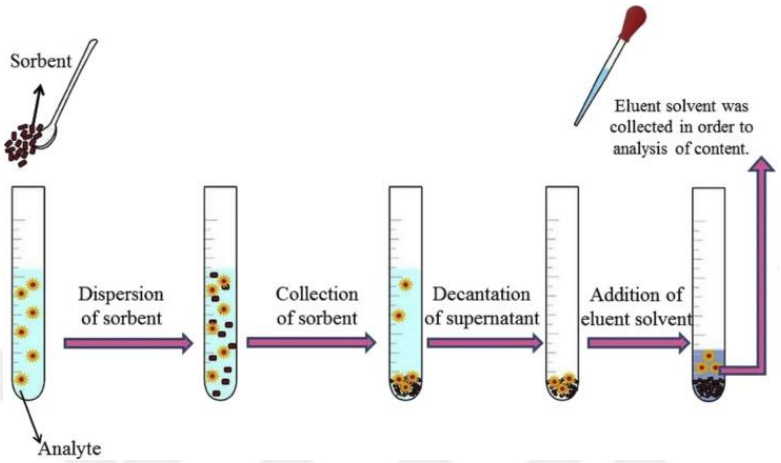


Figure 2.9 An illustrative scheme of D- μ-SPE procedure [179]

Magnetic solid-phase extraction (MSPE) is a contemporary adaptation of the SPE technique that utilizes magnetic sorbents [181]. The categorization of MSPE as either a dispersive or non-dispersive approach relies on the dispersion state of the magnetic extractant. Most MSPE systems employ the dispersive technique, which uniformly disperses the magnetic extractant across a water-based solution or suspension. The surface area of the extractant that comes into contact with the analyte in solution is enhanced during the dispersion process. While the dispersive method is commonly used, the non-dispersive method focuses on localizing the magnetic sorbent on a thin film or bulk material [182].

MSPE has several advantages compared to traditional SPE such as;

- eliminating the tedious and time-consuming column SPE process.
- providing efficient and rapid separation of analytes without the need for filtration or centrifugation.
- using magnetic extractants that provide a high degree of selectivity, enabling them to effectively isolate analytes from complex biological and environmental samples.

- given that the majority of pollutants present in samples have diamagnetic properties, the use of magnetic extractants can effectively minimize interference from these contaminants during the separation process.
- being suitable to combine with instrumental techniques, such as flow injection analysis, enables automation for routine analysis [183].

An external magnetic field is required to separate magnetic sorbents that adsorb the analytes from the original sample solution. The MSPE separation process eliminates the need for traditional filtration and centrifugation methods, as it relies solely on the use of magnets. The analysis tracks the desorbed analytes from the magnetic adsorbent, similar to prior methods of SPE using appropriate and small amounts of solvent [184]. Recently, novel materials have been devised for the purpose of magnetic separation [181]. The performance of the D-μ-SPE method is directly influenced by the surface area, adsorption specificity, and adsorption capacity of the adsorbent [185]. Nanoparticles have been employed in various fields of analytical chemistry to qualitatively and quantitatively detect several analytes. Considerable research has also focused on their capacity to extract medicines, proteins, pesticides, and explosives for instrumental investigation. Nanomaterials are very suitable for analytes found in small quantities because of their specific attraction and large surface area [186]. Adsorbents with superparamagnetic characteristics can also be used in D-μ-SPE applications. These adsorbents provide a more effective separation process after extraction using an external magnetic field [187].

2.4 Instrumental Detection Techniques

Modern instrumental techniques have replaced classical methods of determination due to their efficiency, selectivity, sensitivity, precision, and ability to determine multiple analytes simultaneously. In contrast, traditional methods are labor-intensive, time-consuming, non-selective, non-specific, and have low precision and accuracy [188]. The competitiveness between device manufacturers has led to advancements and improvements in instrumental methods in recent decades. The main advancement includes enhanced sensitivities that enable the detection of lower quantities that are at trace or ultratrace levels and the simultaneous identification of several compounds.

In literature, inorganic analytes are mainly determined by different instrumental detection techniques including spectroscopic methods; UV-Vis (ultraviolet-visible spectroscopy) [189], [190], AAS (atomic absorption spectrometry) [191]–[196], ICP-MS (inductively coupled plasma mass spectrometry) [197]–[199] and ICP-OES (inductively coupled plasma optical emission spectrometry) [199]–[201] electrochemical techniques; stripping voltammetry (SV) [202]–[204], pulse polarography [205], [206] and potentiometry [207], [208] and other techniques [209]–[211]. On the other hand, organic analytes have been determined using various chromatographic techniques including GC-FID (gas chromatography flame ionization detector) [212], [213], GC-MS (gas chromatography mass spectrometry) [213]–[217], HPLC (high performance liquid chromatography), [218], [219], and tandem systems including GC-MS/MS (gas chromatography tandem mass spectrometry) [220], [221], GC-HRMS (gas chromatography high resolution mass spectrometry) [221], LC-MS/MS (liquid chromatography tandem mass spectrometry) [220], and HPLC-MS/MS (high performance liquid chromatography-tandem mass spectrometry) [219]. However, the applicability of these instrumental detection techniques for the determination of both inorganic and organic analytes can be extended by conducting derivatization of analytes into forms that align with the instruments' working principle [222].

2.4.1 Spectroscopic Methods

The spectroscopic methods rely on the interference of beams passing through multiple optical channels to produce a signal. The grating uses only a small quantity of beams, determined by the number of grooves, in contrast to the prism, which utilizes an infinite quantity of beams [223]. In the method, a light is employed to stimulate or interact with a chemical of interest, enabling the assessment of its intensity or structure by measuring the analyte's response to the energy of the light using specific instruments. Light is a form of electromagnetic radiation that may be utilized for tracking different features of a substance. The particular properties that can be determined depend on the intensity and emitted energy of the light. Spectrometric techniques have emerged as the predominant method for determining elements.

2.4.1.1 Inductively Coupled Plasma Optical Emission Spectrometry

Inductively coupled plasma optical emission spectrometry (ICP-OES), known as a multi-functional and modern analytical technique, has been commonly employed for the quantification of elements in different real samples of environmental, industrial, plant, tissue, and pharmaceutical origins [224]. The method has gained attention as one of the hyphenated techniques having the ability of rapid and precise measurement of multiple elements at parts per billion (ppb) to parts per million (ppm) levels with very little interference [225]. The fundamental concept of ICP-OES relies on the emission of photons that occur spontaneously from ions or atoms. These ions and atoms are stimulated by a radio frequency (RF) discharge, causing them to excite in quantised energy level structure. Hence, the wavelength of photons can be used to quantify the elements because the total quantity of photons is directly proportional to the concentration of the element in the sample [226]. The samples are initially introduced into an argon plasma that is inductively connected using a sample injection equipment. Prior to being stimulated, the molecules in the plasma undergo atomization and ionization. Echelle or Rowland circle optics separate individual emission wavelengths and direct the emitted light to a detector by capturing the electrons transitioning from a higher energy level to a lower energy level. The process leads to ion or atomic emission [224]. A nebulizer is a device that converts liquid samples into tiny droplets or aerosols. The nebulization process involves the transfer of aerosol into the plasma core by introducing argon gas flow in the designated zone [227]. The liquid sample is transformed into an aerosol through the process of aerosol nebulization. Previously, solid materials required acid digestion or extraction, while gas samples could be directly introduced into the instrument. Currently, the majority of samples are introduced into the central channel of the device by radiofrequency (RF) produced argon plasma [224]. An ICP torch is comprised of three gas tubes: an outside tube, an intermediate tube, and an inner tube, all made of concentric fused-silica. The exterior gas tube sizes vary between 9.0 and 27 mm. The flow of argon gas (7–18 liters per minute) in the outer tube maintains the plasma and cools the walls of the torch, so preventing melting and enabling the monitoring of analyte emissions. Encircling the upper part of the torch is an RF generator, which is connected to a copper coil (known as a load coil) consisting of two or three turns. This coil is cooled using either water or gas. Certain

instruments possess coils that are interwoven. The RF generator supplies an alternating current (AC) that oscillates at a frequency proportionate to the generator's frequency, which can be either 27.12 or 40.68 MHz. The torch's tip generates an electromagnetic field by the oscillation of high-frequency electricity. The Tesla spark is employed to ionize specific argon atoms in the load coil area using a radio frequency power source (750-1500W) supplied to the coil and argon gas flowing through the torch [228].

2.4.1.2 Inductively Coupled Plasma Mass Spectrometry (ICP-MS)

Houk et al. introduced an inductively coupled plasma-mass spectrometry (ICP-MS) technique in 1980, which ionizes atoms by disrupting chemical bonds using high-temperature plasma [229]. Because of its capacity to enhance the determination of the majority of elements on the periodic table at ng L^{-1} detection limits with one to two minute spectral scanning, the ICP-MS technology launched a quantum leap for elemental analysis [230]. The ICP-MS is highly favoured and utilized extensively because of its exceptional sensitivity, long-lasting performance, and capacity to efficiently measure isotope ratios [231]. Argon ICP is widely recognized as the benchmark for ion sources in commercial inductively ICP-MS and shares the same functionality as those found in inductively coupled plasma optical emission spectroscopy (ICP-OES) systems. Plasma is generated by surrounding a quartz torch filled with argon with a coil that produces radio frequency magnetic fields in a spiral pattern. The plasma is initiated by introducing electrons from a high-voltage spark, which collide with argon atoms, resulting in the ionization of argon [232]. Similar to ICP-OES, ICP-MS utilizes a plasma medium near the Cu coil to vaporize and atomize analytes. This plasma medium is located in the same general area as the load coil [233]. Ions are transferred from the surrounding atmospheric pressure to a highly evacuated environment by employing a sampler and a skimmer. Ion lenses and quadrupoles are utilized to concentrate ions onto a mass filter, which then segregates them based on their mass-to-charge ratio (m/z). The ions identified by the detector are then quantified [234].

2.4.1.3 Flame Atomic Absorption Spectrometry

Kirchhoff and Bunsen conducted pioneering experiments on the "line reversal" phenomenon of alkaline earth spectra in the late nineteenth century. They utilized

a visible-band light source to demonstrate the fundamental relationship between radiation absorption and emission [235]. Atomic absorption spectroscopy (AAS) is an analytical technique that relies on the absorption of different beams emitted by atoms in the gaseous phase of a radiation source. Flame atomic absorption spectrophotometry (FAAS) is the most often employed method of AAS [236]. The FAAS, invented by Alan Walsh in 1955 [237], has found widespread analytical use in several sample types including clinical, environmental, metallurgical, and biological due to its simple, reliable, and cost-effective characteristics [238]. The standard components of such a system are light, lenses, a flame atomizer, a nebulizer, a monochromator, and a detector. Figure 2.10 depicts a standard representation of the components of the FAAS [239]. In essence, a lens is used to focus the light emitted by the specific light source onto the atomizer. Upon traversing a second lens, it passes through the flame consisting of fuel and oxidizing gas and is conveyed to the monochromator, where it undergoes filtration prior to ultimately reaching the detector. The solution containing the analyte is transported to the flame after conversion into an aerosol by the nebulizer. At extremely elevated temperatures, the process of atomization occurs within the flame, causing the atoms produced to engage with and assimilate a portion of the light that traverses the flame. As a result, the detector receives less light, which leads to the generation of absorption signals. These signals are then analyzed using a computer connected to the device [240].

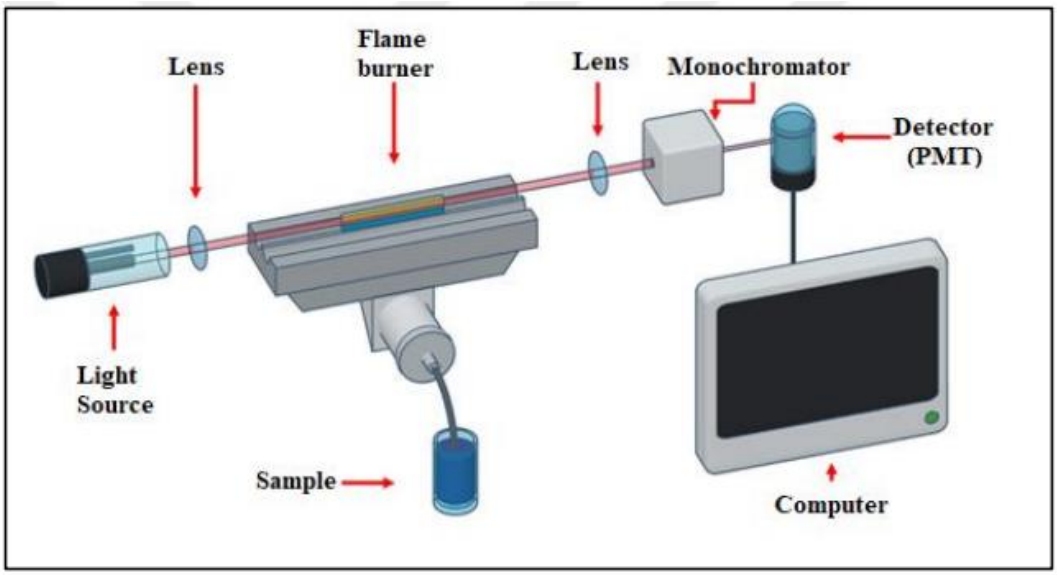


Figure 2.10 An illustration of FAAS system [239]

An atom absorbs light at specific wavelengths. In order to assess the extent of light absorption with optimal sensitivity, it is necessary to employ a line source that emits specific wavelengths that can be absorbed by the atom [241]. Figure 2.11 depicts a hollow cathode lamp (HCL) consisting of an anode and a cathode enclosed within a sealed glass tube filled with either argon or neon, both of which are inert gases [242]. The cathode contains an element that is necessary for the production of a specific spectrum, either in its pure form or as part of an officially accepted alloy. Quartz is chosen as the material for the front window of the HCL tube due to its ability to prevent the absorption of UV rays, unlike glass [243].

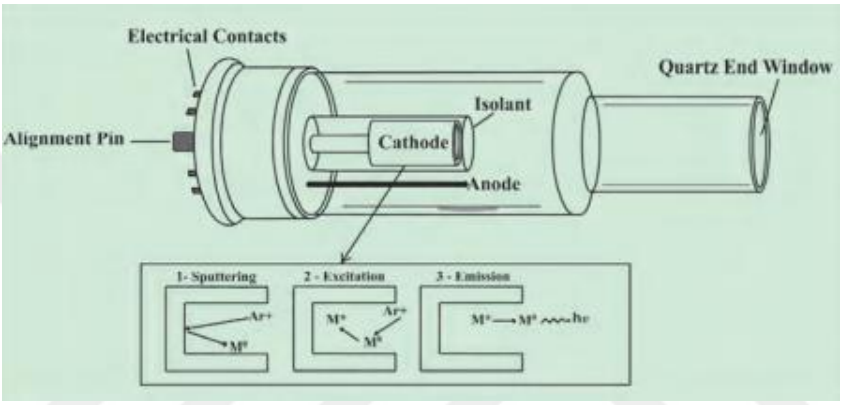


Figure 2.11 A diagram of a hollow cathode lamp [242]

The predominant sample inlet units in the FAAS system are gas-assisted nebulizers The nebulizer consists of a gas aperture and a central capillary tube that is used to inject the aqueous sample for analysis. The gas, often an oxidant, moves rapidly, resulting in a decrease in pressure inside the capillary due to a venture effect. This effect pulls the solution and promptly injects it as a fine aerosol into the nebulizer chamber. Typically, a flow rate of 3.0-5.0 mL/minute is reached for this type of nebulizers [244]. A method of categorizing AAS systems is based on the atomizers employed. There are two main categories of atomizers: electrothermal and flame atomization devices. Even when the temperature is lower than the point at which a substance melts, the pressure of the vaporized form of the substance may not go above the maximum pressure it can reach because of the tiny amount of the substance present in the flame, which is less than 10^{-3} atm [245]. The most prevalent flames are those formed by the combination of acetylene and air, reaching temperatures ranging from 2100 to 2400 °C, and the flames resulting from the

reaction between acetylene and nitrous oxide can reach temperatures between 2600 and 2900 °C [246].

The relationship between the quantity of analyte in solution and radiation absorption is represented mathematically by the measurement of monochromatic radiation, which possesses a distinct wavelength. However, it is important to note that photons and radiation in the visible and ultraviolet regions are generally detected by detectors. To determine the correct wavelength, however, a device is required to separate the detector from the source [244]. Monochromators utilizing the Ebert, Littrow, or Czerny-Turner designs are the most prevalent type of wavelength selector in AAS [245], [247]. An appropriate transducer is necessary to measure the magnitude of light passing through the exit slit of a wavelength selector. To accomplish this objective, a photomultiplier tube (PMT) is frequently employed [244]. The PMT possesses several captivating characteristics, such as its extensive wavelength range, significant amplification gains, wide dynamic range, and minimal noise. Nevertheless, there is presently a prevailing inclination to substitute PMTs with multichannel detectors consisting of numerous individual, minuscule adjacent detectors referred to as pixels. Charge transfer device detectors, utilizing charge injection or charge-coupled device technologies, are also utilized in this field [247].

2.4.2 Chromatographic Methods

Russian botanist Mikhail Tswett first used the chromatographic separation method in 1903 to isolate certain plant colors from a mixture. As the separated species in that experiment were passed through a calcium carbonate-filled glass column, coloured bands were discovered to have formed. The word "*chromatography*" was derived from the Greek words "*chroma*" meaning "*color*" and "*graphy*" meaning "*writing*"; the two words were joined together based on this discovery [248].

Chromatography is a widely used technique for separating organic compounds in order to enable their detection by an appropriate detector. Chromatography is particularly suitable for the initial step in analytical chemistry, which involves separating the desired substances from the surrounding substances in a sample. This separation is crucial for enhancing the accuracy and precision of the measurement and identification processes. The chromatographic solution is partitioned between

the mobile phase and the stationary phase [249]. The migration rates of the analytes in the mobile phase and their interactions with the stationary phase are utilized to achieve their separation.

It is usual practice to dissect chromatography into its constituent elements because of the wide scope of the discipline. Classification is based on several important criteria, with the most notable being the classification of the mobile phase's physical state. Other critical criteria include the classification of the stationary phase's physical state, the physical form of the separation mechanism, and the physical form of the chromatographic bed shape [250]. Table 2.3 presents a comprehensive classification of column chromatographic procedures [240].

Table 2.3 Categorization of column chromatographic techniques [240].

General Classification	Specific Method	Stationary Phase	Equilibrium Type
GC	Gas-solid	Solid	Adsorption
	Gas-liquid chromatography (GLC)	Liquid adsorbed or bonded to a solid surface	Partition between gas and liquid
LC	Liquid-solid, or adsorption	Solid	Adsorption
	Liquid-liquid, or partition	Liquid adsorbed or bonded to a solid surface	Partition between immiscible liquids
	Size exclusion	Liquid in interstices of a polymeric solid	Partition/sieving
	Ion-exchange	Ion-exchange resin	Ion-exchange
	Affinity	Group specific liquid bonded to a solid surface	Partition between surface liquid and mobile liquid

Table 2.4 Categorization of column chromatographic techniques [240] (Continued)

SFC (mobile phase: supercritical fluid)	-	Organic species bonded to a solid	Partition between supercritical fluid and bonded surface

2.4.2.1 Liquid Chromatography (LC)

While Giddings [251] had previously illustrated the potential benefits of liquid chromatography (LC) over gas chromatography (GC) in relation to column yields and analysis speed, it is generally agreed that the publication of Huber and Hulsman [252] in 1967 marked the beginning of LC's emergence on a comparable basis to GC [253]. LC has advanced to an incredible level with the rapid development of new instruments among all chromatographic procedures. High performance liquid chromatography (HPLC), an enhanced type of LC, was first considered a complement to GC. However, in recent years, HPLC has absorbed a significant portion of GC's application space due to its versatility. In contrast to GC, HPLC has no constraints on compound volatility, molecular weight, or thermal stability. With advancements in column packing for specific applications, optimal mobile phase combinations, and the use of improved and sensitive detectors, the HPLC method has become a perfect alternative for detecting environmental contaminants, agrochemicals, pharmaceuticals, and many other organic compounds [254]. The working principle of HPLC is that the analytes in the sample are dissolved in the mobile phase and passed through the column containing the solid packing material of the stationary phase at different speeds depending on their affinity for the mobile phase or stationary phase. Because the polarities of the analytes are different, they pass through the column at different rates and therefore have different retention times [255][256]. A typical HPLC equipment comprises an injector unit, mobile phase pumps, a column, a detector, and a data output device. Many HPLC systems employ valve injectors. The high pressure eluent system is separated from the sample introduction process by employing valve injectors with a constant volume

loop. To introduce the sample into the column, a smooth transition of the valve from the load position to the injection position is performed. These injectors are generally dependable and precise. The pumps typically deliver the mobile phase of the system at a flow rate ranging from 0.40 to 1.0 mL min^{-1}. Reciprocating pumps are commonly used to provide power to HPLC systems [257]. Through the use of a column containing a packaging material (stationary phase), the sample components are separated. HPLC employs a variety of separation mechanisms, including size exclusion chromatography, gel permeation, and ion exchange, all of which utilize distinct stationary phases. Characteristics of the particles comprising the stationary phase have a direct impact on the separation and retention periods of components. Normal phase columns and reverse phase columns, which consist of polar and non-polar stationary phases, respectively, are the two most common column varieties utilized in HPLC systems. When employing reverse phase columns, octyl groups (C8) or octadecyl groups (ODS) are the most utilized stationary phases [258]. Mobile phases in normal phase and reverse phase chromatography systems consist of non-polar and polar solvents, respectively [259]. In the chromatographic column, elution may be conducted in gradient mode or isocratic mode. Gradient elution denotes a programmed change in the composition of the mobile phase, whereas isocratic elution pertains to the preservation of a uniform composition of the mobile phase throughout the analysis. Isocratic elution falls short of achieving efficient separation in composites comprising analytes with differing polarities. In such situations, gradient programs that are suitable can increase the separation yield [260].

Various detectors are capable of achieving both qualitative and quantitative detection of compounds subsequent to chromatographic elution. Detectors employed in high-performance liquid chromatography (HPLC) ought to possess a number of qualities including compatibility, favourable linearity and operational range, heightened sensitivity, and resistance to temperature fluctuations and flow rate fluctuations [261]. Ultraviolet visible (UV-Vis), fluorescence, mass spectrometric, refractive index, electrochemical, and conductivity detectors are the most common types of HPLC detectors. Analyte solutes absorb light or radiation at specific wavelengths, which is the basis of the operation of the UV-Vis detector, the most common type of HPLC system detector. Several compounds can be

detected because they contain chromophore groups that allow them to absorb light in the visible and ultraviolet (UV-vis and UV) spectrums (190-600 nm) [262]. According to Beer's Law, the concentration of the sample is directly proportional to its absorption. The equation A = ε.b.c expresses that absorbance (A), the coefficient of absorptivity (ε), the length of the flow cell (b), and the concentration of the analyte (c) are all factors that can vary [263]. Mass spectrometry (MS) detectors, known for their high level of sophistication, are often employed in HPLC for the examination of intricate materials. The combination of mass spectrometry (MS) and high-performance liquid chromatography (HPLC) is a powerful analytical approach because of its exceptional selectivity and sensitivity [264].

2.4.2.2 Gas Chromatography (GC)

James and Martin (1952) were the first to develop the technique of isolating volatile fatty acids using gas chromatography. The GC was compared to distillation and found to be more efficient [265]. Subsequent to substantial progressions, it has emerged as the dominant methodology for the separation, characterization, and quantification of volatile and semi-volatile substances. The separation principle of gas chromatography (GC) entails the equitable distribution of analytes between a stationary phase and a mobile phase, which is comprised of a carrier gas. This procedure is carried out inside an analytical column subsequent to the transformation of the sample into a gaseous state. A comparison can be made between the individual retention times of the analytes that exit the GC column and the retention times of purified standards that underwent chromatographic analysis using the identical conditions [266].

The principal constituent of GC is the column, an elongated tube upon which a liquid is immobilized or deposited on the inner surface. As carrier gases, inert gases including hydrogen, helium, and nitrogen are controlled in tandem with the column to travel from a cylinder to the sample injection unit at a constant flow rate or pressure. The physical or chemical properties of mixture components that are eluted and separated via a column facilitate their detection by a suitable detector. The operational efficiency of GC is significantly impacted by the temperature of the column. Developments since the initial configuration have resulted in hot-air furnaces that offer efficient temperature regulation [267].

Detectors are a crucial part of gas phase GC systems since they significantly influence the specificity and sensitivity for the detection of organic molecules. High-quality detectors are characterized by their reliable analyte qualification, high repeatability, high sensitivity, rapid data acquisition, resilience, low cost, and user-friendliness. So far, improvements have been made to several characteristics of certain gas chromatography detectors, such as their ability to produce linear results, their sensitivity, selectivity, and the way they operate [266]. Flame ionization detector (FID) [268], electron capture detector (ECD) [22], [269], [270], infrared (IR) [271], mass spectrometry (MS) [22], [270], and thermal conductivity detector (TCD) [268], [272] are all prevalent detector types that can be conveniently integrated into GC to facilitate the identification of distinct organic analytes.

2.4.2.3 Gas Chromatography-Mass Spectrometry

GC-MS is a highly dependable, sensitive, specific, and consistent analytical technique used to separate and detect volatile organic compounds [273]. Optimizing the separation of volatile organic components is achieved by carefully selecting the column and setting the temperature, taking into account the different vapor pressures of the compounds [274]. Chemical ionization (CI) and electron ionization (EI) are the two ionization sources most commonly used in gas chromatography–mass spectrometry (GC–MS) analyses. The GC-MS system that uses an EI source is becoming more popular since it has access to libraries that include extensive databases of chemicals with mass spectra or fragmentation patterns. Costs and running times for EI-based systems are reasonable, and this straightforward method provides useful data for compound verification [273]. The mass spectrum library developed by the National Institute of Science and Technology (NIST) is a valuable resource for researchers conducting compound identification experiments because ionization using the EI source yields ion fragments of compounds that are highly repeatable for replication tests [275].

The ionization procedure entails transforming the chemicals present in the sample into ions through an appropriate method. Subsequently, the ion fragments obtained are subjected to sorting in a mass analyzer that employs an electrostatic field and radio frequency to regulate the movement of charged ions based on their distinct *m/z* (mass to charge ratio). The signals are collected and shown as a mass spectrum, which illustrates the proportional abundance of ion fragments in relation to their

m/z ratios, resulting from the interaction of ions with the detector. In order to prevent any possible interactions or collisions with other charged species, these procedures are conducted in a thoroughly evacuated environment [276].

The electron multiplier is the most commonly used detector in mass spectrometry. The signal undergoes amplification when a sequence of strategically positioned dynodes makes contact with ion fragments emitted by the mass analyzer. Subsequently, these electrons are liberated when the ions collide with a photocathode located next to an electron multiplier [277]. The GC-MS system has two main modes for collecting data: scan mode and selective ion monitoring (SIM). During scan mode, data is collected for ion fragment signals throughout a broad range of m/z ratios. Conversely, in SIM mode, data is collected for a limited number of specifically chosen ion fragments. The scan mode efficiently acquires a substantial amount of data, perhaps resulting in the loss of certain analyte signals. The detection power is enhanced by a factor of 10 to 100 because of the higher number of analyte signals collected in the SIM mode per unit of time [278]. Figure 2.12 presents a simplified schematic representation of the numerous components comprising a conventional GC-MS system [279].

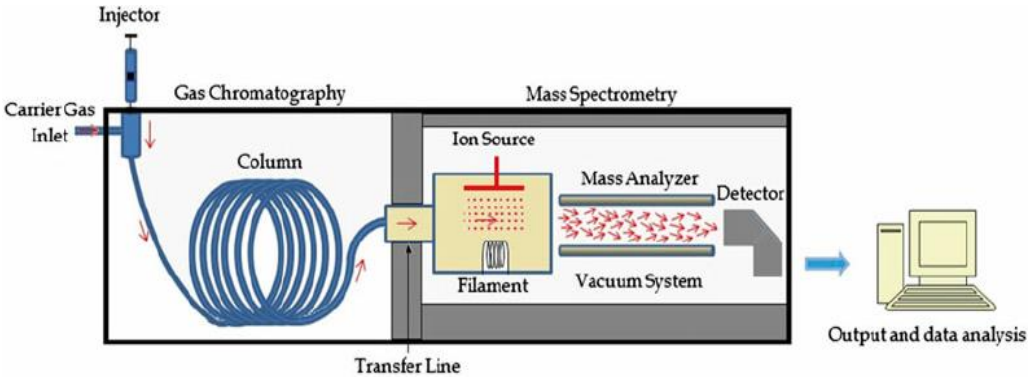


Figure 2.12 An instructive schematic illustration of the various constituents of a GC-MS system [279]

2.5 Quantification of Analytes

Estimating the exact quantities of an analyte is equally crucial for identifying the constituents of a sample. The readable, recordable and measurable signals are needed to be converted from response of the detectors' to the analyte [280]. The

undetermined values of these signals can be ascertained by comparing and subsequently quantifying them with the signals of standard solutions. The most reliable method for quantitative analysis is standard calibration, which produces highly linear results (R^2>0.99) by analyzing working standards with varying concentrations. The linear response of the analyte can be determined by applying the equation $y = mx + n$, where y represents the detector's response, m represents the slope, x represents the analyte's concentration, and n represents the y-axis intercept. The method of quantification known as external standard calibration is widely recognized and frequently employed. Measurements can vary due to electrical fluctuations and irregular infusions, which can change the signal output of analytes, as a disadvantage of the method, it lacks the ability to resolve such challenges [281].

2.5.1 Standard Addition and Matrix-Matching Calibration Strategies

During the analysis of real samples, the accuracy of measuring a specific substance can be significantly influenced by the composition of the sample. This can result in either an underestimated or overestimated system response. Relative errors in determining analytes are more frequent in complex sample matrices due to interference effects, in contrast to standard solutions prepared with pure solvents and deionized water. Matrix matching calibration and standard addition processes are techniques often employed to mitigate the influence of interference effects on quantitative data, hence enhancing their accuracy. The standard addition method involves creating a calibration plot by gradually increasing the amount of the analyte standard solution in the sample solutions [282]. In order to achieve uniform matrix effects for all sample calibration standards, equivalent quantities of sample solution are measured for each calibration point. excessive dilution of the sample matrix should be prevented, thus, it is crucial to add extremely small amounts of standard volumes and top-up solutions or solvents. The calibration chart, which plots concentration versus analytical system response, is used to calculate the analyte's concentration by extrapolating the plot to the negative x-axis and taking the absolute value. The concentration (x) of the analyte in a sample can be estimated using the linear calibration equation (y=mx+n) by calculating the absolute value of the y-intercept over the slope (n/m) when y is set to zero [283].

Utilizing a matrix matching strategy can effectively address the issue of quantification errors in analyte measurements resulting from matrix effects. Calibration standards are prepared by employing a sample solution that has a matrix composition similar to the sample being analyzed [284]. It is essential to carry out blank determinations on the matrix matching sample to verify the presence of the analyte, prior to performing spiking or making appropriate blank corrections. Locating a sample that is an exact match to the one being analyzed can provide challenges when employing the matrix matching strategy. Performing a comprehensive qualitative and quantitative evaluation of all sample components to get an exact match is neither feasible nor practical. However, a representative sample that closely mimics the composition of the real sample can be utilized to produce calibration standards, thereby mitigating the influence of matrix effects. To verify the accuracy of a blank analysis when investigating a contaminated portion of a large sample, one can obtain uncontaminated samples from clean parts. In order to obtain same outcomes when dealing with samples prepared with reagents, it is important to provide the sample reagents to the calibration standards in a consistent manner [285].

Other techniques that can be used to enhance the accuracy of quantitative measurements include isotope dilution mass spectrometry (IDMS) [215] [216] and internal standard [286], [287].

2.6 Method Validation

Analytical methods might vary significantly in terms of characteristics, methodology, scope, and applicability since there is no universality. Therefore, it is not attainable to provide a solitary set of directives that may be employed to authenticate all existing methods. There are some similarities that can be evaluated for their reliability in use and the acquired measurements. Thus, the results should be validated according to standard requirements to be considered as a reliable analytical method. In this case, some parameters are used in the validation of analytical methods including limit of detection (LOD), limit of quantification (LOQ), dynamic working range, robustness, accuracy, precision, selectivity, sensitivity and ruggedness [288]. Following the method validation, the majority of these parameters remain applicable for subsequent measurements; however, it is imperative to ascertain the precision and accuracy of various sets of measurement

data. Percent relative standard deviation (%RSD), is a measure of precision in measurement. The calculation involves dividing the standard deviation (SD) by the mean of repeated measurements. The %RSD provides a more relevant statement than the traditional SD when assessing the proximity of repeated measurements [289]. There are three specific methods to classify the degree of precision in repeated measurements, depending on the analytical method and laboratory conditions. "*Repeatability"* pertains to the level of precision attainable when a solitary analyst employs an identical instrument to do numerous measurements within a brief time-frame. "*Intermediate precision"* refers to the level of accuracy of measurements achieved under conditions that are comparable to repeatability, but in more varied circumstances. The term "*reproducibility*" refers to the level of precision achieved when numerous analysts in different laboratories carry out the same analysis [290].

The term "*trueness*" refers to how close a measured result is to its reference value. Precision and trueness are two separate metrics that, when combined, serve to verify the accuracy of the analytical technique. The *accuracy* of a method is confirmed by examining a certified or standard reference material (CRM/SRM) at the same time as the standards used to measure the components in a sample. The degree of accuracy of the approach is determined by how close the experimental findings are to the certified value. When a CRM or SRM is not readily available, one might establish calibration control standards by measuring the concentration of analytes in the initial sample that is evaluated after instrument calibration [282].

2.7 Treatment Strategies of Water Sources

Access to freshwater is a fundamental requirement for the survival of both humans and wildlife. The provision of drinkable water is vital for sustaining a healthy and well-being existence. Notwithstanding the annually escalation of global water demand, different types of contamination have undermined potable water reservoirs. Additionally, scientific studies have revealed that the adverse consequences of climate change, including the increased temperatures and alterations to the hydrological cycle, have the potential to intensify the aforementioned water-related predicaments. This may lead to amplified instances of flooding, heightened severity of droughts, and augmented toxicity of chemical pollutants in the environment [291]–[293]. The presence of pollutants in water

sources may cause a significant damage to human health. As a result of this contamination, exposure to pathogens or toxic chemicals can occur through several sources including irrigation of plants with contaminated water, consumption of toxins in aquatic organisms, or the use of contaminated surface water for recreational activities like swimming [294]. However, the consumption of contaminated water continues to be the primary cause of human health problems for the majority of individuals in developing nations.

In the developing world, heavy metal contamination has been on the significant rise due to the growing prevalence of urban and industrial activities. The discharge of contaminated wastewater from various industries, such as coal-fired power plants [295], mining [296], operations including electronic devices' waste disposal and waste recycling [297]–[299], represents a significant origin of pollution. In addition, emissions from vehicles and other urban activities have also contributed to the pollution [300], [301]. According to the United Nations, approximately 80% of municipal and industrial wastewater in underdeveloped countries is released into the environment without performing any form of pre-treatment [302]. Moreover, it should be noted that contamination in water can also be attributed to multitude of sources including rainwater transport into potential drinking water sources, polluted urban storm water runoff, agricultural runoff, and other sources [303]. The detrimental effects caused by the toxic and carcinogenic properties of heavy metals, have gained considerable apprehension among researchers [304], [305]. The issue of heavy metal pollution is a significant concern due to the inefficacy of various drinking water treatment methods employed in developing nations, such as chlorination, boiling, and solar disinfection, in eliminating heavy metals [306].

Several review papers have examined the distribution of heavy metals in drinking water sources in various regions in developing countries [307]–[310] and detrimental effects of heavy metal contamination that are associated with human health [311]–[313]. Furthermore, owing to the extensively recorded effects of heavy metals on human health, a substantial body of research has been undertaken to investigate techniques for eliminating heavy metals from potable water sources, as well as industrial and municipal wastewater, and other water sources. Heavy metal removal efficiencies that are particularly noteworthy have been discussed in a number of recent review publications. These methods are currently being explored

for implementation in several developed countries. The methods include carbon nanotechnology [314]–[316], modified adsorbents [317]–[319], electrocoagulation [320], [321], membrane filtration [322], and microbial remediation [323], [324]. Nevertheless, the implementation of these technologies may not be viable or economically efficient in the context of developing nations. In order to address water treatment in developing regions, it is imperative that the proposed technologies are easily accessible, can be constructed by individuals with limited education, and have minimal operating and maintenance expenses.

2.7.1 Chemical Based Removal Procedures

2.7.1.1 Precipitation

Chemical precipitation, also known as coagulation precipitation, is a widely utilized technique in various industries and is recognized as a highly efficient and well-established approach. The process involves the conversion of dissolved metal ions into solid particles, which aids in their sedimentation. The coagulant reagent is capable of precipitating metal ions through alterations in pH, electro-oxidizing potential, or co-precipitation [325]. Typically, the elimination of sediments ensues. Figure 2.13 illustrates a basic diagram of the chemical precipitation procedure [326].

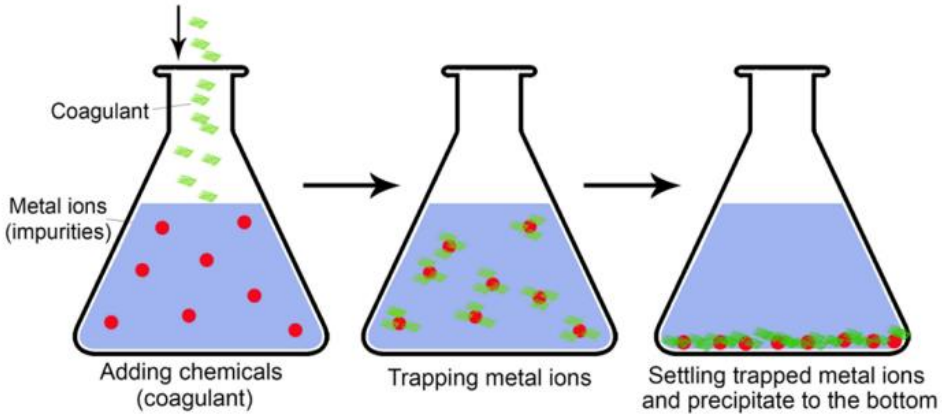


Figure 2.13 A simple schematic display of the chemical precipitation process [326]

2.7.1.2 Coagulation and Flocculation

The process of coagulation involves the disruption of colloidal stability by counteracting the intermolecular forces that maintain their dispersion, whereas

flocculation pertains to the clustering of destabilized particles [327]. Aluminum sulfate, and iron coagulants in their ferric form are commonly utilized as conventional coagulants for the purpose of ion charge neutralization by producing ferric hydroxide floc when exposed to bicarbonate acids [328]. Flocculation is a process that involves the use of a flocculant, such as polyaluminum chloride (PAC), polyferric sulfate (PFS), polyacrylamide (PAM), and other macromolecule flocculants, to bond particles together and form larger agglomerates [329]. The practicality of polyelectrolytes (PE) as a flocculation agent has been widely reported, however, it is worth noting that the resulting sludge may contain toxic elements [327]. Flocculants are typically synthetic and exhibit low biodegradability [330]. The procedure is depicted in Figure 2.14, encompassing the sedimentation process [326]. Several limitations have been identified in the use of coagulants. These include the potential for toxicity and health hazards associated with inorganic coagulants, the generation of a significant volume of sludge, selectivity for certain metals, inefficiency in removing emerging contaminants, increasing effluent color, inefficiency when using natural coagulants, and complexity in scaling up the process [331].

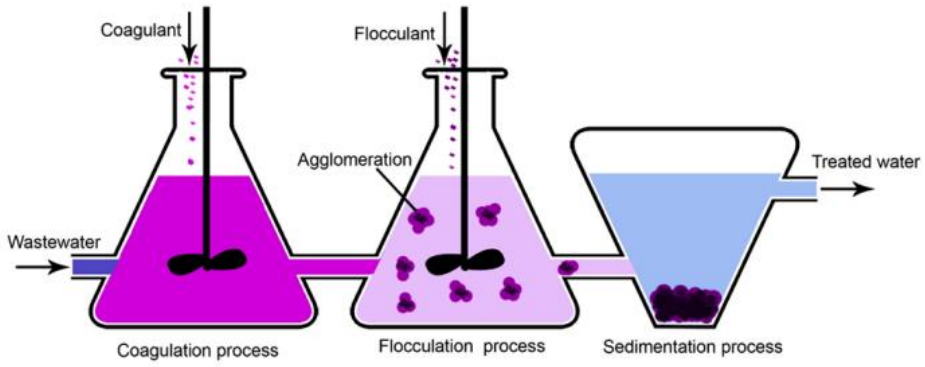


Figure 2.14 An illustrative depiction of the coagulation-flocculation treatment process [326]

2.7.2 Adsorption Based Removal Methods

The mechanism of adsorption is determined by the physicochemical characteristics of both the adsorbate and adsorbent, together with the conditions under which the process is carried out, including temperature, quantity of adsorbent used, pH level, duration of adsorption, and initial concentration of metal ions. In general, it has

been observed that heavy metal ions possess the ability to undergo adsorption onto the surface of adsorbents, as depicted in Figure 2.15. The aforementioned technique has been documented to possess economical operational expenses, substantial elimination efficacy, uncomplicated execution, and simple processing via the restoration of the adsorbed substance [332].

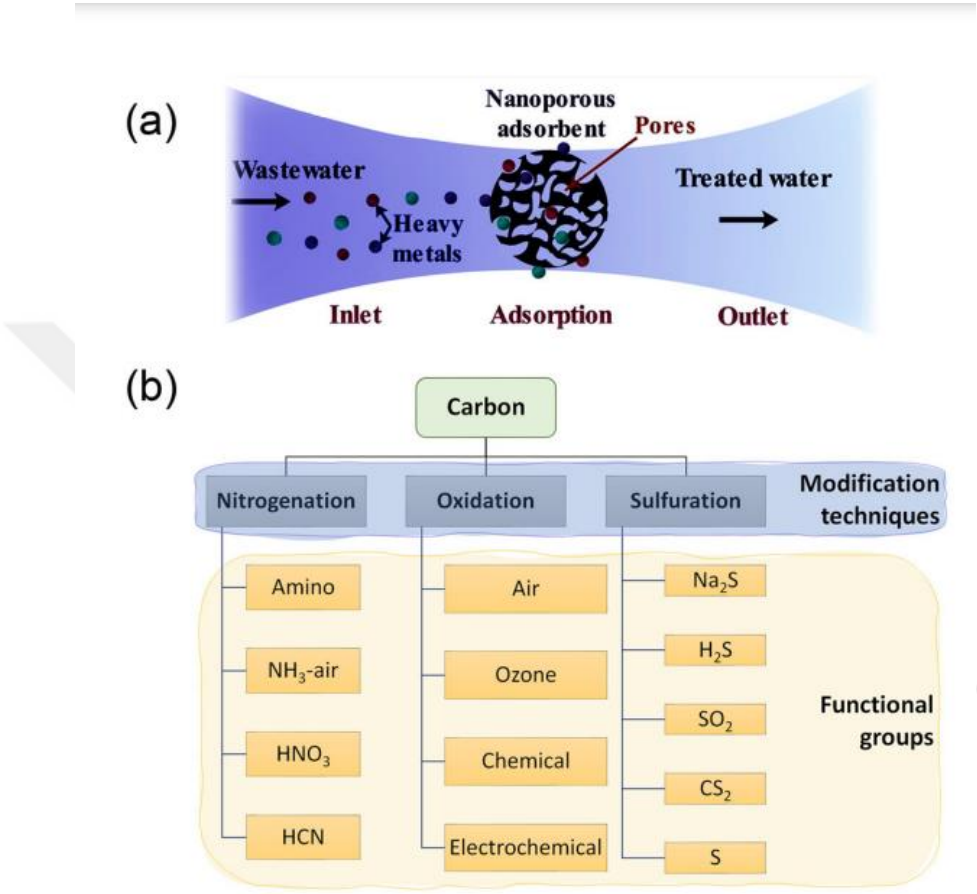


Figure 2.15 Adsorption process used for water treatment [326]

The process of adsorption of heavy metal ions involves the binding of these ions from wastewater onto the surface of nano-adsorbents, which have a large surface area as a result of their porosity. The adsorption process may demonstrate selectivity towards certain metals over others. Regeneration can be achieved by employing a suitable desorbing agent. Different modification processes, such as oxidation, nitrogenation, and sulfuration, can be applied to add various functional groups to nanoparticle atom. Functionalization increases the adsorption ability of the nanoparticles and retain molecules, as well as improves the overall stability.

Different adsorbent materials have been employed for the treatment of wastewater. The materials are often classified as either natural adsorbents obtained from natural

sources, or synthetic adsorbents, which are artificially manufactured [333]. Natural adsorbents include a range of substances such as zeolites, clays, clay minerals, charcoal, and ores [334]. The three main origins of intricate adsorbents include:

i) agricultural sources and by-products such as fruits and vegetables;

ii) agricultural wastes and residues;

iii) economical sources that can be utilized for the production of activated carbons via the pyrolysis of agricultural sources.

The "green adsorbents" are expected to exhibit lesser adsorption capacities in comparison to the highly adsorbent materials documented in literature, such as activated carbons, modified chitosan, and inorganic composite materials with intricate architectures. Nevertheless, their cost-effectiveness makes them a viable and competitive option [335]. Synthetic adsorbents encompass adsorbents sourced from diverse origins, such as agricultural products, waste materials from agriculture, sewage sludge, industrial waste, home trash, and polymeric materials. Adsorbents possess unique characteristics such as their pore structure, porosity, and the makeup of their adsorbing surface [334].

2.7.2.1 Nanoadsorbents

The exceptional sorption ability of nanoadsorbents can be attributed to their large surface area and sorption sites, adjustable pore size, decreased intraparticle-diffusion distance, and heightened surface activity. These characteristics makes them capable to efficiently adsorb a wide range of organic and other pollutants [336], [337]. Utilizing nanoadsorbents is beneficial because of their ability to easily undergo functionalization, which allows them to demonstrate strong selectivity towards different contaminants [338]. Adsorption has demonstrated a significant efficacy in removing persistent organic pollutants (POPs) such as phenols, hydrocarbons, insecticides, dyes, detergents, medicines, and biphenyls, during the remediation process. Nanoadsorbents are classified into different groups including metal-metal oxide nanoparticles, nanostructured mixed oxides, and magnetic nanoparticles, according to their specific functions in the process of adsorption. Additionally, carbonaceous nanomaterials (CNMs) have been produced in different shapes such as nanoparticles, nanosheets, and nanotubes. The efficiency of nanoadsorbents is dependent on various particular characteristics, such as surface

chemistry, crystal structure, average size, shape, chemical composition, aggregation state, fractal dimension, and solubility [339]. In general, nanomaterials have distinct properties that deviate significantly from their larger counterparts as a result of their smaller size. The properties of nanomaterials often undergo substantial changes to form nanoparticles with desired shape and size using nanotechnology [340]. Nanomaterials with many corners and sharp edges, including nanotubes, nanowires, and nanorods, demonstrate improved electrocatalytic capabilities [341]. Nanomaterials are generally acknowledged due to their distinctive electrical, optical mechanical, chemical and thermal properties, which play a critical role in the field of biomedical applications [342]. Surface atoms generally exhibit greater reactivity than the atoms placed in the central areas, and they have an important role in phenomena such as increased catalytic current. Conversely, a larger surface area shows a greater quantity of atoms that might potentially interact, thereby elevating the sensitivity [343]. The special morphological properties of a surface is essential for accurately identifying targeted substances [341].

Carbon-based Nanoadsorbents

The unique properties of carbonaceous nanomaterials based on the sp^2 hybridization of carbon bonds, results in remarkable mechanical, chemical and electrical capabilities at the nanoscale [344]. The atomic structures and intermolecular forces of carbon-based nanomaterials have substantially influence on their characteristics [345]. Carbon-based nanomaterials have outstanding features in the areas of electricity, mechanics, optics, and the surface area to volume ratio compared to conventional nanomaterials [346]. As a result, carbon-based nanomaterials have gained considerable attention by scientists and the industrial community because of their unique characteristics that show potential for a wide range of advanced applications in fields such as wastewater treatment, electronics, tissue engineering, heterogeneous catalysis, membranes, batteries, capacitors, cancer therapy, drug delivery, imaging, and bio-sensing [346], [347]. There are different allotropes with varied dimensions, such as fullerenes (0-D), carbon nanotubes (1-D), and graphene nanomaterials (2-D). Graphene is a carbon-based material that consists of a single layer of carbon atoms arranged in a honeycomb crystal lattice, with the carbon atoms bonded together in sp^2 configuration. It

functions as an essential precursor for the production of several other carbon allotropes. As an example, rolled graphene results in the formation of carbon nanotubes (CNTs), whereas twisted graphene leads to the formation of fullerenes. Fullerenes, also known as molecular carbon, have three-dimensional structures made up of a single-atom-thick sheet of graphite that is twisted into pentagonal and hexagonal shapes. Carbon nanotubes are seamless cylindrical structures with a diameter ranging from 1 to 100 nms [346].

Metallic Nanoadsorbents

Most metal nanoadsorbents that are defined in the literature consist mainly of iron oxide, cobalt oxide and nickel oxide based nanomaterials, commonly known as magnetic nanoparticles (MNPs) due to their high magnetic properties [348], [349]. The magnetic properties of these nanoparticles allow them to be easily separated from water media by applying an external magnetic field [350]. However, partitioning small-sized magnetic nanoparticles have some limitations, which requires the use of stronger external magnetic fields. This contributes to the overall cost of the treatment and disposal process [351]. Recently, there is a considerable attention in the employment of MNPs, such as magnetite (Fe_3O_4), maghemite (γ-Fe_2O_3), ferrite colloids, and hematite (α-Fe_2O_3), for the purpose of water treatment [352]. In applications of biology and the biomedical industry, Fe_3O_4 and γ- Fe_2O_3 possess unique nanoscale properties that make them well-suited and very efficient for these application areas [349]. Nevertheless, bare magnetite nanoparticles are vulnerable to oxidation and corrosion especially in acidic media. In addition, they have the propensity to become agglomerated as a consequence of magnetic forces. This agglomeration leads to a reduction in magnetic intensity and adsorption capability of the MNPs. Therefore, it is crucial to ensure surface protection for magnetic nanoparticles to prevent their aggregation. Hence, the stability of MNPs are improved by widely using polymeric/oxide compounds (particularly biocompatible polymers) and surfactants [353]. In addition, organic compounds are also used in the modification of MNP surfaces for a wide range of applications [354].

Polymeric Nanoadsorbents

Polymeric adsorbents provide a porous structure that enhances their effectiveness in adsorbing acids, alcohols, phenols, ketones, aldehydes, and furans from aqueous solutions, which can be achieved by Van der Waals intermolecular interactions [355]. Polymer-based materials are mostly composed of organic compounds and are known for having specific surface area with microporous structures [356]. These types of materials consist of membranes, ion exchange resins, molecularly imprinted polymers (MIPs), covalent organic polymers (COPs), and microporous organic polymers (MOPs). These adsorbents are exceedingly valuable due to their efficacy and the possibility of multitude combinations of polymers with clay, metal, ceramic, or another polymer [357]. These nanoadsorbents have gained the attention of researchers in several environmental contexts. Nevertheless, the existing information on these adsorbents are deficient in the necessary level of reliability and precision. Especially, polymers like polypyrrole (PPy), polyaniline, and their mixtures have favourable electrical conductivity and have garnered significant interest as promising adsorbents [358]. In order to achieve some desired properties such low toxicity, water and colloidal solution stability, and biocompatibility, surface modification of magnetic nanoparticles (MNPs) using various coatings and biological molecules is widely used in biomedical applications [359]. For this aim, small organic molecules such as monocarboxylic fatty acids and both artificial and natural polymers are predominantly utilized [360]–[362].

2.7.3 Equilibrium Isotherm Models

Adsorption isotherms are commonly used to evaluate changes in adsorption capacity as a function of equilibrium concentration from the curves obtained. Pore size distribution and volume, surface area, and adsorption performance of adsorbents can be calculated by employing these isotherms [363]. For this purpose, different isotherm models have been introduced, among them some isotherm models have garnered greater attention due to their wide application area and simplicity in use. The number of independent variables incorporated in the model determine the accuracy of the isotherm model, while its prevalence in application of the process is generally determined by the model's mathematical simplicity [364]. In simple terms, the more complex the adsorption isotherms become, the lesser they are utilized [365]. The isotherms currently used in the literature for

adsorption assessments are Langmuir [366]–[370], Freundlich [26], [368], [369], combined Langmuir-Freundlich [371]–[373], Temkin [370], [374], and BET (Brunauer-Emmett-Teller) [375]–[377] equation models.

2.8 Nanotechnology

Richard Philips Feynman's lecture in 1959 titled "There's Plenty of Room at the Bottom," is considered one of the most noteworthy scientific presentations of the twentieth century. Feynman envisioned a technology that could manipulate and govern objects at a microscopic scale, allowing for the production of nano-sized structures. After 15 years, the term "nanotechnology" was introduced in 1974 by Norio Taniguchi at Tokyo Science University. It encompasses the manipulation and modification of materials at the nanoscale with practical applications. Some application areas of the nanotechnology is depicted in Figure 2.16 [378].

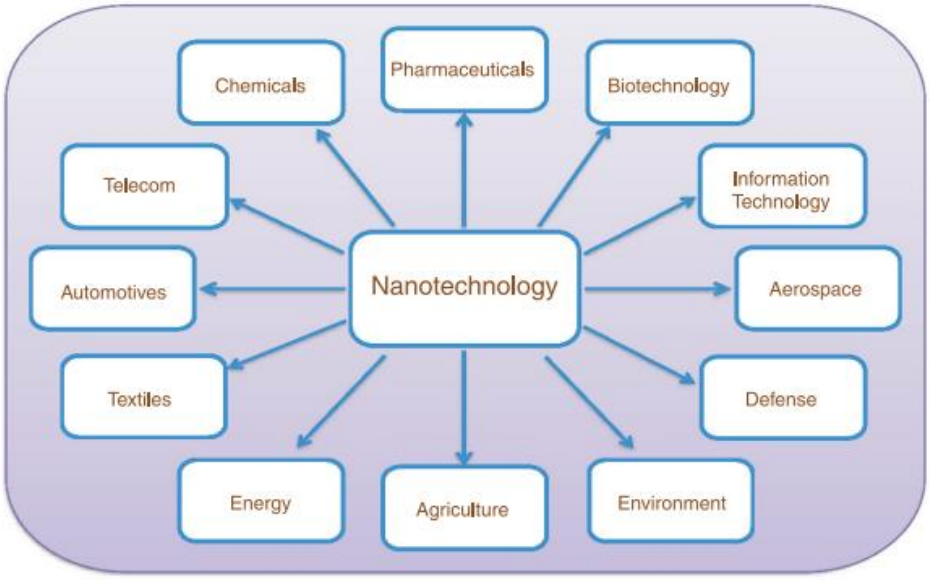


Figure 2.16 Implementation fields of nanotechnology [378]

The field of nanotechnology continues to improve and its influence is being observed across various scientific areas, including animal biotechnology and life sciences. Unavoidably, the field's expansion will continue in the utilization of this technology in the fields of animal nutrition, health, illness diagnostics, and medicine delivery. It enables the manipulation and observation of atomic and molecular structures on a scale between 1 and 100 nm. This makes it possible for

the creation, understanding, and utilization of new materials and technologies with unique characteristics and functions due to their very small size [379].

Noble metal nanoparticles have gained considerable use in the biomedical applications facilitated by advancements in nanotechnology. The noble metal nanoparticles have a size distribution that spans at least one dimension within the range of 100 nm. The extensive utilization of noble metal nanoparticles in biomedicine is attributed to their substantial specific surface area, exceptional biological characteristics, convenient synthesis, remarkable effectiveness, and minimal toxicity [380]. A great deal of study is currently being carried out on the possible implementations of noble metal nanoparticles in numerous fields, such as targeted drug delivery in living organisms, photodynamic therapy for cancerous tumours, cure of skin diseases, biocidal disinfection, auxiliary materials for tissue imaging, catalysis, and other areas. The exceptional sensitivity of noble metal nanoparticles' optical spectra to even the slightest alterations in the electrodynamic characteristics of their surrounding medium enables the development of biological and chemical sensors designed upon them [381]. The techniques and systems in utilizing noble metal nanoparticles for biomedical applications are shown in Figure 2.17 [380].

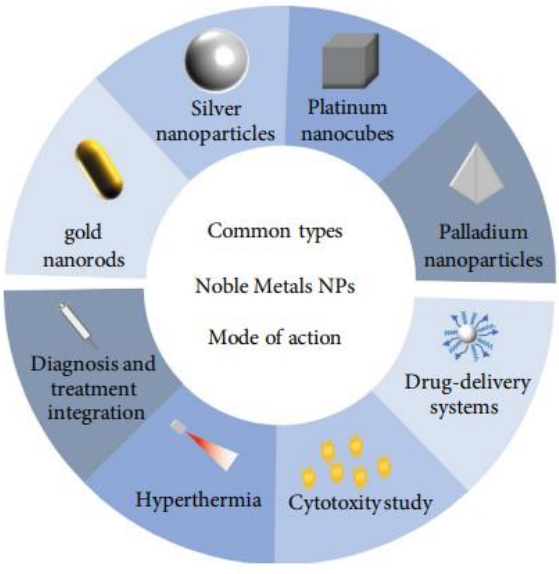


Figure 2.17 Noble metal nanoparticles and some of their usage areas [380]

Among the noble metal nanoparticles, gold nanoparticles (GNPs) have been consistently published as effective catalysts for many applications. The GNPs have

garnered considerable attention due to their diverse and distinguishing functional properties, as well as their simple synthesis process. The inherent optical, electronic, and physicochemical properties of GNPs can be modified by altering their characters, including form, size, and aspect ratio for biological applications. These applications include medication and gene administration, photo-thermal therapy (PTT), photodynamic therapy (PDT), radiation therapy (RT), diagnostics, X-ray imaging and computed tomography (CT) [27].

2.8.1 Synthesis of Gold Nanoparticles

Gold nanoparticles have been fabricated using a wide array of methods and pathways to achieve different sizes, shapes and surface functionality [382]. The synthesis procedures are typically categorized into two approaches. The top-down approach is based on the decomposition of bulk metals into smaller particles, resulting in the assembly of the desired nanostructure. The second approach, the bottom-up approach includes the assembly of individual atoms or molecules to form bigger nanostructures, resulting in the production of materials at the nanoscale [383]. The synthesis of these compounds has been carried out with physical, chemical, and biological techniques. Every fabrication technique possesses its unique benefits and drawbacks.

In physical methods, synthesis procedure was conducted through the process of evaporation-condensation using a tube furnace under atmospheric pressure [384]. Conventional physical methods such as arc discharge and pyrolysis have also been used in the synthesis procedures [385], [386]. The benefits of physical procedures include utilization of radiation as reducing agents [387], rapidity [388], and absence of hazardous chemicals [389]. However, the methods have some drawbacks such as low productivity, contamination by solvents, substantial energy consumption, and inadequate uniformity of distribution [390].

The prevailing technique used in the production of GNPs is the chemical approach. Generally, a metal precursor, a reducing agent, and/or stabilizing/capping agents are used in the synthesis procedures [383]. The chemical synthesis approaches are based on the reduction the concentration of metal ions in solution under conditions that enable the subsequent production of small metal clusters or aggregates [390].

Gold exists in three oxidation states: aurous (Au^{1+}), auric (Au^{3+}), and its un-oxidized state (Au°). The ultimate state of desire for nanoparticles is accepted as Au°. Thus, reducing Au^{1+}, or Au^{3+}, to Au° by adding an electron donor (reducing agent) is the primary step in the synthesis of GNPs. The precursor favored by the majority in the literature sources is chloroauric acid ($HAuCl_4$) in which gold is oxidized to Au^{3+} [391]. A multitude of chemicals are used as reductants in the synthesis procedure and the common ones can be listed as sodium borohydride ($NaBH_4$), sodium citrate ($Na_3C_6H_5O_7$), and hydrazine (N_2H_4). Moreover, to prevent agglomeration, stabilizing agents including surfactants, chitosan, phosphorus ligands, trisodium citrate dihydrate ($C_6H_9Na_3O_9$), cetyltrimethylammonium bromide (CTAB), and other polymers are incorporate onto the surface of the GNPs [383]. Among the numerous synthesis procedures, the Turkevich method, in which colloids in the range of 15–20 nm in diameter are formed by reducing $[AuCl_4]^-$ in heated aqueous solution using sodium citrate as reductant [392]. Although, the method had restricted applications due to the narrow spectrum of GNPs that could be produced using this technique, multiple advancements in the fundamental procedure have empowered scientists to expand the particle size range [393]. The other common methods are seeding growth method [394], electrochemical method [395], Brust-Schiffrin method [396], and digestive ripening method [397].

While chemical methods remain the predominant approach for producing metallic nanoparticles, their practical uses are constrained by the demand of expensive and harmful reagents to function as reducing and stabilizing/capping agents. Additionally, their detrimental effects reduce the use of produced nanoparticles in biomedical applications [398]. As a result, the need to develop environmentally sustainable and economically viable methods of nanoparticles synthesis, which are devoid of the use of hazardous chemicals has increased. In the last decades, biological synthesis of nanoparticles has received considerable interest as an environmentally benign and green method. GNPs are synthesized through biological processes that rely on different enzymes, microorganisms (bacteria, fungi, algae, etc.), and plants or plant extracts [399]. General aspects of both chemical and biological synthesis procedures are compared in Table 2.5 in terms of advantages and disadvantages [400].

Table 2.5 Comparison of synthesis methods by their advantages and disadvantages to each other [400]

Synthesis Type	Advantages	Disadvantages
Chemical Synthesis	- Require low energy in the reduction step; - High controlled size, shape and crystallinity with homogenous nanoparticle formation; - Use of stabilizing agents that have low complexity	- Toxic solvents and chemical reductant use; - Hazardous chemicals and residuals use or generation; - Expensive precursors; - Low stability and biocompatibility and high toxically properties for the use of biomedical applications;
Biological Synthesis	- Low by-products and waste generation; - Reduced consumption of poteantially hazardous solvents and reagents; - Energy consumption at low levels; - Ambient temperature and pressure requirement for carrying out the reduction reaction; - Sustainable raw and natural resources employment; -Costly-effective synthesis procedure	- Use of stabilizing agents that have high complexity (biomolecules); - Difficulties in purifaction porcess

Algaes (photosynthetic prokaryotes and/or eukaryotes) have great capability to remove contaminants from the environment and carry out harmless reactions in biotransformation processes [401]. They also possess an outstanding capacity to produce a diverse array of natural and organic products, including saponins, carbohydrates, steroids, proteins, alkaloids, phenols, and flavonoids which notably contribute to the reduction of metallic ions and facilitate their conversion into nanoparticles [402]. In GNP syntheses, macro (multicellular) algae including *Acanthophora spicifera* [403], *Kappaphycus alvarezii* [404], *Sargassum wightii* [405], *Sargassum myriocystum* [406], *Stoechospermum marginatum* [407], and *Laminaria japonica* [408] have been utilized.

Padina pavonica is an abundant macro-algae found in intertidal zones along coastlines globally. It is one of the two brown algae types currently recognized by scientists. $CaCO_3$ is precipitated in the form of needle-shaped aragonite, that has vertical ventral stripe shapes observed. Extensive researches have been carried out on *P. pavonica,* due to its importance for environment and medical applications. It is widely used in different areas as an antioxidant, an antibacterial agent, a feedstock in heavy-metal biosorption, a trace metal biomonitor, a bioindicator for pollution, an anticancer drug (by inducing apoptosis of cancer cells) and a bioinsecticide [409]. In a research conducted in methanolic extract of *P. Pavonica,* the total phenolic, proanthocyanidin and flavonoid contents were recorded as about of 2.007 ± 0.104 mg GAE/g DM (milligrams of gallic acid equivalents per gram of dry sample), 4.611 ± 0.346 mg CE/g DM (milligrams of catechin equivalents per gram of dry sample), and 1.132 ± 0.091 mg CE/g DM, respectively [410]. In another study, the extract was obtained by using different solvents (methanol, ethanol and water) and total phenolic compounds (TPC) and total flavonoid compounds (TFC) were determined. The results varied from 11.8 to 76.8 µg GAEs/mg extract and 6.8 to 29.5 µg Quercetin/mg extract for TPC and TFC, respectively [411]. In this case, *P. pavonica* can be considered as a suitable reducing and stabilizing agent to rapidly produce extracellular gold nanoparticles that are exceptionally stable, surpassing the time required for other biological processes [412].

3
MATERIALS AND METHODS

3.1 Chemicals and Reagents

All chemicals and reagents used throughout the study were ensured to be of analytical quality purity. All chemicals were obtained from Merck (Darmstadt, Germany) unless otherwise stated. Details about the pesticides and endocrine disruptors for which qualitative and quantitative determinations were made in the study are given in Table 3.1. Each analyte was supplied as solid standards, from which individual stock standard solutions separetely prepared in acetonitrile (98-101%, Merck). Mixed standard solutions of the analytes at desired concentrations were prepared using these stock solutions. All standard solution used throughout the study were prepared gravimetrically using an analytical balance. The prepared stock and mixed stock solutions were stored in a refrigerator at -22 °C, away from moisture and sunlight. All standard and sample solutions used in the study were prepared by diluting the prepared mix stock solution with deionized water (conductivity, 18.2 MΩ cm^{-1}) obtained from an ELGA Pureflex III (London, United Kingdom) ultrapure water purification system. In the extraction procedure, 1,2-dichloroethane and dichloromethane were used as binary extraction solvents. The borate-HCl buffer solution used to adjust standard/sample solution at optimum pH was prepared with 0.025M disodium tetraborate decahydrate, which was in turn adjusted to 9.0 with 0.10 M HCl solution (37%). In the study, 99.995% pure helium (He) gas used as a carrier gas in the GC-MS system was obtained from a gas supplying company in İstanbul.

Table 3.1 Pesticides and endocrine disruptors that were qualitatively and quantitatively determined in the study

CAS Number	Analyte	Vendor
309-00-2	Aldrin	Sigma-Aldrich
80-05-7	Bisphenol A	Sigma-Aldrich
319-84-6	alfa-BHC	Dr. Ehrenstorfer
319-85-7	beta-BHC	Dr. Ehrenstorfer
319-86-8	delta-BHC	Dr. Ehrenstorfer
72-54-8	4,4-DDD	Dr. Ehrenstorfer
72-55-9	4, 4-DDE	Dr. Ehrenstorfer
50-20-3	4, 4-DDT	Dr. Ehrenstorfer
333-41-5	Diazinon	Sigma-Aldrich
60-57-1	Dieldrin	Sigma-Aldrich
33286-22-5	Diltiazem HCL	Sigma-Aldrich
959-98-8	α – Endosulfan	Sigma-Aldrich
33213-65-9	β – Endosulfan	Sigma-Aldrich
1031-07-8	Endosulfan Sulphate	Dr. Ehrenstorfer
72-20-8	Endrin	Dr. Ehrenstorfer
53494-70-5	Endrin keton	Dr. Ehrenstorfer
50-28-2	ß-Estradiol	Sigma-Aldrich
53-16-7	Estrone	Sigma-Aldrich
57-63-6	17α-Ethyleneestradiol	Sigma-Aldrich
1222-05-5	1,3,4,6,7,8-Hekzahydro-4,6,6,7,8,8-hexane (Galaxolide)	Sigma-Aldrich
76-44-8	Heptachlor	Sigma-Aldrich
298-46-4	Carbamazepine	Sigma-Aldrich
5103-71-9	cis-chlordan	Sigma-Aldrich
58-89-9	Lindane	Dr. Ehrenstorfer
121-75-5	Malathion	Sigma-Aldrich
72-43-5	Metoxychlor	Dr. Ehrenstorfer
104-40-5	4-n-Nonylphenol	Sigma-Aldrich
76738-62-0	Paclobutrazol	Sigma-Aldrich
298-00-0	Parathion Methyl	Sigma-Aldrich
4640-01-1	Triclosan methyl	Sigma-Aldrich
68694-11-1	Triflumizole	Sigma-Aldrich

In the removal study, 1000 mg kg^{-1} aqueous stock solution was prepared by dissolving solid $CdSO_4.8/3H_2O$ with deionized water produced from the ELGA PureFlex III ultrapure water purification system. Further dilutions throughout the study was performed by using this stock solution. The magnetic $CuFe_2O_4$ nanoparticles were synthesized using $CuSO_4.5H_20$ and $FeSO_4.7H_20$. Sodium hydroxide was employed for pH modulation in both the synthesis protocol and the formulation of borate-hydrochloric acid (HCl) buffer with a pH of 9.0.

In the synthesis procedure of gold nanoparticles, $HAuCl_4.2H_2O$ stock solution (30%wt) in HCl (Sigma-Aldrich) was utilized as the Au ion source. The stock solution was diluted with deionized water befor the synthesis procedure.

3.2 Instruments

The separation, qualitative and quantitative determinations of organic analytes were made with a Hewlett Packard HP 6890 series gas chromatograph with a Hewlett Packard 5973 model mass selective detector. Samples were sent to the chromatographic system through the HP 6890 model autosampler. OHAUS Pioneer PA214C model analytical balance was used in the gravimetric preparation of calibration and sample standards.

Identification and quantification of the analytes were performed on the Hewlett Packard HP 6890 model gas chromatography mass spectrometry (GC-MS) system. Chromatographic separation was performed on HP-5MS (Agilent, USA) capillary column (30 m x 0.32 mm I.D., 0.25 μm film thickness). Helium gas of 99.995% purity was used as the carrier gas at a constant flow rate of 0.8 mL min^{-1}. Qualitative and quantitative determinations of the analytes were performed with a Hewlett Packard 5973 model mass spectrometer (MS). The ionization energy of the MS detector was 70 eV, the quadrupole temperature was 150 °C, and the ion source temperature was 230 °C. An SGE Analytical Scince (Melbourne, Australia) microinjector with a total volume of 10 μL was used for injection. The volume of sample/standard solution injected into the system was determined as 2.0 μL, and the injection was applied in splitless mode. The injection site and mass transfer path temperatures were set as 250 °C and 290 °C, respectively. A deactivated inlet liner was installed in the sample introduction port. This liner has an inner diameter of 4.0 mm and an exterior diameter of 6.47 mm. The apparatus features a solitary conical structure that incorporates glass wool at the intersection with the analytical column. The entire volume is 900 μL, and the length is 78.5 mm. The flow rate for the purge was adjusted to 60 mL/min, and the purge duration was set at 1.0 minute.

Cadmium was detected and quantified with a SolAAR 929 model flame-type atomic absorption spectrophotometer manufactured by ATI UNICAM (United Kingdom), with deuterium (D_2) lamp for background correction provided by Varian (United States). A light source in the form of a hollow cathode lamp (HCL)

was utilized at a wavelength of 228.8 nm. The cadmium HCL (Varian, USA) was operated at a working current of 15 mA, while the spectral band pass was set to 0.50 nm. Stoichiometric proportion of acetylene and air was used to generate the flame. Additionally, the other devices utilized in all experimental procedures are listed in Table 3.2.

Table 3.2 Laboratory devices used in the study

Laboratory devices	**Brand/Model**
Analytical Balance	Ohaus Pioneer PA214C
Centrifuge	BIOBASE BKC-TL5II
pH meter	Mettler Toledo – S210
Automatic Pipette	Eppendorf
Automatic Pipette	Brand
Oven	Heraeus D-6450
Mechanical shaker	Kermanlar
Ultrasonic bath	HAPA M-100
Vortex	Isolab

The UV-Vis absorption spectra of prepared GNP solutions were measured using a Shimadzu UV-2600 model UV-Vis spectrophotometer (Shimadzu corperation, Japan) at room temperature. The measurements were taken in 1.0 cm optical path quartz cuvettes. Zeta potential values of the GNPs were determined with Malvern Zetasizer Nano ZS (Malvern Instruments Ltd.,UK). BMG LABTECH SPECTROstar® Nano device (BMG LABTECH, Germany) was employed as a microplate reader in MTT studies.

3.3 Simultaneous Determination of Endocrine Disruptor Compounds and Pesticides in GC-MS System

3.3.1 Spraying Apparatus

Within the scope of the study, in order to carry out the extraction process with a more efficient and environmentally friendly approach, the distribution of the extraction solvent mixture into the aqueous solution as small droplets was provided with a spray apparatus. This apparatus was designed using a 20 mL inner volume container of a commercially available nasal spray product in Türkiye. A hole was made at the midpoint of the test tube's cap to fit the diameter (approximately 2.0 mm) of the spray apparatus' nozzle. The pierced test tube cap was placed on the tip of the spray apparatus. The extraction solvent mixture was filled into the 20 mL spray apparatus tank, and spraying was done with PTFE tubing with a length of 2.5 cm and a diameter of 3.0 mm. The illustration of the designed apparatus is given in Figure 3.1 [413].

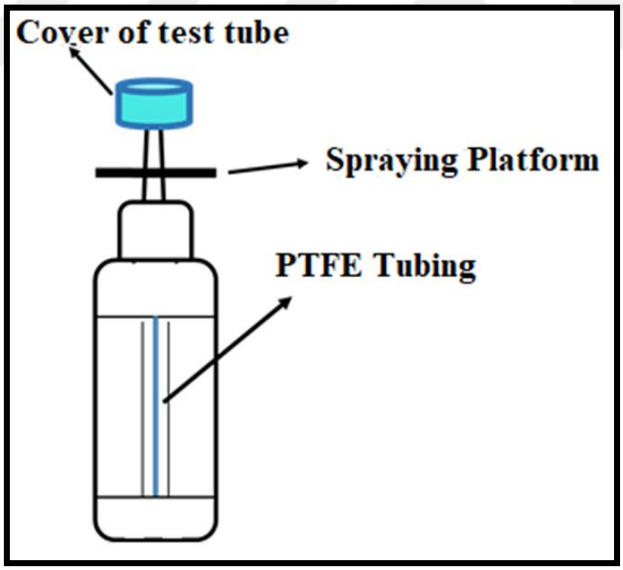


Figure 3.1 Spray apparatus used to create droplets in the study

3.3.2 Spray Assisted Droplet Formation based Liquid Phase Microextraction Procedure

In the developed method, 5.0 mL of aqueous sample or standard solution was taken into a clean 15 mL polypropylene test tube. After adding 0.50 mL of 50 mM borate-HCl buffer solution (pH 9.0) to the sample solution, the mixture was vortexed for 5.0 s to ensure effective distribution of the buffer solution into the aqueous solution.

Then, the extraction solvent mixture containing 1,2-dichloroethane and dichloromethane in a ratio of 1:1 by volume was dispersed into the aqueous solution by spraying twice with the spraying apparatus described in the section above. The solution was mixed with the help of vortex for 15 s in order to further enhance the interaction of the extraction solvent with the analytes. The resulting cloudy solution was stirred for 2.0 min by centrifugation at 3460 *g* for rapid phase separation. As a result, the analyte-rich organic phase was collected at the conical bottom of the test tube. The clear aqueous phase remaining on the top was carefully removed with a pipette. The organic phase collected into a 200 µL inner vial, which was in turn placed in a 1.5 mL glass vial. The vial was tightly closed with a plastic vial cap with a PTFE septum, and the sample was stored in a refrigerator at -16.0 °C until analysis.

3.3.3 Preparation of Real Sample Used in Spiked Recovery Experiments

3.3.3.1 Seawater Samples

Two different seawater samples were randomly selected from seawater samples collected from around Horseshoe Island of the Antarctic Continent and used in recovery experiments. Before using the seawater samples, they were stored at +4.0 ± 0.8 °C in completely closed polypropylene containers away from sunlight. After applying the appropriate dilution process to the water samples, they were spiked with mixed standards of the analytes at determined concentrations.

3.3.3.2 Soil Samples

Two soil samples were collected from different parts of Turkey. Initially, 20-25 g the soil samples were weighed and taken to the oven, where they were kept at 55-60 °C for two days to remove water and moisture. The dried soil was ground using a blender, then passed through a sieve with a pore diameter of 100 µm. Then, 5.0 g of the prepared soil samples were weighed into a clean polypropylene test tube before adding 25 g of acetonitrile. In order to ensure the distribution of acetonitrile in the soil sample, the sample was mixed with vortex for 1.0 minutes, then mixed on a mechanical shaker for 45 minutes and to ensure sufficient extraction of the analytes from the soil sample into the solvent. A final mixing procedure was performed in an ultrasonic bath (at a frequency of 45 mHz) for 10 minutes. Afterwards, the sample solution was centrifuged at 3000 rpm for 2.0 min and soil

particles were collected at the bottom of the test tube. In the last step, the sample solution was filtered with a filter paper of 11 μm pore size. The obtained liquid soil sample extract was stored in closed polypropylene test tubes in a refrigerator at -20 °C before standard additions.

3.3.3.3 Moss Samples

Since moss samples from the Antarctic Continent's Horseshoe Island and Farue Island surroundings are scarce and must be kept for use in real sample analysis, moss samples were collected from different districts of İstanbul, Türkiye, for recycling studies. After collecting the moss samples, they were washed thoroughly with tap water to remove unwanted matter. Then, the same process was carried out with ultrapure water. The washed moss samples were kept in an oven at 55-60 °C for two days to remove water/moisture. The dried moss samples were ground into powder in a mortar. Then, 40 g of acetonitrile was added to 8.0 g of moss sample and the extraction process applied to the soil samples was applied. The moss samples were also stored in sealed polypropylene test tubes at -20 °C in a refrigerator until sample analysis was performed.

3.3.4 Preparation of Real Samples Collected from Antarctic Region

Different environmental samples obtained from the Horseshoe (67° 51′ G 67° 12′ B) and Faure (68° 06' S, 68° 52' W) Islands during the 4th National Antarctic Science Expedition of Türkiye in February 2020 (TÜBİTAK Project Number: 119Z846) were analyzed in this study. Rock and soil samples (n=92), ocean water samples (n=42), lake water samples (n=12) moss and seaweed samples (n=43) and feces samples (n=14) were collected from the two islands within the scope of the expedition. The rock, soil, moss, seaweed and feces samples were weighed and dried in an oven at 50-55 °C. The dried samples were weighed again to determine water ingredient (water loss) of the samples. Then, the rock and soil samples (5.0 g) and moss, seaweed and feces samples (1.0 g) were weighed and extracted with 25 mL of ACN. Mixing process was applied with mechanical shaker for 45 min and ultrasonication for 15 min in order to achieve complete extraction of the analytes [414]. Finally, the aqueous sample solutions were prepared following the same procedure briefly described given in *Section 3.3.3 Preparation of Real Sample Used in Spiked Recovery Experiments* prior to instrumental analysis.

3.4 Magnetic $CuFe_2O_4$ Nanoparticle Assisted Batch Type Adsorption Based Removal Strategy

3.4.1 Magnetic $CuFe_2O_4$ Nanoparticle Synthesis Procedure

The study utilized nanoparticles as an adsorbent, which were synthesized through a precipitation-based method. The synthesis method employed entailed the weighing and dissolution of 0.0050 mol $CuSO_4.5H_2O$ and 0.010 mol $FeSO_4.7H_2O$ in 15 mL of deionized water, facilitated by ultrasonication. Subsequently, the pH of the solution was adjusted to a range of 10.00 -10.35 with 5.0 M NaOH solution. The formation of dark-brown precipitates was promptly observed upon the commencement of NaOH addition. Following the pH adjustment, the final volume of the solution was brought to 20 mL by adding deionized water. Subsequently, the mixture was subjected to ultrasonic treatment for a duration of 15 minutes at room temperature, followed by mechanical agitation for 30 minutes using a shaker. Finally, the precipitates were isolated using an Nb magnet. Subsequently, the $CuFe_2O_4$ nanoparticles were meticulously cleansed with deionized water and technical grade ethanol sequentially to eliminate any potential impurities. The drying procedure was employed in an oven at 55 - 60 °C to evaporate all solvents and remove moisture from the nanoparticles before use.

3.4.2 Magnetic $CuFe_2O_4$ Nanoparticle Assisted Batch Type Adsorption Based Removal Procedure

In the experimental procedure of the developed method, a volume of 40 mL of an aqueous solution containing Cd ions was carefully transferred into a sterile 50 mL polypropylene centrifuge tube. The pH of the sample solution was modified to pH 9.0 by utilizing 2.0 mL of 0.50 M borate buffer solution. In addition, a quantity of 100 mg of $CuFe_2O_4$ was expeditiously introduced into the solution of interest. The $CuFe_2O_4$ nanoparticles were dispersed with the aid of a vortex mixer for a duration of 60 s. The samples underwent centrifugation for a duration of 2.0 minutes at a rate of 3000 rpm, resulting in the collection of all $CuFe_2O_4$ nanoparticles at the base of the centrifuge tube. The effluent (4.0 mL of the supernatant) was transferred to another clean test tube. Subsequently, absorbance measurement was conducted

using flame atomic absorption spectrometry to assess the efficacy of the removal process.

3.4.3 Preparation of Synthetic Wastewater Samples

The synthetic wastewater utilized throughout the experiment was prepared with the chemicals given below in the Table 3.3 [415]. All the chemicals are acquired from Sigma-Aldrich Chemie GmbH (Germany).

Table 3.3 The chemicals and their concentrations contains in synthetic wastewater samples [415]

Chemicals	Concentrations
Glucose	400 mg L^{-1}
Yeast Extract	14 mg L^{-1}
Bactopeptone	115 mg L^{-1}
$(NH_4)_2SO_4$	104.8 mg L^{-1}
KH_2PO_4	21.75 mg L^{-1}
$MgSO_4$	15.63 mg L^{-1}
$FeCl_3$	0.075 mg L^{-1}
$CaCl_2$	2.45 mg L^{-1}
$MnSO_4$	1.8 mg L^{-1}
$NaHCO_3$	255.5 mg L^{-1}

All characteristic of the synthetic wastewater used was summarized in Table 3.4 [415].

Table 3.4 Synthetic wastewater characterization [415]

Parameter	Mean Value
pH	7.34
Conductivity, µS (20 °C)	807.38
Chemical Oxygen Demand (COD), mg L^{-1}	461.46
NH_4-N, mg L^{-1}	24.29
Total Kheljdal Nitrogen (TKN), mg L^{-1}	36.71
O_4-P, mg L^{-1}	3.94
Alkalinity, mg $CaCO_3$ L^{-1}	194.31
COD/TKN	12.57

3.4.4 Evaluation of Removal Efficiency of the Magnetic $CuFe_2O_4$ Nanoparticle Assisted Batch Type Adsorption Based Removal Strategy

The percent removal efficiency (%RE) of the batch adsorption process was calculated via Equation 3.1, where A_e and A_i represent the equilibrium and initial adsorption levels, respectively. In all the optimization experiments, A_e and A_i values were denoted by the peak areas of each adsorbate. In the equilibrium studies under the optimum conditions, these values were denoted by the initial spike concentrations and equilibrium concentrations calculated via the calibration plots of peak areas vs. concentrations for A_i and A_e, respectively. The q_e value, which denotes the equilibrium adsorption capacity (mass of adsorbates collected by the adsorbent) (mg/g) is calculated via Equation 3.2 and in this equation, C_i and C_e represent the initial and equilibrium (residual) adsorbate concentrations in the aqueous samples (mg/L), while m and V represent adsorbent amount (g) and the volume of the aqueous sample solution (L), respectively. The calculated C_e and q_e values were used in the Freundlich and Langmuir isotherm models.

$$\%RE = \frac{A_i - A_e}{A_i} X\ 100 \qquad \textbf{(Equation 3.1)}$$

$$q_e = \frac{(C_i - C_e)\,V}{m} \qquad \textbf{(Equation 3.2)}$$

3.4.5 Langmuir Isotherm Model

The Langmuir equation, which is based on the theory that there are a limited number of homogenously distributed binding sites over the adsorbent surface, is known to be the most frequently used isotherm model [416], [417]. The non-linear equation of this Langmuir isotherm model is shown in Equation 3.3.

$$q_e = \frac{q_m K_L C_e}{1+K_L C_e} \qquad \textbf{(Equation 3.3)}$$

In the Langmuir equation, q_m and K_L represent the maximum adsorption capacity of a monolayer (mg/g) and the Langmuir constant (L/mg) related to the apparent adsorption energy. Calculating q_m and K_L as regression constants requires linearization of the mathematical model followed by linear regression on the dependent variable q_e against the independent variable C_e. Linearization of Equation 3.3 can be accomplished by one of the four transformations presented in Table 3.5 [418], [419].

Table 3.5 Linearization of the Langmuir model [418], [419]

Type	Linear form	Plot	Slope	Intercept
Type 1	$\frac{C_e}{q_e} = \frac{C_e}{q_m} + \frac{1}{K_L\, q_m}$	$\frac{C_e}{q_e}$ against Ce	$\frac{1}{q_m}$	$\frac{1}{K_L\, q_m}$
Type 2	$\frac{1}{q_e} = \frac{1}{K_L\, q_m\, C_e} + \frac{1}{q_m}$	$\frac{1}{q_e}$ against $\frac{1}{C_e}$	$\frac{1}{K_L\, q_m}$	$\frac{1}{q_m}$
Type 3	$q_e = q_m - \frac{q_e}{K_L\, C_e}$	q_e against $\frac{q_e}{C_e}$	$-\frac{1}{K_L}$	q_m
Type 4	$\frac{q_e}{C_e} = K_L\, q_m - K_L\, q_e$	$\frac{q_e}{C_e}$ against q_e	$-K_L$	$K_L\, q_m$

The R_L value is a dimensionless constant separation factor (Equation 3.4) that states the Langmuir isotherm characteristics and indicates the type of the isotherm to be either $R_L = 0$ (irreversible), $0 < R_L < 1$ (favourable), $R_L = 1$ (linear), or $R_L > 1$ (undesirable).

$$\boldsymbol{R_L = \frac{1}{1+K_L\, C_i}} \qquad \textbf{(Equation 3.4)}$$

3.5 Synthesis of Gold Nanoparticles and Their Toxicological Assessment

3.5.1 Synthesis of Gold Nanoparticles

3.5.1.1 Preparation of Macro-algae Extract

The macro-algae species, *Padina pavonica* was used as a source of reducing agent in the biogenic synthesis of nanoparticles [412]. For this purpose, the collected invasive macro-algae species was first removed from the necrotic samples and the remaining macro-algae sample was washed with tap water to remove the epiphytes. Then, the macro-algae was rinsed with ultrapure water to avoid any contamination on the macro-algae surface. The drying process was carried out in daylight to avoid any deterioration due to heat. After the drying process, the completely dried macro-algae sample was grounded into a homogeneous powder sample with the help of a grinder to increase the surface area. Following the preparation of the sample, extraction of the species which are used as reducing agents and also a stabilizing agent in the synthesis was carried out. For this purpose, 12.5 g of dried macro-algae sample was stirred vigorously in 187.5 mL of deionized water at 50-55 °C for 1.0 hour and the reducing species was extracted into the water medium. The resulting aqueous solution was filtered with black dot quantitative filter paper (125 mm) to remove the solid particles remaining in the medium. The filtrate was used for gold nanoparticle synthesis.

3.5.1.2 Biogenic Synthesis of Gold Nanoparticles (GNPs)

The synthesis of gold nanoparticles was done by using $HAuCl_4.2H_2O$ solution (30% wt) as gold ion source and the solution containing Au ions at the concentration determined in the synthesis procedure (1.0 mM) was prepared by diluting the solution with deionized water. The macro-algae extract solution (5.0 mL) was heated to 40 °C and the synthesis reaction was initiated by dropwise addition of the aqueous solution containing Au ions to this solution. The resulting solution was stirred at constant temperature for 1.0 hour for the synthesis of metallic gold nanoparticles. A schematic representation of the synthesis procedure is given in Figure 3.2.

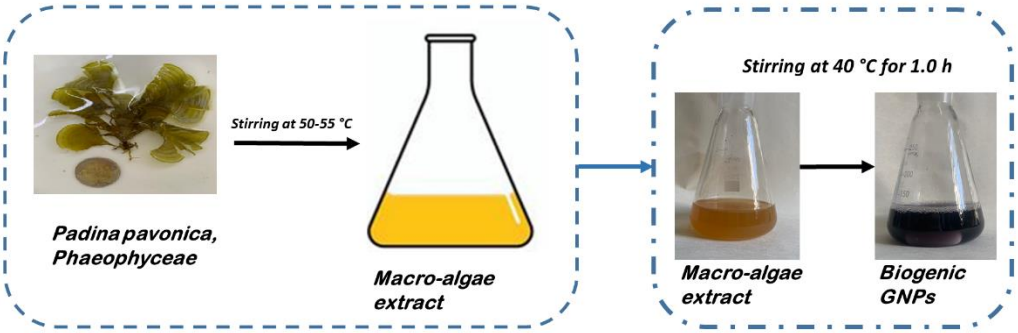


Figure 3.2 Schematic display of the biogenic GNP synthesis procedure

3.5.2 Test organisms and experiments to examine the lethal doses

In the genotoxicological assessment studies, *Daphnia magna* (from Iskenderun Technical University, Türkiye) was chosen as test organisms. All experiments during the assessment were conducted by following Test No. 202: Daphnia sp. Acute Immobilisation Test standardized by the Organization for Economic Co-operation and Development (OECD) [420]. The cultures were grown in an aquarium under controlled circumstances, with an ambient temperature of 20.5 ± 1.0 °C, a medium pH of 8.40 ± 0.05, and a photoperiod of 16 hours of light followed by 8 hours of darkness. The average size of the neonates used in the bioassay was 3.0 mm. The gravid female daphnia were separated from the aquarium to simplify the care of the infants. Subjected female daphnia were fed with a diet consisting of a mixture of algae (*S. subspicatus*). Neonates less than 24 hours old starting from the moment of egg fertilization were subjected to both acute and chronic toxicity assessments. In the evaluation experiments, the cell suspension obtained from *Daphnia magna* was centrifuged at a speed of 3000 rpm for 5.0 minutes in a phosphate buffer solution at a temperature of +4.0 °C. Afterwards, the samples were prepared by mixing 10 µL of cell suspension with 100 µL of 0.7% low melting point agarose (LMPA). Subsequently, a volume of 100 µL of this mix sample was put onto slides that were coated with agarose with a normal melting point (NMPA) and then exposed to freezing conditions. The preparations were placed in lysis solution and kept at a temperature of +4.0 °C overnight. They were then transferred to electrophoresis buffer and incubated at the maintained temperature for 20 minutes. The alkaline electrophoresis procedure was carried out with 24 V voltage and 300 mA operating current for 40 mins at 4.0 °C. Following that, the samples were

subjected to treatment with 100 µL of ethidium bromide solution (10 µL mL^{-1}). The samples were analyzed using fluorescence microscopy (Leica Microsystems, Germany). Following that, the scoring method was used to determine the Arbitrary Unit and other index values. The extent of DNA damage in total 100 cells per slide was assessed using a scale of 5 grades: "*N_0 -undamaged,* "*N_1-mildly damaged",* "*N_2-moderately damaged",* "*N_3-from moderately to heavily damaged",* "*N_4-heavily damaged* based on the length of the tail extending from the nucleus [421].

3.5.3 Cell Viability Tests

The toxicological assessment for gold nanoparticles Human Umbilical Vein Endothelial Cells (HUVEC) line and Human Colorectal Carcinoma Cell (HCT116) line were employed. The cell lines were cultured in Dulbecco's Modified Eagle Medium (DMEM media) supplemented with L-glucose, 1.0% penicillin-streptomycin (10,000 U/mL) antibiotic and 10% fetal bovine serum (FBS). The cells were incubated in a humidified incubator at 37 °C and 5.0% CO_2 for a day. When the cell density reached an appropriate level, the culture dish was sterilized with phosphate buffered saline (PBS) and 3.0 mL of trypsin was used for detaching cells from the culture dish's surface. The culture dish was incubated at 37 ℃ for 3 more minutes after trypsin addition. Once the cells were detached from the surface of the culture dish, the culture dish was moved to a laminar air circulation cabinet and 3.0 mL of fresh DMEM medium was added. The cells were then transferred to a sterile centrifuge tube and centrifuged at 1500 rpm for 5.0 min. Then, 1.0 mL of fresh DMEM medium was added to the cell lines which are accumulated at the bottom of the centrifuge tube, and pipetted precisely with a disposable sterile serological pipette.

In the MTT cell viability experiments, the impact of different doses of GNPs on both HUVEC and HCT116 cell lines was evaluated. The cells were distributed into 96-well plates at a density of 1×10^3 cells per well. After incubating overnight, various quantities (ranging from 1.0 to 50 µg mL^{-1}) of GNPs were prepared in a regular culture medium. After 24 hours, the GNPs media was removed from the plate wells and replaced with 10 µL of 0.5 mg mL^{-1} 3-(4,5-Dimethylthiazol-2-yl)-2,5-Diphenyltetrazolium Bromide (MTT) solution to evaluate cell viability. At the end of the 4.0-hour incubation period, the MTT solution was replaced from the wells and 100 µL of DMSO (dimethyl sulfoxide) was employed to dissolve the

violet-purple formazan crystals. Figure 3.3 presents a picture of the experimental plate with formazan crystals. Ultimately, the absorbance readings were quantified using an ELISA microplate reader at a wavelength of 540 nm. The % cell viability was calculated using the Equation 3.5, based on the observed results.

$$\boldsymbol{Cell\ viability}\ (\%) = \frac{\boldsymbol{ABS_{540}\ Sample}}{\boldsymbol{ABS_{540}\ Control}} \times \mathbf{100} \qquad \textbf{(Equation 3.5)}$$

ABS_{540}: Absorbance value in 540 nm

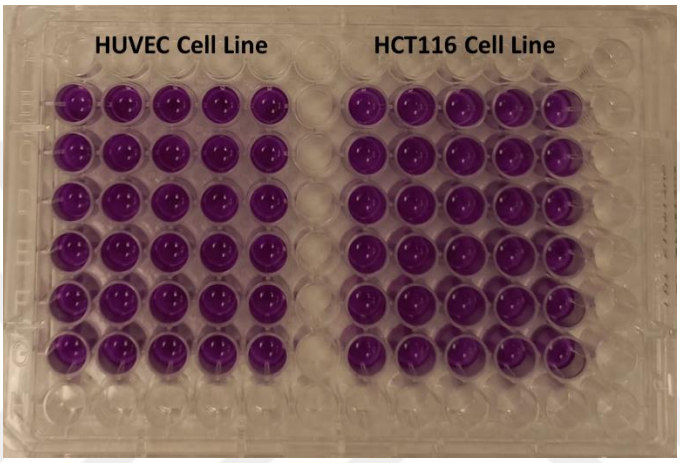


Figure 3.3 96-well plates with formazon crystals

4
RESULTS AND DISCUSSION

4.1 Simultaneous Determination of Endocrine Disruptor Compounds and Pesticides in GC-MS System

This section of the thesis has been published in the *Environmental Science and Pollution Research* journal (DOI: 10.1007/s11356-023-31750-8.) as a research article. The scope of this study was to develop and validate an accurate and precise SADF-LPME-GC-MS method for the simultaneous determination of the twenty-nine selected analytes in soil, sea water and moss samples. For real sample applications, the developed method was applied to rock and soil samples (n=92), ocean water samples (n=42), lake water samples (n=12) moss and seaweed samples (n=43) and feces samples (n=14), all collected from the Horseshoe and Faure Islands in (Anctarctica).

4.1.1 Chromatographic Elution of the Endocrine Disruptor Compounds and Pesticides

In order to determine the optimum chromatographic conditions for the qualitative determination of the analytes, an appropriate elution temperature program was determined for the GC-MS system. To achieve this, different temperature programs were applied to 50 mg/kg mixed standard solutions of the analytes in order to attain transient peaks for easy identification. Table 4.1 lists the different temperature programs applied in order to determine the appropriate chromatographic conditions that will enable the separation of each of the 29 analytes for which qualitative and quantitative determinations would be carried out in the study.

Table 4.1 Temperature ramps attempted to determine suitable chromatographic conditions for separation of analytes

Temperature Ramp	**Initial Temperature, ˚C**	**Finale Temperature, ˚C**	**Analysis Period, min**	**Flow Rate, mL min^{-1}**	**Injection volume, µL**
Program 1	40	300	27.00	1.80	1.0
Program 2	50	300	48.00	0.50	1.0
Program 3	50	300	13.00	2.50	1.0
Program 4	70	300	16.00	2.00	1.0
Program 5	70	300	25.00	2.50	1.0
Program 6	70	300	16.00	2.50	1.0
Program 7	80	300	13.00	2.50	1.0
Program 8	80	300	19.00	2.00	1.0
Program 9	80	300	22.00	2.00	1.0
Program 10	80	285	21.00	2.00	1.0
Program 11	80	285	12.50	2.00	1.0
Program 12	100	295	13.00	2.00	1.0
Program 13	100	295	13.50	1.80	1.0
Program 14	100	300	20.00	0.50	1.0
Program 15	100	300	15.00	0.50	1.0
Program 16	100	300	21.00	0.50	1.0
Program 17	100	300	25.00	0.50	1.0
Program 18	100	300	38.00	0.50	1.0
Program 19	100	300	27.00	0.80	1.0
Program 20	100	300	27.50	1.00	1.0

When the total ion chromatograms obtained were compared, it was seen that the most suitable temperature program for the analytes was 'Program 19'. With the analysis temperature program used, it was determined that the peak of 29 of 30 analytes could be observed in total ion chromatography. This involved an initial temperature of 100 °C, then the temperature was increased to 200 °C with a rate of 15 °C per minute. After waiting at 200 °C for 1.0 minute, the temperature reached 280 °C with an increase rate of 5.0 °C per minute, and the temperature was kept constant for 1.0 minute. Then, the oven temperature was increased to the final temperature (300 °C) within 2.0 minutes. The total analysis time was determined as 27 minutes. In Table 4.2, the values of the method parameters applied in the simultaneous determination of the analytes are given. The total ion chromatogram (TIC) obtained under the determined optimum chromatographic conditions is presented in Figure 4.1

Table 4.2 Method parameters applied in the GC-MS device used in the simultaneous determination of pesticides and endocrine disruptors

Parameter	**Value**
Injector Total Volume	10 µL
Injection Volume	2.0 µL
Inlet Temperature	250 °C
Pressure	7.86 psi
Total Flow	63.3 mL min^{-1}
Injection Mode	Splitless
Purge Rate	60 mL min^{-1}
COLUMN PARAMETERS	
Coating Material	%5.0 methyl-phenylpolysiloxane
Column Size	30 m x 0.32 mm I.D., 0.25 µm film thickness
Mode	Constant Flow
Flow Rate	0.8 mL min^{-1}

Table 4.3 Method parameters applied in the GC-MS device used in the simultaneous determination of pesticides and endocrine disruptors (Continued)

Pressure		7.86 psi
Velocity		33 cm s^{-1}
OVEN PARAMETERS		
Initial Temperature		100 °C
Ramp, °C min^{-1}	**Finale Temperature, °C**	**Period, min**
15	200	6.67
0.0	200	1.0
5.0	280	23.67
0.0	280	1.0
10	300	26.67
0.0	300	0.33

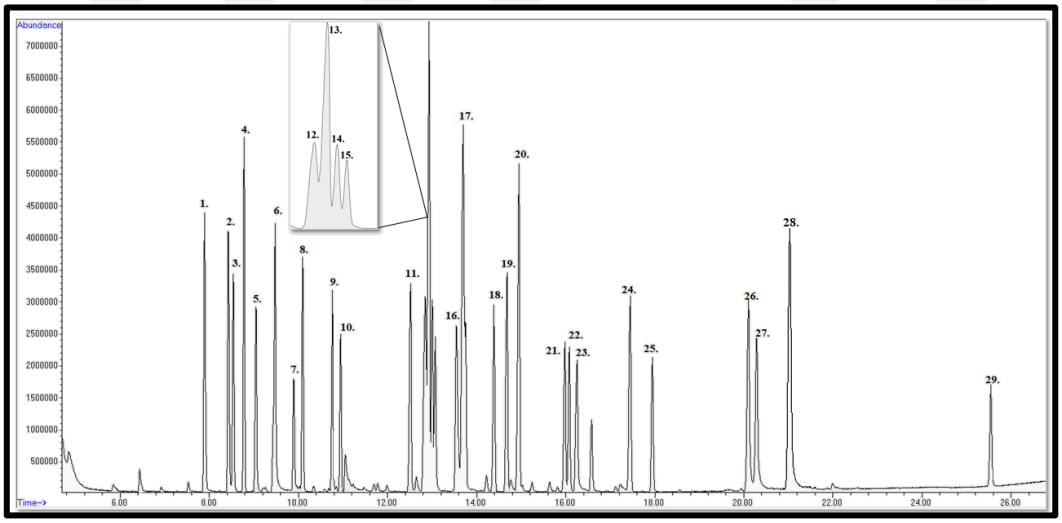


Figure 4.1 Total ion chromatography obtained for 50 mg kg^{-1} mix standard solution containing all the pesticide and endocrine disruptor determined in the study

Retention times (RT) were determined in order to clarify the peaks of the analyte in the chromatogram obtained as a result of the analysis. For this purpose, the NIST

Mass Spectrometer Resource Library (MSRL) was used. Here, according to the information on the analyte, the ions with the 5 mass/charge (m/z) ratios that form the largest peak were selected. Chromatograms were displayed for these selected ions and RT values of each analyte were determined. To confirm the results, the prominent m/z ions are extracted where the occurrence of all ions at the same retention time suggests the compound of interest. In Figure 4.2, overlapping peaks of five prominent mass fragments of sertraline is shown at the retention time of the analyte. The identification of the analyte in interest was then confirmed with the NIST MSRL in the ChemStation software as depicted in Figure 4.3. Presented in Table 4.4 are the ion values with the 5 major fragment ions, which constitutes the largest peak of the pesticides and endocrine disruptors and their respective retention times. The chronological of the analytes preented in the table are also depicted on the peaks of the TIC in Figure 4.1. Quantification of the analytes was performed by calculating the peak area values of the analyte signal obtained by extracting the most prominent ion of the main 5 fragments.

Table 4.4 Chromatographic informations of the targeted analytes in the study

Peak Number	Analyte	Molecular weight, g mol^{-1}	The 5 major fragment ions with the highest peak area	Retention Time, min
1	alfa-benzenehexachloride (alfa-BHC)	290.83	**183**, 181, 219, 217, 111	7.9
2	beta-benzenehexachloride (beta-BHC)	290.83	**219**, 181, 109, 183,217	8.425
3	Lindane (gama-BHC)	290.83	**181**, 183, 219, 217, 109	8.553
4	Diazinon	304.35	**179**, 137, 152, 199, 304	8.758
5	Delta-benzenehexachloride (delta-BHC)	290.83	**109**, 219, 183, 181, 217	9.046
6	Galaxolide	258.4	**243**, 213, 258, 244, 171	9.435

Table 4.5 Chromatographic informations of the targeted analytes in the study (Continued)

6	4-n-Nonylphenol	220.35	**107**, 220, 108, 77, 221	9.503
7	Parathion Methyl	263.21	**109**, 263, 125, 79, 63	9.892
8	Heptachlor	373.32	100, **272**, 274, 270, 65	10.096
9	Malathion	330.36	125, **173**, 93, 127, 29	10.763
10	Aldrin	364.91	66, **263**, 265, 261, 91	10.947
11	Triflumizole	345.75	73, **278**, 206, 179, 287	12.504
12	Paclobutrazol	293.79	**236**, 125, 82, 238, 57	12.847
13	Triclosan methyl	303.57	**290,** 288, 218, 63, 51	12.936
14	cis-chlordane	409.78	373, **375**, 377, 371, 237	13.076
15	Bisphenol A	228.29	**213**, 228, 119, 214, 91	13.590
16	4, 4-dicholorodiphenyl dichloroethylene (4,4-DDE)	318.03	**246**, 318, 248, 316, 176	13.686
17	Dieldrin	380.91	**79**, 81, 82, 77, 263	13.749
18	Endrin	380.91	**81**, 79, 263, 67, 82	14.391
19	α – Endosulfan	406.93	**241,** 239, 195, 237, 339	14.684
19	β – Endosulfan	406.93	195, **241,** 237, 239, 207	14.684
20	4,4-dichlorodiphenyl dichloroethane (4,4-DDD)	320.04	**235**, 237, 165, 236, 199	14.95
21	Endosulfan sulphate	422.92	**387**, 272, 274, 389, 385	15.98

Table 4.6 Chromatographic informations of the targeted analytes in the study (Continued)

22	4, 4- dichlorodiphenyl trichloroethane (4,4-DDT)	354.49	**235**, 237, 165, 236, 199	16.075
23	Carbamazepine	236.27	**193**, 192, 236, 194, 191	16.24
24	Endrin ketone	380.91	**67**, 317, 315, 319, 139	17.441
25	Metoxychlor	345.65	**227**, 228, 212, 196, 195	17.95
26	Estrone	270.37	**270,** 146, 185, 172, 145	20.064
27	ß-Estradiol	272.38	**272**, 160, 146, 172, 159	20.251
28	17α-Ethynylestradiol	296.40	**213**, 296, 160, 133, 159	21.294
29	Diltiazem HCl	450.98	**58**, 71, 72, 121, 150	25.506

***Ions with m/z from which quantitative determinations performed were indicated in bold.**

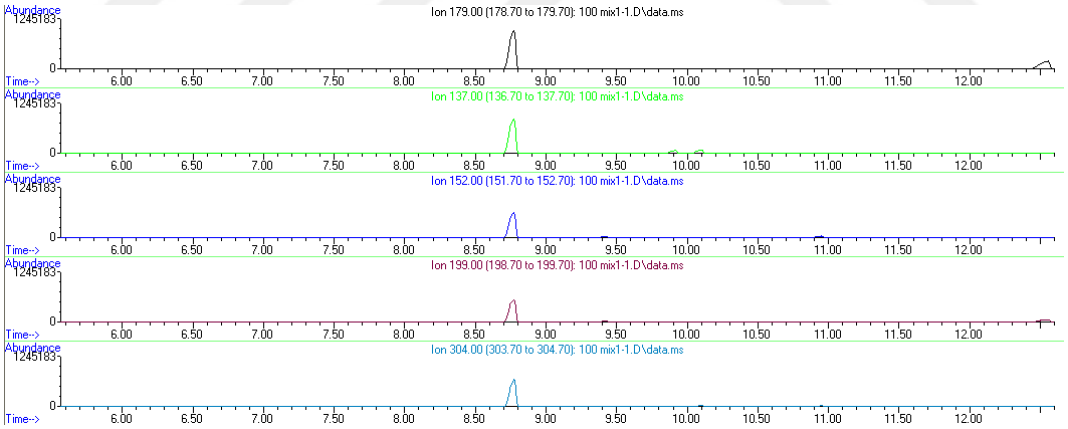


Figure 4.2 Extracted ion chromatogram of diazinon's five prominent mass fragments (*m/z*: 179, 137, 152, 199, 304)

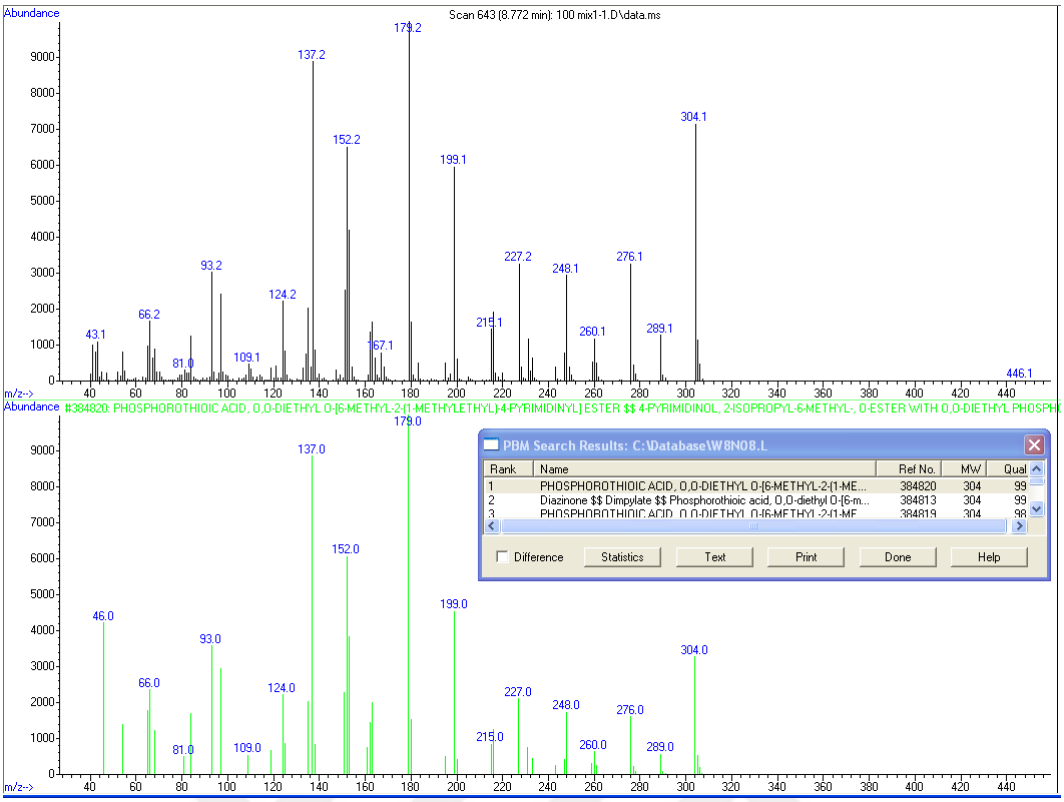


Figure 4.3 Identification of diazinone via NIST compound database based on compound's mass spectrum similarity to library spectrum

4.1.2 Analytical Figures of Merit

In order to determine the detection limits of pesticides and endocrine disrupting substances in the GC-MS system with the developed chromatographic method, a series of mixed standard solutions were prepared and measurements were carried out under optimum instrumental conditions. The peak areas were calculated with the MSD ChemStation software program in the chromatograms obtained by using the m/z ratio ion with the highest relative abundance of each analyte. Calibration charts were then generated showing the peak area versus the concentration of each analyte. With the obtained calibration curve, the dynamic working range of each analyte was determined under the determined instrumental conditions. The calibration plots created showed a high coefficient of determination (in the range of 0.9983 - 1.0), showing that high linearity was achieved in the determination of the analytes with the developed chromatographic method.

In the developed system, the detection limit (LOD) and the quantification limit (LOQ) of the analytes were calculated using the equation obtained from the

calibration plots. Equations 4.1 and 4.2 given below were used in determining the LOD and LOQ values;

$$LOD = \frac{3 * SD}{m} \quad \textbf{(Equation 4.1)}$$

$$LOQ = \frac{10 * SD}{m} \quad \textbf{(Equation 4.2)}$$

The expression SD in the equation denotes the standard deviation obtained from 7 replicate measurements of the lowest analyte concentration in the dynamic operating range, and m denotes the slope of the calibration line obtained from the calibration graph. System analytical performance values for the analyte are given in Table 4.7.

The calibration plots of the GC-MS showed a high coefficient of determination (R^2) ranging from 0.9983 to 1.000, showing that there was a strong linear relationship between the analytes and the optimal chromatographic conditions. The LOD and LOQ values for the GC-MS system were determined in the ranges of 3.6 – 419.7 ng g^{-1} and 12 – 1399 ng g^{-1}, respectively. The %RSD of all 29 analytes were recorded below 18%, demonstrating satisfactory precision for duplicate instrumental measurements. The analytical features of the GC-MS system for the simultaneous determination of the analytes are described in Table 4.7.

Table 4.7 System performance values for each analyte under optimum chromatographic conditions

Analyte	LOD, ng g^{-1}	LOQ, ng g^{-1}	R^2	Linear Range, ng g^{-1}	%RSD
alfa-BHC	24.4	81.2	0.9993	109.7 – 7331	11.8
beta-BHC	23.6	78.8	0.9994	103.3 – 9079	13.0
Lindane (gama-BHC)	14.4	48.1	0.9995	52.4 – 9367	13.4
Diazinon	25.6	85.5	0.9983	102.2 – 19109	9.9
delta-BHC	89.9	299.6	0.9985	531.4 – 19951	8.1
1,3,4,6,7,8-Hekzahidro-4,6,6,7,8,8-hekzam	72.0	240.0	0.9989	396.6 – 15014	5.4
4-n-Nonylphenol	31.2	104.0	0.9995	199.0 – 18930	4.4
Parathion Methyl	75.9	252.9	0.9989	507.4 – 19209	17.3
Heptachlor	24.2	80.6	0.9989	104.2 – 7016	9.3
Malathion	41.5	138.4	0.9989	201.5– 19168	12.9
Aldrin	36.9	123.1	0.9987	201.8 – 6921	4.0
Triflumizole	38.8	129.5	0.9991	200.2 – 19049	10.5
Paclobutrazol	44.4	148.0	0.9991	204.8 – 9236	9.1
Trichlosan methyl	106.4	354.5	0.9996	488.2 – 18482	7.1
cis-chlordane	41.2	137.4	0.9985	201.7 – 6916	3.9
Bisphenol A	60.8	202.6	1.00	201.9 – 19202	6.9
4,4-DDE	19.1	63.6	0.9984	101.8 – 8948	6.9
Dieldrin	28.4	94.5	0.9988	103.2 – 6949	10.5

Table 4.8 System performance values for each analyte under optimum chromatographic conditions (Continued)

Endrin	52.9	176.2	0.9986	504.9 -18958	2.6
Endosulfan**	123.8	412.7	0.9995	404.2 – 13860	7.6
4,4-DDD	9.3	31.0	0.9987	52.2 – 19703	10.4
Endosulfan sulfate	43.0	143.3	0.9997	205.6 – 38716	11.7
4,4-DDT	91.4	304.8	0.9989	524.0 – 19675	8.5
Carbamazepine	201.0	669.9	0.9997	1012 – 19386	13.4
Endrin ketone	62.0	206.6	0.9986	203.5 – 19206	6.9
Methoxychlor	3.6	12.0	0.9992	52.3 – 9354	6.9
Estrone	285.2	950.8	0.9993	1007 – 19307	13.0
ß-Estradiol	419.7	1398.9	0.9984	2034 – 19458	11.7
17α-Ethinylestradiol	56.9	189.9	0.9991	201.5 – 19168	14.2
Diltiazem Hydrochloride	24.3	80.9	0.9995	200.8 – 19103	5.3

***Standard deviation value for 6 replicate measurements of the lowest analyte concentration in the dynamic operating range.**

****Total analyte concentration (α-Endosulfan + β-Endosulfan).**

4.1.3 Determination of Proper Liquid Phase Microextraction Method for Simultaneous Preconcentration of the Analytes

The detection limits recorded for the GC-MS system was not low enough for trace level determinations and this required the development of a suitable liquid phase microextraction method that would enable the separation and preconcentration of the analytes from sample matrix for quantification at trace levels. For this purpose, three methods that are frequently used in the literature were tested and the method that would provide the most efficient extraction of analytes was determined. Hereby, switchable solvent based liquid phase microextraction (SS-LPME), dispersive liquid-liquid microextraction (DLLME) and spray assisted droplet formation based liquid phase microextraction method (SADF-LPME) were applied to the same concentration and volume of aqueous standard solutions of the analyte. In order to determine the appropriate method, mixed standard solutions of the analyte in the concentration range of 0.036 - 0.1668 mg kg^{-1} were prepared. The experimental parameters applied for each extraction method are summarized in Table 4.9. The results obtained are graphically depicted in Figure 4.4 The results of the extraction methods applied to determine the appropriate extraction method. The average value of the improvement factor in the peak areas of the analytes in the SADF-LPME method was 50.30 times. The improvement factors were determined as 40.81 times for DLLME and 41.25 times for SS-LPME. It is clearly seen that the enhancement recorded for the SADF-LPME method for the vast majority of analytes is higher compared to other extraction methods. Therefore, it was decided to apply the SADF-LPME method for the simultaneous determination of the analytes and to develop optimum experimental parameters to ensure maximum extraction output. The fact that the method provides a more environmentally friendly approach is one of the important reasons why the method was preferred over the DLLME method, which requqires a disperser solvent. When compared to the SS-LPME method that utilizes the relatively toxic dimethyl benzylamine (DMBA), the SADF-LPME method emerged as a safer approach. In addition, with the SADF-LPME method, it is aimed to reduce the possibility of relative error by reducing the extraction experimental steps compared to the other two methods. In the light of these results, SADF-LPME method was selected and optimized to achieve highly accurate and precise results for the selected analytes.

Table 4.9 Experimental parameters of the extraction methods applied in order to determine the appropriate extraction method

Extraction Method	Sample volume	Extraction solvent	Extraction solvent volume	Dispersive solvent and its volume	NaOH solution concentration and its volume
SS-LPME	8.0 mL	DMBA	500 µL	-	2.0 M; 1.0 mL
DLLME	8.0 mL	Chloroform	300 µL	Ethanol; 2.0 mL	-
SADF-LPME	8.0 mL	Chloroform	≅ 200 µL	-	-

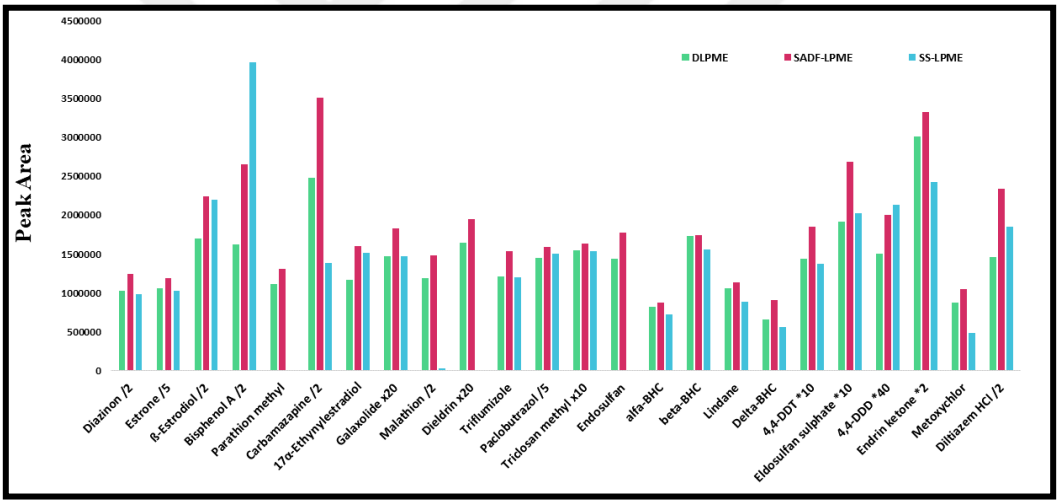


Figure 4.4 The results of the extraction methods applied to determine the appropriate extraction method

Within the scope of this study, the parameters affecting the extraction output of the SADF-LPME method were optimized using the single variable-based optimization studies. Variables of each parameter were tested on mixed standard solutions to determine the optimum condition. All experimental and instrumental conditions, except for the parameter whose optimum condition was sought, were kept constant for each sample during the optimization study stages. The mean peak area value, standard deviation and relative standard deviation value of each variable were determined with at least two replicate samples, and the variable that provided the

highest extraction output and high reproducibility for the majority of analytes was determined as the optimum experimental parameter.

4.1.4 Optimization Studies

The main parameters that were optimized in this work for the SADF-LPME method were the sample pH, buffer solution volume, extraction solvent type, binary solvent mixture ratio, and number of replicate spraying used to determine the right amount of extraction solvent. At each optimization phase, the optimum values or parameters were selected based on the highest peak area mean of extraction measurements, which were obtained from at least four measurements of two replicate samples.

4.1.4.1 Determination of the pH of the Sample Solution

The form of organic compounds in aqueous solution are very important for their mass transfer into an extractant phase. In order to provide this transfer, accelerate it and increase its efficiency, it is necessary to determine the ionic balance of the sample solution. For this purpose, the mass transfer of the analytes to the extraction solvent can be done quickly and safely by using a buffer that will provide the appropriate pH medium. Since it is aimed to carry out the extraction of many analytes simultaneously in this study, the presence of the sample solution at the appropriate pH is a parameter that directly affects their respective extraction outputs. Therefore, extraction was carried out using buffer solutions at pH 3.0, 5.0, 7.0 and 9.0. In addition, the extraction process was carried out under unbuffered conditions in order to examine the extraction efficiency of the solution in its own pH (pH 2.73) without any external intervention. As can be seen in the graphs in Figure 4.5 and Figure 4.6, low extraction efficiency and high relative error were obtained in the natural pH. In the results obtained for the buffered solutions, it was observed that most of the analytes were extracted in the basic region (pH 9.0) more efficiently. In the acidic region (pH 3.0), where the rest of the analytes appear to give the highest signal, only a 1.0-1.2-fold decrease was determined in the trials of the same analytes with borate-HCl buffer. Since it was thought that this difference did not have a significant effect on the extraction of the analytes and it was seen that many analytes could be extracted with high reproducibility and efficiency in a

pH 9.0 environment, it was decided to continue the study with this buffer solution. Table 4.10 lists the constant experimental conditions applied in this optimization step.

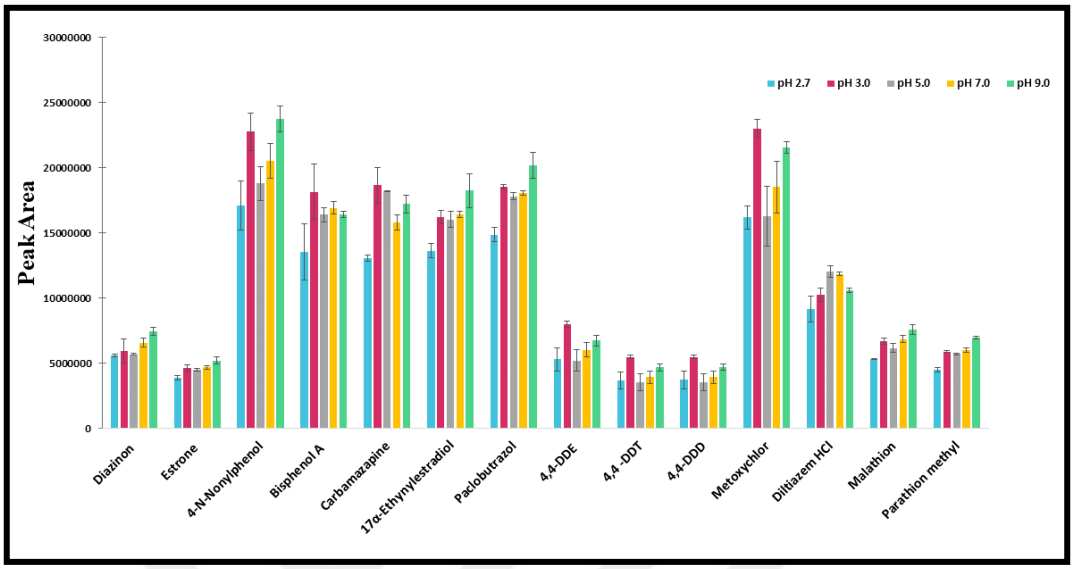


Figure 4.5 Determination of optimum solution pH (Group 1)

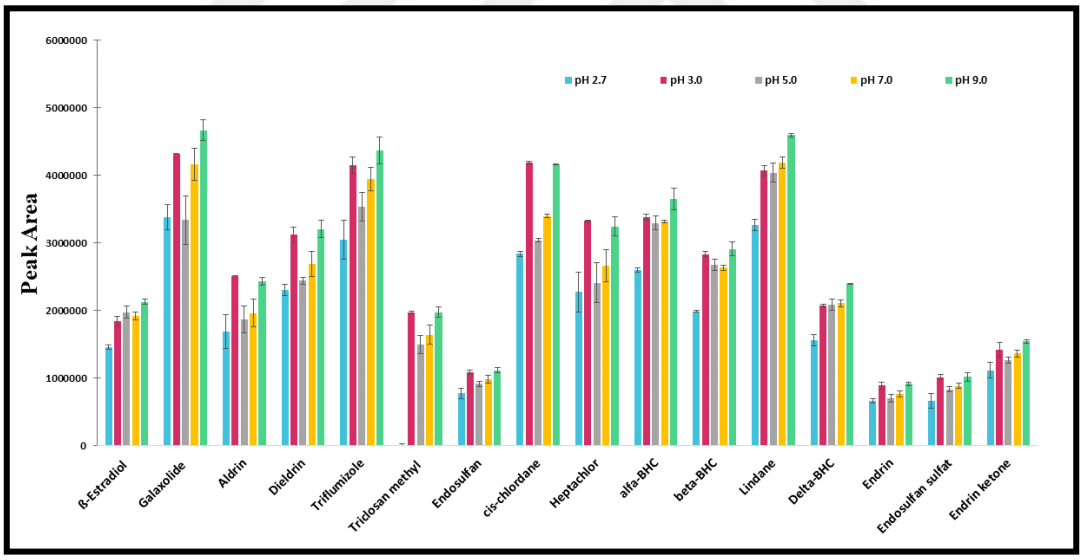


Figure 4.6 Determination of optimum solution pH (Group 2)

Table 4.10 Experimental parameters used in the optimization study to determine the solution pH

Concentration of the aqueous mix standard solution	500 ng mL^{-1}
Volume of the aqueous mix standard solution	5.0 mL
Buffer Solution	pH 3.0; 5.0; 7.0; 9.0 (In progress)
Volume of the buffer solution	1.0 mL
Extraction solvent	Chloroform
Spraying repetition	2
Vortex period	15 s

4.1.4.2 Determination of the Buffer Solution Volume

The buffer capacity of the buffer solution used is decisive for determining the appropriate pH in the sample solution. The buffer capacity is also proportional to the concentration. While adding buffer solution to the sample solution, in addition to adding buffer solution at a concentration that will provide the right buffer capacity, a volume should be selected to prevent the dilution of the analytes in the solution. For this aim, 0.25, 0.50, 1.0 and 2.0 mL of 50 mM borate-HCl buffer solution were added and extraction was performed under constant conditions (Table 4.11). As expected, a downward trend was observed in the signals due to the dilution effect on the analytes for the increasing volumes. The highest extraction efficiency was obtained for 0.25 mL buffer solution for 17 out of the 29 analytes (Figure 4.7 and Figure 4.8). However, since it was predicted that this volume would not be sufficient in studies with real samples and it was determined that there was only a 1.5-fold improvement compared to 0.50 mL, the optimum buffer solution volume was chosen as 0.50 mL.

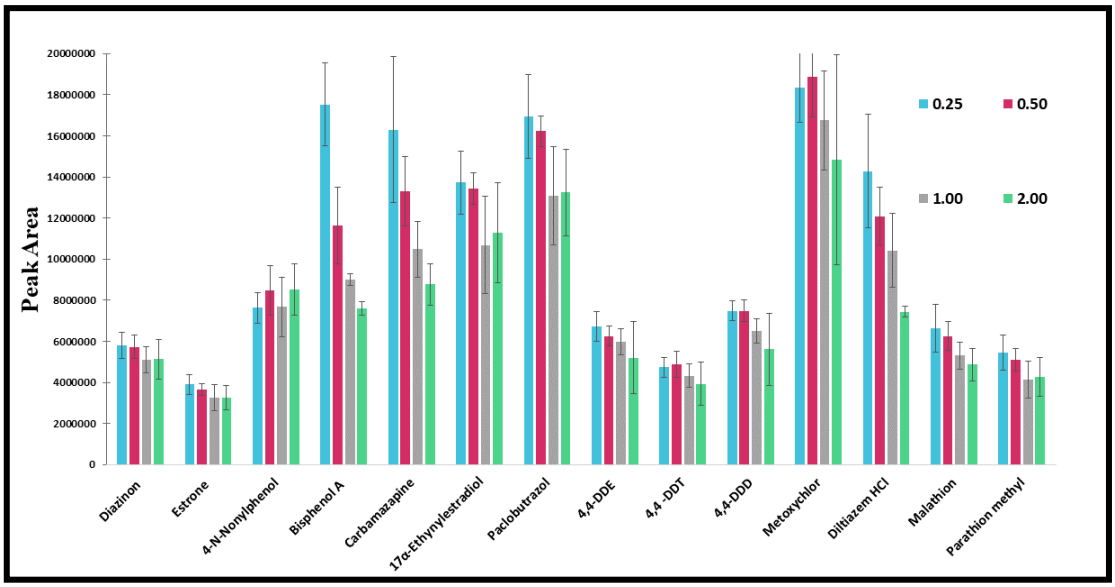


Figure 4.7 Determination of the optimum volume of buffer solution (Group 1)

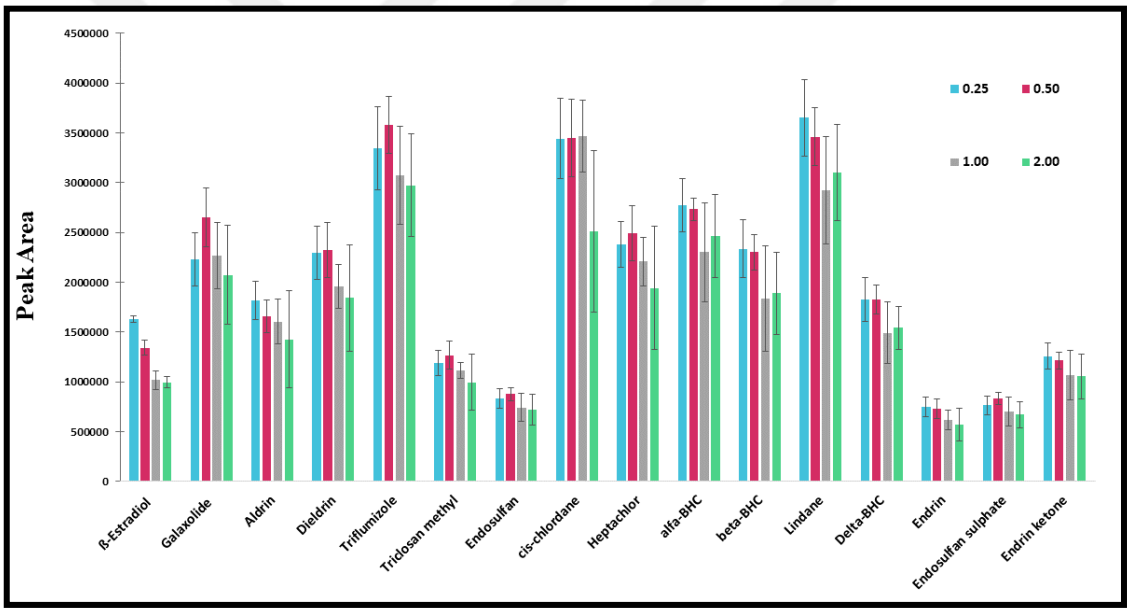


Figure 4.8 Determination of the optimum volume of buffer solution (Group 2)

Table 4.11 Experimental parameters used in the optimization study to determine the buffer solution volume

Concentration of the aqueous mix standard solution	500 ng mL^{-1}
Volume of the aqueous mix standard solution	5.0 mL
Buffer Solution	pH 9.0 (50 mM borate-HCl buffer)
Volume of the buffer solution	0.25; 0.50; 1.0; 2.0 mL (In progress)
Extraction solvent	Chloroform
Spraying repetition	2
Vortex period	15 s

4.1.4.3 Determination of Appropriate Extraction Volume

The use of suitable organic solvents in liquid phase extraction methods is an important parameter that directly affects the extraction efficiency. The main factor that determines the suitability of a solvent is its ability to dissolve the target analyte(s) in high amounts [422]. In the selection of the solvent, the properties of the organic solvent such as density, volatility, melting point, toxicity, cost and environmental factors should be considered. In addition, it is necessary to choose a solvent appropriate for the analytical instrumental method. Finally, the efficiency of the solvent in the extraction varies depending on the forces of attraction such as ionic, hydrogen bonds and London forces with the analyte(s) [423]. In this study, it is not possible to obtain the maximum extraction output of each analyte in a single extraction solvent due to the determination of more than one analyte. For this reason, it was decided to use binary mixtures of extraction solvents to create a more suitable polarity for the analytes. Here, chloroform (CHL), dichloromethane (DCM), 1,2-dichloroethane (DCE), binary mixtures of these solvents (CHL:DCM; CHL:DCE; DCM:DCE) and a ternary solvent mixture were used to determine the most suitable solvent/solvent mixture for simultaneous determination of the analytes (Figure 4.9- Figure 4.10). The prepared solvent mixtures were prepared in

a ratio of 1:1 by volume, and it was aimed to create a homogeneous solution for each extraction by mixing the solution container by vortex for 5.0 s before using the mixtures for each sample. The results obtained in this step showed that solvent mixtures of CHL:DCM (18 analytes) and DCE:DCM (12 analytes) achieved the highest extraction outputs. However, the relative standard deviation values between 9.9 and 64.3% for the analytes with the highest peak area in the CHL:DCM solvent mixture revealed low reproducibility. In contrast, the %RSD values for the DCE:DCM solvent mixture were below 10% for each analyte (1.3 – 8.8%). In addition, when the average peak areas were compared, it was seen that there was only a 1.0-1.3-fold difference between the average peak area values of the analytes recorded for the DCE:DCM solvent mixture and the CHL:DCM solvent mixture. In order to increase the precision of the method with satisfactory enrichment, it was decided to use the DCE:DCM solvent mixture. The fixed experimental conditions of this optimization step are summarized in Table 4.12.

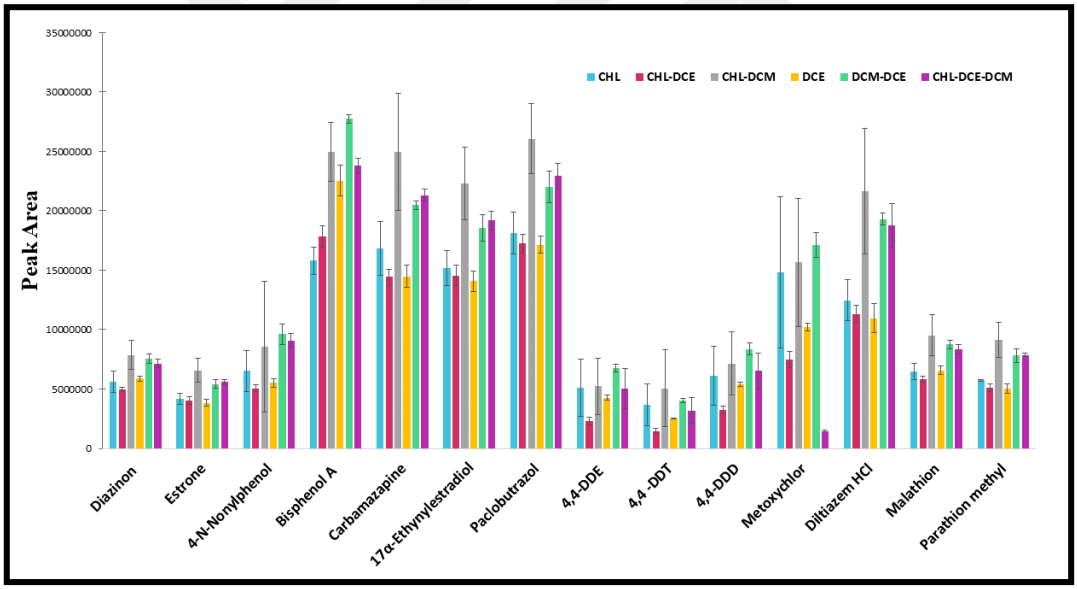


Figure 4.9 Determination of the appropriate solvent/solvent mixture (Group 1)

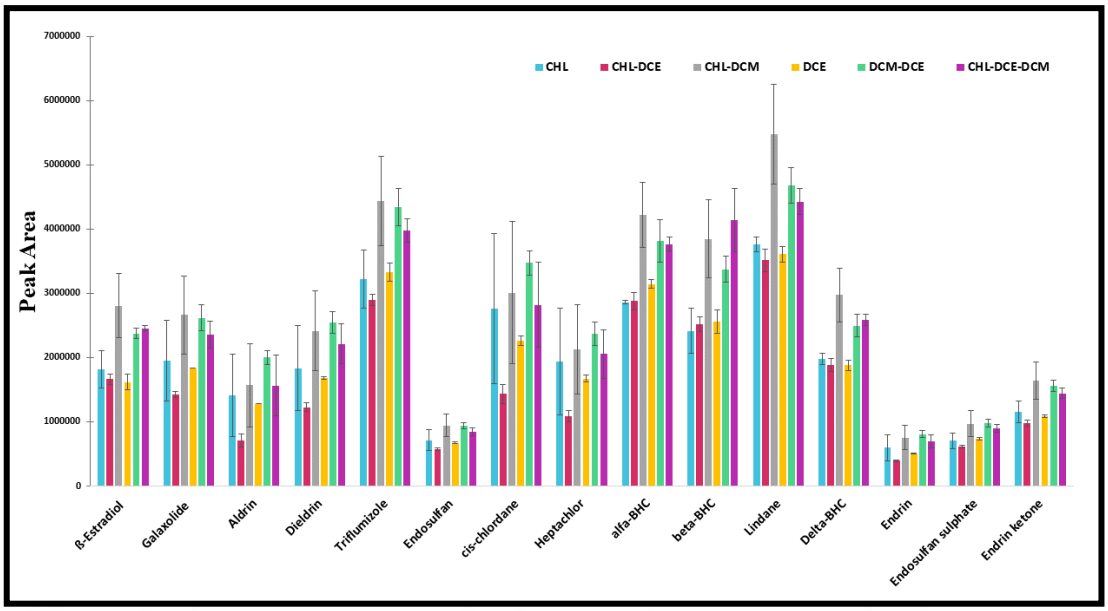


Figure 4.10 Determination of the appropriate solvent/solvent mixture (Group 2)

Table 4.12 Experimental parameters used in the optimization study to determine the extraction solvent

Concentration of the aqueous mix standard solution	500 ng mL^{-1}
Volume of the aqueous mix standard solution	5.0 mL
Buffer Solution	pH 9.0 (50 mM borate-HCl buffer)
Volume of the buffer solution	0.50 mL
Extraction solvent	CHL; DCE; DCM; DCE:CHL; DCE:DCM; CHL:DCM; CHL:DCM:DCE (In progress)
Binary mixture ratio	1:1 (v:v)
Spraying repetition	2
Vortex period	15 s

4.1.4.4 Determination of Extraction Solvent Mixture Ratio (v/v)

The polarity of each solvent is different and there is a constant for each solvent as depicted in the Hildebrand polarity scale [422]. The polarity of the prepared solvent mixture is very important to ensure the solubility of the analytes in the organic phase

and their efficient extraction. In this case, the ratio of the used extraction solvents in the prepared solvent mixture is a critical parameter for the method as it will directly determine the polarity of the solution. At the same time, the ratio of the solvent mixture is of great importance for the formation of the extraction solvent phase with different solubility percentages in water and to ensure proper preconcentration. This optimization step was therefore performed to determine the ratio DCE:DCM binary mixture, which was determined as the optimum extractant combination solvent. In this optimization step, the binary solvent was prepared in the ratios of 1:1, 1:2, 2:1, 1:3 and 3:1 (DCE:DCM) by volume, and the extraction method was applied with each one under constant conditions (Table 4.13). As can be seen in the results obtained in Figure 4.11 and Figure 4.12, a decrease was obtained in the peak areas of the analytes as the DCE ratio increased. This is likely due to the high solubility of DCM in water and the higher probability of contact with analytes in aqueous solution. In addition, it was observed that the organic phase obtained with the increasing amount of DCM was very low. It was decided to continue the study with the 1:1 (v:v) DCE:DCM mixture.

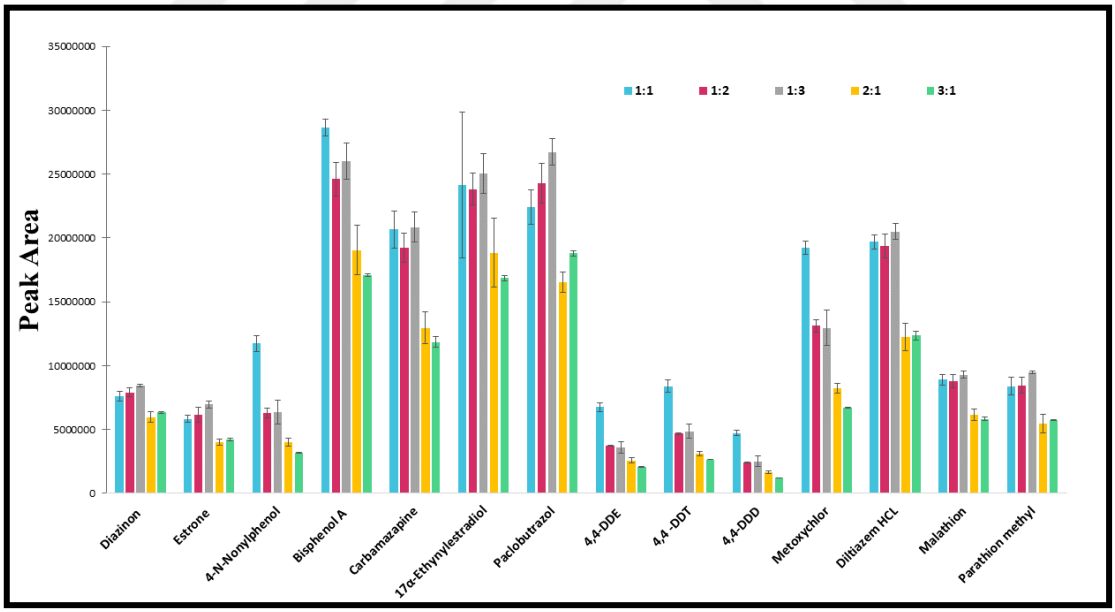


Figure 4.11 Determination of the optimum solvent mixture volume ratio (Group 1)

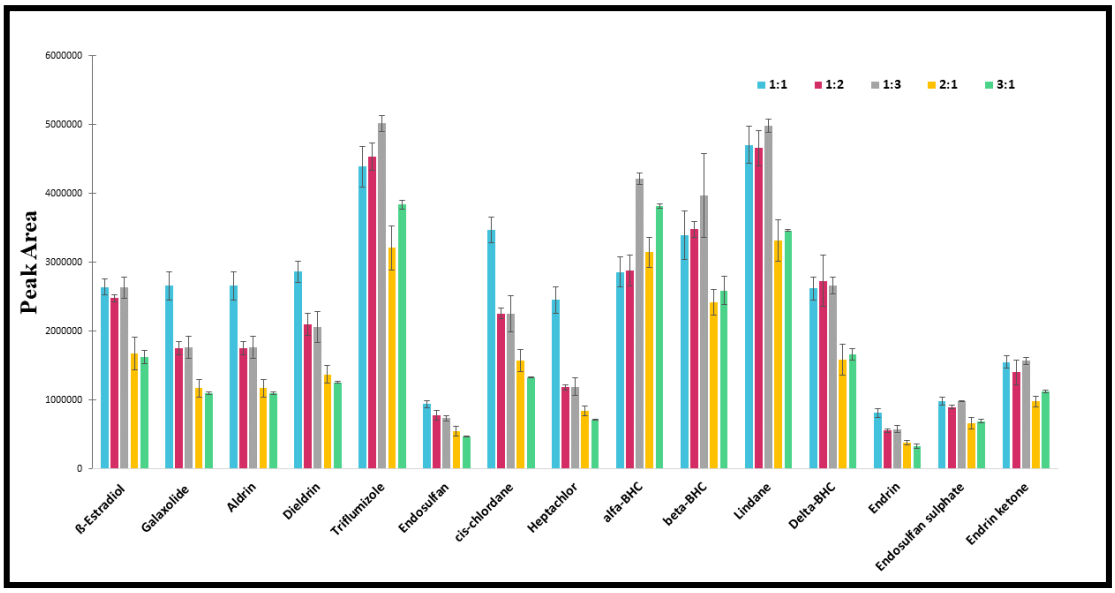


Figure 4.12 Determination of the optimum solvent mixture volume ratio (Group 2)

Table 4.13 Experimental parameters used in the optimization study to determine the ratio extraction solvents in the extraction mixture

Concentration of the aqueous mix standard solution	500 ng mL^{-1}
Volume of the aqueous mix standard solution	5.0 mL
Buffer Solution	pH 9.0 (50 mM borate-HCl buffer)
Volume of the buffer solution	0.50 mL
Extraction solvent	DCE:DCM
Binary mixture ratio	1:1; 1:2; 1:3; 2:1; 3:1 (v:v) (In progress)
Spraying repetition	2
Vortex period	15 s

4.1.4.5 Determination of Spray Repetition for Sufficient Extraction Solvent Mixture Volume

Disperser solvents have been widely used in the literature to rapidly disperse extraction solvents as small droplets in all sample/standard solutions [424]. However, the use of a disperser solvents that are magnitudes higher in volume than extraction solvents increase the overall volume of organic solvents used. In this study, the extraction solvent was dispersed into the standard/sample solution as microdroplets by air pressure, without using a disperser solvent. In this optimization study, since the spray number and the amount of extraction solvent were directly proportional, the spray number of the extraction solvent was one of the factors affecting the extraction efficiency and pre-concentration factor. However, adjusting the binary extraction mixture solution volumes, volume of the spray apparatus used in this experiment was not possible due to the manual spray apparatus. Therefore, the volume of extraction solvent was defined using the number of sprays. Primarily, the precision scale was used to figure out the solvent volume consumed per spraying. For this purpose, the average volume of extraction solvent mixture consumed in one spray cycle was recorded as 0.1326±0.0045 g with 15 replicate measurements. Then, 1, 2, and 3 times spray numbers were tested in order to evaluate the influence of extraction solvent mixture volume. As a result of this experiment, as seen in Figure 4.13Figure 4.14, the obtained signals decreased as the number of sprays increased. This is because the analytes are diluted with increasing solvent mix volume as the number of sprays increases. However, the phase obtained with 1 spray cycle was quite small. Since this situation was foreseen to cause difficulties in the extraction process for real samples and for the low reproducibility recorded, it was decided to perform the method with 2 sprays ($\cong 0.265\ g$). Table 4.14 presents the experimental conditions in the optimization study.

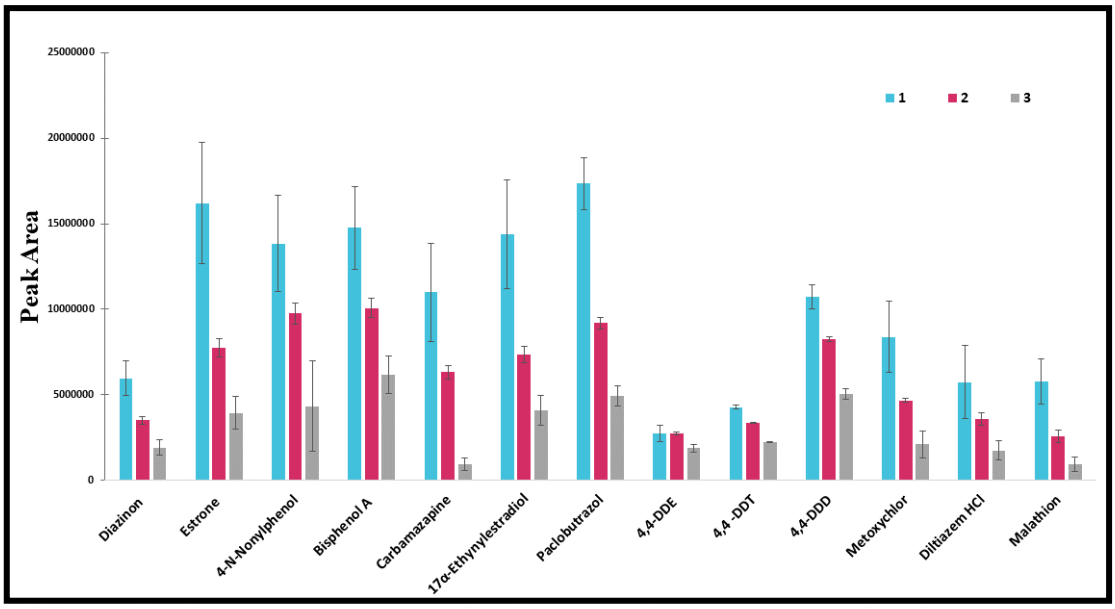


Figure 4.13 Determination of the optimum volume of extraction solvent mixture by spraying repetition (Group 1)

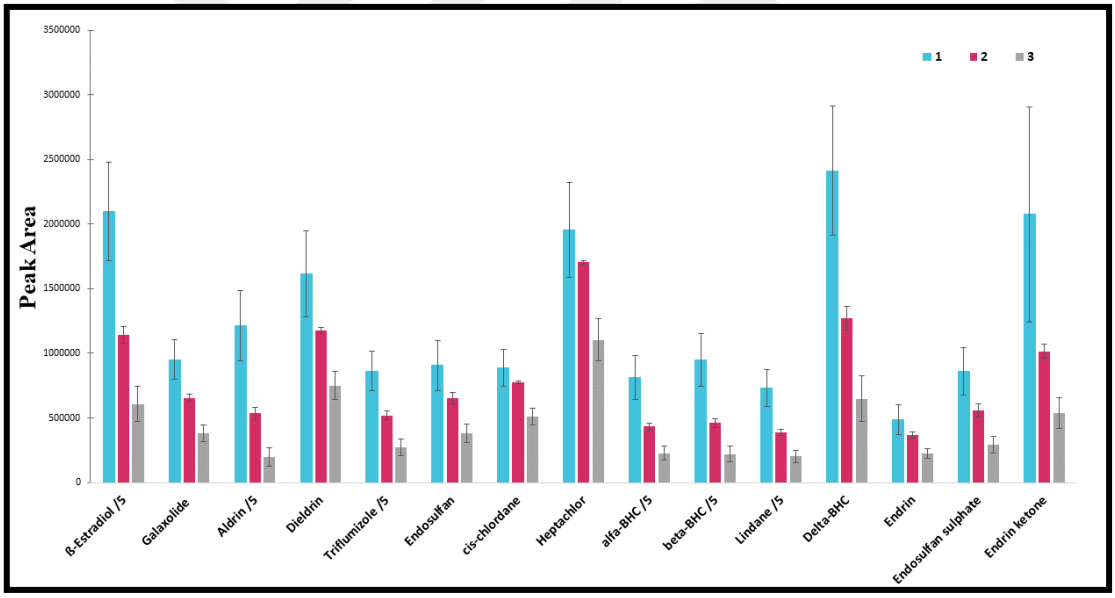


Figure 4.14 Determination of the optimum volume of extraction solvent mixture by spraying repetition (Group 2)

Table 4.14 Experimental parameters used in the optimization study to determine the spraying repetition

Concentration of the aqueous mix standard solution	500 ng mL^{-1}
Volume of the aqueous mix standard solution	5.0 mL
Buffer Solution	pH 9.0 (50 mM borate-HCl buffer)
Volume of the buffer solution	0.50 mL
Extraction solvent	DCE:DCM
Binary mixture ratio	1:1 (v:v)
Spraying repetition	1; 2; 3 (In progress)
Vortex period	15 s

4.1.5 Validation of the SADF-LPME Method

4.1.5.1 Evaluation of Analytical Performance of the SADF-LPME-GC-MS Method

The performance of this extraction method was evaluated by studying the linearity, sensitivity, accuracy, LOD, and LOQ values. The calibration plots for all the EDCs were generated using several standards within the range of about 50-100000 ng g^{-1}. These standards solutions were extracted using the most optimum extraction conditions determined in the univariate optimization study. The approach demonstrated a strong correlation with R^2 values ranging from 0.9830 to 1.000. The LOD and LOQ values obtained with the SADF-LPME-GC-MS method ranged from 1.0 to 6.6 ng $g^{-1}$and 3.2 to 22.1 ng g^{-1}, respectively. The enhancement of detection power (EDP) of the method involved comparing the LODs of each system under investigation. To evaluate the exact effect of the optimized method, the LOD values were compared with the LOD values of the GC-MS directly used to determine the analytes. The EDP values for the target analytes ranged from 3.7 to 158.9. The quantitative performance characteristics of the SADF-LPME-GC-MS method are displayed in Table 4.15. The method's precision, as assessed by

repeatability, was found to be high, as confirmed by %RSD values below 20% for the lowest concentration of the linear working range of all 29 analytes.

Table 4.15 Analytical figures of merit of the SADF-LPME-GC-MS combined method for EDCs

Analyte	LOD, ng g^{-1}	LOQ, ng g^{-1}	Linear Range, ng g^{-1}	R^2	%RSD	EDP
alfa-BHC	6.6	21.9	13.8 – 205.0	0.9950	7.2	3.7
beta-BHC	2.4	7.9	6.4 – 205.0	0.9991	3.8	10.1
Lindane (gama-BHC)	2.6	8.7	8.1 – 205.0	0.9958	12.5	5.4
Diazinon	1.4	4.5	4.8 – 89.7	0.9987	8.0	19.1
delta-BHC	5.4	17.9	13.8 – 205.0	0.9942	6.4	16.8
1,3,4,6,7,8-Hexahydro-4,6,6,7,8,8-hekzame (Galaxolide)	1.3	4.3	3.8 – 154.4	0.9961	10.9	56.0
4-n-Nonylphenol	1.0	3.3	4.7 – 194.7	0.9940	16.4	31.8
Parathion Methyl	1.2	4.1	4.8 – 90.1	0.9979	8.9	62.3
Heptachlor	2.3	7.5	8.0 – 202.6	0.9937	19.4	10.6
Malathion	1.4	4.8	4.8 – 197.1	0.9991	8.3	29.0
Aldrin	3.8	12.6	13.2 – 201.3	0.9987	8.1	9.8
Triflumizole	2.7	9.1	12.5 – 195.9	0.9976	14.1	14.3
Paclobutrazol	1.6	5.3	4.9 – 200.4	0.9981	6.8	27.9
cis-chlordane	2.7	9.1	13.4 – 202.5	0.9996	6.1	15.0
Bisphenol A	1.4	4.7	4.8 – 499.3	0.9992	5.5	43.3
4,4-DDE	2.4	8.1	14.6 – 205.0	0.9830	4.5	7.8
Dieldrin	3.0	10.1	13.2 – 201.7	0.9955	5.3	9.2

Table 4.16 Analytical figures of merit of the SADF-LPME-GC-MS combined method for EDCs (Continued)

Endrin	3.2	10.6	13.8 – 205.0	0.9922	5.5	16.7
Endosulfan	2.2	7.2	13.2 – 201.4	0.9972	3.1	57.2
4,4-DDD	1.5	5.0	13.8 – 205.0	0.9897	11.8	6.0
Endosulfan sulfate	1.4	4.5	4.8 – 89.7	0.9987	8.0	31.6
4,4-DDT	1.7	5.7	8.1 – 205.0	0.9931	17.1	53.6
Carbamazepine	1.3	4.2	4.9 – 504.0	0.9990	5.2	158.9
Endrin ketone	1.3	4.2	6.4 – 205.0	0.9990	6.3	49.3
Methoxychlor	1.1	3.5	13.8 – 205.0	0.9875	16.2	3.8
Estrone	3.5	11.8	12.6 – 198.6	1.00	8.5	80.6
ß-Estradiol	6.6	22.1	24.1 – 505.9	0.9986	9.4	63.5
17α-Ethinylestradiol	1.1	3.8	4.8 – 197.2	0.9990	5.3	50.0
Diltiazem Hydrochloride	1.0	3.2	4.8 – 196.5	0.9949	10.0	24.7

4.1.5.2 Recovery Experiments of the SADF-LPME Method

A validation experiment was conducted to determine the percentage of recoveries for the 29 EDCs and pesticides in seawater, soil, and moss samples. The selected test samples were subjected to the aforementioned procedure and analyzed using the GC-MS system. In order to assess the feasibility of the approach, real sample solutions were prepared using various concentrations of the desired analytes. These solutions were generated using spiking concentrations that fell within the linear operating range of the SADF-LPME-GC-MS method. The peak regions of the analytes spiked in the real sample and deionized water were compared, and the components of the sample matrices were found to have decreasing/increasing effects on the signals of the analytes. Significant disparities can be observed between the signals obtained from the real sample solution, containing the same amount of analyte added artificially, and the signal obtained from the standard solution prepared in deionized water. The matrix matching approach was adopted to eliminate any potential matrix interferences from the sample matrices. Each of the selected samples was augmented with varying standard concentrations in order to generate calibration plots. The specifics may be found in *Section 3.3.3 Preparation of Real Sample Used in Spiked Recovery Experiments*. Each sample was analyzed in four replicates during the recovery trials. The calibration plots of the spiked HS-D-7 coded seawater, soil A, and moss A samples were used to derive an equation for calculating the % recoveries of the spiked HS-D-26 coded seawater, soil B, and moss B samples. Similarly, the calibration plot of the spiked HS-D-26 coded seawater, soil B, and moss B samples was used to derive an equation for calculating the % recoveries of the spiked HS-D-7 coded seawater, soil A, and moss A samples. The study identified the analytes and recorded their percent recovery values at different concentrations in HS-D-26 and HS-D-7 coded seawater samples. The specific details can be found in Table 4.17 and Table 4.20, respectively. The seawater samples exhibited recovery values ranging from 71% to 128%. The findings indicated that the provided method is suitable for conducting analysis of seawater samples. The low standard deviations registered by the analytes signified high repeatability. Since satisfactory recovery results were not recorded for endrin ketone and parathion methyl (70%-130%), a precise matrix matching experiment was performed for the two analytes.

Table 4.17 Percent recovery results using matrix matching approach on seawater sample coded HS-D-26 *(n=4)*

Analyte	Spiked concentration, ng g^{-1}	%Recovery ± SD
alfa-BHC	100.7	95.8 ± 6.7
	170.6	106.5 ± 3.4
beta-BHC	100.7	91.0 ± 5.4
	170.6	105.8 ± 4.5
Lindane (gama-BHC)	51.1	80.3 ± 1.2
	100.7	103.5 ± 3.8
	170.6	109.7 ± 1.4
Diazinon	97.7	94.9 ± 8.0
	196.7	108.3 ± 2.2
	472.5	106.1 ± 4.5
delta-BHC	51.1	92.9 ± 6.9
	100.7	103.9 ± 2.5
	170.6	116.7 ± 2.8
1,3,4,6,7,8-Hekzahydro-4,6,6,7,8,8-hekzame (Galaxolide)	76.8	106.9 ± 2.0
	154.6	110.3 ± 2.6
	371.3	97.6 ± 3.5
4-n-Nonylphenol	96.8	95.8 ± 10.8
	194.9	113.8 ± 1.4
	468.1	96.3 ± 4.8
Parathion Methyl *	49.1	95.4 ± 6.5
	98.2	101.0 ± 4.0
	197.8	106.0 ± 4.2
Heptachlor	100.1	108.0 ± 8.4
	185.5	117.7 ± 0.4
	443.1	77.6 ± 1.4
Malathion	49	105.6 ± 5.8
	98	114.1 ± 3.5
	197.4	112.7 ± 1.9
	474	99.1 ± 1.4
Aldrin	50.1	71.2 ± 3.7
	99.4	126.0 ± 1.3
	439.8	76.8 ± 1.5

Table 4.18 Percent recovery results using matrix matching approach on seawater sample coded HS-D-26 *(n=4)* (Continued)

Triflumizole	48.7	98.0 ± 6.2
	97.4	118.1 ± 8.2
	196.1	114.7 ± 1.9
	405	126.6 ± 13.1
Paclobutrazol	99.6	112.8 ± 1.4
	200	116.5 ± 5.4
	481.8	119.6 ± 5.3
cis-chlordane	99.8	79.1 ± 4.3
	179.6	109.5 ± 0.8
	428	75.6 ± 2.6
Bisphenol A	49.1	114.7 ± 8.0
	98.2	110.9 ± 5.4
	197.7	98.5 ± 5.9
	478.8	100.1 ± 3.3
4,4-DDE	100.7	98.2 ± 3.2
	170.6	106.4 ± 2.6
Dieldrin	50.2	93.2 ± 1.2
	99.6	101.8 ± 2.8
	184.6	109.6 ± 2.0
	440.8	82.9 ± 1.0
Endrin	98.2	78.9 ± 8.6
	197.7	94.1 ± 1.0
Endosulfan	50.1	92.9 ± 2.1
	99.5	123.2 ± 6.0
	184.3	121.4 ± 2.1
	440.1	108.2 ± 1.4
4,4-DDD	100.7	96.0 ± 8.5
	170.6	111.5 ± 0.8
Endosulfan sulphate	51.1	97.7 ± 4.4
	100.7	103.7 ± 6.0
	170.6	113.3 ± 3.0
4,4-DDT	100.7	94.6 ± 6.7
	170.6	112.5 ± 1.6

Table 4.19 Percent recovery results using matrix matching approach on seawater sample coded HS-D-26 *(n=4)* (Continued)

Carbamazepine	49.6	112.1 ± 6.3
	99.1	113.1 ± 2.1
	199.6	109.0 ± 1.1
	479.4	105.6 ± 3.8
Endrin Ketone*	51.1	89.1 ± 5.8
	100.7	95.0 ± 5.4
Metoxychlor	49.1	82.2 ± 9.0
	98.2	116.8 ± 8.3
	197.7	116.0 ± 2.4
Estrone	49.8	79.7 ± 2.7
	99.5	99.6 ± 6.8
	200.4	110.7 ± 5.3
	481.2	104.0 ± 2.9
ß-Estradiol	49.4	80.9 ± 3.1
	98.7	99.8 ± 6.8
	198.8	110.9 ± 5.2
	477.4	103.7 ± 2.2
17α-Ethinylestradiol	49	74.0 ± 4.5
	98	100.4 ± 5.8
	197.4	120.7 ± 2.7
	474	115.8 ± 4.7
Diltiazem HCl	49.1	84.9 ± 8.8
	98.2	95.8 ± 7.7
	197.7	114.5 ± 3.3
	474.8	110.3 ± 3.4

**Exact matrix matching was employed.*

Table 4.20 Percent recovery results using matrix matching approach on seawater sample coded HS-D7 *(n=4)*

Analyte	Spiked concentration, ng g^{-1}	%Recovery ± SD
alfa-BHC	114.8	93.6 ± 3.5
	175.4	96.5 ± 1.9
beta-BHC	114.8	92.3 ± 2.7
	175.4	93.8 ± 1.5
Lindane (gama-BHC)	54.3	123.8 ± 1.9
	114.8	90.4 ± 2.1
	175.4	92.1 ± 1.2
Diazinon	97.6	101.8 ± 4.6
	202.3	97.4 ± 1.6
	493.3	93.6 ± 4.9
delta-BHC	54.3	97.2 ± 4.4
	114.8	87.5 ± 4.3
	175.4	93.4 ± 3.7
1,3,4,6,7,8-Hexahydro-4,6,6,7,8,8-hekzame	87.5	94.9 ± 2.0
	159	94.1 ± 3.6
	387.6	82.0 ± 7.2
4-n-Nonylphenol	97.6	102.6 ± 7.0
	202.3	105.5 ± 3.3
	493.3	100.1 ± 7.6
Parathion Methyl *	112	113.4 ± 8.0
	203.4	88.8 ± 10.8
Heptachlor	114.1	95.0 ± 1.9
	190.8	92.9 ± 1.3
	462.6	77.7 ± 4.2
Malathion	111.8	97.3 ± 2.8
	202.9	98.9 ± 3.8
	494.8	98.7 ± 3.4
Aldrin	53.2	110.9 ± 2.1
	113.4	89.4 ± 1.2
	189.4	78.1 ± 2.8

Table 4.21 Percent recovery results using matrix matching approach on seawater sample coded HS-D7 *(n=4)* (Continued)

Triflumizole	51.8	107.7 ± 8.2
	111.1	91.3 ± 5.8
	201.7	89.9 ± 3.8
	422.8	78.7 ± 0.4
Paclobutrazol	113.6	99.6 ± 0.6
	205.7	98.7 ± 2.2
	503	81.8 ± 3.3
cis-chlordane	113.8	110.9 ± 4.8
	184.7	98.0 ± 1.9
	446.9	76.8 ± 1.0
Bisphenol A	112	98.6 ± 2.1
	203.3	97.8 ± 2.1
	495.7	100.2 ± 2.3
4,4-DDE	114.8	92.0 ± 1.6
	175.4	98.6 ± 1.1
Dieldrin	53.3	125.0 ± 7.2
	113.6	98.7 ± 1.1
	189.8	94.5 ± 2.3
Endrin	112	122.1 ± 0.9
	203.3	96.8 ± 2.7
Endosulfan	53.3	105.3 ± 5.0
	113.5	98.8 ± 0.7
	189.5	94.5 ± 1.8
	459.5	89.4 ± 2.5
4,4-DDD	114.8	91.8 ± 2.6
	175.4	94.8 ± 2.0
Endosulfan sulphate	54.3	110.1 ± 2.7
	114.8	84.0 ± 3.2
	175.4	91.4 ± 1.4
4,4-DDT	114.8	88.3 ± 2.2
	175.4	96.4 ± 2.8
Carbamazepine	113	98.0 ± 1.5
	205.2	94.2 ± 1.3
	500.5	88.7 ± 2.6

Table 4.22 Percent recovery results using matrix matching approach on seawater sample coded HS-D7 *(n=4)* (Continued)

Endrin Ketone*	54.3	122.4 ± 6.0
	114.8	105.2 ± 0.4
	175.4	110.4 ± 3.4
Metoxychlor	112	97.6 ± 3.1
	203.3	92.8 ± 2.5
Estrone	113.5	92.9 ± 3.1
	206	99.7 ± 1.9
	502.3	94.7 ± 0.8
ß-Estradiol	112.6	102.3 ± 3.4
	204.4	103.6 ± 2.1
	498.4	97.2 ± 0.7
17α-Ethinylestradiol	52.2	127.7 ± 2.2
	111.8	80.3 ± 1.0
	202.9	91.7 ± 1.4
Diltiazem Hydrochloride	112	93.1 ± 2.2
	203.3	96.7 ± 3.2
	495.7	89.6 ± 3.7

**Exact match matrix matching was employed.*

The recovery data obtained for soil A and B are given in Table 4.23 and Table 4.27, respectively. The recovery values found for soil A and B samples were comparable, ranging from 73.7% to 130.3% and 74.1% to 130.8%, respectively. Furthermore, a precise matrix matching approach was utilized for parathion methyl. The method can be readily employed to ascertain and regulate the specific EDCs in soil samples.

Table 4.23 Percent recovery results using matrix matching approach on soil sample coded A *(n=4)*

Analyte	Spiked concentration, ng g^{-1}	S
alfa-BHC	54.6	82.5 ± 1.4
	118.2	95.6 ± 5.5
	162.4	100.5 ± 13.6
	455.3	91.9 ± 5.4
beta-BHC	118.2	81.6 ± 6.9
	162.4	103.4 ± 4.6
	455.3	96.8 ± 2.8
Lindane (gama-BHC)	54.6	82.9 ± 1.4
	118.2	92.5 ± 5.5
	162.4	97.0 ± 7.3
	455.3	85.1 ± 2.9
Diazinon	52.2	97.6 ± 7.1
	114.7	119.0 ± 9.2
	187.2	107.9 ± 12.6
	531.5	95.0 ± 5.0
delta-BHC	54.6	81.4 ± 0.7
	118.2	86.0 ± 1.8
	162.4	87.7 ± 10.4
	455.3	79.5 ± 1.1
1,3,4,6,7,8-Hexahydro-4,6,6,7,8,8-hekzame (Galaxolide)	90.1	98.2 ± 1.9
	147.1	91.2 ± 8.7
	417.6	80.8 ± 1.7
4-n-Nonylphenol	51.7	76.6 ± 4.3
	113.7	109.1 ± 11.3
	185.5	102.2 ± 14.5
	526.5	83.7 ± 4.5
Parathion Methyl	188.2	79.2 ± 2.3
	534.3	85.8 ± 5.5

Table 4.24 Percent recovery results using matrix matching approach on soil sample coded A *(n=4)* (Continued)

Heptachlor	53.9	84.8 ± 1.8
	117.5	103.1 ± 3.8
	176.5	99.6 ± 4.0
	498.4	76.4 ± 3.9
Malathion	52.4	75.5 ± 4.1
	115.1	106.6 ± 2.0
	187.8	103.1 ± 4.9
	533.1	97.5 ± 5.7
Aldrin	53.5	110.1 ± 1.8
	116.7	115.8 ± 3.2
	175.2	120.1±1.4
	494.7	82.4±4.4
Triflumizole	52.1	102.2 ± 3.9
	114.4	91.1 ± 3.8
	188.6	89.4 ± 5.5
	455.5	87.5 ± 4.0
Paclobutrazol	117	97.5 ± 7.0
	190.3	101.5 ± 5.7
	541.9	80.3 ± 3.4
cis-chlordane	53.9	88.7 ± 4.6
	117.2	81.4 ± 0.6
	170.9	74.4 ± 1.3
Bisphenol A	115.3	83.0 ± 0.6
	188.1	81.4 ± 10.1
	534.1	76.7 ± 4.0
4,4-DDE	54.6	115.3 ± 10.5
	118.2	103.8 ± 2.0
	162.4	115.7 ± 13.8

Table 4.25 Percent recovery results using matrix matching approach on soil sample coded A *(n=4)* (Continued)

Dieldrin	53.6	113.0 ± 5.1
	117	109.7 ± 6.7
	175.6	115.9 ± 5.5
Endrin	115.3	126.9 ± 7.1
	188.1	99.6 ± 0.9
	534.1	75.9 ± 2.0
Endosulfan	53.6	95.4 ± 4.6
	116.8	88.2 ± 2.4
	175.4	120.1 ± 5.7
	495	118.0 ± 5.0
4,4-DDD	118.2	103.5 ± 3.0
	162.4	115.2 ± 16.8
Endosulfan sulphate	54.6	88.4 ± 11.3
	118.2	110.7 ± 15.5
	162.4	113.7 ± 14.6
	455.3	100.4 ± 4.4
4,4-DDT	54.6	105.4 ± 5.8
	118.2	107.9 ± 6.6
	162.4	116.5 ± 11.1
	455.3	102.9 ± 5.1
Carbamazepine	116.4	83.4 ± 6.5
	189.9	130.3 ± 9.3
	539.2	116.7 ± 4.8
Endrin ketone	54.6	92.1 ± 8.7
	118.2	116.7 ± 8.9
	162.4	123.4 ± 19.4
	455.3	80.7 ± 4.3
Methoxychlor	52.5	74.7 ± 9.2
	115.3	111.1 ± 9.3
	188.1	114.6 ± 2.2

Table 4.26 Percent recovery results using matrix matching approach on soil sample coded A *(n=4)* (Continued)

Estrone	116.8	77.6 ± 3.1
	190.7	82.9 ± 13.3
	541.2	85.8 ± 7.6
ß-Estradiol	115.9	89.5 ± 3.0
	189.2	88.5 ± 12.2
	537	87.5 ± 6.9
17α-Ethinylestradiol	52.4	78.5 ± 3.5
	115.1	88.3 ± 3.9
	187.8	80.7 ± 2.7
	533.1	92.7 ± 5.1
Diltiazem Hydrochloride	115.3	79.4 ± 2.3
	188.1	92.1 ± 2.4
	534.1	73.7 ± 5.2

**Exact match matrix matching was employed.*

Table 4.27 Percent recovery results using matrix matching approach on soil sample coded B *(n=4)*

Analyte	**Spiked concentration, ng g^{-1}**	**%Recovery ± SD**
alfa-BHC	62.7	100.5 ± 7.5
	104.3	113.3 ± 12.5
	201	83.9 ± 6.3
beta-BHC	104.3	118.3 ± 25.1
	201	114.8 ± 12.7
	419.2	87.6 ± 3.6
Lindane (gama-BHC)	62.7	97.9 ± 1.2
	104.3	118.1 ± 10.9
	201	79.6 ± 3.4

Table 4.28 Percent recovery results using matrix matching approach on soil sample coded B *(n=4)* (Continued)

Diazinon	60	83.2 ± 3.4
	101.2	105.5 ± 7.8
	231.7	93.1 ± 1.9
	489.3	105.0 ± 3.4
delta-BHC	62.7	100.3 ± 16.5
	104.3	110.9 ± 4.8
	419.2	123.6 ± 5.3
1,3,4,6,7,8-Hexahydro-4,6,6,7,8,8-hekzame (Galaxolide)	47.1	74.1 ± 3.8
	384.5	122.3 ± 3.2
4-n-Nonylphenol	59.4	82.0 ± 4.7
	229.6	129.1 ± 2.0
	484.7	113.7 ± 5.1
Parathion Methyl *	101.8	102.6 ± 2.8
	233	123.4 ± 0.2
Heptachlor	61.9	103.8 ± 3.9
	103.7	100.0 ± 5.1
	218.5	105.3 ± 1.0
Malathion	60.2	119.2 ± 7.4
	101.6	118.9 ± 10.1
	232.5	87.8 ± 1.2
	490.8	100.9 ± 4.2
Aldrin	61.5	78.9 ± 3.7
	103	93.0 ± 3.1
	216.9	119.5 ± 2.7
Triflumizole	59.8	89.0 ± 5.4
	100.9	118.0 ± 9.8
	231	89.2 ± 0.9
	419.4	114.1 ± 5.6

Table 4.29 Percent recovery results using matrix matching approach on soil sample coded B *(n=4)* (Continued)

Paclobutrazol	61.2	84.1 ± 3.1
	103.2	111.0 ± 1.1
	235.6	105.1 ± 4.1
cis-chlordane	19.7	99.2 ± 4.0
	61.9	97.2 ± 2.2
Bisphenol A	62.7	107.2 ± 3.9
	104.3	129.8 ± 2.0
	201	127.4 ± 4.1
4,4-DDE	62.7	86.6 ± 2.2
	104.3	105.6 ± 9.5
	201	101.2 ± 25.4
Dieldrin	61.6	77.5 ± 0.7
	103.2	89.6 ± 4.2
	217.4	87.9 ± 0.7
Endrin	201	111.2 ± 3.7
	419.2	130.8 ± 2.4
Endosulfan	61.5	119.8 ± 3.8
	103.1	110.5 ± 8.6
	217.1	90.0 ± 4.3
	455.7	84.7 ± 4.6
4,4-DDD	62.7	105.5 ± 4.0
	104.3	113.1± 13.3
	201	87.5 ± 3.5
Endosulfan sulphate	62.7	96.0 ± 1.1
	104.3	96.2 ± 12.5
	201	111.0 ± 2.2
4,4-DDT	62.7	107.9 ± 1.0
	104.3	104.2 ± 5.0
	201	80.8 ± 11.0
Carbamazepine	102.7	115.0 ± 2.7
	235.1	81.6 ± 1.0

Table 4.30 Percent recovery results using matrix matching approach on soil sample coded B *(n=4)* (Continued)

Endrin Ketone	104.3	96.8 ± 17.1
	201	79.6 ± 14.0
Methoxychlor	62.7	109.9 ± 1.8
	104.3	116.1 ± 2.5
	201	92.1 ± 3.2
Estrone	61.1	92.3 ± 5.7
	498.3	115.1 ± 2.7
ß-Estradiol	60.6	91.9 ± 5.9
	102.3	117.1 ± 8.2
	494.4	113.5 ± 2.6
17α-Ethinylestradiol	101.6	130.5 ± 4.5
	232.5	101.2 ± 8.4
	490.8	110.3 ± 5.4
Diltiazem Hydrochloride	62.7	87.9 ± 0.5
	201	127.4 ± 10.0

*Exact match matrix matching was employed.

The recovery values for moss A and B samples are provided in Table 4.31Table 4.34, respectively. Here, good recovery levels, similar to other sample matrices were achieved. The impact of matrix interferences on the signals of the analytes was assessed for 4-n-nonylphenol, parathion methyl, heptachlor, 4,4-DDE, dieldrin, and endrin ketone. The precise and accurate determination of these analytes was achieved by employing the matrix matching approach. The percent recovery values obtained for moss A and B samples were in the ranges of 77.6–126.9% and 75.9 – 132.4%, respectively.

Table 4.31 Percent recovery results using matrix matching approach on moss sample coded A *(n=4)*

Analyte	Spiked concentration, ng g^{-1}	%Recovery ± SD
alfa-BHC	52.4	112.8 ± 1.2
	104.7	120.8 ± 22.3
beta-BHC	52.4	108.6 ± 3.5
	104.7	101.1 ± 3.9
	173.7	113.1 ± 6.1
Lindane (gama-BHC)	52.4	94.4 ± 1.5
	104.7	91.8 ± 16.2
	173.7	105.7 ± 3.2
Diazinon	50.1	92.0 ± 1.6
	101.7	107.2 ± 4.3
	200.2	99.8 ± 4.7
	483.9	103.3 ± 5.1
delta-BHC	52.4	108.4 ± 7.4
	104.7	104.9 ± 6.2
	173.7	119.5 ± 7.0
	414.6	109.0 ± 1.1
1,3,4,6,7,8-Hexahydro-4,6,6,7,8,8-hekzame (Galaxolide)	157.3	91.2 ± 0.8
	380.2	84.4 ± 5.5
4-n-Nonylphenol *	100.7	84.3 ± 5.9
	198.4	104.3 ± 19.1
Parathion Methyl *	102.2	98.6 ± 7.9
	201.3	106.3 ± 5.8
Heptachlor *	104.1	92.2 ± 3.3
	188.8	95.2 ± 6.2
Malathion	102	126.9 ± 17.4
	200.9	115.7 ± 7.4
	485.4	99.1 ± 3.0

Table 4.32 Percent recovery results using matrix matching approach on moss sample coded A *(n=4)* (Continued)

Aldrin	51.4	120.5 ± 2.3
	103.4	102.9 ± 2.8
	187.4	105.1 ± 7.5
	450.4	92.1 ± 0.5
Triflumizole	50	100.3 ± 5.4
	101.3	99.5 ± 4.9
	199.6	86.6 ± 11.7
	414.8	85.8 ± 3.8
Paclobutrazol	51.1	92.6 ± 3.1
	103.6	104.8 ± 5.0
	203.6	114.8 ± 1.8
	493.4	110.8 ± 2.8
cis-chlordane	103.9	105.5 ± 6.3
	182.8	96.6 ± 2.7
Bisphenol A	50.4	114.9 ± 1.9
	102.2	111.8 ± 3.7
	201.2	105.3 ± 1.8
	486.3	91.7 ± 1.4
4,4-DDE*	52.4	122.0 ± 14.2
	104.7	110.5 ± 4.9
Dieldrin*	103.7	116.2 ± 8.0
	187.8	107.6 ± 10.0
Endrin	201.2	106.5 ± 2.8
	486.3	86.0 ± 7.0
Endosulfan	187.6	114.9 ± 4.4
	450.7	94.3 ± 4.9
4,4-DDD	104.7	82.4 ± 9.9
	173.7	97.5 ± 6.1
	414.6	87.9 ± 1.0

Table 4.33 Percent recovery results using matrix matching approach on moss sample coded A *(n=4)* (Continued)

Endosulfan sulphate	52.4	116.1 ± 8.8
	104.7	113.6 ± 9.0
	173.7	80.6 ± 3.4
4,4-DDT	104.7	122.2 ± 12.2
	173.7	105.3 ± 2.6
	414.6	77.6 ± 5.5
Carbamazepine	50.8	100.9 ± 6.2
	103.1	110.4 ± 4.9
	203.2	102.3 ± 7.9
	491	91.6 ± 1.9
Endrin Ketone*	173.7	95.5 ± 4.7
Methoxychlor	50.4	96.6 ± 4.8
	102.2	120.2 ± 7.2
	201.2	89.5 ± 0.5
	486.3	87.4 ± 4.7
Estrone	51	88.3 ± 2.6
	103.5	99.4 ± 7.2
	203.9	106.7 ± 5.6
	492.8	100.8 ± 4.3
ß-Estradiol	102.7	93.0 ± 7.5
	202.3	104.5 ± 5.9
	489	101.5 ± 4.0
17α-Ethinylestradiol	50.3	117.9 ± 9.3
	102	122.5 ± 1.0
	200.9	111.3 ± 1.8
	485.5	102.3 ± 2.0
Diltiazem Hydrochloride	201.2	116.0 ± 7.8
	486.3	108.5 ± 2.9

* Exact match matrix matching was employed.

Table 4.34 Percent recovery results using matrix matching approach on moss sample coded B *(n=4)*

Analyte	Spiked concentration, ng g^{-1}	%Recovery ± SD
alfa-BHC	51.6	101.6 ± 2.8
	102.7	80.6 ± 3.5
beta-BHC	51.6	101.5 ± 0.7
	102.7	84.7 ± 3.5
	196.5	91.8 ± 3.9
Lindane (gama-BHC)	51.6	107.2 ± 0.1
	102.7	91.9 ± 1.1
	196.5	98.7 ± 6.1
Diazinon	49.4	98.1 ± 8.8
	99.7	108.5 ± 3.9
	226.6	93.3 ± 3.7
	473.1	97.7 ± 0.6
delta-BHC	51.6	86.5 ± 1.9
	102.7	82.1 ± 1.8
	196.5	95.3 ± 1.8
	405.3	90.0 ± 2.5
1,3,4,6,7,8-Hexahydro-4,6,6,7,8,8-hekzame (Galaxolide)	38.8	94.9 ± 1.8
	78.3	79.2 ± 2.2
	178	108.6 ± 1.8
	371.7	121.7 ± 0.9
4-n-Nonylphenol *	98.7	99.4 ± 8.4
	224.5	91.2 ± 1.8
Parathion Methyl *	102.2	80.0 ± 4.9
	227.8	112.9 ± 1.4
Heptachlor *	102.1	83.1 ± 4.4
	213.7	102.3 ± 3.1
Malathion	100	81.4 ± 3.5
	227.3	91.9 ± 3.9
	474.5	99.5 ± 1.2

Table 4.35 Percent recovery results using matrix matching approach on moss sample coded B *(n=4)* (Continued)

Aldrin	50.6	99.1 ± 2.4
	101.4	81.6 ± 1.4
	212.1	92.8 ± 5.7
	440.3	107.9 ± 3.0
Triflumizole	99.3	105.6 ± 1.0
	225.9	102.3 ± 8.4
	405.5	120.4 ± 5.4
Paclobutrazol	50.4	96.6 ± 1.7
	101.6	99.3 ± 1.8
	230.4	88.5 ± 1.8
	482.3	90.2 ± 0.7
cis-chlordane	50.9	75.9 ± 7.2
	206.9	100.7 ± 4.2
Bisphenol A	49.6	91.9 ± 9.9
	100.1	99.4 ± 5.7
	227.7	99.2 ± 3.2
	475.4	108.2 ± 5.8
4,4-DDE*	51.6	114.3 ± 4.4
	102.7	94.1 ± 2.5
Dieldrin*	101.6	92.0 ± 6.9
	212.6	93.7 ± 11.1
Endrin	227.7	92.6 ± 5.0
	475.4	120.1 ± 6.6
Endosulfan	212.3	83.1 ± 5.3
	440.6	107.6 ± 1.9
4,4-DDD	51.6	92.9 ± 4.0
	196.5	114.6 ± 14.4
	405.3	108.1 ± 4.6
Endosulfan sulphate	102.7	106.4 ± 8.0
	196.5	128.2 ± 5.7

Table 4.36 Percent recovery results using matrix matching approach on moss sample coded B *(n=4)* (Continued)

4,4-DDT	196.5	113.3 ± 12.0
	405.3	132.4 ± 15.9
Carbamazepine	50.1	79.3 ± 0.8
	101.1	99.2 ± 0.5
	229.9	97.5 ± 2.7
	479.9	109.6 ± 3.7
Endrin Ketone*	102.7	88.6 ± 0.4
	196.5	97.7 ± 4.8
Methoxychlor	49.6	78.4 ± 7.3
	100.1	99.6 ± 2.8
	227.7	121.8 ± 9.3
	475.4	112.3 ± 6.7
Estrone	50.3	91.3 ± 6.4
	101.5	123.5 ± 28.6
	230.7	90.4 ± 6.2
	481.7	99.5 ± 3.6
ß-Estradiol	49.9	91.9 ± 9.0
	229	89.9 ± 6.3
	478	99.1 ± 3.5
17α-Ethinylestradiol	100	89.5 ± 0.5
	227.3	89.4 ± 2.9
	474.5	97.5 ± 0.7
Diltiazem Hydrochloride	100.1	88.8 ± 7.6
	227.7	93.8 ± 2.7
	475.4	89.1± 2.5

* Exact match matrix matching was employed.

4.1.5.3 Real Sample Applications

The SADF-LPME-GC-MS method was used to evaluate two hundred samples collected from the Horseshoe and Faure Islands, Antarctica. This method was utilized to accurately quantify the quantities of 29 distinct pesticides and EDCs. Aqueous standard solutions were prepared for these samples, following the procedures described in the document "*3.3.4 Preparation of Real Samples Collected from Antarctic Region".* The analytes were examined using the most suitable chromatographic conditions following the extraction of samples using the optimum SADF-LPME procedure. Based on the detection limits of the developed method, none of the samples analyzed displayed any analytical signals specific to pesticides or EDCs. In order to reassess the samples for the matrix effect, a concentrated mixture of standard solutions of EDCs (5000 ng g^{-1}) was introduced to the original samples. Figure 4.15 displays both the initial signal and the signal obtained for diazinone after introducing a 5000 ng g^{-1} standard to the seaweed sample. The results demonstrated exceptional accuracy and precision in measuring the analytes, without any noticeable influence from the matrix. These findings support the notion that the proposed extraction approach can be utilized to assess and track potential EDCs in Antarctica.

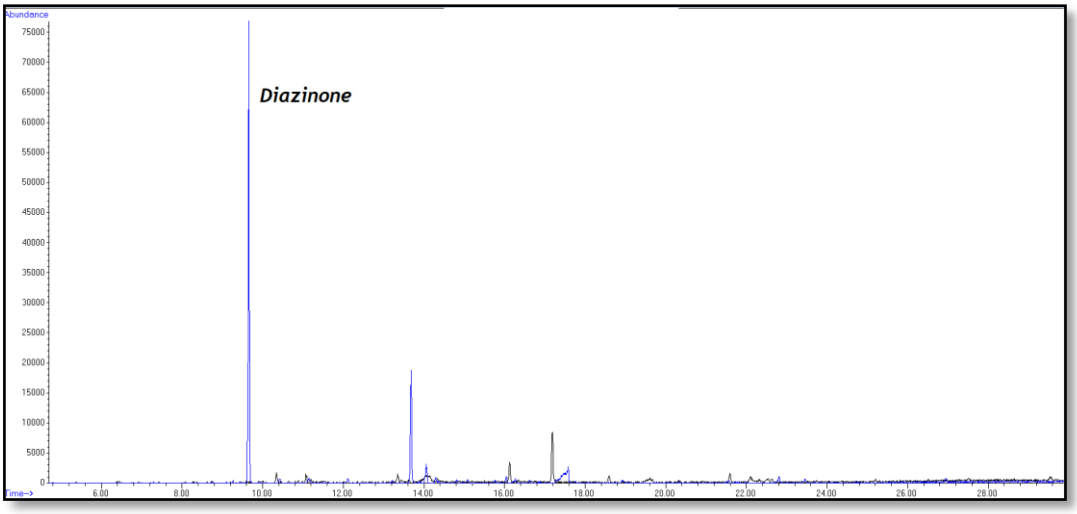


Figure 4.15 The selected ion chromatograms were acquired utilizing the diazinon analyte from a seaweed sample collected from Horseshoe Island, along with a 5000 ng/g mixed reference solution of the same material. (m/z: 179)

4.2 Removal of Cadmium Ions From Wastewater by Using $CuFe_2O_4$ Nanoparticle Assisted Batch Type Surface Adsorption Procedure Based Treatment Strategy

4.2.1 Characterization of Magnetic $CuFe_2O_4$ Nanoparticles

The morphology characteristic of the synthesized magnetic $CuFe_2O_4$ nanoparticles was determined by FE-SEM analysis to examine the surface area of the synthesized material at the nanoscale as shown in Figure 4.16.Figure 4.16 FE-SEM images obtained for CuFe2O4 nanoparticles at different magnification (a) 5 µm (b) 1 µm

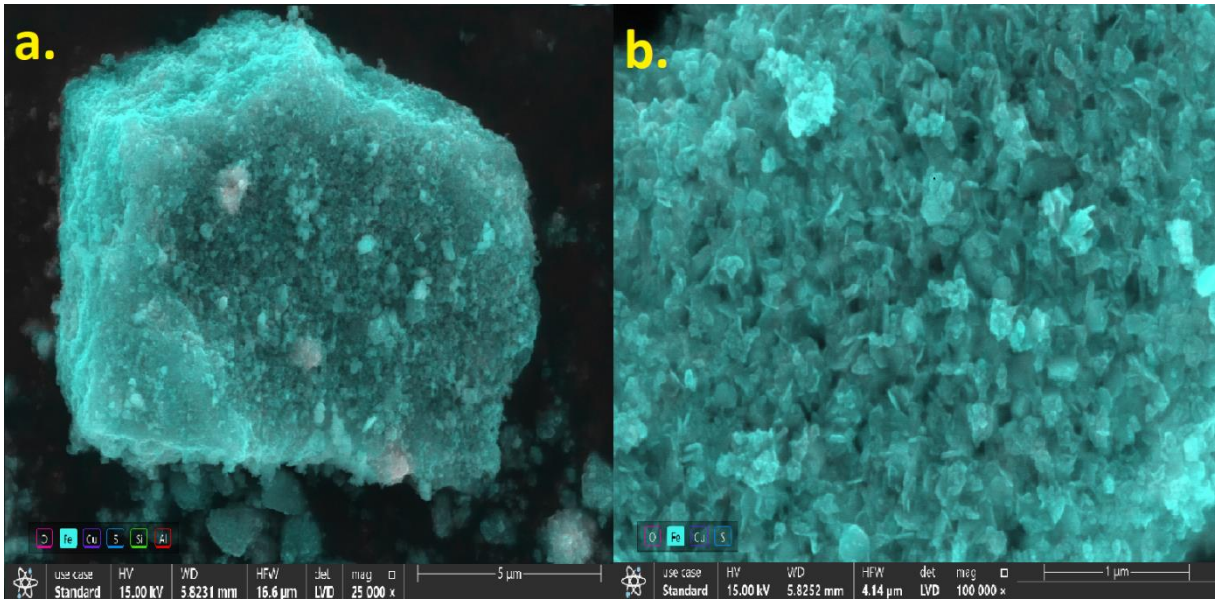


Figure 4.16 FE-SEM images obtained for $CuFe_2O_4$ nanoparticles at different magnification (a) 5 µm (b) 1 µm

Figure 4.17 displays the phase composition and crystal structure of the specimen analyzed through X-ray diffraction. Based on the X-ray diffraction (XRD) analysis, it was determined that the material comprised the distinct constituents of $CuFe_2O_4$.The diffraction peaks observed in the $CuFe_2O_4$ samples were at 35.81°, 36.53°, 42.42°, 57.14°, and 61.57°. The observed diffraction peaks indicated consistence of the crystallographic planes of $CuFe_2O_4$ (JCPDC 01-077-0010) [425].

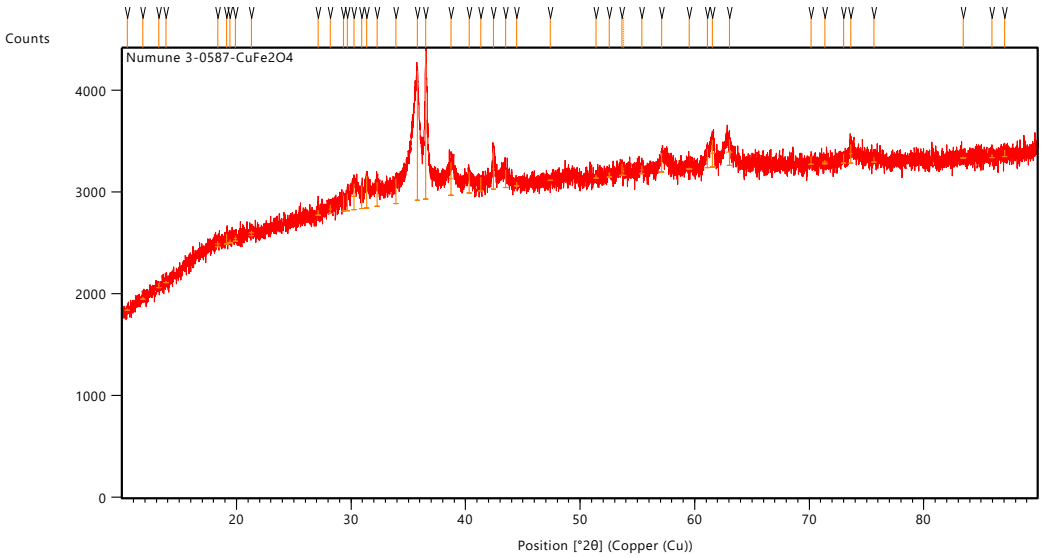


Figure 4.17 Powder XRD pattern obtained for $CuFe_2O_4$ nanoparticles

The surface area of the synthesized $CuFe_2O_4$ nanoparticles was examined by the Brunauer-Emmett-Teller Method (BET) and the specific surface area of the nanoparticles were calculated as 5.810 m^2 g^{-1}. The multi-point BET results are shown in Figure 4.18. The C constant was determined as 45.331, which indicates the magnitude of the $CuFe_2O_4$ nanoparticles/cadmium ions. The linear equation was reported as y = 586.18x + 1322 with 0.9987 R^2 value.

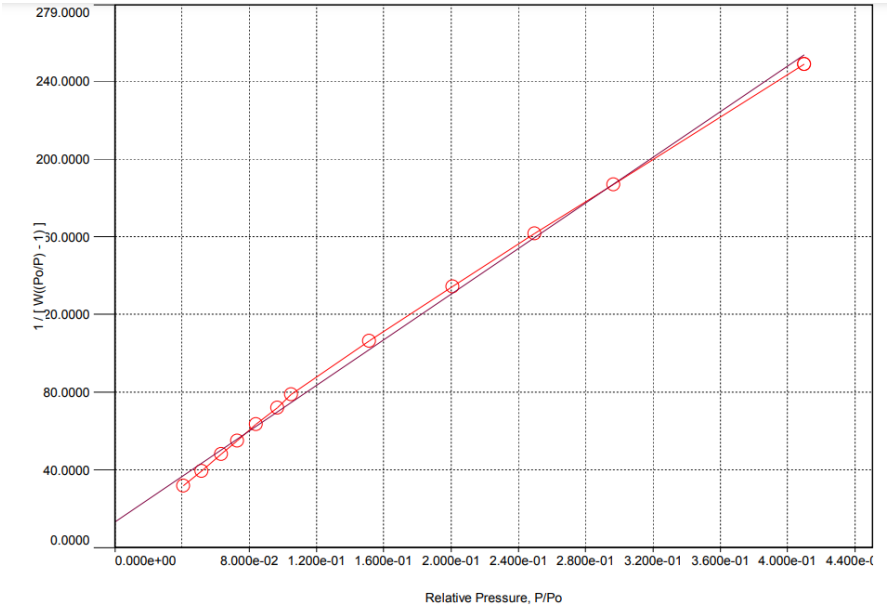


Figure 4.18 The linear regression of $CuFe_2O_4$ nanoparticles obtained by multi-point BET

4.2.2 Optimization of the $CuFe_2O_4$ Nanoparticle Assisted Batch Type Surface Adsorption Based Treatment Procedure

In order to achieve accurate predictions of future experimental outcomes, it is imperative to optimize the adsorbent properties, the adsorption conditions, and the physicochemical composition of the contaminants. Through meticulous analysis and precise adjustments of these factors, the precision and reliability of the generated models can be substantially enhanced. Consequently, this may result in a significant decrease in the quantity of required experiments [426]. Thus, the experimental parameters were optimized within the scope of the study to achieve the highest possible removal efficiency for cadmium ions from wastewater. The present study employed a univariate optimization strategy to assess the experimental parameters that had a direct impact on the removal efficiency of the analyte. These parameters included buffer solution type, buffer solution volume, magnetic $CuFe_2O_4$ nanoparticle amount, mixing type, and period. The study involved determining the optimal value of each variable and evaluating the impact of these variables on the removal efficiency while maintaining constant experimental conditions for other factors. In order to assess the efficacy of the magnetic $CuFe_2O_4$ nanoparticle in removing Cd^{2+} from aqueous solutions, the absorbance value of a 4.0 mg L^{-1} Cd^{2+} aqueous standard solution (influent) was compared to the absorbance values obtained after the removal procedure was applied to aqueous standard solutions containing Cd^{2+} at the same concentration (effluent). The percent removal efficiency (%RE) was subsequently calculated. The %RE was computed using the equation presented in Equation 3.1. The optimal condition was determined by selecting the parameter with the highest %RE value, which was calculated based on low standard deviation values obtained from three replicate samples.

$$\%RE = \frac{A_i - A_f}{A_i} X\ 100 \qquad \textbf{(Equation 3.1)}$$

A_i = absorbance value of the influent solution

A_f = absorbance value of the effluent solution

4.2.2.1 Determination of pH of the Solution and Buffer Solution Volume

The influence of solution pH on the surface charge of the adsorbent material, as well as ionization and speciation of the adsorbate are critical factors in the adsorption process of heavy metals [427]. To enhance the interaction between the analyte and nanocomposite and attain optimal adsorption efficiency, the aqueous solution was subjected to pH adjustments using buffer solutions. The impact of solution pH on treatment efficiency was subsequently examined. Buffer solutions with pH values ranging from 5.0 to 10 were employed for this purpose. Throughout the experiments, the pH of the buffered solution was monitored with a pH meter, while the pH of the buffered solution was evaluated following the addition of the nanomaterial. The findings indicated that the absorbance values remained constant in the acidic range (pH 5.0-7.0) irrespective of the influent absorbance value, thereby suggesting the absence of cadmium removal at these pH levels. It was discovered that the interaction between the analyte and the magnetic $CuFe_2O_4$ nanoparticle was hindered due to the lack of an appropriate ionic balance. The reduced removal efficiency observed under low pH conditions can be attributed to the electrostatic repulsion forces between positively charged H_3O^+ and Cd^{2+} ions. At acidic pH levels, H_3O^+ exhibits a higher concentration than Cd(II) ions, resulting in a competition for active sites of magnetic $CuFe_2O_4$ nanoparticle. Consequently, Cd^{2+} ions remain unbound and present in the solution. The rise in pH levels resulted in the substitution of H_3O^+ ions by Cd^{2+} ions, thereby enhancing the adsorption yield of Cd^{2+} ions. The high %RE value recorded in the basic region is depicted in Figure 4.19.

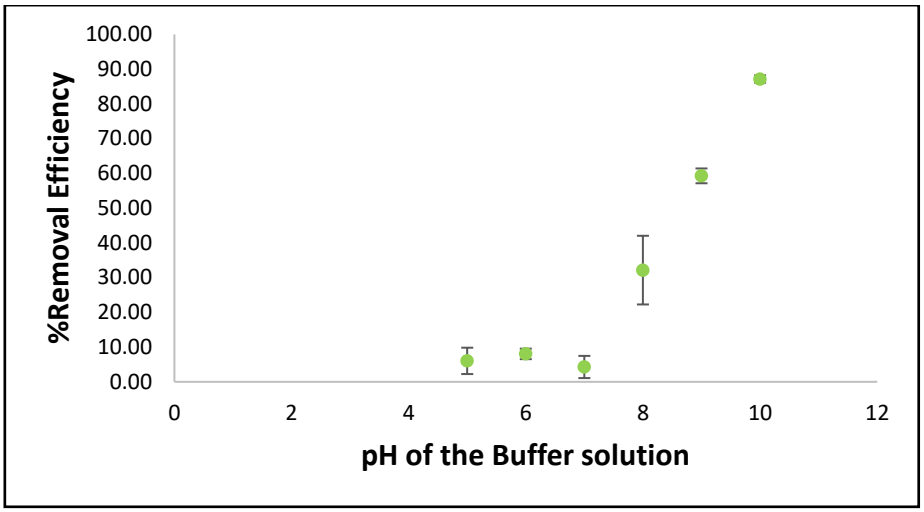


Figure 4.19 A plot of %RE against different buffer solutions, n=3 for the error bars (*Experimental conditions: 40 mL 4.0 mg L^{-1} Cd^{2+} aqueous standard solution;2.0 mL of buffer solution; 50 mg $CuFe_2O_4$ nanoparticle; 60 s contact period with the aid of vortex mixing*)

The aforementioned scenario can be elucidated through various adsorption mechanisms expounded in literature sources. Reed and Matsumoto proposed (Figure 4.20) that pH can influence the formation of different cadmium species [428]. The significance of the hydrolysis extent of Cd^{2+} ions is negligible until a pH of approximately 7.5. Evidently, the concentration of $Cd(OH)^{+}$ ions attains its maximum level at approximately pH 9.5. At pH levels exceeding 8.0, the removal of Cd^{2+} ions may occur through both adsorption and precipitation mechanisms, whereby the ions are converted into $Cd(OH)_2$.

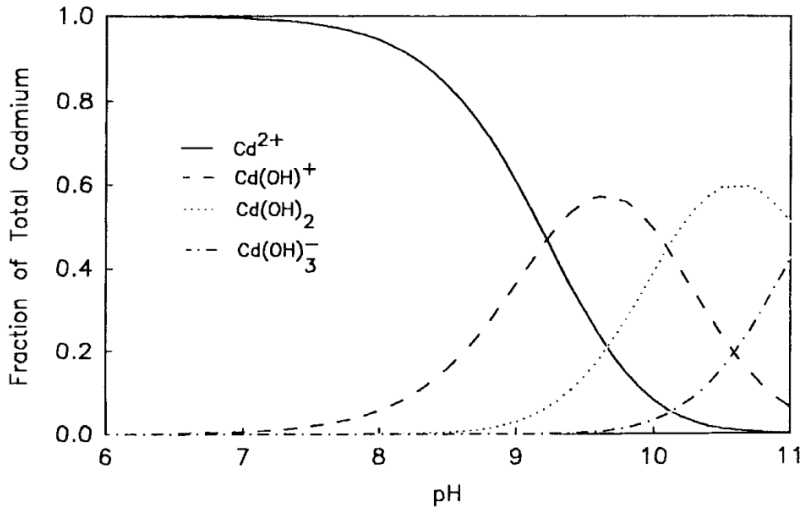


Figure 4.20 Fractions of Cd(II) depending on the pH [428]

The observed alteration in pH could potentially signify the displacement of the -OH^- ion instead of the nanomaterial with the analyte, thereby elucidating the phenomenon of cadmium removal. To substantiate this hypothesis, an experiment was conducted on a sample without magnetic $CuFe_2O_4$ nanoparticle, and it was observed that there was noteworthy disparity between the analyte signal in the effluent and influent at pH 10. The removal efficiency was recorded as 44.6% in the absence of the nanoparticle. On the other hand, the removal efficiency of the samples prepared at pH 9.0 without nanoparticle use was only 6.9%. By comparing this result with the experiment performed with the nanoparticles at the same pH value, the difference in removal efficiency was noted as 60.0%. Since a significant percentage of the removal of the analyte was attributed to the pH of the solution at the pH 10 value, pH 9.0 was selected as the optimal condition for subsequent experiments due to the nanoparticles playing a more significant role in the removal process.

Following the determination of the optimal pH level, experiments were conducted to ascertain the quantity of buffer solution necessary to establish a stable ionic equilibrium conducive for adsorption in the aqueous medium. The samples were subjected to analysis under equivalent conditions after being prepared with buffer solutions of varying volumes (1.0, 1.5, 2.0, and 2.5 mL). The findings as presented in Figure 4.21 shows increasing %REs with increasing buffer solution volume up to 2.0 mL before it declined at 2.5 mL. Thus, the optimal volume of the buffer solution was selected as 2.0 mL.

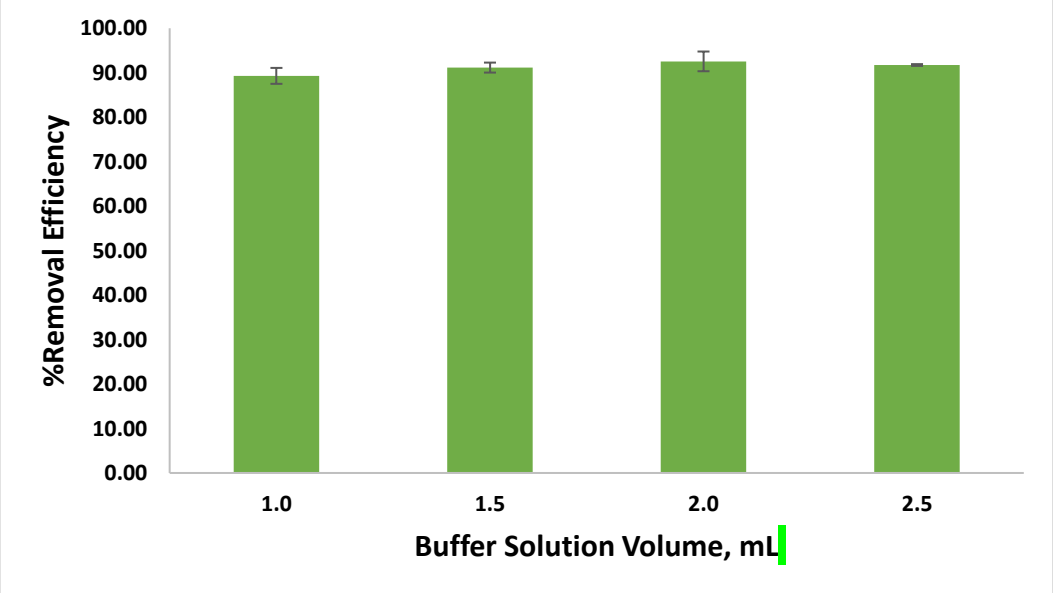


Figure 4.21 A plot of %RE values against different volumes of buffer solution, n=3 for the error bars (*Experimental conditions: 40 mL 4.0 mg L^{-1} Cd^{2+} aqueous standard solution;0.50 M borate-HCl buffer solution; 50 mg $CuFe_2O_4$ nanoparticle; 60 s contact period with the aid of vortex mixing*)

4.2.2.2 Determination of Magnetic $CuFe_2O_4$ Nanoparticle Amount

The amount of adsorbent employed is a critical factor that can significantly influence the adsorption of heavy metals from solution [429]. The application of a considerable amount of nanomaterial has been noted to increase the surface area, thereby exerting a notable influence on the process of adsorption. The reason for this phenomenon is that a greater surface area enables a higher adsorption capacity of the analyte, leading to an enhanced interaction between the magnetic $CuFe_2O_4$ nanoparticle surface and the analyte. In light of the aforementioned factors, varying amounts (50, 75, 100, and 150 mg) of the nanoparticle were employed in the removal process to ascertain the optimal amount for effective removal of cadmium ions. As illustrated in Figure 4.22, a positive correlation was observed between the %RE and the quantity of magnetic $CuFe_2O_4$ nanoparticle, with all four tested amounts recording over 80% removal efficiency. Similar results were observed for 100 mg and 150 mg as indicated by the absence of analytical signals of cadmium in the FAAS measurements. The 100 mg amount was selected as optimum value because it produced a very low relative standard deviation and was more economical relative to the 150 mg amount.

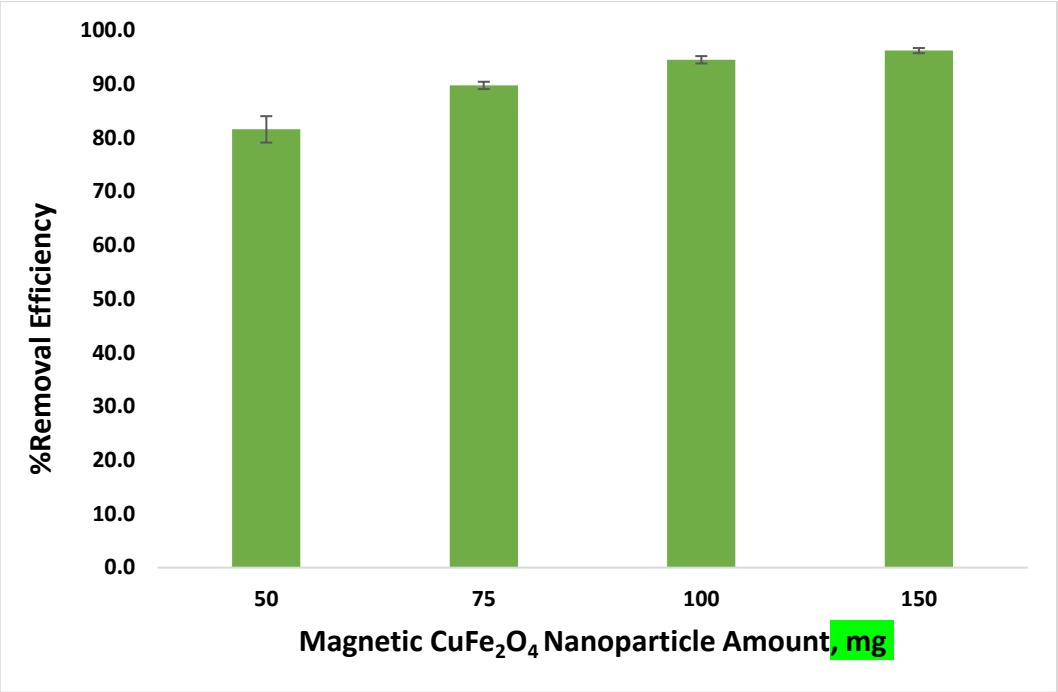


Figure 4.22 A plot of %RE values against different amounts of magnetic $CuFe_2O_4$ nanoparticle, n=3 for the error bars (*Experimental conditions: 40 mL 4.0 mg* L^{-1} Cd^{2+} *aqueous standard solution;2.0 mL of 0.50 M borate-HCl buffer solution; 60 s contact period with the aid of vortex mixing*)

4.2.2.3 Determination of Agitation Type and Period

The mixing procedure is a crucial step that facilitates optimal interaction between the target analyte and the adsorbent. To ascertain the optimal %RE, three mixing approaches including ultrasonication, vortexing, and mechanical shaking were employed for a duration of 60 seconds. In addition, one experiment was performed without mixing in order to determine the true impact of mixing on removal efficiency. The outcomes of the experiment carried out without mixing exhibited significantly low efficiency, as depicted in Figure 4.23. The results indicated that the vortex mixing technique is the most suitable option due to its straightforward implementation and relatively reliable %RE results.

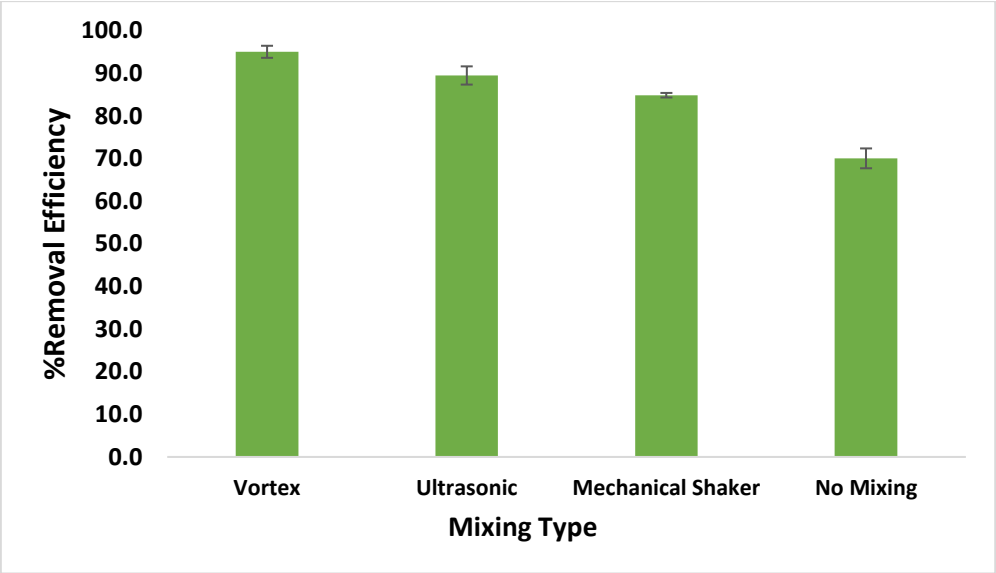


Figure 4.23 A plot of %RE values against different mixing types, n=3 for the error bars (*Experimental conditions: 40 mL 4.0 mg* L^{-1} Cd^{2+} *aqueous standard solution;2.0 mL of 0.50 M borate-HCl buffer solution; 100 mg* $CuFe_2O_4$ *nanoparticle; 60 s contact period with the aid of mixing*)

The final optimized parameter pertained to the mixing period, which was aimed at further maximizing the interaction between the analyte of interest and the magnetic $CuFe_2O_4$ nanoparticle. Extended mixing duration may result in the liberation of the targeted analyte from the surface of the adsorbent back into solution. Conversely, the efficiency of the nanomaterial in collecting the analyte may be compromised by a limited duration or short-time of mixing. The occurrence of periodic issues may result in reduced efficiency of removal. In this instance, the mixing procedure was implemented for varying durations of 30, 45, 60, 75, and 90 seconds using the vortex apparatus to ascertain the optimal mixing period that yields the highest %RE. The applied durations were compared, and it was observed that a significant increase was attained by increasing the mixing period from 30 to 60 seconds. For the longer periods, the removal efficiency decreased and remain similar for the highest two periods. The contact period of 60 seconds was deemed optimal due to its highest %RE value with high repeatability, as presented in Figure 4.24.

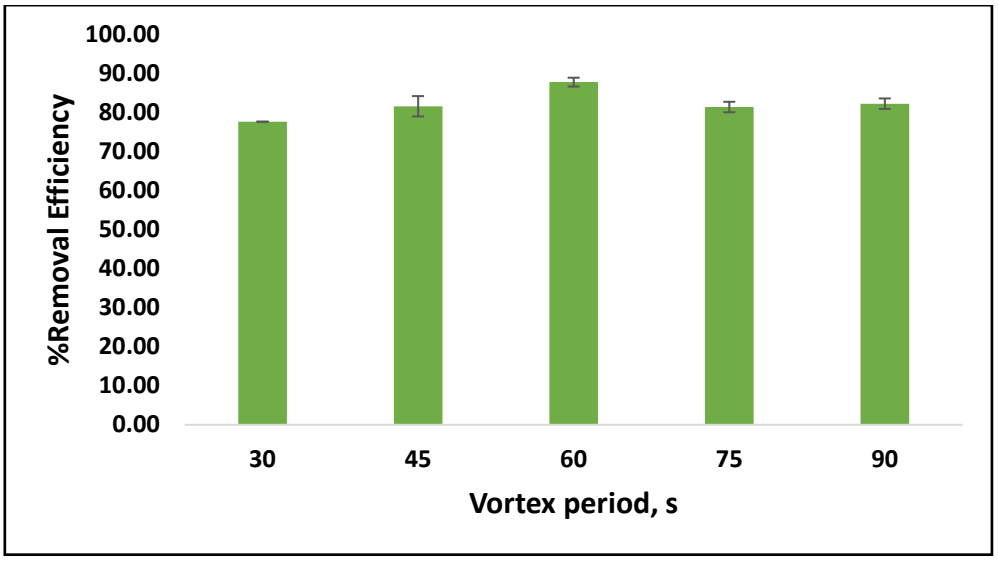


Figure 4.24 A plot of %RE values against different vortex periods, n=3 for the error bars (*Experimental conditions: 40 mL 4.0 mg L^{-1} Cd^{2+} aqueous standard solution; 2.0 mL of 0.50 M borate buffer solution; 100 mg $CuFe_2O_4$ nanoparticle; contact period with the aid of vortex mixing*)

4.2.3 Evaluation of Removal Efficiency of the Developed Method

The effectiveness of the removal method was evaluated by conducting removal efficiency studies with synthetic wastewater samples. Prior to this, the optimal removal parameters were identified through univariate optimizations. This assessment aimed to determine the feasibility and efficiency of the devised removal method. To accomplish this objective, synthetic wastewater samples were spiked with cadmium at predetermined quantities (ranging from 0.25 to 15 mg L^{-1}) to attain samples with ascending levels of concentration. Prior to commencing the removal experiments, the aforementioned samples were denoted as influent specimens and subjected to measurement in the FAAS system. The instrumental system's ability to measure cadmium in synthetic wastewater samples was assessed by generating a calibration plot of recorded absorbance values against increasing cadmium concentrations (Figure 4.25).

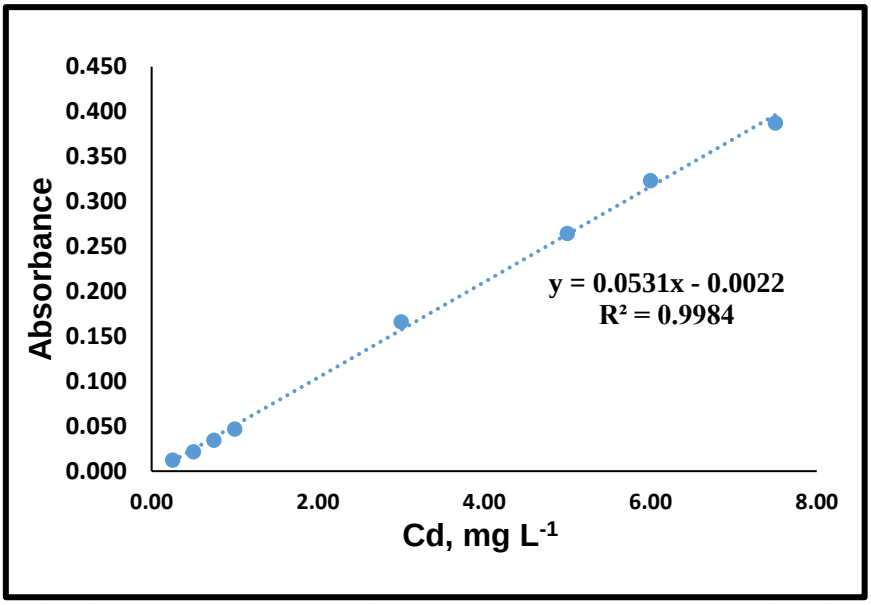


Figure 4.25 Calibration plot indicates the linear working range of the FAAS system for cadmium(II) ions in synthetic wastewater samples

The linear operating range of the calibration plot was determined to be between 0.25 and 7.50 mg L^{-1} with good linearity as indicated by 0.9984 coefficient of determination. The LOD and LOQ of the analytes were calculated using Equations 4.1 and 4.2, respectively, where the SD was derived from 6 repetitive measurements of the lowest analyte concentration in the dynamic operating range. As a result, the calculated LOD and LOQ values were found to be 0.06 and 0.20 mg L^{-1}, respectively.

$$\mathbf{LOD}=\frac{3*SD}{m} \qquad \textbf{(Equation 4.1)}$$

$$\mathbf{LOQ}=\frac{10*SD}{m} \qquad \textbf{(Equation 4.2)}$$

Following the application of the optimal removal procedure to the influent solutions, the final solutions (effluents) were subjected to analysis under ideal conditions of the FAAS system. The linear equation of the calibration plot was used to calculate the concentration of cadmium that corresponded to the absorbance value obtained from the effluent solutions. The estimation of removal efficiency was conducted for each concentration utilizing the aforementioned Equation 3.1. In cases where effluent solutions yielded no discernible analytical signal (S/N≤3), the concentration of the effluent was deemed to represent the method's estimated limit of detection, and the equation was subsequently employed to calculate the removal

efficiency. Table 4.37 displays the removal efficiency through the enumeration of outcomes.

Table 4.37 The percent removal efficiency results for different concentrations of cadmium

Influent concentration, mg L^{-1}	**Effluent concentration, mg L^{-1}**	**%Removal efficiency ± standard deviation**
1	-**	≥ 91.0
2	0.22 ± 0.04	88.9 ± 2.0
4	0.47 ± 0.08	88.2 ± 1.9
8	1.75 ± 0.17	78.2 ± 2.2
10	2.54 ± 0.22	74.6 ± 2.2
15	4.89 ± 0.52	67.4 ± 3.4

Calculated from linear equation

****Calculated from the LOD value***

The findings presented in Table 4.37 demonstrated an inverse correlation between the concentration of cadmium and the removal efficiency. However, it was ascertained that a removal efficiency exceeding 68% could be attained even at the highest tested concentration of 15 mg L^{-1}, which is quite a high concentration for environmental water resources. This validated the magnetic $CuFe_2O_4$ nanoparticles as a suitable adsorbent for the removal of cadmium under optimum conditions of the method.

Consequently, the equilibrium data of the adsorption process in synthetic wastewater was analyzed via the Langmuir adsorption model with the aim of determining the suitable model.

The Langmuir equation, which is based on the theory that there are a limited number of homogenously distributed binding sites over the adsorbent surface, is known to be the most frequently used isotherm model [416][417]. The non-linear equation of this Langmuir isotherm model is shown in Equation 3.3.

$$\boldsymbol{q_e = \frac{q_m K_L C_e}{1+K_L C_e}} \qquad \textbf{(Equation 3.3)}$$

In the Langmuir equation, q_m and K_L represent the maximum adsorption capacity of a monolayer (mg/g) and the Langmuir constant (L/mg) related to the apparent adsorption energy. Calculating q_m and K_L as regression constants requires linearization of the mathematical model followed by linear regression on the dependent variable q_e against the independent variable C_e (Table 4.38).

Table 4.38 Linearization of the Langmuir model [419]

Linear form	Plot	Slope	Intercept
$\boldsymbol{\frac{1}{q_e} = \frac{1}{K_L q_m C_e} + \frac{1}{q_m}}$	$\frac{1}{q_e}$ against $\frac{1}{C_e}$	$\frac{1}{K_L q_m}$	$\frac{1}{q_m}$

The R_L value is a dimensionless constant separation factor that states the Langmuir isotherm characteristics and indicates the type of the isotherm to be either $R_L = 0$ (irreversible), $0 < R_L < 1$ (favourable), $R_L = 1$ (linear), or $R_L > 1$ (undesirable).

$$\boldsymbol{R_L = \frac{1}{1+K_L C_e}} \qquad \textbf{(Equation 3.4)}$$

In this modeling study, the Langmuir isotherm was linearized by plotting the $1/q_e$ values against the $1/C_e$ values, as shown in

Figure 4.26. A good fit of the Langmuir model to the adsorption of cadmium was indicated by the R^2 value of 0.9937. The adsorption capacity of $CuFe_2O_4$ nanoparticles was satisfactory for cadmium regarding the q_m value, which was 4.67 mg L^{-1} as shown in Table 4.39. On the other hand, the higher K_L value calculated as 0.8209 L mg^{-1} implied stronger bonding onto $CuFe_2O_4$ nanoparticles. As shown in Table 4.40, the calculated R_L values showed that the adsorption was more

favorable for the low initial concentrations of the adsorbates. However, all the R_L values were calculated between 0 and 1, which represented favorable adsorption conditions for all the initial concentrations in the range of 2.0 – 15 mg L^{-1}. All the calculated isotherm constants indicated satisfactory efficiency and good fit of the Langmuir model, suggesting the monolayer adsorption of cadmium ions on the $CuFe_2O_4$ nanoparticles.

Table 4.39 Calculated parameter values of the Langmuir isotherm model by the linear method

Langmuir isotherm model, Type 2		
q_m, mg g^{-1}	**K_L, L mg^{-1}**	**R^2**
4.67	0.8209	0.9937

Table 4.40 Calculated R_L values of the Langmuir isotherm model for different initial concentrations

C_e, mg L^{-1}	**R_L**
2.0	0.3785
4.0	0.2334
8.0	0.1321
10	0.1086
15	0.0751

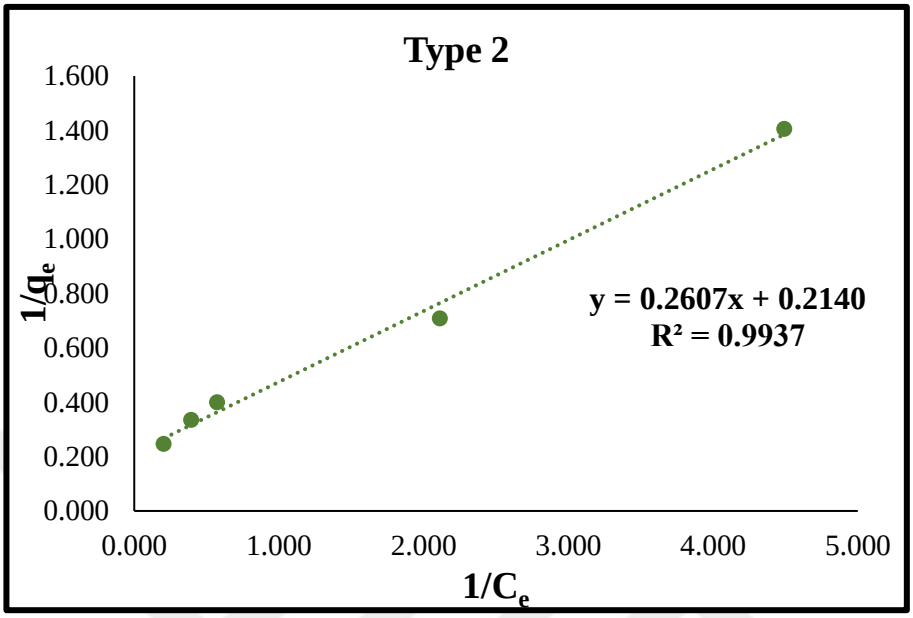


Figure 4.26 A plot of Langmuir isotherm for cadmium adsorption on $CuFe_2O_4$ nanoparticles under optimum conditions in synthetic wastewater

4.3 Development of Biogenic Gold Nanoparticles (GNP) Synthesis and its Cytotoxic and Genotoxic Assessment

Gold nanoparticles were synthesized by using macro-algae extract for the reduction of Au ions. The study investigated the impact of varying parameters on the synthesis yield, specifically the quantity of extract in sample solution and the temperature of the reaction medium. The formation of GNPs was determined by monitoring the colour change with the naked eye, indicated by the yellow solution turning into a purple solution. In the optimization processes, the GNP solutions obtained for each condition were examined using UV-Vis spectrometer measurements. The experimental condition that showed the highest peak in the GNP-specific Surface Plasmon Resonance (SPR) band (542 nm) was considered to have the highest reaction yield. Afterwards, the characterization of GNPs obtained under the most favorable reaction conditions was conducted using transmission electron microscope (TEM), Zeta-sizer, and Zeta potential analysis. Finally, the

cytotoxic and genotoxic characteristics of the nanoparticles were assessed by the MTT test and Comet Assay analysis.

4.3.1 Optimization Studies

4.3.1.1 Determination of macro-algae extract volume in colloidal sample solution

A wide scale of phytochemicals, such as phenols, flavonoids, and terpenoids can be found in plant extracts and these can function as reducing and stabilizing agents in the production of nanoparticles [430]. Therefore, the content and amount of the plant extract utilized in plant-based biogenic synthesis approaches may play a vital role in determining the efficiency of synthesis as well as the physical characteristics, such as size and shape of the resulting nanoparticle. Accordingly, different volumes of the same macro-algae extract were used in the synthesis of the GNPs in order to determine the most suitable phytochemical content for the reduction reaction. In the optimization study, 1.0, 2.0, 4.0 and 5.0 mL of macro-algae extract was added to the GNP colloidal solution to prepare solutions containing 4.0%, 8.0%, 16% and 20% extract, respectively. After adding aqueous solution containing 1.0 mM Au ions to these solutions, the solutions were kept on a magnetic stirrer at 500 rpm for 1.0 hour. Aqueous solutions containing the same amounts of macro-algae extract were also prepared. At the end of the mixing time, no color change was observed in the GNP colloidal solutions containing 4.0% and 8.0% macro-algae extracts, indicating that the reduction reaction did not occur in these solution media. For the solutions containing 16% and 20% macro-algae extracts, purple-colored solutions specific to the GNP colloidal solution was obtained. All solutions were scanned in the UV-Vis spectrometer between 400-700 nm. No absorbance signal was obtained for the GNP colloidal solutions containing 4.0% and 8.0% macro-algae extracts, which supported the assumption of insufficient biological precursors for the reduction of Au ions. The absorbance value obtained from each GNP colloidal solution was subtracted from the absorbance value obtained in aqueous solution containing the same amount of macro-algae extract to mitigate any scattering from the extract solution resulting in interference with the SPR peaks of GNPs. As depicted in the absorption measurements of Figure 4.27, the corrected absorption peak of the GNP colloidal solution containing 20% macro algae extract is higher than the GNP colloidal solution containing 16% macro algae extract corrected

absorption peak. Consequently, it was decided to work with 20% macro algae extract in order to achieve the most appropriate reaction conditions.

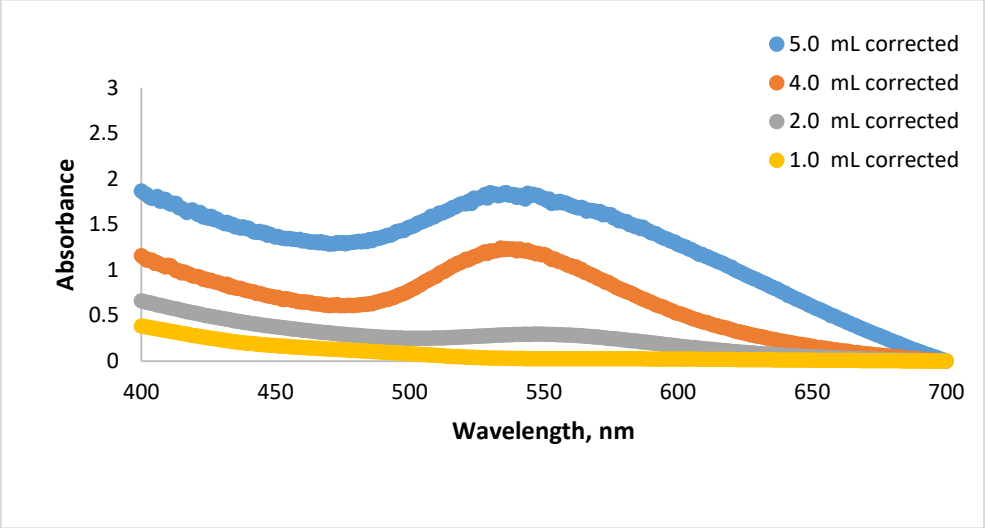


Figure 4.27 The absorption spectrums giving SPR band for GNPs in different macro-algae extract contains

4.3.1.2 Determination of sufficient temperature of the reaction medium

The temperature at which that reaction take place is a crucial parameter in determining both the effectiveness of the product and the specific qualities of the products acquired during biogenic reduction processes [431]. On the other hand, carrying out the reaction at high temperatures can result in the thermal degradation of phytochemicals potentially present in the macro-algae and reduce their biological activities [432]. Taking all these into consideration, the bio-reduction reaction was applied under constant conditions of room temperature (≈20 °C), 30, 40 and 50 °C. The GNP colloidal solution containing 20% macro-algae extract was mixed at 500 rpm for 1.0 hour at these temperatures. Aqueous solutions containing 20% macro-algae extract were also prepared and subjected to the same heat treatments as control samples. The resulting absorption peaks are given in Figure 4.28. As clearly seen in the spectra, there was a fluctuation in the signal baseline. In order to overcome this and obtain highly accurate results, peak heights were calculated with the help of a ruler, by subtracting the lowest absorbance value in each absorption peak from the highest peak height. Accordingly, very similar results were obtained at 30, 40 and 50 °C, demonstrating that the reaction medium must be heated for the bio-reduction reaction to occur quickly and effectively. The 40 °C variable was

selected as the optimum temperature because the GNPs showed more stable characteristics.

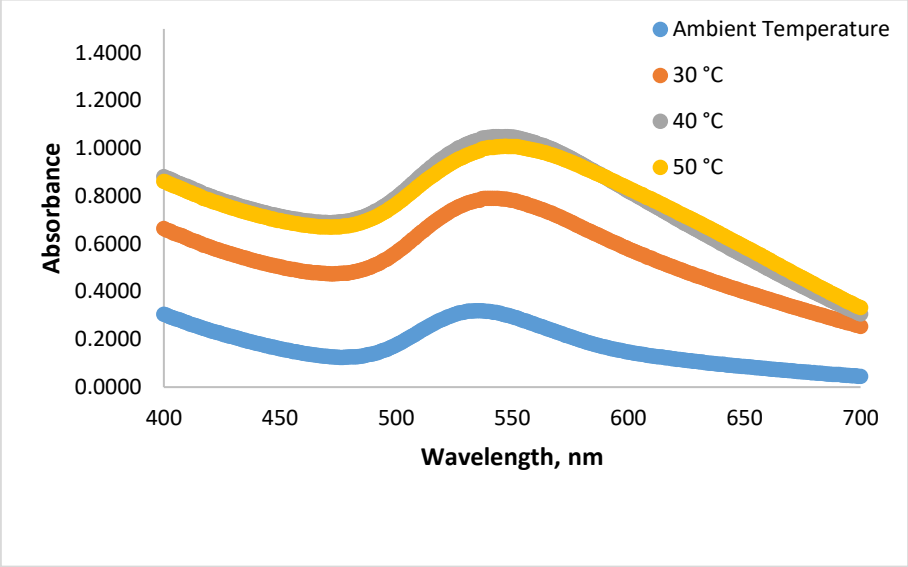


Figure 4.28 The absorption spectrums giving SPR band for GNPs at different temperatures

After determining the conditions that provided the maximum synthesis yield, the GNP synthesis was carried out simultaneously in 3 different flasks to determine the reproducibility of the developed synthesis procedure. The samples were then analyzed by UV-Vis spectrometry. Considering the absorbance values of the SPR peak of GNP at 542 nm, the %RSD calculated for the three separate syntheses was 6.8%. This demonstrated that the GNPs obtained by the developed synthesis method can be used in analytical applications with high precision and certainty.

4.3.2 Characterization Studies

Colloidal GNP solutions have a highly vibrant color, which is not displayed by the bulk biogenic material or individual atoms. Resonance is attributed to the collective oscillation of free conduction electrons excited by an interaction with the electromagnetic region, which is defined as an SPR feature [433]. The UV–Vis absorption spectra in Figure 4.29 clearly demonstrated the formation of GNPs. The prominent peak at 542 nm was observed in the UV-Vis spectrum scanned in the range of 400-700 nm indicating the distinctive SPR band of the GNPs [434], [435]. The absorbance of SPR is exceptionally responsive to the dimensions, and

morphology of the synthesized particles, as well as the gaps between the particles and the surrounding media [436].

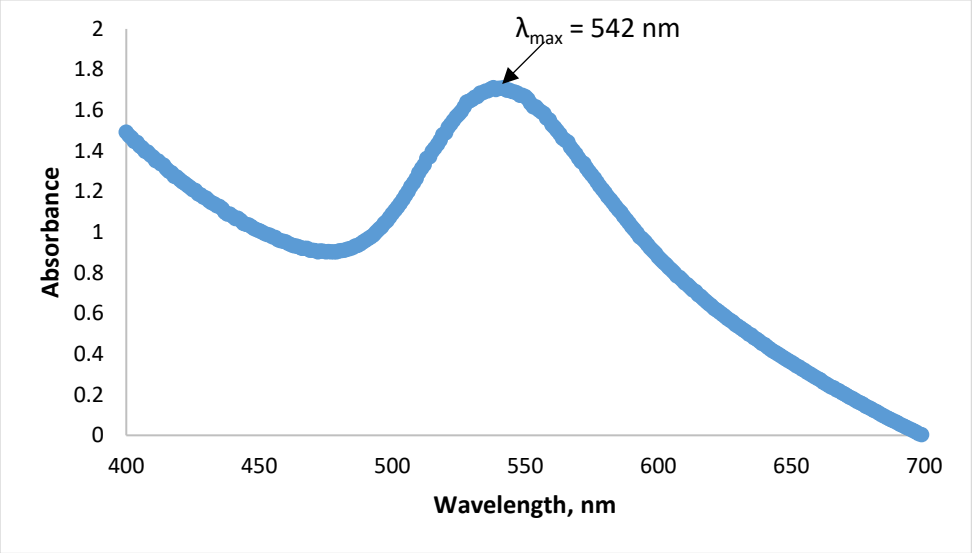


Figure 4.29 The UV-Vis spectrum of synthesized biogenic GNPs

Employing advanced microscopy techniques provides the characterization of nanoparticles including their elemental content, structure, and even charges or force measurements [437]. The average diameter of a particle (i.d), the distribution of their sizes, and their charge have an impact on the physical stability and *in vivo* distribution of nanoparticles. Electron microscopy techniques are commonly employed to ascertain the overall morphology of nanoparticles, which can influence their toxicological properties [438]. Thus, the morphology and diameter distributions with shape spectrum of GNPs formed was investigated utilizing the transmission electron microscopy (TEM). Typically, the biogenic synthesis pathway yields nanoparticles of varying form and sizes due to the chemical composition of the biogenic source [439]. Figure 4.30 displays that the GNPs were predominantly spherical and other particles of anisotropic structures with irregular shapes.

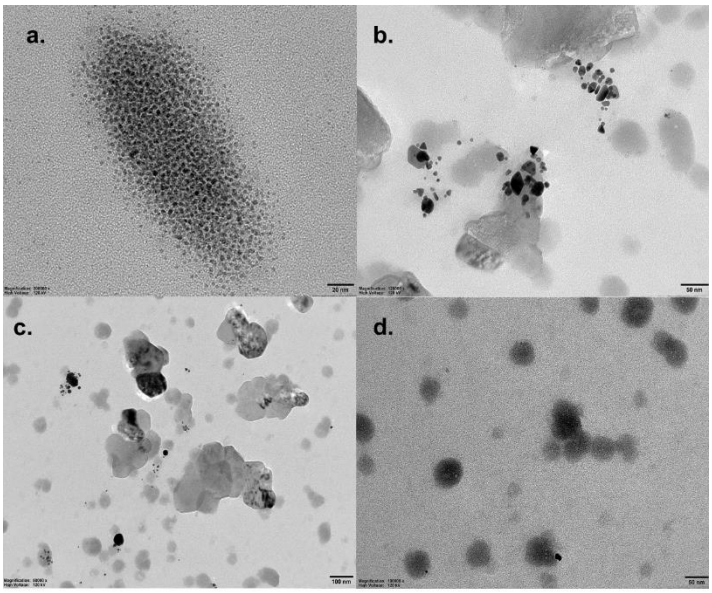


Figure 4.30 TEM images of the biogenic GNPs

The GNPs exhibited a narrow particle size distribution with sizes ranging from 1.87 – 4.74 nm with the average size as 2.96 ± 0.55 nm, according to the TEM analysis (Figure 4.30). The smaller nanoparticles were observed to have a spherical morphology, whereas the bigger particles revealed different geometrical shapes including triangles, hexagons, and rods (Figure 4.31a, b, c, d). In the literature, nanoparticles with irregular shapes have larger sizes in contrast to those with spherical shapes [440]. This is attributed to the insufficient amount of biomolecules that are responsible for capping and stabilizing the formed nanoparticles, resulting in the formation of larger anisotropic nanoparticles [441].

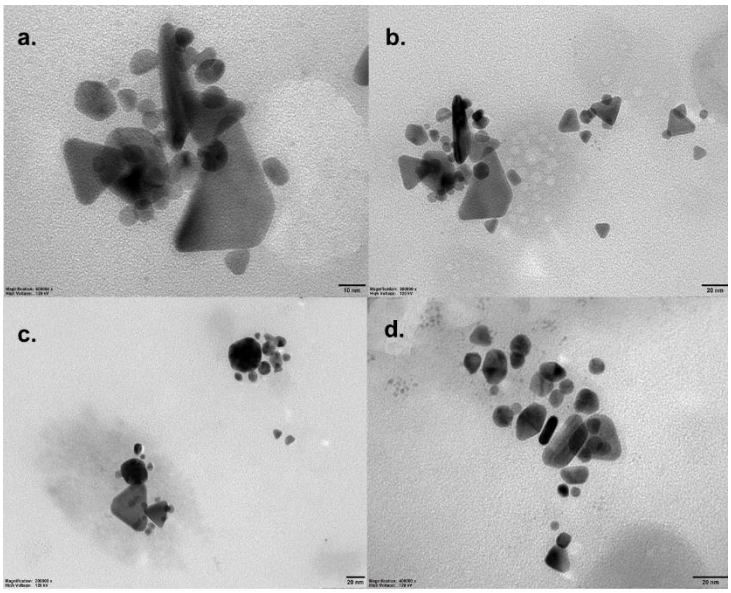


Figure 4.31 TEM images of the biogenic GNPs

The zeta potential (ZP) is a frequently utilized method to measure of surface charge, revealing data regarding the overall charge of particles in a solution. Its value is intricately related to the stability of suspension and the coating on the surface of the particle. As a result, it is commonly used to examine particle stability and surface adsorption. The ZP is an electro kinetic potential referred to as the potential at the slipping plane, where the potential of the bulk solution is zero. The electric double layer (EDL) in a liquid neutralizes a particle's surface charge by containing an excess of opposite-charge ions. The Stern layer is immobile and the diffuse layer allows ion diffusion [442]. Zeta potential of the GNPs was investigated with the instrumental conditions given in Table 4. 41 in order to shed light on the stability of the colloidal golds in the solution.

Table 4. 41 Instrumental conditions conducted in zeta measurements of GNPS

Temperature (°C): 25.0	**Zeta runs: 12**
Count Rate (kcps): 164.3	**Measurement Position (mm): 2.00**
Cell Description: Clear disposable zeta cell	**Attenuator: 6**

The zeta potential distribution of the GNPs is depicted in Figure 4.32. The average potential was recorded as -28.4 ± 4.2 mV with conductivity recorded as 1.31 mS

cm^{-1}. The results validated high stability of the GNPs as supported by other findings in the literature [434], [443], [444].

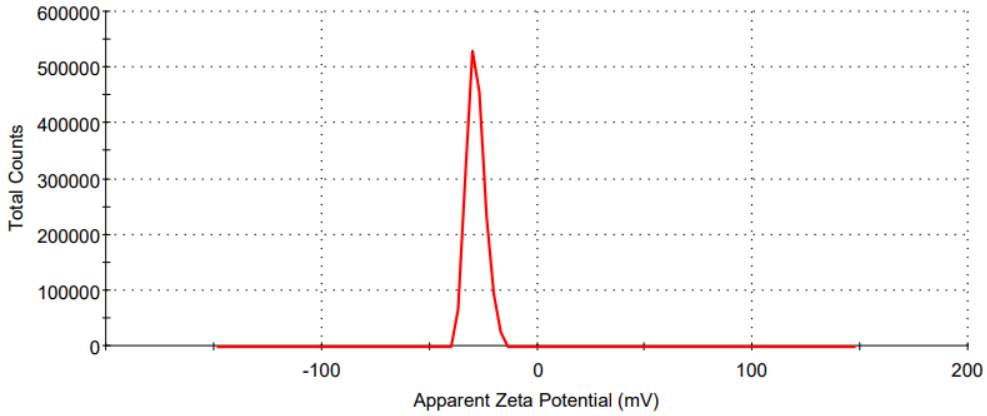


Figure 4.32 Distribution graph of zeta potential obtained for GNPs

4.3.3 Evaluation of Toxicological Profile of GNPs

4.3.3.1 Comet Assay

Comet Assay protocol was recently established and standardized for water fleas, *Daphnia magna, Crustacea, Cladocera* (Figure 4.33), which is a widely used model organism [445]. This advancement was prompted by the need of using this test method in future eco-genotoxicological investigations on freshwater ecosystems. The benefit of using this protocol for freshwater monitoring is that breeding daphnids is simple, affordable, rapid and does not require big and special spaces [446]. The potential implementation of the Comet Assay with *Daphnia magna* to detect DNA damage attributed to particular substances has recently gained considerable attention [447]–[449]. However, this bioassay has not yet been applied in field biomonitoring.

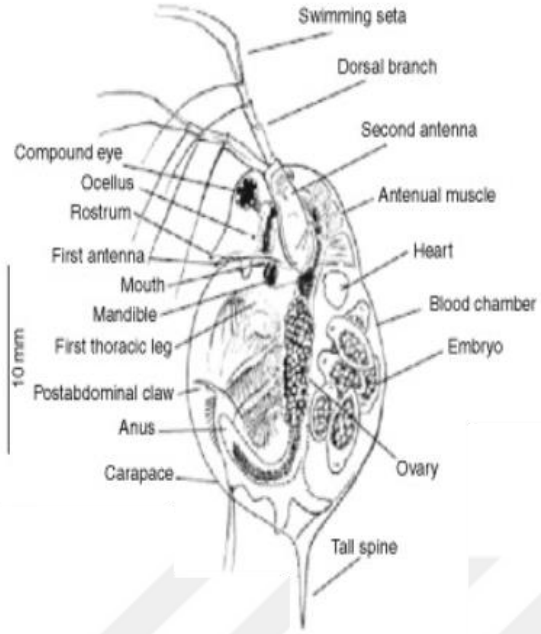


Figure 4.33 Representative image of Daphnia magna used as a model organism in the study [450]

The acute toxicity of the GNPs was investigated by exposing test organisms to various dosages (0.5, 1.0, 2.0, 3.0, 4.0 and 5.0 μM) of the nanoparticles in a fixed medium for durations of one to four days. Each experimental setting was performed with three replicates, with a total of 10 individuals in each aquarium. Feeding was not implemented during the test period. The control groups were compared with the other dose groups and it was observed that the dosage groups displayed behavioural issues as given in Table 4.42.

Table 4.42 Behavioral respects of Daphnia magna in acute toxicity tests

Duration	Swimming Ability	Activities	Antenna movements
24 h (1. Day)	Normal	Normal movement, harmonious, peaceful	Normal
48 h (2. Day)	Fast	Rapid behavioral responses	Normal
72 h (3. Day	Slow	Restless random swimming, another, aggressive behavior against the individual, adverse straight movement, sinking	Slow
96 h (4. Day)	Very slow	Restlessness in movement, inability to maintain balance	Very slow

According to the criterion of the EU-Directive 93/67/EEC, the LC_{50} value for GNP was determined with 95% confidence level to be 1.32 μM using probit analysis. As a result, GNPs were considered to have a slightly harmful (damage level of 2) based on the LC_{50} value [451][452]. The evaluation of subacute toxicity was conducted using a semi-static apparatus with continuous ventilation. Twenty individual *Daphnia magna* neomata were exposed to GNPs in a 100 mL borosilicate beaker for a period of fourteen days. Three subacute dosages for GNPs were used for the LC_{50} value: subacute I (app. 1/10 of LC_{50}, or 0.13 μM), subacute II (app. 1/4 of LC_{50}, or 0.33 μM), and subacute III (app. 1/2 of LC_{50}, or 0.66 μM). Throughout the experiments, all groups were fed with algal culture (*S. subspinosus*) bi-daily. The positive control consisted of 5.0 mg L^{-1} mutagen ethylmethane sulfonate for a period of 14 days. The neomates were periodically removed from the experimental medium each day to determine the results. The experimental results are displayed in Table 4.43.

Table 4.43 The DNA damage values in neomates that were subjected to various concentrations of GNPs

Groups (µM)	Damage Frequency (%)	Arbitrary Unit (AU)	Genetical Damage Index (DI) (%)
Positive Control (5.0 mg L^{-1} ethylmethane sulfonate)	99.00±1.00	396.67±1.15	3.96±0.01
Negative Control (0.0)	22.33±1.52	57.00±6.25	0.57±0.06
0.13	23.67±1.15	53.33±5.69	0.53±0.05
0.32	26.33±1.53	72.33±8.39	0.72±0.08
0.66	27.33±1.15	71.67±3.06	0.71±0.03
P	***	***	***

: P≤0.05; **P≤0.01;P≤0.001**

It was observed that the positive control group, which is known to be mutagenic, exhibited the highest level of DNA damage at 99.00±1.00%. This difference was statistically significant (P<0.0001) in comparison to the other groups used in the experiments. The negative control group that did not contain any GNPs or other substances, showed the least DNA damage percentage, with a calculated value of 22.33±1.52%. On the other hand, the level of DNA damage was marginally increased by the increased concentration of GNPs in the experimental medium recorded between 24 and 27%. However, the DNA damage level exhibited similar results with the negative control group, and DNA damage rate was almost a quarter of the DNA damage percentage observed in the mutagenic positive control group. Based on the data obtained, it was concluded that the GNPs does not exhibit significant genotoxic effects.

4.3.3.2 Cell Viability Tests

The measurement of cell viability plays an important role for all forms of cell culture. Cell viability is used as the main objective of the experiment, as in toxicity assays, or to correlate cell behavior with cell number [453]. Cell-based assays are studies used to determine whether test molecules have effects on cell proliferation or show direct cytotoxic effects that eventually lead to cell death [454]. Cell culture studies are the first step for cytotoxicity evaluation of nanoparticles due to their advantages such as low cost, rapid response, ethical, easy control and replication [455]. *In vitro* toxicity assays are primarily used to investigate the generic cytotoxicity or genotoxicity of chemicals [456]. One of the most common examples of tetrazolium salts used in bioassays is 3-(4,5-dimethylthiazol-2-yl)-2,5-diphenyl tetrazolium bromide (MTT). MTT procedures are widely applied to fungi, bacteria and mammalian cell lines [457]. The MTT assay is based on enzymatic activity in cells, but is significantly affected by certain interfering factors, including cell culture media solubility of formazan crystals in solvents and various drug compounds added to the assay [458]. MTT is a colorimetric assay that provides information about living and non-living cells by processing NPs. Since active cells have the ability to reduce this dye to colored formazan, a clear distinction is made between living and non-living cells [459]. For this case, in order to assess the cytotoxicity of the GNPs, MTT analysis was conducted by using Human Umbilical Vein Endothelial Cells (HUVEC) line and Human Colorectal Carcinoma Cell (HCT116) line, which is a typical colon cancer cell. The data were analyzed using statistical analyzer GraphPad Prism 9.4.0 software. The Tukey post-hoc test and one-way ANOVA test were employed for statistical analysis of the results as given in Figure 4.34, for each cell line respectively.

Ordinary one-way ANOVA Multiple comparisons	HCT116 Cell Line		
Number of families	1		
Number of comparisons per family	15		
Alpha	0.05		
Tukey's multiple comparisons test	**Mean Diff.**	**95.00% CI of diff.**	**Below threshold?**
Control vs. 1	12.16	5.368 to 18.95	Yes
Control vs. 5	18.28	11.49 to 25.07	Yes
Control vs. 10	15.63	8.844 to 22.42	Yes
Control vs. 25	28.68	21.90 to 35.47	Yes
Control vs. 50	53.34	46.55 to 60.13	Yes
1 vs. 5	6.118	-0.6713 to 12.91	No
1 vs. 10	3.476	-3.313 to 10.27	No
1 vs. 25	16.53	9.738 to 23.32	Yes
1 vs. 50	41.18	34.39 to 47.97	Yes
5 vs. 10	-2.642	-9.432 to 4.148	No
5 vs. 25	10.41	3.620 to 17.20	Yes
5 vs. 50	35.06	28.27 to 41.85	Yes
10 vs. 25	13.05	6.262 to 19.84	Yes
10 vs. 50	37.70	30.91 to 44.49	Yes
25 vs. 50	24.65	17.86 to 31.44	Yes

Ordinary one-way ANOVA Multiple comparisons	HUVEC Cell Line		
Number of families	1		
Number of comparisons per family	15		
Alpha	0.05		
Tukey's multiple comparisons test	**Mean Diff.**	**95.00% CI of diff.**	**Below threshold?**
Control vs. 1	4.922	-2.138 to 11.98	No
Control vs. 5	2.770	-4.290 to 9.830	No
Control vs. 10	-2.102	-9.163 to 4.958	No
Control vs. 25	19.12	12.06 to 26.18	Yes
Control vs. 50	39.62	32.56 to 46.68	Yes
1 vs. 5	-2.152	-9.212 to 4.908	No
1 vs. 10	-7.024	-14.08 to 0.03568	No
1 vs. 25	14.20	7.137 to 21.26	Yes
1 vs. 50	34.70	27.64 to 41.76	Yes
5 vs. 10	-4.873	-11.93 to 2.188	No
5 vs. 25	16.35	9.289 to 23.41	Yes
5 vs. 50	36.85	29.79 to 43.91	Yes
10 vs. 25	21.22	14.16 to 28.28	Yes
10 vs. 50	41.73	34.67 to 48.79	Yes
25 vs. 50	20.50	13.44 to 27.56	Yes

Figure 4.34 ANOVA statistical results for HCT116 (leftside) and HUVEC (rightside) Cell lines at MTT Cell Viability tests

The data indicated no effect on HUVEC line cell viability at GNP concentrations of 1.0 – 10 µg mL^{-1} (Figure 4.35). However, a significant decrease in cell viability was observed at increasing concentrations and cell viability decreased to 60.4±4.6% for the highest dose determined in the study (50 µg mL^{-1}). Furthermore, as a result of the experiment performed in the HCT116 line, cell viability for 1.0 – 50 µg mL^{-1} was recorded as 87.8±1.8, 81.7±4.3, 84.4±3.7, 71.3±4.6, and 46.7±5.0%, respectively. In the light of these results, the synthesized GNPs showed an acceptable cytotoxic effect on the cancer cell line.

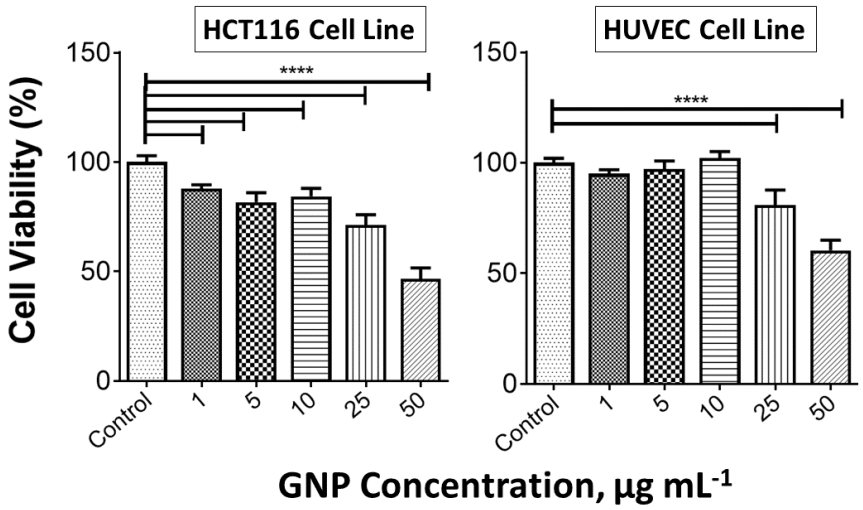


Figure 4.35 MTT test results obtained for both HUVEC and HCT116 cell lines for different concentrations of GNPs

Flavonoids are quite popular due to their known lethal effects on various types of human cancer cells but having minimal or absent impact on normal human cells. This makes the flavonoids as possible chemotherapeutics for the treatment of cancer [460]. Therefore, the MTT analysis was also carried out with equivalent concentrations of macro-algae extract solutions (1.0 - 50 μg mL^{-1}) with both cell lines in order to evaluate the cytotoxic effect of GNPs (. In the MTT analysis performed, the cell viability remained around 100% for both cell lines, which indicated the non-cytotoxic impact of macro-algae extract on both HCT116 line and HUVEC line.

5
CONCLUSION

In the scope of this thesis, methods have been developed for the determination, removal and monitoring of pollutants at trace levels, which are known to have adverse effects on human health and the environment. Furthermore, gold nanoparticles were synthesized with a green approach and the toxicological attributes were assessed.

In the first part of the thesis, a liquid phase microextraction method was developed for the simultaneous preconcentration of selected 29 endocrine disruptor compounds and pesticides. This involved the combination of spray assisted droplet formation based liquid phase microextraction and gas chromatography mass spectrometry (SADF-LPME-GC-MS) for the accurate and precise simultaneous determination of the targeted analytes in seawater, seaweeds, and rock-soil samples obtained from the Antarctic region. The chromatographic and extraction conditions were rigorously enhanced, and the SADF-LMPE method eliminated the need for disperser solvents, making it conform with the principle of 'green chemistry' on solvent usage. The detection limits and quantification limits for all analytes were recorded between 1.0 and 6.6 ng g^{-1} and 3.2 and 22.1 ng g^{-1}, respectively. The low detection limits of the SADF-LPME method correlated with high enhancement factors ranging from 3.7 to 158.9 folds. The method was validated using seawater, moss, soil samples. The recoveries of all analytes were found to be within an acceptable range for all studied samples, and this validated the feasibility and applicability of the method for complex sample matrices. Environmental samples collected from the Horseshoe and Faure Islands in the Antarctic region were also analyzed under the optimum conditions of the developed SADF-LPME-GC-MS method. The GC-MS-based extraction approach was applicable for the detection of the specified EDCs and pesticides at exceptionally low concentrations, and can be utilized for the monitoring of these analytes at different locations and environmental matrices, especially in the Antarctic region.

In the second part of the thesis, a nanomaterial assisted batch type adsorption based removal strategy was optimized for the remediation of cadmium ions from synthetic

wastewater. The co-precipitation method was used to synthesize the $CuFe_2O_4$ nanoparticles that was employed as adsorbent for the study. The effectiveness of the magnetic $CuFe_2O_4$ nanoparticle under optimum conditions of the developed method was assessed for the removal of cadmium. The removal efficiency of the method in synthetic wastewater was recorded between 67 and 89% in the linear working range of cadmium as detected and quantified by a flame atomic absorption spectrophotometry system. The Langmuir isotherm modeling studies were conducted to examine the types of adsorption isotherms for the developed procedure, and the results depicted that the model fitted well to the experimental data. The fitted models validated the favorable adsorptive removal of cadmium from synthetic wastewater by the magnetic $CuFe_2O_4$ nanoparticle.

In the third part of the thesis, gold nanoparticles were synthesized using invasive macro-algae extract as biological precursor. The biosynthesis procedure was optimized comprehensively to yield nano-sized colloidal golds. The morphology, and physicochemical properties of the produced GNPs were investigated with zeta-potential, and TEM analysis. The average hydrodynamic diameter of the GNPs was calculated as 2.96 ± 0.55 nm and zeta potential was recorded as -28.4 ± 4.2 mV. The results showed the high surface area and stability of the biogenic GNPs. The toxicological assessment of the GNPs was achieved by employing MTT cell viability and single-cell electrophoresis (Comet Assay) tests. The MTT cell viability assays performed on colon cancer cell line (HCT116) revealed the destructive effect of the synthesized GNPs on tumor cells. In addition, evaluations in healthy cell lines (HUVEC) showed that GNPs had no negative effect on cell viability except at certain concentration levels ($60.4 \pm 4.6\%$ for 50 $\mu g\ mL^{-1}$). Moreover, the genotoxic properties of the GNPs were examined by Comet Assay. According to the low DNA damage percentages obtained in the evaluations performed with *Daphnia magna* species, the effect of the GNPs on the species was determined as *'mildly damaged'*.

REFERENCES

[1] P. O. Ukaogo, U. Ewuzie, and C. V Onwuka, "21 - Environmental pollution: causes, effects, and the remedies," P. Chowdhary, A. Raj, D. Verma, and Y. B. T.-M. for S. E. and H. Akhter, Eds. Elsevier, 2020, pp. 419–429.

[2] J. G. Speight, "9 - Pollution prevention," J. G. B. T.-N. W. R. Speight, Ed. Butterworth-Heinemann, 2020, pp. 305–336.

[3] P. Chowdhary, R. N. Bharagava, S. Mishra, and N. Khan, "Role of industries in water scarcity and its adverse effects on environment and human health," *Environ. Concerns Sustain. Dev. Vol. 1 Air, Water Energy Resour.*, pp. 235–256, 2020.

[4] B. Chen *et al.*, "In search of key: Protecting human health and the ecosystem from water pollution in China," *J. Clean. Prod.*, vol. 228, pp. 101–111, 2019, doi: https://doi.org/10.1016/j.jclepro.2019.04.228.

[5] L. Lin, H. Yang, and X. Xu, "Effects of water pollution on human health and disease heterogeneity: a review," *Front. Environ. Sci.*, vol. 10, p. 880246, 2022.

[6] S. Gundry, J. Wright, and R. Conroy, "A systematic review of the health outcomes related to household water quality in developing countries," *J. Water Health*, vol. 2, no. 1, pp. 1–13, 2004.

[7] UNESCO, *The United Nations World Water Development Report 2021: Valuing Water*. United Nations, 2021.

[8] S. Ullah, M. W. Javed, M. Shafique, and S. F. Khan, "An integrated approach for quality assessment of drinking water using GIS: A case study of Lower Dir.," *J. Himal. Earth Sci.*, vol. 47, no. 2, 2014.

[9] S. Nabizadeh, F. Barzegar, M. Babaei, M. Kamankesh, and A. Mohammadi, "New and efficient direct-SLM two-phase hollow fiber electromembrane extraction coupled to GC/MS for the analysis of nitrosamines in different types of sausage: Investigation of meat type, meat percent and cooking methods," *Food Chem.*, vol. 416, p. 135759, 2023, doi: https://doi.org/10.1016/j.foodchem.2023.135759.

[10] M. B. Bloom, E. Sisco, and I. S. Lurie, "Development and validation of a rapid GC–MS method for seized drug screening," *Forensic Chem.*, vol. 33, p. 100479, 2023, doi: https://doi.org/10.1016/j.forc.2023.100479.

[11] N. Vidović, V. Antić, and J. Schwarzbauer, "Determination of the water-soluble polymer poly(ethyleneimine) (PEI) in wastewater by continuous-flow off-line pyrolysis GC/MS," *J. Anal. Appl. Pyrolysis*, vol. 172, p. 106001, 2023, doi: https://doi.org/10.1016/j.jaap.2023.106001.

[12] F. H. Thamer and N. Thamer, "Gas chromatography – Mass spectrometry (GC-MS) profiling reveals newly described bioactive compounds in Citrullus colocynthis (L.) seeds oil extracts," *Heliyon*, p. e16861, 2023, doi: https://doi.org/10.1016/j.heliyon.2023.e16861.

[13] K. Jiang, K. Xu, J. Wang, F. Meng, and B. Wang, "Based on HS-SPME-GC-MS combined with GC-O-MS to analyze the changes of aroma compounds in the aging process of Citri Reticulatae Pericarpium," *Food Biosci.*, p. 102798, 2023, doi: https://doi.org/10.1016/j.fbio.2023.102798.

[14] Y. Bakırcıoğlu, S. Akman, N. Bıçak, and F. Şenkal, "Determination of some trace heavy metals in some water samples by FAAS after their

preconcentration using DETA," *J. trace microprobe Tech.*, vol. 21, no. 2, pp. 239–248, 2003.
[15] M. Soylak and I. Murat, "Determination of copper, cobalt, lead, and iron in table salt by FAAS after separation using violuric acid and multiwalled carbon nanotubes," *Food Anal. Methods*, vol. 5, pp. 1003–1009, 2012.
[16] V. Y. Durguti, S. Aliu, F. Laha, and F. Feka, "Determination of iron, copper and zinc in the wine by FAAS," *Emerg. Sci. J.*, vol. 4, no. 5, pp. 411–417, 2020.
[17] G. Dalgıç Bozyiğit, M. Fırat Ayyıldız, D. Selali Chormey, G. Onkal Engin, and S. Bakırdere, "Accurate Quantification of Nervous System Drugs in Aqueous Samples at Trace Levels by Binary Solvent Dispersive Liquid–Liquid Microextraction-Gas Chromatography Mass Spectrometry," *Environ. Toxicol. Chem.*, vol. 40, no. 6, pp. 1570–1575, 2021.
[18] K. A. Ago, S. A. Kitte, G. Chirfa, and A. Gure, "Effervescent powder-assisted floating organic solvent-based dispersive liquid-liquid microextraction for determination of organochlorine pesticides in water by GC–MS," *Heliyon*, vol. 9, no. 1, p. e12954, 2023, doi: https://doi.org/10.1016/j.heliyon.2023.e12954.
[19] S. Bodur, S. Erarpat, Ö. T. Günkara, and S. Bakırdere, "One step derivatization and dispersive liquid-liquid microextraction of hydroxychloroquine sulfate for its sensitive and accurate determination using GC–MS," *J. Pharmacol. Toxicol. Methods*, vol. 113, p. 107130, 2022, doi: https://doi.org/10.1016/j.vascn.2021.107130.
[20] A. Kul and O. Sagirli, "A novel method for the therapeutic drug monitoring of biperiden in plasma by GC-MS using salt-assisted liquid–liquid microextraction," *Clin. Chim. Acta*, vol. 543, p. 117322, 2023, doi: https://doi.org/10.1016/j.cca.2023.117322.
[21] U. Balçık, D. S. Chormey, M. F. Ayyıldız, and S. Bakırdere, "Liquid phase microextraction based sensitive analytical strategy for the determination of 22 hazardous aromatic amine products of azo dyes in wastewater and tap water samples by GC-MS system," *Microchem. J.*, vol. 155, p. 104712, 2020, doi: https://doi.org/10.1016/j.microc.2020.104712.
[22] A. Altınışık Tağaç, P. Erdem, S. Seyhan Bozkurt, and M. Merdivan, "Utilization of montmorillonite nanocomposite incorporated with natural biopolymers and benzyl functionalized dicationic imidazolium based ionic liquid coated fiber for solid-phase microextraction of organochlorine pesticides prior to GC/MS and GC/ECD," *Anal. Chim. Acta*, vol. 1185, p. 339075, 2021, doi: https://doi.org/10.1016/j.aca.2021.339075.
[23] E. Akkaya, G. D. Bozyiğit, and S. Bakirdere, "Simultaneous determination of 4-tert-octylphenol, chlorpyrifos-ethyl and penconazole by GC–MS after sensitive and selective preconcentration with stearic acid coated magnetic nanoparticles," *Microchem. J.*, vol. 146, no. January, pp. 1190–1194, 2019, doi: 10.1016/j.microc.2019.01.077.
[24] E. Ö. Er, A. Çağlak, G. Ö. Engin, and S. Bakirdere, "Ultrasound-assisted dispersive solid phase extraction based on Fe3O4/reduced graphene oxide nanocomposites for the determination of 4-tert octylphenol and atrazine by gas chromatography–mass spectrometry," *Microchem. J.*, vol. 146, pp. 423–428, 2019, doi: https://doi.org/10.1016/j.microc.2019.01.040.
[25] R. F. Ajayi *et al.*, "Chapter 18 - Nanoparticles in biosensor development for the detection of pathogenic bacteria in water," T. Dalu and N. T. B. T.-E. F.

P. Tavengwa, Eds. Elsevier, 2022, pp. 331–358.
[26] R. Kodešová *et al.*, "Assessment of potential mobility of selected micropollutants in agricultural soils of the Czech Republic using their sorption predicted from soil properties," *Sci. Total Environ.*, vol. 865, p. 161174, 2023, doi: https://doi.org/10.1016/j.scitotenv.2022.161174.
[27] X. Hu, Y. Zhang, T. Ding, J. Liu, and H. Zhao, "Multifunctional gold nanoparticles: a novel nanomaterial for various medical applications and biological activities," *Front. Bioeng. Biotechnol.*, vol. 8, p. 990, 2020.
[28] P. R. Chandran and R. T. Thomas, "Chapter 14 - Gold Nanoparticles in Cancer Drug Delivery," S. Thomas, Y. Grohens, and N. B. T.-N. A. for T. E. Ninan, Eds. Oxford: William Andrew Publishing, 2015, pp. 221–237.
[29] J. Yguerabide and E. E. Yguerabide, "Light-Scattering Submicroscopic Particles as Highly Fluorescent Analogs and Their Use as Tracer Labels in Clinical and Biological Applications: I. Theory," *Anal. Biochem.*, vol. 262, no. 2, pp. 137–156, 1998, doi: https://doi.org/10.1006/abio.1998.2759.
[30] S. Yirmibeşoğlu, Ö. Oktar, and B. Özsoy, "Ulusal Antarktik Bilim Seferi (TAE-1) Gözlemleri ile Kutuplarda Denizcilik Meteorolijisi," in *Kutup (Arktik ve Antarktik) Bilim Programı Çalıştayı*, 2017, p. 19.
[31] L.-M. . van der Watt, "Antarctica," *Encyclopedia Britannica*, 2023. https://www.britannica.com/place/Antarctica (accessed Jan. 30, 2024).
[32] R. Kunverji, "Antarctica's Kiss-Shot," *J. Interdiscip. Sci. Top.*, vol. 10, 2023.
[33] P. Convey, "Antarctic Ecosystems," S. A. B. T.-E. of B. (Second E. Levin, Ed. Waltham: Academic Press, 2013, pp. 179–188.
[34] L. T. Oppedal, J. Bakke, Ø. Paasche, J. P. Werner, and W. G. M. van der Bilt, "Cirque glacier on South Georgia shows centennial variability over the last 7000 years," *Front. Earth Sci.*, vol. 6, p. 2, 2018.
[35] S. J. Pyne, "Heart of Whiteness: The Exploration of Antarctica," *Environ. Rev.*, vol. 10, no. 4, pp. 231–246, Dec. 1986, doi: 10.2307/3984348.
[36] J. Hanessian, "The Antarctic Treaty 1959," *Int. Comp. Law Q.*, vol. 9, no. 3, pp. 436–480, 1960, doi: DOI: 10.1093/iclqaj/9.3.436.
[37] D. M. Bergstrom, P. Convey, and A. H. L. Huiskes, *Trends in Antarctic terrestrial and limnetic ecosystems*. Springer, 2006.
[38] R. Bargagli, "Environmental contamination in Antarctic ecosystems," *Sci. Total Environ.*, vol. 400, no. 1, pp. 212–226, 2008, doi: https://doi.org/10.1016/j.scitotenv.2008.06.062.
[39] R. B. Aronson, S. Thatje, J. B. McClintock, and K. A. Hughes, "Anthropogenic impacts on marine ecosystems in Antarctica," *Ann. N. Y. Acad. Sci.*, vol. 1223, no. 1, pp. 82–107, Mar. 2011, doi: https://doi.org/10.1111/j.1749-6632.2010.05926.x.
[40] T. Deblonde, C. Cossu-Leguille, and P. Hartemann, "Emerging pollutants in wastewater: A review of the literature," *Int. J. Hyg. Environ. Health*, vol. 214, no. 6, pp. 442–448, 2011, doi: https://doi.org/10.1016/j.ijheh.2011.08.002.
[41] H. J. M. Verhaar, C. J. Van Leeuwen, and J. L. M. Hermens, "Classifying environmental pollutants," *Chemosphere*, vol. 25, no. 4, pp. 471–491, 1992.
[42] T. Suzuki, T. Hidaka, Y. Kumagai, and M. Yamamoto, "Environmental pollutants and the immune response," *Nat. Immunol.*, vol. 21, no. 12, pp. 1486–1495, 2020.
[43] K. Y. Bell, M. J. M. Wells, K. A. Traexler, M. Pellegrin, A. Morse, and J. Bandy, "Emerging pollutants," *Water Environ. Res.*, vol. 83, no. 10, pp.

1906–1984, 2011.
[44] A. Chavoshani, M. Hashemi, M. Mehdi Amin, and S. C. Ameta, “Chapter 1 - Introduction,” A. Chavoshani, M. Hashemi, M. Mehdi Amin, and S. C. B. T.-M. and C. Ameta, Eds. Elsevier, 2020, pp. 1–33.
[45] M. O. Barbosa, N. F. F. Moreira, A. R. Ribeiro, M. F. R. Pereira, and A. M. T. Silva, “Occurrence and removal of organic micropollutants: An overview of the watch list of EU Decision 2015/495,” *Water Res.*, vol. 94, pp. 257–279, 2016, doi: https://doi.org/10.1016/j.watres.2016.02.047.
[46] Y. Luo *et al.*, “A review on the occurrence of micropollutants in the aquatic environment and their fate and removal during wastewater treatment,” *Sci. Total Environ.*, vol. 473–474, pp. 619–641, 2014, doi: https://doi.org/10.1016/j.scitotenv.2013.12.065.
[47] M. Hforouzanfar *et al.*, “Global, regional, and national comparative risk assessment of 79 behavioural, environmental and occupational, and metabolic risks or clusters of risks, 1990-2015: a systematic analysis for the Global Burden of Disease Study 2015,” *Lancet*, 2016.
[48] A. T. Mathew and M. P. Saravanakumar, “Removal of micropollutants through bio-based materials as a transition to circular bioeconomy: Treatment processes involved, perspectives and bottlenecks,” *Environ. Res.*, vol. 214, p. 114150, 2022, doi: https://doi.org/10.1016/j.envres.2022.114150.
[49] J. Santana *et al.*, “Preliminary toxicological assessment of phthalate esters from drinking water consumed in Portugal,” *Environ. Sci. Pollut. Res.*, vol. 21, no. 2, pp. 1380–1390, 2014, doi: 10.1007/s11356-013-2020-3.
[50] L. Fitzgerald and D. S. Wikoff, “Persistent organic pollutants,” 2014.
[51] I. Mahmood, S. R. Imadi, K. Shazadi, A. Gul, and K. R. Hakeem, “Effects of pesticides on environment,” in *Plant, soil and microbes*, Springer, 2016, pp. 253–269.
[52] S. A. Nsibande and P. B. C. Forbes, “Fluorescence detection of pesticides using quantum dot materials – A review,” *Anal. Chim. Acta*, vol. 945, pp. 9–22, 2016, doi: https://doi.org/10.1016/j.aca.2016.10.002.
[53] C. N. B. Grey, M. J. Nieuwenhuijsen, and J. Golding, “The use and disposal of household pesticides,” *Environ. Res.*, vol. 97, no. 1, pp. 109–115, 2005, doi: https://doi.org/10.1016/j.envres.2004.07.008.
[54] M. Tudi *et al.*, “Exposure routes and health risks associated with pesticide application,” *Toxics*, vol. 10, no. 6, p. 335, 2022.
[55] M. K. Javaid, M. Ashiq, and M. Tahir, “Biodegradation and Environmental Impacts of Pesticides.,” *Scientifica (Cairo).*, 2016.
[56] I. C. Yadav and N. L. Devi, “Pesticides classification and its impact on human and environment,” *Environ. Sci. Eng.*, vol. 6, pp. 140–158, 2017.
[57] J. Martín Reina, J. A. Duarte, L. Cerrillos, J. D. Bautista Palomas, and I. M. Moreno Navarro, “Insecticide reproductive toxicity profile: organophosphate, carbamate and pyrethroids,” *J. Toxins, 4 (1), 1-7.*, 2017.
[58] F. P. Garcia, S. Y. C. Ascencio, J. C. G. Oyarzún, A. C. Hernandez, and P. V. Alavarado, “Pesticides: classification, uses and toxicity. Measures of exposure and genotoxic risks,” *J. Res. Environ. Sci. Toxicol*, vol. 1, no. 11, pp. 279–293, 2012.
[59] R. C. Gupta, “Carbamate pesticides,” *Encycl. Toxicol.*, pp. 661–664, 2014.
[60] S. M. Waliszewski *et al.*, “Persistent organochlorine pesticide levels in bovine fat from Mexico,” *Food Addit. Contam.*, vol. 21, no. 8, pp. 774–780,

Aug. 2004, doi: 10.1080/02652030410001712736.
[61] W. Tang *et al.*, "Pyrethroid pesticide residues in the global environment: An overview," *Chemosphere*, vol. 191, pp. 990–1007, Jan. 2018, doi: 10.1016/j.chemosphere.2017.10.115.
[62] M. A. Sogorb and E. Vilanova, "Enzymes involved in the detoxification of organophosphorus, carbamate and pyrethroid insecticides through hydrolysis," *Toxicol. Lett.*, vol. 128, no. 1, pp. 215–228, 2002, doi: https://doi.org/10.1016/S0378-4274(01)00543-4.
[63] European Commission, "How are EU MRLs set?," *Maximum Residue Levels*, 2018. https://food.ec.europa.eu/plants/pesticides/maximum-residue-levels/how-are-eu-mrls-set_en.
[64] C. A. O. Midega, A. W. Murage, J. O. Pittchar, and Z. R. Khan, "Managing storage pests of maize: Farmers' knowledge, perceptions and practices in western Kenya," *Crop Prot.*, vol. 90, pp. 142–149, 2016, doi: https://doi.org/10.1016/j.cropro.2016.08.033.
[65] Environmental Protection Agency, "About Pesticide Tolerances," *Pesticide Tolerances*, 2023. https://www.epa.gov/pesticide-tolerances/about-pesticide-tolerances.
[66] P. Van Hoi, A. Mol, and P. Oosterveer, "State governance of pesticide use and trade in Vietnam," *NJAS Wageningen J. Life Sci.*, vol. 67, no. 1, pp. 19–26, 2013.
[67] H. Tyagi, T. Gautam, and P. Prashar, "Survey of pesticide use patterns and farmers' perceptions: a case study from cauliflower and tomato cultivating areas of district Faridabad, Haryana, India," *Int. J. MediPharm Res.*, vol. 1, no. 03, pp. 139–146, 2015.
[68] P. Lu *et al.*, "Biodegradation of chlorpyrifos and 3, 5, 6-trichloro-2-pyridinol by Cupriavidus sp. DT-1," *Bioresour. Technol.*, vol. 127, pp. 337–342, 2013.
[69] World Health Organization, *Public health impact of pesticides used in agriculture*. World Health Organization, 1990.
[70] S. Imanishi *et al.*, "Prenatal exposure to permethrin influences vascular development of fetal brain and adult behavior in mice offspring," *Environ. Toxicol.*, vol. 28, no. 11, pp. 617–629, Nov. 2013, doi: https://doi.org/10.1002/tox.20758.
[71] C. Chang *et al.*, "Current pesticide profiles in blood serum of adults in Jiangsu Province of China and a comparison with other countries," *Environ. Int.*, vol. 102, pp. 213–222, 2017.
[72] C. A. Damalas and I. G. Eleftherohorinos, "Pesticide Exposure, Safety Issues, and Risk Assessment Indicators," *International Journal of Environmental Research and Public Health*, vol. 8, no. 5. pp. 1402–1419, 2011, doi: 10.3390/ijerph8051402.
[73] K.-H. Kim, E. Kabir, and S. A. Jahan, "Exposure to pesticides and the associated human health effects," *Sci. Total Environ.*, vol. 575, pp. 525–535, 2017, doi: https://doi.org/10.1016/j.scitotenv.2016.09.009.
[74] P. Chawla, R. Kaushik, V. J. S. Swaraj, and N. Kumar, "Organophosphorus pesticides residues in food and their colorimetric detection," *Environ. nanotechnology, Monit. Manag.*, vol. 10, pp. 292–307, 2018.
[75] S. Hiller-Sturmhöfel and A. Bartke, "The endocrine system: an overview," *Alcohol Health Res. World*, vol. 22, no. 3, p. 153, 1998.
[76] Diagrams, "The Human Body Hormone System," *DIAGRAMS*, 2018. http://all-diagram.blogspot.com/2018/06/the-human-body-hormone-

system.html?m=.
[77] K. Woods, “Endocrine Disorders: Common Types and Their Treatments,” *Endocrinology and Metabolism*, 2022. https://www.healthgrades.com/right-care/endocrinology-and-metabolism/endocrine-disorders.
[78] W. Mnif, A. I. H. Hassine, A. Bouaziz, A. Bartegi, O. Thomas, and B. Roig, “Effect of endocrine disruptor pesticides: a review,” *Int. J. Environ. Res. Public Health*, vol. 8, no. 6, pp. 2265–2303, 2011.
[79] Å. Bergman, J. J. Heindel, S. Jobling, K. Kidd, T. R. Zoeller, and W. H. Organization, *State of the science of endocrine disrupting chemicals 2012*. World Health Organization, 2013.
[80] J. M. Braun, “Early-life exposure to EDCs: role in childhood obesity and neurodevelopment,” *Nat. Rev. Endocrinol.*, vol. 13, no. 3, pp. 161–173, Mar. 2017, doi: 10.1038/nrendo.2016.186.
[81] P. Grandjean and A. A. Jensen, “Breastfeeding and the weanling’s dilemma,” *Am. J. Public Health*, vol. 94, no. 7, p. 1075, 2004.
[82] M. C. Fossi and L. Marsili, “Effects of endocrine disruptors in aquatic mammals,” *Pure Appl. Chem.*, vol. 75, no. 11–12, pp. 2235–2247, 2003.
[83] I. Suhani, S. Sahab, V. Srivastava, and R. P. Singh, “Impact of cadmium pollution on food safety and human health,” *Curr. Opin. Toxicol.*, vol. 27, pp. 1–7, Sep. 2021, doi: 10.1016/J.COTOX.2021.04.004.
[84] K. D. Fasae and A. O. Abolaji, “Interactions and toxicity of non-essential heavy metals (Cd, Pb and Hg): lessons from Drosophila melanogaster,” *Curr. Opin. Insect Sci.*, vol. 51, p. 100900, 2022, doi: 10.1016/j.cois.2022.100900.
[85] M. S. Sankhla, M. Kumari, M. Nandan, R. Kumar, and P. Agrawal, “Heavy metals contamination in water and their hazardous effect on human health-a review,” *Int. J. Curr. Microbiol. App. Sci*, vol. 5, no. 10, pp. 759–766, 2016.
[86] P. Gangaiya, J. Tabudravu, R. South, and S. Sotheeswaran, “Heavy metal contamination of the Lami coastal environment, Fiji,” *South Pacific J. Nat. Appl. Sci.*, vol. 19, no. 1, pp. 24–29, 2001.
[87] A. U. Rehman *et al.*, “Toxicity of heavy metals in plants and animals and their uptake by magnetic iron oxide nanoparticles,” *J. Mol. Liq.*, vol. 321, 2021, doi: 10.1016/j.molliq.2020.114455.
[88] R. Shrestha *et al.*, “Technological trends in heavy metals removal from industrial wastewater: A review,” *J. Environ. Chem. Eng.*, vol. 9, no. 4, p. 105688, 2021, doi: 10.1016/j.jece.2021.105688.
[89] R. Verma and P. Dwivedi, “Heavy metal water pollution-A case study,” *Recent Res. Sci. Technol.*, vol. 5, pp. 98–99, Jan. 2013.
[90] G. Genchi, M. S. Sinicropi, G. Lauria, A. Carocci, and A. Catalano, “The effects of cadmium toxicity,” *Int. J. Environ. Res. Public Health*, vol. 17, no. 11, Jun. 2020, doi: 10.3390/IJERPH17113782.
[91] H. Zhang and M. Reynolds, “Cadmium exposure in living organisms: A short review,” *Sci. Total Environ.*, vol. 678, pp. 761–767, 2019, doi: 10.1016/j.scitotenv.2019.04.395.
[92] S. QIN *et al.*, “Toxicity of cadmium and its competition with mineral nutrients for uptake by plants: A review,” *Pedosphere*, vol. 30, no. 2, pp. 168–180, 2020, doi: 10.1016/S1002-0160(20)60002-9.
[93] J. Thompson and J. Bannigan, “Cadmium: Toxic effects on the reproductive system and the embryo,” *Reprod. Toxicol.*, vol. 25, no. 3, pp. 304–315, 2008, doi: 10.1016/j.reprotox.2008.02.001.

[94] Y. Ma, D. Ran, X. Shi, H. Zhao, and Z. Liu, “Cadmium toxicity: A role in bone cell function and teeth development,” *Sci. Total Environ.*, vol. 769, p. 144646, 2021, doi: 10.1016/j.scitotenv.2020.144646.
[95] H. Horiguchi, E. Oguma, and F. Kayama, “Cadmium and cisplatin damage erythropoietin-producing proximal renal tubular cells,” *Arch. Toxicol.*, vol. 80, pp. 680–686, 2006.
[96] “scholar (12).” .
[97] J. Alexander *et al.*, “SCIENTIFIC OPINION Cadmium in food Scientific Opinion of the Panel on Contaminants in the Food Chain,” *EFSA J*, vol. 980, pp. 1–139, 2009.
[98] A. Kubier, R. T. Wilkin, and T. Pichler, “Cadmium in soils and groundwater: A review,” *Appl. Geochemistry*, vol. 108, p. 104388, 2019, doi: https://doi.org/10.1016/j.apgeochem.2019.104388.
[99] X.-S. Li, G.-T. Zhu, Y.-B. Luo, B.-F. Yuan, and Y.-Q. Feng, “Synthesis and applications of functionalized magnetic materials in sample preparation,” *TrAC Trends Anal. Chem.*, vol. 45, pp. 233–247, 2013.
[100] A. Przyjazny, “Liquid-phase microextraction,” 2017.
[101] A. B. Kanu, “Recent developments in sample preparation techniques combined with high-performance liquid chromatography: A critical review,” *J. Chromatogr. A*, vol. 1654, p. 462444, 2021, doi: https://doi.org/10.1016/j.chroma.2021.462444.
[102] I. Ali, M. Suhail, O. M. L. Alharbi, and I. Hussain, “Advances in sample preparation in chromatography for organic environmental pollutants analyses,” *J. Liq. Chromatogr. Relat. Technol.*, vol. 42, no. 5–6, pp. 137–160, 2019.
[103] C. M. M. Almeida, “Overview of Sample Preparation and Chromatographic Methods to Analysis Pharmaceutical Active Compounds in Waters Matrices,” *Separations*, vol. 8, no. 2. 2021, doi: 10.3390/separations8020016.
[104] A. Gałuszka, Z. M. Migaszewski, P. Konieczka, and J. Namieśnik, “Analytical Eco-Scale for assessing the greenness of analytical procedures,” *TrAC Trends Anal. Chem.*, vol. 37, pp. 61–72, 2012, doi: https://doi.org/10.1016/j.trac.2012.03.013.
[105] C. Ribeiro, A. R. Ribeiro, A. S. Maia, V. M. F. Gonçalves, and M. E. Tiritan, “New Trends in Sample Preparation Techniques for Environmental Analysis,” *Crit. Rev. Anal. Chem.*, vol. 44, no. 2, pp. 142–185, Apr. 2014, doi: 10.1080/10408347.2013.833850.
[106] S. N. Atapattu and J. M. Rosenfeld, “Solid phase analytical derivatization as a sample preparation method,” *J. Chromatogr. A*, vol. 1296, pp. 204–213, Jun. 2013, doi: 10.1016/j.chroma.2013.03.020.
[107] S. N. Atapattu and J. M. Rosenfeld, “Solid Phase Analytical Derivatization,” *Ref. Modul. Chem. Mol. Sci. Chem. Eng.*, Jan. 2018, doi: 10.1016/B978-0-12-409547-2.14248-9.
[108] R. Urkude, V. Dhurvey, and S. Kochhar, “15 - Pesticide Residues in Beverages,” A. M. Grumezescu and A. M. B. T.-Q. C. in the B. I. Holban, Eds. Academic Press, 2019, pp. 529–560.
[109] P. B. Kyle, “Chapter 7 - Toxicology: GCMS,” H. Nair and W. B. T.-M. S. for the C. L. Clarke, Eds. San Diego: Academic Press, 2017, pp. 131–163.
[110] G. Vas, K. Nagy, and K. Vékey, “Chapter 4 - Biomedical sampling,” K. Vékey, A. Telekes, and A. B. T.-M. A. of M. S. Vertes, Eds. Amsterdam:

Elsevier, 2008, pp. 37–59.
[111] E. Verette, “CHROMATOGRAPHY | Automation,” I. D. B. T.-E. of S. S. Wilson, Ed. Oxford: Academic Press, 2000, pp. 343–352.
[112] B. A. de Marco, B. S. Rechelo, E. G. Tótoli, A. C. Kogawa, and H. R. N. Salgado, “Evolution of green chemistry and its multidimensional impacts: A review,” *Saudi Pharm. J.*, vol. 27, no. 1, pp. 1–8, 2019, doi: https://doi.org/10.1016/j.jsps.2018.07.011.
[113] J. Howard-Grenville, A. J. Nelson, A. G. Earle, J. A. Haack, and D. M. Young, “‘If chemists don’t do it, who is going to?’ Peer-driven occupational change and the emergence of green chemistry,” *Adm. Sci. Q.*, vol. 62, no. 3, pp. 524–560, 2017.
[114] A. Gałuszka, Z. Migaszewski, and J. Namieśnik, “The 12 principles of green analytical chemistry and the SIGNIFICANCE mnemonic of green analytical practices,” *TrAC Trends Anal. Chem.*, vol. 50, pp. 78–84, 2013, doi: https://doi.org/10.1016/j.trac.2013.04.010.
[115] M. Sajid, “Dispersive liquid-liquid microextraction: Evolution in design, application areas, and green aspects,” *TrAC Trends Anal. Chem.*, vol. 152, p. 116636, 2022, doi: 10.1016/j.trac.2022.116636.
[116] Á. I. López-Lorente, F. Pena-Pereira, S. Pedersen-Bjergaard, V. G. Zuin, S. A. Ozkan, and E. Psillakis, “The ten principles of green sample preparation,” *TrAC Trends Anal. Chem.*, vol. 148, p. 116530, 2022, doi: https://doi.org/10.1016/j.trac.2022.116530.
[117] H. Liu and P. K. Dasgupta, “Analytical chemistry in a drop. solvent extraction in a microdrop,” *Anal. Chem.*, vol. 68, no. 11, pp. 1817–1821, 1996, doi: 10.1021/ac960145h.
[118] M. A. Jeannot and F. F. Cantwell, “Solvent microextraction into a single drop,” *Anal. Chem.*, vol. 68, no. 13, pp. 2236–2240, 1996.
[119] A. Yohannes, T. Tolesa, Y. Merdassa, and N. Megersa, “Single drop microextraction analytical technique for simultaneous separation and trace enrichment of atrazine and its major degradation products from environmental waters followed by liquid chromatographic determination,” *J. Anal. Bioanal. Tech*, vol. 7, no. 5, 2016.
[120] J. S. Câmara, R. Perestrelo, B. Olayanju, C. V Berenguer, A. Kabir, and J. A. M. Pereira, “Overview of Different Modes and Applications of Liquid Phase-Based Microextraction Techniques,” *Processes*, vol. 10, no. 7. 2022, doi: 10.3390/pr10071347.
[121] C. Nerin, “Basic principles and applications of liquid phase microextraction techniques,” *Sci Chromatogr*, vol. 8, pp. 137–142, 2016.
[122] Y. B. Pakade and D. K. Tewary, “Development and applications of single-drop microextraction for pesticide residue analysis: A review,” *J. Sep. Sci.*, vol. 33, no. 23-24, pp. 3683–3691, 2010.
[123] M. A. Jeannot, A. Przyjazny, and J. M. Kokosa, “Single drop microextraction—Development, applications and future trends,” *J. Chromatogr. A*, vol. 1217, no. 16, pp. 2326–2336, 2010, doi: https://doi.org/10.1016/j.chroma.2009.10.089.
[124] I. Delove Tegladza *et al.*, “Direct immersion single-drop microextraction of semi-volatile organic compounds in environmental samples: A review,” *J. Hazard. Mater.*, vol. 393, p. 122403, 2020, doi: https://doi.org/10.1016/j.jhazmat.2020.122403.
[125] N. S. Pano-Farias, S. G. Ceballos-Magaña, R. Muñiz-Valencia, J. M. Jurado,

Á. Alcázar, and I. A. Aguayo-Villarreal, “Direct immersion single drop micro-extraction method for multi-class pesticides analysis in mango using GC–MS,” *Food Chem.*, vol. 237, pp. 30–38, 2017.

[126] A. A. Rincón, V. Pino, J. H. Ayala, and A. M. Afonso, “Headspace-single drop microextraction (HS-SDME) in combination with high-performance liquid chromatography (HPLC) to evaluate the content of alkyl- and methoxy-phenolic compounds in biomass smoke,” *Talanta*, vol. 85, no. 3, pp. 1265–1273, 2011, doi: https://doi.org/10.1016/j.talanta.2011.05.046.

[127] G.-J. Wang, L. Tian, Y.-M. Fan, and M.-L. Qi, “Headspace single-drop microextraction gas chromatography mass spectrometry for the analysis of volatile compounds from Herba Asari,” *J. Anal. Methods Chem.*, vol. 2013, 2013.

[128] S. Jahan *et al.*, “A highly efficient three-phase single drop microextraction technique for sample preconcentration,” *Analyst*, vol. 140, no. 9, pp. 3193–3200, 2015, doi: 10.1039/C4AN02324B.

[129] S. Jeong *et al.*, “Facile and highly efficient three-phase single drop microextraction in-line coupled with capillary electrophoresis,” *J. Chromatogr. A*, vol. 1655, p. 462520, 2021, doi: https://doi.org/10.1016/j.chroma.2021.462520.

[130] H.-F. Wu, J.-H. Yen, and C.-C. Chin, “Combining Drop-to-Drop Solvent Microextraction with Gas Chromatography/Mass Spectrometry Using Electronic Ionization and Self-Ion/Molecule Reaction Method To Determine Methoxyacetophenone Isomers in One Drop of Water,” *Anal. Chem.*, vol. 78, no. 5, pp. 1707–1712, Mar. 2006, doi: 10.1021/ac052076p.

[131] K. Shrivas and D. K. Patel, “Matrix-assisted laser desorption/ionization mass spectrometry for quantitative determination of β-blocker drugs in one-drop of human serum sample,” *J. Chromatogr. B*, vol. 879, no. 1, pp. 35–40, 2011.

[132] D. B. G. Williams, M. J. George, and L. Marjanovic, “Rapid Detection of Atrazine and Metolachlor in Farm Soils: Gas Chromatography–Mass Spectrometry-Based Analysis Using the Bubble-in-Drop Single Drop Microextraction Enrichment Method,” *J. Agric. Food Chem.*, vol. 62, no. 31, pp. 7676–7681, Aug. 2014, doi: 10.1021/jf502411t.

[133] K. Chullasat, Z. Huang, O. Bunkoed, P. Kanatharana, and H. K. Lee, “Bubble-in-drop microextraction of carbamate pesticides followed by gas chromatography-mass spectrometric analysis,” *Microchem. J.*, vol. 155, p. 104666, 2020, doi: https://doi.org/10.1016/j.microc.2020.104666.

[134] D. B. G. Williams, M. J. George, R. Meyer, and L. Marjanovic, “Bubbles in Solvent Microextraction: The Influence of Intentionally Introduced Bubbles on Extraction Efficiency,” *Anal. Chem.*, vol. 83, no. 17, pp. 6713–6716, Sep. 2011, doi: 10.1021/ac201323z.

[135] W. Liu and H. K. Lee, “Continuous-Flow Microextraction Exceeding1000-Fold Concentration of Dilute Analytes,” *Anal. Chem.*, vol. 72, no. 18, pp. 4462–4467, Sep. 2000, doi: 10.1021/ac000240x.

[136] Y. He and H. K. Lee, “Continuous flow microextraction combined with high-performance liquid chromatography for the analysis of pesticides in natural waters,” *J. Chromatogr. A*, vol. 1122, no. 1, pp. 7–12, 2006, doi: https://doi.org/10.1016/j.chroma.2006.04.078.

[137] S. Pedersen-Bjergaard and K. E. Rasmussen, “Liquid− liquid− liquid microextraction for sample preparation of biological fluids prior to capillary electrophoresis,” *Anal. Chem.*, vol. 71, no. 14, pp. 2650–2656, 1999.

[138] V. Sharifi, A. Abbasi, and A. Nosrati, “Application of hollow fiber liquid phase microextraction and dispersive liquid–liquid microextraction techniques in analytical toxicology,” *J. food drug Anal.*, vol. 24, no. 2, pp. 264–276, 2016.
[139] H. Zhang, Z. Du, Y. Ji, and M. Mei, “Simultaneous trace determination of acidic non-steroidal anti-inflammatory drugs in purified water, tap water, juice, soda and energy drink by hollow fiber-based liquid-phase microextraction and ultra-high pressure liquid chromatography coupled to tandem ,” *Talanta*, vol. 109, pp. 177–184, 2013, doi: https://doi.org/10.1016/j.talanta.2013.02.048.
[140] L. M. Madikizela, V. E. Pakade, S. Ncube, H. Tutu, and L. Chimuka, “Application of hollow fibre-liquid phase microextraction technique for isolation and pre-concentration of pharmaceuticals in water,” *Membranes (Basel).*, vol. 10, no. 11, p. 311, 2020.
[141] E. Bozorgzadeh, S. Shariati, and A. Esmaeilnejad, “Central composite design for optimizing hollow fiber liquid phase microextraction of carbamazepine from aqueous and biological samples,” *J. Anal. Chem.*, vol. 75, pp. 154–160, 2020.
[142] M. Tajik, Y. Yamini, A. Esrafili, and B. Ebrahimpour, “Automated hollow fiber microextraction based on two immiscible organic solvents for the extraction of two hormonal drugs,” *J. Pharm. Biomed. Anal.*, vol. 107, pp. 24–31, 2015, doi: https://doi.org/10.1016/j.jpba.2014.12.028.
[143] S. Cunha, J. Fernandes, and M. Oliveira, “Current Trends in Liquid-Liquid Microextraction for Analysis of Pesticide Residues in Food and Water,” in *Pesticides - Strategies for Pesticides Analysis*, 2011.
[144] M. R. K. Zanjani, Y. Yamini, S. Shariati, and J. Å. Jönsson, “A new liquid-phase microextraction method based on solidification of floating organic drop,” *Anal. Chim. Acta*, vol. 585, no. 2, pp. 286–293, 2007.
[145] F. R. Mansour and N. D. Danielson, “Solidification of floating organic droplet in dispersive liquid-liquid microextraction as a green analytical tool,” *Talanta*, vol. 170, pp. 22–35, 2017.
[146] X. Zhang *et al.*, “A Natural Monoterpene Enol for Dispersive Liquid–Liquid Microextraction Based on Solidification of Floating Organic Droplets for Determination of Benzophenone Compounds in Water Samples,” *Separations*, vol. 10, no. 1. 2023, doi: 10.3390/separations10010001.
[147] Y. Liu, M. He, B. Chen, and B. Hu, “Solidification of floating organic drop microextraction combined with gas chromatography-flame photometric detection for the analysis of organophosphorus pesticides in water samples,” *Anal. Methods*, vol. 7, no. 15, pp. 6182–6189, 2015.
[148] B. Chen and Y. Huang, “Dispersive Liquid-Phase Microextraction with Solidification of Floating Organic Droplet Coupled with High-Performance Liquid Chromatography for the Determination of Sudan Dyes in Foodstuffs and Water Samples,” *J. Agric. Food Chem.*, vol. 62, no. 25, pp. 5818–5826, Jun. 2014, doi: 10.1021/jf5006403.
[149] Z. M. Memon, E. Yilmaz, and M. Soylak, “Switchable solvent based green liquid phase microextraction method for cobalt in tobacco and food samples prior to flame atomic absorption spectrometric determination,” *J. Mol. Liq.*, vol. 229, pp. 459–464, 2017.
[150] Y. Hamid and M. R. Fat’hi, “A fast and green preconcentration method based

on surfactant ion pair-switchable solvent dispersive liquid–liquid microextraction for determination of phenazopyridine in pharmaceutical and biological samples," *J. Iran. Chem. Soc.*, vol. 15, no. 8, pp. 1813–1820, 2018, doi: 10.1007/s13738-018-1378-z.

[151] H. Musarurwa and N. T. Tavengwa, "Switchable solvent-based micro-extraction of pesticides in food and environmental samples," *Talanta*, vol. 224, p. 121807, 2021, doi: https://doi.org/10.1016/j.talanta.2020.121807.

[152] Y. Bazel, M. Rečlo, and Y. Chubirka, "Switchable hydrophilicity solvents in analytical chemistry. Five years of achievements," *Microchem. J.*, vol. 157, p. 105115, 2020, doi: https://doi.org/10.1016/j.microc.2020.105115.

[153] M. Hassan, F. Uzcan, U. Alshana, and M. Soylak, "Switchable-hydrophilicity solvent liquid–liquid microextraction prior to magnetic nanoparticle-based dispersive solid-phase microextraction for spectrophotometric determination of erythrosine in food and other samples," *Food Chem.*, vol. 348, p. 129053, 2021, doi: https://doi.org/10.1016/j.foodchem.2021.129053.

[154] A. Quigley, W. Cummins, and D. Connolly, "Dispersive Liquid-Liquid Microextraction in the Analysis of Milk and Dairy Products: A Review," *J. Chem.*, vol. 2016, p. 4040165, 2016, doi: 10.1155/2016/4040165.

[155] M. Saraji and M. K. Boroujeni, "Recent developments in dispersive liquid–liquid microextraction," *Anal. Bioanal. Chem.*, vol. 406, pp. 2027–2066, 2014.

[156] M. Rezaee, Y. Assadi, M.-R. M. Hosseini, E. Aghaee, F. Ahmadi, and S. Berijani, "Determination of organic compounds in water using dispersive liquid–liquid microextraction," *J. Chromatogr. A*, vol. 1116, no. 1–2, pp. 1–9, 2006.

[157] O. Zuloaga, M. Olivares, P. Navarro, A. Vallejo, and A. Prieto, "Dispersive liquid–liquid microextraction: Trends in the analysis of biological samples," *Bioanalysis*, vol. 7, no. 17, pp. 2211–2225, 2015.

[158] T. Y. Hwang, Kin, Chai Mee, and W. L. Shing, "A review on extraction solvents in the dispersive liquid-liquid microextraction," *Malaysian J. Anal. Sci.*, vol. 22, no. 2, pp. 166–174, 2018, doi: https://doi.org/10.17576/mjas-2018-2202-01.

[159] G. K. S. Alcantara, L. A. Calixto, L. A. B. de Moraes, R. H. C. Queiroz, A. R. M. de Oliveira, and C. M. de Gaitani, "Determination of levetiracetam in human plasma by dispersive liquid-liquid microextraction followed by gas chromatography-mass spectrometry," *J. Anal. Methods Chem.*, vol. 2016, 2016.

[160] M. Rezaee, Y. Yamini, and M. Faraji, "Evolution of dispersive liquid-liquid microextraction method," *Journal of Chromatography A*, vol. 1217, no. 16. pp. 2342–2357, Apr. 2010, doi: 10.1016/j.chroma.2009.11.088.

[161] Y. Wang, J. Li, D. Sun, S. Yang, H. Liu, and L. Chen, "Strategies of dispersive liquid-liquid microextraction for coastal zone environmental pollutant determination," *J. Chromatogr. A*, vol. 1658, p. 462615, 2021, doi: https://doi.org/10.1016/j.chroma.2021.462615.

[162] F. R. Mansour and M. A. Khairy, "Pharmaceutical and biomedical applications of dispersive liquid–liquid microextraction," *J. Chromatogr. B*, vol. 1061–1062, pp. 382–391, 2017, doi: https://doi.org/10.1016/j.jchromb.2017.07.055.

[163] J. L. P. Pavón, S. H. Martín, C. G. Pinto, and B. M. Cordero, "Determination

of trihalomethanes in water samples: a review," *Anal. Chim. Acta*, vol. 629, no. 1–2, pp. 6–23, 2008.
[164] J. Grau, C. Azorín, J. L. Benedé, A. Chisvert, and A. Salvador, "Use of green alternative solvents in dispersive liquid-liquid microextraction: A review," *J. Sep. Sci.*, vol. 45, no. 1, pp. 210–222, 2022.
[165] M. Tobiszewski, P. Bigus, and J. Namieśnik, "Determination of parent and methylated polycyclic aromatic hydrocarbons in water samples by dispersive liquid–liquid microextraction–two dimensional gas chromatography–time-of-flight mass spectrometry," *Anal. methods*, vol. 6, no. 17, pp. 6678–6687, 2014.
[166] B. Ç. Özkan, M. Fırat, D. S. Chormey, and S. Bakırdere, "Accurate and sensitive determination of harmful aromatic amine products of azo dyes in wastewater and textile samples by GC–MS after multivariate optimization of binary solvent dispersive liquid-liquid microextraction," *Microchem. J.*, vol. 145, pp. 84–89, 2019.
[167] D. S. Chormey, M. Fırat, and S. Bakırdere, "Multivariate Optimization of Binary Solvent Microextraction for the Simultaneous Determination of Endocrine Disruptive Phenolic Compounds and Organochlorine Pesticides in Wastewater and Sludge Samples by GC-MS," *Water, Air, Soil Pollut.*, vol. 229, no. 11, p. 370, 2018.
[168] E. S. Koçoğlu, O. Sözüdoğru, O. T. Komesli, A. E. Yılmaz, E. Ö. Er, and S. Bakırdere, "Sensitive Determination of Selected Drug Active Compounds in Wastewater Matrices by LC-QTOF-MS/MS after Vortex Assisted Binary Solvents Dispersive Liquid-Liquid Microextraction," *Chem. Lett.*, vol. 49, no. 5, pp. 546–549, Apr. 2020, doi: 10.1246/cl.200066.
[169] S. Berijani, Y. Assadi, M. Anbia, M.-R. M. Hosseini, and E. Aghaee, "Dispersive liquid–liquid microextraction combined with gas chromatography-flame photometric detection: very simple, rapid and sensitive method for the determination of organophosphorus pesticides in water," *J. Chromatogr. A*, vol. 1123, no. 1, pp. 1–9, 2006.
[170] J. M. Kokosa, "Advances in solvent-microextraction techniques," *TrAC Trends Anal. Chem.*, vol. 43, pp. 2–13, 2013.
[171] F. A. Hansen and S. Pedersen-Bjergaard, "Emerging extraction strategies in analytical chemistry," *Anal. Chem.*, vol. 92, no. 1, pp. 2–15, 2019.
[172] N. B. Turan and S. Bakirdere, "A miniaturized spray-assisted fine-droplet-formation-based liquid-phase microextraction method for the simultaneous determination of fenpiclonil, nitrofen and fenoxaprop-ethyl as pesticides in soil samples," *Rapid Commun. Mass Spectrom.*, vol. 35, no. 1, p. e8943, 2021.
[173] J. L. M. Viana, A. A. Menegário, and A. H. Fostier, "Preparation of environmental samples for chemical speciation of metal/metalloids: A review of extraction techniques," *Talanta*, vol. 226, no. September 2020, 2021, doi: 10.1016/j.talanta.2021.122119.
[174] C. L. Arthur and J. Pawliszyn, "Solid phase microextraction with thermal desorption using fused silica optical fibers," *Anal. Chem.*, vol. 62, no. 19, pp. 2145–2148, 1990.
[175] J. Li, Y.-B. Wang, K.-Y. Li, Y.-Q. Cao, S. Wu, and L. Wu, "Advances in different configurations of solid-phase microextraction and their applications in food and environmental analysis," *TrAC Trends Anal. Chem.*, vol. 72, pp. 141–152, 2015, doi: https://doi.org/10.1016/j.trac.2015.04.023.

[176] C. Duan, Z. Shen, D. Wu, and Y. Guan, “Recent developments in solid-phase microextraction for on-site sampling and sample preparation,” *TrAC Trends Anal. Chem.*, vol. 30, no. 10, pp. 1568–1574, 2011, doi: https://doi.org/10.1016/j.trac.2011.08.005.
[177] M. Lashgari, V. Singh, and J. Pawliszyn, “A critical review on regulatory sample preparation methods: Validating solid-phase microextraction techniques,” *TrAC Trends Anal. Chem.*, vol. 119, p. 115618, 2019, doi: https://doi.org/10.1016/j.trac.2019.07.029.
[178] V. Jalili, A. Barkhordari, and A. Ghiasvand, “Solid-phase microextraction technique for sampling and preconcentration of polycyclic aromatic hydrocarbons: A review,” *Microchem. J.*, vol. 157, p. 104967, 2020, doi: https://doi.org/10.1016/j.microc.2020.104967.
[179] T. Khezeli and A. Daneshfar, “Development of dispersive micro-solid phase extraction based on micro and nano sorbents,” *TrAC Trends Anal. Chem.*, vol. 89, pp. 99–118, 2017, doi: https://doi.org/10.1016/j.trac.2017.01.004.
[180] M. Ghorbani, M. Aghamohammadhassan, M. Chamsaz, H. Akhlaghi, and T. Pedramrad, “Dispersive solid phase microextraction,” *TrAC Trends Anal. Chem.*, vol. 118, pp. 793–809, 2019, doi: https://doi.org/10.1016/j.trac.2019.07.012.
[181] I. Vasconcelos and C. Fernandes, “Magnetic solid phase extraction for determination of drugs in biological matrices,” *TrAC Trends Anal. Chem.*, vol. 89, pp. 41–52, 2017, doi: https://doi.org/10.1016/j.trac.2016.11.011.
[182] W. Li and Y. Shi, “Recent advances and applications of carbon nanotubes based composites in magnetic solid-phase extraction,” *TrAC Trends Anal. Chem.*, vol. 118, pp. 652–665, 2019, doi: https://doi.org/10.1016/j.trac.2019.06.039.
[183] C. Herrero-Latorre, J. Barciela-García, S. García-Martín, R. M. Peña-Crecente, and J. Otárola-Jiménez, “Magnetic solid-phase extraction using carbon nanotubes as sorbents: A review,” *Analytica Chimica Acta*, vol. 892. Elsevier B.V., pp. 10–26, Sep. 10, 2015, doi: 10.1016/j.aca.2015.07.046.
[184] G. D. Bozyiğit, Y. Kılınç, B. T. Zaman, D. S. Chormey, and S. Bakırdere, “Polystyrene-coated magnetic nanoparticles based dispersive solid phase extraction for the determination of cadmium in cigarette ash prior to slotted quartz tube flame atomic absorption spectrometry system,” *Anal. Sci.*, vol. 38, no. 6, pp. 843–849, 2022, doi: 10.1007/s44211-022-00104-8.
[185] N. Ma *et al.*, “Determination of Tetracyclines in Chicken by Dispersive Solid Phase Microextraction Based on Metal-Organic Frameworks/Molecularly Imprinted Nano-polymer and Ultra Performance Liquid Chromatography,” *Food Anal. Methods*, vol. 13, no. 5, pp. 1211–1219, 2020, doi: 10.1007/s12161-020-01744-0.
[186] A. Azzouz *et al.*, “Review of nanomaterials as sorbents in solid-phase extraction for environmental samples,” *TrAC Trends Anal. Chem.*, vol. 108, pp. 347–369, 2018, doi: https://doi.org/10.1016/j.trac.2018.08.009.
[187] H. I. Mokhtar, R. A. Abdel-Salam, and G. M. Hadad, “A nanocomposite of silica coated magnetite nanoparticles and aniline-anthranilic acid co-polymeric nanorods with improved stability and selectivity for fluoroquinolones dispersive micro solid phase extraction,” *J. Chromatogr. B*, vol. 1206, p. 123350, 2022, doi: https://doi.org/10.1016/j.jchromb.2022.123350.
[188] Bhanot, D., “What are the benefits offered by Modern Analytical

Instrumental methods over Non-Instrumental methods?,” 2023. .
[189] S. Watanabe, T. Sato, M. Nakaya, T. Yoshida, and J. Onoe, “Chemical forms of molybdenum ion in nitric acid solution studied using liquid-phase X-ray absorption fine structure, Ultraviolet–Visible absorption spectroscopy and first-principles calculations,” *Chem. Phys. Lett.*, vol. 723, pp. 76–81, 2019, doi: https://doi.org/10.1016/j.cplett.2019.02.049.
[190] C. Du, B. Liu, J. Hu, and H. Li, “Determination of iodine number of activated carbon by the method of ultraviolet–visible spectroscopy,” *Mater. Lett.*, vol. 285, p. 129137, 2021, doi: https://doi.org/10.1016/j.matlet.2020.129137.
[191] M. Hassan, Z. Erbas, U. Alshana, and M. Soylak, “Ligandless reversed-phase switchable-hydrophilicity solvent liquid–liquid microextraction combined with flame-atomic absorption spectrometry for the determination of copper in oil samples,” *Microchem. J.*, vol. 156, p. 104868, 2020, doi: https://doi.org/10.1016/j.microc.2020.104868.
[192] M. Şaylan, B. Metin, H. Akbıyık, F. Turak, G. Çetin, and S. Bakırdere, “Microwave assisted effective synthesis of CdS nanoparticles to determine the copper ions in artichoke leaves extract samples by flame atomic absorption spectrometry,” *J. Food Compos. Anal.*, vol. 115, p. 104965, 2023, doi: https://doi.org/10.1016/j.jfca.2022.104965.
[193] J. R. K. Silveira, L. C. Brudi, S. R. Waechter, P. A. Mello, A. B. Costa, and F. A. Duarte, “Copper determination in beer by flame atomic absorption spectrometry after extraction and preconcentration by dispersive liquid–liquid microextraction,” *Microchem. J.*, vol. 184, p. 108181, 2023, doi: https://doi.org/10.1016/j.microc.2022.108181.
[194] L. M. Costa *et al.*, “Direct magnetic sorbent sampling flame atomic absorption spectrometry (DMSS-FAAS) for highly sensitive determination of trace metals,” *Anal. Chim. Acta*, p. 340709, 2022, doi: https://doi.org/10.1016/j.aca.2022.340709.
[195] M. Anastácio, A. P. M. dos Santos, M. Aschner, and L. Mateus, “Determination of trace metals in fruit juices in the Portuguese market,” *Toxicol. Reports*, vol. 5, pp. 434–439, 2018, doi: https://doi.org/10.1016/j.toxrep.2018.03.010.
[196] S. M. Farid and M. A. Enani, “Levels of trace elements in commercial fruit juices in Jeddah, Saudi Arabia,” *Med. J. Islam. World Acad. Sci.*, vol. 18, no. 1, pp. 31–38, 2010.
[197] C. U. Desem, R. Maas, J. Woodhead, G. Carr, and A. Greig, “The utility of rapid throughput single-collector sector-field ICP-MS for soil Pb isotope studies,” *Appl. Geochemistry*, vol. 143, p. 105361, 2022, doi: https://doi.org/10.1016/j.apgeochem.2022.105361.
[198] T. Y. Guselnikova, A. R. Tsygankova, and N. S. Medvedev, “Matrix volatilization in a flow reactor for multi-element analysis of high purity germanium by ICP-MS,” *Spectrochim. Acta Part B At. Spectrosc.*, vol. 197, p. 106544, 2022, doi: https://doi.org/10.1016/j.sab.2022.106544.
[199] Y. Rodríguez Giraldo, E. Rodriguez Sánchez, L. G. Torres, A. C. Montenegro, and M. A. Pichimata, “Development of validation methods to determine cadmium in cocoa almond from the beans by ICP-MS and ICP-OES,” *Talanta Open*, vol. 5, 2022, doi: 10.1016/j.talo.2021.100078.
[200] F. Di Donato, A. Biancolillo, M. Foschi, V. Di Cecco, L. Di Martino, and A. A. D’Archivio, “Authentication of typical Italian bell pepper spices by ICP-OES multi-elemental analysis combined with SIMCA class modelling,” *J.*

Food Compos. Anal., vol. 115, p. 104948, 2023, doi: https://doi.org/10.1016/j.jfca.2022.104948.
[201] S. H. Santos *et al.*, "Development of Analytical Method for Determination of Inorganic Constituents in Powder Refreshment Using Dilute Mineral Acids and Detection by ICP OES," *J. Braz. Chem. Soc.*, vol. 32, pp. 1361–1372, 2021.
[202] S. Phal, H. Nguyễn, A. Berisha, and S. Tesfalidet, "In situ Bi/carboxyphenyl-modified glassy carbon electrode as a sensor platform for detection of Cd2+ and Pb2+ using square wave anodic stripping voltammetry.," *Sens. Bio-Sensing Res.*, vol. 34, p. 100455, 2021, doi: https://doi.org/10.1016/j.sbsr.2021.100455.
[203] M. Nodehi, M. Baghayeri, and A. Kaffash, "Application of BiNPs/MWCNTs-PDA/GC sensor to measurement of Tl (1) and Pb (II) using stripping voltammetry," *Chemosphere*, vol. 301, p. 134701, 2022, doi: https://doi.org/10.1016/j.chemosphere.2022.134701.
[204] Y. Zhang and R. G. Compton, "Anodic stripping voltammetry using underpotential deposition allows sub 10 ppb measurement of Total As and As(III) in water," *Talanta*, vol. 247, p. 123578, 2022, doi: https://doi.org/10.1016/j.talanta.2022.123578.
[205] Y. Ni and L. Wang, "Simultaneous polarographic determination of Lead (II) and Tin (II) by multivariate calibration," 1999.
[206] C. Hubert *et al.*, "Development and validation of a quantitative method for the selective determination of tin species in tin octoate by differential pulse polarography," *Talanta*, vol. 80, no. 3, pp. 1413–1420, 2010.
[207] H. Aghaie, M. Giahi, M. Monajjemi, M. Arvand, G. H. Nafissi, and M. Aghaie, "Tin (II)-selective membrane potentiometric sensor using a crown ether as neutral carrier," *Sensors Actuators B Chem.*, vol. 107, no. 2, pp. 756–761, 2005.
[208] M. Arvand, A. M. Moghimi, A. Afshari, and N. Mahmoodi, "Potentiometric membrane sensor based on 6-(4-nitrophenyl)-2, 4-diphenyl-3, 5-diaza-bicyclo [3.1. 0] hex-2-ene for detection of Sn (II) in real samples," *Anal. Chim. Acta*, vol. 579, no. 1, pp. 102–108, 2006.
[209] L. C. Peruchi *et al.*, "Determination of inorganic nutrients in wheat flour by laser-induced breakdown spectroscopy and energy dispersive X-ray fluorescence spectrometry," *Spectrochim. Acta Part B At. Spectrosc.*, vol. 100, pp. 129–136, 2014, doi: https://doi.org/10.1016/j.sab.2014.08.025.
[210] E. Marguí, B. Zawisza, and R. Sitko, "Trace and ultratrace analysis of liquid samples by X-ray fluorescence spectrometry," *TrAC Trends Anal. Chem.*, vol. 53, pp. 73–83, 2014, doi: https://doi.org/10.1016/j.trac.2013.09.009.
[211] E. Poboży and M. Trojanowicz, "Application of Capillary Electrophoresis for Determination of Inorganic Analytes in Waters," *Molecules*, vol. 26, no. 22. 2021, doi: 10.3390/molecules26226972.
[212] M. Paolini, L. Tonidandel, and R. Larcher, "Development, validation and application of a fast GC-FID method for the analysis of volatile compounds in spirit drinks and wine," *Food Control*, vol. 136, p. 108873, 2022, doi: https://doi.org/10.1016/j.foodcont.2022.108873.
[213] R. Aparicio-Ruiz *et al.*, "Method for the analysis of volatile compounds in virgin olive oil by SPME-GC-MS or SPME-GC-FID," *MethodsX*, vol. 10, p. 101972, 2023, doi: https://doi.org/10.1016/j.mex.2022.101972.
[214] G. D. Bozyiğit *et al.*, "Removal of selected pesticides, alkylphenols,

hormones and bisphenol A from domestic wastewater by electrooxidation process," *Water Sci. Technol.*, vol. 85, no. 1, pp. 220–228, 2022.
[215] S. Bodur *et al.*, "A sensitive determination method for trace bisphenol A in bottled water and wastewater samples: Binary solvent liquid phase microextraction-quadrupole isotope dilution-gas chromatography-mass spectrometry," *Microchem. J.*, vol. 159, p. 105532, 2020, doi: https://doi.org/10.1016/j.microc.2020.105532.
[216] S. Bodur *et al.*, "Assessment of different isotope dilution strategies and their combination with switchable solvent-based liquid phase microextraction prior to the quantification of bisphenol A at trace levels *via* GC-MS," *New J. Chem.*, 2020, doi: 10.1039/D0NJ02706E.
[217] H. Sari Erkan *et al.*, "Binary Dispersive Liquid-Liquid Microextraction Strategy for Accurate and Precise Determination of Micropollutants in Lake, Well and Wastewater Matrices," *Bull. Environ. Contam. Toxicol.*, vol. 103, no. 6, pp. 841–847, Dec. 2019, doi: 10.1007/s00128-019-02722-x.
[218] T. U. Gösterişli, S. Oflu, S. Keyf, and S. Bakırdere, "Development of a double monitoring system for the determination of Cr(VI) in different water matrices by HPLC–UV and digital image-based colorimetric detection method with the help of a metal sieve-linked double syringe system in complexation," *Environ. Monit. Assess.*, vol. 194, no. 10, p. 691, 2022, doi: 10.1007/s10661-022-10392-2.
[219] Y. Zhang *et al.*, "Simultaneous determination of 20 phenolic compounds in propolis by HPLC-UV and HPLC-MS/MS," *J. Food Compos. Anal.*, vol. 115, p. 104877, 2023, doi: https://doi.org/10.1016/j.jfca.2022.104877.
[220] R. D. Damale *et al.*, "Multiresidue analysis of pesticides in four different pomegranate cultivars: Investigating matrix effect variability by GC-MS/MS and LC-MS/MS," *Food Chem.*, vol. 407, p. 135179, 2023, doi: https://doi.org/10.1016/j.foodchem.2022.135179.
[221] B. Lyu, X. Zhang, J. Li, L. Zhang, Y. Zhong, and Y. Wu, "Determination of polychlorinated dibenzo-p-dioxins and furans in food samples by gas chromatography-triple quadrupole mass spectrometry (GC-MS/MS) and comparison with gas chromatography-high resolution mass spectrometry (GC-HRMS)," *J. Food Compos. Anal.*, vol. 115, p. 104947, 2023, doi: https://doi.org/10.1016/j.jfca.2022.104947.
[222] C. F. Poole, "Chapter 2 - Derivatization in Liquid Chromatography," S. Fanali, P. R. Haddad, C. F. Poole, P. Schoenmakers, and D. B. T.-L. C. Lloyd, Eds. Amsterdam: Elsevier, 2013, pp. 25–56.
[223] J. Bland-Hawthorn and G. Cecil, "18 - Classical Spectroscopy," in *Atomic, Molecular, and Optical Physics: Atoms and Molecules*, vol. 29, F. B. Dunning and R. G. B. T.-E. M. in the P. S. Hulet, Eds. Academic Press, 1996, pp. 363–391.
[224] S. R. Khan, B. Sharma, P. A. Chawla, and R. Bhatia, "Inductively Coupled Plasma Optical Emission Spectrometry (ICP-OES): a Powerful Analytical Technique for Elemental Analysis," *Food Anal. Methods*, vol. 15, no. 3, pp. 666–688, 2022, doi: 10.1007/s12161-021-02148-4.
[225] A. M. Pollard, C. M. Batt, B. Stern, and Y. S. M. M, "Elemental Analysis by Absorption and Emission Spectroscopies in the Visible and Ultraviolet," in *Analytical chemistry in archaeology*, New York, USA: Cambridge University Press, 2007.
[226] A. J. Majumdar and N. Dubey, "Applications of inductively coupled plasma-

atomic emission spectrometry (ICP-OES) in impurity profiling of Pharmaceuticals.," *Int. J. Pharm. Life Sci.*, vol. 8, no. 1, 2017.
[227] X. Hou and B. T. Jones, "Inductively coupled plasma/optical emission spectrometry," *Encyclopedia of analytical chemistry*, vol. 2000. John Wiley & Sons Chichester, UK, pp. 9468–9485, 2000.
[228] Y. Makonnen and D. Beauchemin, "Chapter 1 - The inductively coupled plasma as a source for optical emission spectrometry and mass spectrometry," D. B. T.-S. I. S. in I. and I. Beauchemin, Ed. Amsterdam: Elsevier, 2020, pp. 1–55.
[229] R. S. Houk, V. A. Fassel, G. D. Flesch, H. J. Svec, A. L. Gray, and C. E. Taylor, "Inductively coupled argon plasma as an ion source for mass spectrometric determination of trace elements," *Anal. Chem.*, vol. 52, pp. 2283–2289, 1980, doi: 10.1021/ac50064a012.
[230] T. Rettberg, "The Development of Inductively-Coupled Plasma Mass Spectrometry (ICP-MS)," *Encycl. Mass Spectrom.*, pp. 87–91, 2016, doi: 10.1016/b978-0-08-043848-1.00197-8.
[231] C. G. Vogiatzis and G. A. Zachariadis, "Tandem mass spectrometry in metallomics and the involving role of ICP-MS detection: A review," *Anal. Chim. Acta*, vol. 819, pp. 1–14, 2014, doi: 10.1016/j.aca.2014.01.029.
[232] F. Cubadda, "Inductively coupled plasma mass spectrometry," *Food Toxicants Anal.*, pp. 697–751, 2007, doi: 10.1016/B978-044452843-8/50020-1.
[233] P. N. Soltanpour, G. W. Johnson, S. M. Workman, J. B. Jones, and R. O. Miller, "Advances in ICP Emission and ICP Mass Spectrometry," *Adv. Agron.*, vol. 64, no. C, pp. 27–113, 1998, doi: 10.1016/S0065-2113(08)60502-7.
[234] R. Thomas, "Practical Guide to ICP-MS and Other Atomic Spectroscopy Techniques: A Tutorial for Beginners," 2023.
[235] B. Welz, H. Becker-Ross, S. Florek, U. Heitmann, and M. G. R. Vale, "High-resolution continuum-source atomic absorption spectrometry - What can we expect?," *J. Braz. Chem. Soc.*, vol. 14, no. 2, pp. 220–229, 2003, doi: 10.1590/S0103-50532003000200007.
[236] J. R. Dean, D. J. Ando, and E. D. Metcalfe, *Atomic Absorption and Plasma Spectroscopy*. 1997.
[237] A. Walsh, "The application of atomic absorption spectra to chemical analysis," *Spectrochim. Acta - Part A Mol. Spectrosc.*, vol. 7, pp. 108–117, 1955, doi: 10.1016/S0584-8539(89)80272-7.
[238] P. Wu, S. He, B. Luo, and X. Hou, "Flame furnace atomic absorption spectrometry: a review," *Appl. Spectrosc. Rev.*, vol. 44, no. 5, pp. 411–437, 2009.
[239] S. Bakirdere, "Ultraviyole fotokimyasal uçucu bileşen oluşturma-atom tuzak-alevli atomik absorpsiyon spektrofotometri sistemi ile Pb, Cd, Ni, Co elementlerinin eser seviyelerde tayinleri," 2020.
[240] D. A. Skoog, F. J. Holler, and S. R. Crouch, *Principles of instrumental analysis*. Cengage learning, 2017.
[241] R. D. Beaty and J. D. Kerber, *Concepts, instrumentation and techniques in atomic absorption spectrophotometry*. Perkin-Elmer USA, 1978.
[242] H. J. I. Filho, R. F. dos Santos Salazar, M. da Rosa Capri, Â. C. Neto, M. A. K. de Alcântara, and A. L. de Castro Peixoto, "State-of-the-Art and Trends in Atomic Absorption Spectrometry," *At. Absorpt. Spectrosc.*, p. 13, 2012.

[243] M. Moldovan, *Atomic Absorption Spectrometry-Flame*. Elsevier Amsterdam, The Netherlands, 2019.
[244] M. A. Farrukh, *Atomic absorption spectroscopy*. BoD–Books on Demand, 2012.
[245] F. Anabitarte, A. Cobo, and J. M. Lopez-Higuera, "Laser-Induced Breakdown Spectroscopy: Fundamentals, Applications, and Challenges," *ISRN Spectrosc.*, vol. 2012, pp. 1–12, 2012, doi: 10.5402/2012/285240.
[246] A. Sanz-Medel, R. Pereiro, and J. M. Costa-Fernández, "A general overview of atomic spectrometric techniques," *RSC Anal. Spectrosc. Ser.*, no. March, pp. 1–50, 2009.
[247] B. Fernández, L. Lobo, and R. Pereiro, "Atomic Absorption Spectrometry: Fundamentals, Instrumentation and Capabilities," 2018.
[248] I. Ali, H. Y. Aboul-Enein, and J. Cazes, "A journey from mikhail tswett to nano-liquid chromatography," *J. Liq. Chromatogr. Relat. Technol.*, vol. 33, no. 5, pp. 645–653, 2010.
[249] Y. I. Yashin and A. Y. Yashin, "Liquid chromatography," *Chem. Anal. Food Tech. Appl.*, vol. 3, pp. 285–310, 2012.
[250] V. B. C. Kumari *et al.*, "Chapter 5 - Chromatographic techniques: types, principles, and applications," C. Egbuna, K. C. Patrick-Iwuanyanwu, M. A. Shah, J. C. Ifemeje, and A. B. T.-A. T. in B. Rasul, Eds. Academic Press, 2022, pp. 73–101.
[251] J. C. Giddings, *Dynamics of chromatography: principles and theory*. CRC Press, 2017.
[252] J. F. K. Huber and J. Hulsman, "A study of liquid chromatography in columns, the time of separation," *Anal. Chim. Acta*, vol. 38, pp. 305–313, 1967.
[253] R. J. Hamilton and P. A. Sewell, "Introduction to high performance liquid chromatography," in *Introduction to high performance liquid chromatography*, Springer, 1982, pp. 1–12.
[254] A. Braithwaite and J. F. Smith, *Chromatographic methods*. Springer Science & Business Media, 2012.
[255] A. P. De Leenheer and W. Lambert, *Modern chromatographic analysis of vitamins: Revised and expanded*, vol. 84. CRC Press, 2000.
[256] V. Gupta, A. D. K. Jain, N. S. Gill, and K. Gupta, "Development and validation of HPLC method-a review," *Int. Res J Pharm. App Sci*, vol. 2, no. 4, pp. 17–25, 2012.
[257] S. S. Nielsen, *Food analysis*. Springer, 1998.
[258] S. C. Moldoveanu and V. David, *Selection of the HPLC method in chemical analysis*. Elsevier, 2016.
[259] P. Jandera, M. Holčapek, and L. Kolářová, "Retention mechanism, isocratic and gradient-elution separation and characterization of (co) polymers in normal-phase and reversed-phase high-performance liquid chromatography," *J. Chromatogr. A*, vol. 869, no. 1–2, pp. 65–84, 2000.
[260] S. Lindsay, *High Performance Liquid Chromatography*. 2008.
[261] R. P. W. B. T.-J. of C. L. Scott, Ed., "Chapter 2 Performance Criteria of Liquid Chromatography Detectors," in *Liquid Chromatography Detectors*, vol. 33, Elsevier, 1986, pp. 7–48.
[262] M. Swartz, "HPLC detectors: a brief review," *J. Liq. Chromatogr. Relat. Technol.*, vol. 33, no. 9–12, pp. 1130–1150, 2010.
[263] N. Y. Morgan and P. D. Smith, "HPLC detectors," *Handb. HPLC*, vol. 7, pp.

207–231, 2010.
[264] M. Pereira Da Costa and C. A. Conte-Junior, “Chromatographic methods for the determination of carbohydrates and organic acids in foods of animal origin,” *Compr. Rev. Food Sci. Food Saf.*, vol. 14, no. 5, pp. 586–600, 2015.
[265] A. T. James and A. J. P. Martin, “Gas-liquid partition chromatography: the separation and micro-estimation of volatile fatty acids from formic acid to dodecanoic acid,” *Biochem. J.*, vol. 50, no. 5, p. 679, 1952.
[266] I. C. Santos and K. A. Schug, “Recent advances and applications of gas chromatography vacuum ultraviolet spectroscopy,” *J. Sep. Sci.*, vol. 40, no. 1, pp. 138–151, 2017.
[267] K. D. Bartle and P. Myers, “History of gas chromatography,” *TrAC Trends Anal. Chem.*, vol. 21, no. 9, pp. 547–557, 2002, doi: https://doi.org/10.1016/S0165-9936(02)00806-3.
[268] H. Budiman, Nuryatini, and O. Zuas, “Comparison between GC-TCD and GC-FID for the determination of propane in gas mixture,” *Procedia Chem.*, vol. 16, pp. 465–472, 2015, doi: https://doi.org/10.1016/j.proche.2015.12.080.
[269] S. Ramezani, V. Mahdavi, H. Gordan, H. Rezadoost, G. Oliver Conti, and A. Mousavi Khaneghah, “Determination of multi-class pesticides residues of cow and human milk samples from Iran using UHPLC-MS/MS and GC-ECD: A probabilistic health risk assessment,” *Environ. Res.*, vol. 208, p. 112730, 2022, doi: https://doi.org/10.1016/j.envres.2022.112730.
[270] V. Nardelli *et al.*, “Box Behnken design-based optimized extraction of non-dioxin-like PCBs for GC-ECD and GC-MS analyses in milk samples,” *Emerg. Contam.*, vol. 6, pp. 303–311, 2020, doi: https://doi.org/10.1016/j.emcon.2020.08.002.
[271] M. Almaghrabi, Y. Abiedalla, M. Dhanasakaran, J. DeRuiter, and C. Randall Clark, “GC–MS and GC–IR of regioisomeric 4-N-bromodimethoxybenzyl derivatives of 3-trifluoromethylphenylpiperazine,” *Forensic Chem.*, vol. 29, p. 100416, 2022, doi: https://doi.org/10.1016/j.forc.2022.100416.
[272] J. Kay, R. Thomas, J. Gruenhagen, and C. J. Venkatramani, “Simultaneous quantitation of water and residual solvents in pharmaceuticals by rapid headspace gas chromatography with thermal conductivity detection (GC-TCD),” *J. Pharm. Biomed. Anal.*, vol. 194, p. 113796, 2021, doi: https://doi.org/10.1016/j.jpba.2020.113796.
[273] D. J. Beale *et al.*, “Review of recent developments in GC–MS approaches to metabolomics-based research,” *Metabolomics*, vol. 14, no. 11, pp. 1–31, 2018.
[274] S. Patel, “Chapter Three - Role of Proteomics in Biomarker Discovery: Prognosis and Diagnosis of Neuropsychiatric Disorders,” vol. 94, R. B. T.-A. in P. C. and S. B. Donev, Ed. Academic Press, 2014, pp. 39–75.
[275] C. J. Wachsmuth, P. J. Oefner, and K. Dettmer, “Equipment and metabolite identification (ID) strategies for mass-based metabolomic analysis,” in *Metabolomics in Food and Nutrition*, Elsevier, 2013, pp. 3–28.
[276] C. Dass, *Fundamentals of contemporary mass spectrometry*. John Wiley & Sons, 2007.
[277] F. A. Mellon, “Mass spectrometry| principles and instrumentation,” 2003.
[278] O. Quehenberger, A. M. Armando, and E. A. Dennis, “High sensitivity quantitative lipidomics analysis of fatty acids in biological samples by gas chromatography–mass spectrometry,” *Biochim. Biophys. Acta (BBA)-*

Molecular Cell Biol. Lipids, vol. 1811, no. 11, pp. 648–656, 2011.
[279] A.-H. Emwas, Z. Al-Talla, Y. Yang, and N. Kharbatia, "Gas Chromatography–Mass Spectrometry of Biofluids and Extracts," *Methods Mol. Biol.*, vol. 1277, pp. 91–112, Feb. 2015, doi: 10.1007/978-1-4939-2377-9_8.
[280] P. W. Brown and S. A. Musil, "Automated data acquisition and processing," in *Environmental Monitoring and Characterization*, Elsevier Inc., 2004, pp. 49–67.
[281] S. Fanse and S. Rajput, "METHOD DEVELOPMENT AND VALIDATION FOR SIMULTANEOUS ESTIMATION OF ASPIRIN AND LANSOPRAZOLE IN BULK AND LABORATORY SAMPLE BY DIFFERENT UV SPECTROPHOTOMETRIC TECHNIQUES," *Int. J. Pharm. Sci. Res.*, vol. 6, no. 8, p. 3534, 2015.
[282] S. Mitra, "Sample preparation techniques in analytical chemistry," 2003.
[283] J. E. T. Andersen, "The standard addition method revisited," *TrAC Trends Anal. Chem.*, vol. 89, pp. 21–33, 2017, doi: https://doi.org/10.1016/j.trac.2016.12.013.
[284] S. Erarpat, S. Bodur, D. S. Chormey, E. Öz, and S. Bakırdere, "Sensitive Determination of 4-n-Nonylphenol in Domestic Wastewater and Liquid Detergent by Binary Solvent Microextraction (BSME) and Gas Chromatography–Mass Spectrometry (GC-MS) with Matrix Matching Calibration," *Anal. Lett.*, vol. 55, no. 7, pp. 1080–1092, May 2022, doi: 10.1080/00032719.2021.1985511.
[285] P. Roper, V. Barwick, S. Burke, R. Walker, and R. Lawn, *Applications of reference materials in analytical chemistry*, vol. 10. Royal Society of Chemistry, 2001.
[286] N. Bakaraki, D. S. Chormey, S. Bakirdere, and G. O. Engin, "Development of a sensitive liquid–liquid extraction method for the determination of N-butyryl-L-homoserine lactone produced in a submerged membrane bioreactor by gas chromatography mass spectrometry and deuterated anthracene as the internal standard," *Anal. Methods*, vol. 8, no. 12, pp. 2660–2665, 2016.
[287] S. Erarpat, G. Özzeybek, D. S. Chormey, F. Erulaş, F. Turak, and S. Bakırdere, "A novel liquid-liquid extraction for the determination of naphthalene by GC-MS with deuterated anthracene as internal standard," *Environ. Monit. Assess.*, vol. 189, no. 10, p. 528, Oct. 2017, doi: 10.1007/s10661-017-6250-6.
[288] J. M. Betz, P. N. Brown, and M. C. Roman, "Accuracy, precision, and reliability of chemical measurements in natural products research," *Fitoterapia*, vol. 82, no. 1, pp. 44–52, 2011.
[289] T. N. Rao, "Validation of Analytical Methods," M. T. Stauffer, Ed. Rijeka: IntechOpen, 2018, p. Ch. 7.
[290] R. Rabena, "4.1. Repeatability, intermediate precision and reproducibility," *LC-MS Method Validation*, 2023. https://sisu.ut.ee/lcms_method_validation/41-precision-trueness-accuracy#:~:text=Intermediate precision (sintermediate precision,account more changes than repeatability. (accessed Jan. 11, 2024).
[291] P. C. D. Milly, R. T. Wetherald, K. A. Dunne, and T. L. Delworth, "Increasing risk of great floods in a changing climate," *Nature*, vol. 415, no. 6871, pp. 514–517, 2002, doi: 10.1038/415514a.

[292] J. Xia, Q.-Y. Duan, Y. Luo, Z.-H. Xie, Z.-Y. Liu, and X.-G. Mo, “Climate change and water resources: Case study of Eastern Monsoon Region of China,” *Adv. Clim. Chang. Res.*, vol. 8, no. 2, pp. 63–67, 2017, doi: https://doi.org/10.1016/j.accre.2017.03.007.
[293] P. D. Noyes *et al.*, “The toxicology of climate change: environmental contaminants in a warming world,” *Environ. Int.*, vol. 35, no. 6, pp. 971–986, 2009.
[294] R. P. Schwarzenbach, T. Egli, T. B. Hofstetter, U. Von Gunten, and B. Wehrli, “Global water pollution and human health,” *Annu. Rev. Environ. Resour.*, vol. 35, pp. 109–136, 2010.
[295] A. Demirak, F. Yilmaz, A. Levent Tuna, and N. Ozdemir, “Heavy metals in water, sediment and tissues of Leuciscus cephalus from a stream in southwestern Turkey,” *Chemosphere*, vol. 63, no. 9, pp. 1451–1458, 2006, doi: https://doi.org/10.1016/j.chemosphere.2005.09.033.
[296] D. Archundia *et al.*, “How Uncontrolled Urban Expansion Increases the Contamination of the Titicaca Lake Basin (El Alto, La Paz, Bolivia),” *Water, Air, Soil Pollut.*, vol. 228, no. 1, p. 44, 2016, doi: 10.1007/s11270-016-3217-0.
[297] S. Herat and P. Agamuthu, “E-waste: a problem or an opportunity? Review of issues, challenges and solutions in Asian countries,” *Waste Manag. Res.*, vol. 30, no. 11, pp. 1113–1129, Jul. 2012, doi: 10.1177/0734242X12453378.
[298] O. B. Olafisoye, T. Adefioye, and O. A. Osibote, “Heavy Metals Contamination of Water, Soil, and Plants around an Electronic Waste Dumpsite.,” *Polish J. Environ. Stud.*, vol. 22, no. 5, 2013.
[299] D. N. Perkins, M.-N. Brune Drisse, T. Nxele, and P. D. Sly, “E-Waste: A Global Hazard,” *Ann. Glob. Heal.*, vol. 80, no. 4, pp. 286–295, 2014, doi: https://doi.org/10.1016/j.aogh.2014.10.001.
[300] J. Pandey and U. Pandey, “Atmospheric Deposition and Heavy Metal Contamination in an Organic Farming System in a Seasonally Dry Tropical Region of India,” *J. Sustain. Agric.*, vol. 33, no. 4, pp. 361–378, May 2009, doi: 10.1080/10440040902834954.
[301] C. Prasse, W. Zech, F. Itanna, and B. Glaser, “Contamination and source assessment of metals, polychlorinated biphenyls, and polycyclic aromatic hydrocarbons in urban soils from Addis Ababa, Ethiopia,” *Toxicol. Environ. Chem.*, vol. 94, no. 10, pp. 1954–1979, Dec. 2012, doi: 10.1080/02772248.2012.737794.
[302] United Nation, “The United Nations world water development report 2018: nature-based solutions for water,” Paris, France., 2018. [Online]. Available: file:///C:/Users/tbuse/Downloads/261424eng.pdf.
[303] L. Joseph, B.-M. Jun, J. R. V Flora, C. M. Park, and Y. Yoon, “Removal of heavy metals from water sources in the developing world using low-cost materials: A review,” *Chemosphere*, vol. 229, pp. 142–159, 2019, doi: https://doi.org/10.1016/j.chemosphere.2019.04.198.
[304] S. Chakraborty, A. R. Dutta, S. Sural, D. Gupta, and S. Sen, “Ailing bones and failing kidneys: a case of chronic cadmium toxicity,” *Ann. Clin. Biochem.*, vol. 50, no. 5, pp. 492–495, Jun. 2013, doi: 10.1177/0004563213481207.
[305] K. M. Gleason *et al.*, “Stunting is associated with blood lead concentration among Bangladeshi children aged 2-3 years,” *Environ. Heal.*, vol. 15, no. 1, p. 103, 2016, doi: 10.1186/s12940-016-0190-4.

[306] M. De Kwaadsteniet, P. H. Dobrowsky, A. Van Deventer, W. Khan, and T. E. Cloete, “Domestic rainwater harvesting: microbial and chemical water quality and point-of-use treatment systems,” *Water, Air, Soil Pollut.*, vol. 224, pp. 1–19, 2013.
[307] S. Chowdhury, M. A. J. Mazumder, O. Al-Attas, and T. Husain, “Heavy metals in drinking water: occurrences, implications, and future needs in developing countries,” *Sci. Total Environ.*, vol. 569, pp. 476–488, 2016.
[308] E. Emmanuel, M. G. Pierre, and Y. Perrodin, “Groundwater contamination by microbiological and chemical substances released from hospital wastewater: Health risk assessment for drinking water consumers,” *Environ. Int.*, vol. 35, no. 4, pp. 718–726, 2009.
[309] M. M. Rahman, R. Naidu, and P. Bhattacharya, “Arsenic contamination in groundwater in the Southeast Asia region,” *Environ. Geochem. Health*, vol. 31, no. 1, pp. 9–21, 2009, doi: 10.1007/s10653-008-9233-2.
[310] H. M. A. Rossiter, P. A. Owusu, E. Awuah, A. M. MacDonald, and A. I. Schäfer, “Chemical drinking water quality in Ghana: Water costs and scope for advanced treatment,” *Sci. Total Environ.*, vol. 408, no. 11, pp. 2378–2386, 2010.
[311] C. N. Amadi, Z. N. Igweze, and O. E. Orisakwe, “Heavy metals in miscarriages and stillbirths in developing nations,” *Middle East Fertil. Soc. J.*, vol. 22, no. 2, pp. 91–100, 2017.
[312] L. Järup, “Hazards of heavy metal contamination,” *Br. Med. Bull.*, vol. 68, no. 1, pp. 167–182, Dec. 2003, doi: 10.1093/bmb/ldg032.
[313] A. O. Odongo, W. N. Moturi, and E. K. Mbuthia, “Heavy metals and parasitic geohelminths toxicity among geophagous pregnant women: a case study of Nakuru Municipality, Kenya,” *Environ. Geochem. Health*, vol. 38, pp. 123–131, 2016.
[314] W. Peng, H. Li, Y. Liu, and S. Song, “A review on heavy metal ions adsorption from water by graphene oxide and its composites,” *J. Mol. Liq.*, vol. 230, pp. 496–504, 2017.
[315] A. I. A. Sherlala, A. A. A. Raman, M. M. Bello, and A. Asghar, “A review of the applications of organo-functionalized magnetic graphene oxide nanocomposites for heavy metal adsorption,” *Chemosphere*, vol. 193, pp. 1004–1017, 2018.
[316] J. Xu *et al.*, “A review of functionalized carbon nanotubes and graphene for heavy metal adsorption from water: Preparation, application, and mechanism,” *Chemosphere*, vol. 195, pp. 351–364, 2018.
[317] Y. Jiang *et al.*, “Polyaniline-based adsorbents for removal of hexavalent chromium from aqueous solution: a mini review,” *Environ. Sci. Pollut. Res.*, vol. 25, pp. 6158–6174, 2018.
[318] M. Sajid, M. K. Nazal, N. Baig, and A. M. Osman, “Removal of heavy metals and organic pollutants from water using dendritic polymers based adsorbents: a critical review,” *Sep. Purif. Technol.*, vol. 191, pp. 400–423, 2018.
[319] E. N. Zare, A. Motahari, and M. Sillanpää, “Nanoadsorbents based on conducting polymer nanocomposites with main focus on polyaniline and its derivatives for removal of heavy metal ions/dyes: a review,” *Environ. Res.*, vol. 162, pp. 173–195, 2018.
[320] Z. Al-Qodah and M. Al-Shannag, “Heavy metal ions removal from wastewater using electrocoagulation processes: a comprehensive review,”

Sep. Sci. Technol., vol. 52, no. 17, pp. 2649–2676, 2017.
[321] E. Bazrafshan, L. Mohammadi, A. Ansari-Moghaddam, and A. H. Mahvi, "Heavy metals removal from aqueous environments by electrocoagulation process–a systematic review," *J. Environ. Heal. Sci. Eng.*, vol. 13, pp. 1–16, 2015.
[322] S. Kim *et al.*, "Removal of contaminants of emerging concern by membranes in water and wastewater: A review," *Chem. Eng. J.*, vol. 335, pp. 896–914, 2018.
[323] A. S. Ayangbenro and O. O. Babalola, "A new strategy for heavy metal polluted environments: a review of microbial biosorbents," *Int. J. Environ. Res. Public Health*, vol. 14, no. 1, p. 94, 2017.
[324] P.-S. Li and H.-C. Tao, "Cell surface engineering of microorganisms towards adsorption of heavy metals," *Crit. Rev. Microbiol.*, vol. 41, no. 2, pp. 140–149, 2015.
[325] M. I. Ojovan, W. E. Lee, and S. N. Kalmykov, *An introduction to nuclear waste immobilisation*. Elsevier, 2019.
[326] N. A. A. Qasem, R. H. Mohammed, and D. U. Lawal, "Removal of heavy metal ions from wastewater: a comprehensive and critical review," *npj Clean Water*, vol. 4, no. 1, p. 36, 2021, doi: 10.1038/s41545-021-00127-0.
[327] D. Ibarra-Rodríguez, J. Lizardi-Mendoza, E. A. López-Maldonado, and M. T. Oropeza-Guzmán, "Capacity of 'nopal' pectin as a dual coagulant-flocculant agent for heavy metals removal," *Chem. Eng. J.*, vol. 323, pp. 19–28, 2017, doi: https://doi.org/10.1016/j.cej.2017.04.087.
[328] D. D. Ratnayaka, M. J. Brandt, and K. M. Johnson, "CHAPTER 7 - Storage, Clarification and Chemical Treatment," D. D. Ratnayaka, M. J. Brandt, and K. M. B. T.-W. S. (Sixth E. Johnson, Eds. Boston: Butterworth-Heinemann, 2009, pp. 267–314.
[329] Q. Chang, M. Zhang, and J. Wang, "Removal of Cu2+ and turbidity from wastewater by mercaptoacetyl chitosan," *J. Hazard. Mater.*, vol. 169, no. 1, pp. 621–625, 2009, doi: https://doi.org/10.1016/j.jhazmat.2009.03.144.
[330] M. Nourani, M. Baghdadi, M. Javan, and G. N. Bidhendi, "Production of a biodegradable flocculant from cotton and evaluation of its performance in coagulation-flocculation of kaolin clay suspension: Optimization through response surface methodology (RSM)," *J. Environ. Chem. Eng.*, vol. 4, no. 2, pp. 1996–2003, 2016, doi: https://doi.org/10.1016/j.jece.2016.03.028.
[331] C. Y. Teh, P. M. Budiman, K. P. Y. Shak, and T. Y. Wu, "Recent Advancement of Coagulation–Flocculation and Its Application in Wastewater Treatment," *Ind. Eng. Chem. Res.*, vol. 55, no. 16, pp. 4363–4389, Apr. 2016, doi: 10.1021/acs.iecr.5b04703.
[332] X. Yang *et al.*, "Surface functional groups of carbon-based adsorbents and their roles in the removal of heavy metals from aqueous solutions: A critical review," *Chem. Eng. J.*, vol. 366, pp. 608–621, 2019, doi: https://doi.org/10.1016/j.cej.2019.02.119.
[333] R. Yousef, H. Qiblawey, and M. H. El-Naas, "Adsorption as a process for produced water treatment: a review," *Processes*, vol. 8, no. 12, p. 1657, 2020.
[334] M. N. Rashed, "Adsorption technique for the removal of organic pollutants from water and wastewater," *Org. Pollut. risk Treat.*, vol. 7, pp. 167–194, 2013.
[335] G. Z. Kyzas and M. Kostoglou, "Green Adsorbents for Wastewaters: A Critical Review," *Materials*, vol. 7, no. 1. pp. 333–364, 2014, doi:

10.3390/ma7010333.
[336] V. K. Yadav *et al.*, “Synthesis and characterization of amorphous iron oxide nanoparticles by the sonochemical method and their application for the remediation of heavy metals from wastewater,” *Nanomaterials*, vol. 10, no. 8, p. 1551, 2020.
[337] S. Homaeigohar, “The nanosized dye adsorbents for water treatment,” *Nanomaterials*, vol. 10, no. 2, p. 295, 2020.
[338] G. Buema *et al.*, “Magnetic Solid-Phase Extraction of Cadmium Ions by Hybrid Self-Assembled Multicore Type Nanobeads,” *Polymers*, vol. 13, no. 2. 2021, doi: 10.3390/polym13020229.
[339] S. Boulkhessaim *et al.*, “Emerging trends in the remediation of persistent organic pollutants using nanomaterials and related processes: A review,” *Nanomaterials*, vol. 12, no. 13, p. 2148, 2022.
[340] G. Sharma *et al.*, “Novel development of nanoparticles to bimetallic nanoparticles and their composites: A review,” *J. King Saud Univ.*, vol. 31, no. 2, pp. 257–269, 2019.
[341] A. V. Bounegru and C. Apetrei, “Carbonaceous nanomaterials employed in the development of electrochemical sensors based on screen-printing technique—A review,” *Catalysts*, vol. 10, no. 6, p. 680, 2020.
[342] K. D. Patel, R. K. Singh, and H.-W. Kim, “Carbon-based nanomaterials as an emerging platform for theranostics,” *Mater. Horizons*, vol. 6, no. 3, pp. 434–469, 2019.
[343] N. Baig, M. Sajid, and T. A. Saleh, “Recent trends in nanomaterial-modified electrodes for electroanalytical applications,” *TrAC Trends Anal. Chem.*, vol. 111, pp. 47–61, 2019.
[344] S. J. Shan, Y. Zhao, H. Tang, and F. Y. Cui, “A Mini-review of Carbonaceous Nanomaterials for Removal of Contaminants from Wastewater,” *IOP Conf. Ser. Earth Environ. Sci.*, vol. 68, no. 1, p. 12003, 2017, doi: 10.1088/1755-1315/68/1/012003.
[345] D. Jariwala, V. K. Sangwan, L. J. Lauhon, T. J. Marks, and M. C. Hersam, “Carbon nanomaterials for electronics, optoelectronics, photovoltaics, and sensing,” *Chem. Soc. Rev.*, vol. 42, no. 7, pp. 2824–2860, 2013.
[346] R. B. Onyancha, U. O. Aigbe, K. E. Ukhurebor, and P. W. Muchiri, “Facile synthesis and applications of carbon nanotubes in heavy-metal remediation and biomedical fields: a comprehensive review,” *J. Mol. Struct.*, vol. 1238, p. 130462, 2021.
[347] Y. M. Manawi and S. Ihsanullah, “A., Al-Ansari, T. & Atieh, MA A review of carbon nanomaterials’ synthesis via the chemical vapor deposition (CVD) method.” Materials, 2018.
[348] P. N. Dave and L. V Chopda, “Application of iron oxide nanomaterials for the removal of heavy metals,” *J. Nanotechnol.*, vol. 2014, 2014.
[349] F. S. A. Khan *et al.*, “Magnetic nanoadsorbents’ potential route for heavy metals removal—a review,” *Environ. Sci. Pollut. Res.*, vol. 27, pp. 24342–24356, 2020.
[350] D. Lisjak and A. Mertelj, “Anisotropic magnetic nanoparticles: A review of their properties, syntheses and potential applications,” *Prog. Mater. Sci.*, vol. 95, pp. 286–328, 2018.
[351] Y. F. Shen, J. Tang, Z. H. Nie, Y. D. Wang, Y. Ren, and L. Zuo, “Preparation and application of magnetic Fe3O4 nanoparticles for wastewater purification,” *Sep. Purif. Technol.*, vol. 68, no. 3, pp. 312–319, 2009.

[352] E. Roy, S. Patra, P. Karfa, R. Madhuri, and P. K. Sharma, “Role of Magnetic Nanoparticles in Providing Safe and Clean Water to Each Individual BT - Complex Magnetic Nanostructures: Synthesis, Assembly and Applications,” S. K. Sharma, Ed. Cham: Springer International Publishing, 2017, pp. 281–316.
[353] D. Stanicki, L. Vander Elst, R. N. Muller, and S. Laurent, “Synthesis and processing of magnetic nanoparticles,” *Curr. Opin. Chem. Eng.*, vol. 8, pp. 7–14, 2015.
[354] T. Osaka, T. Matsunaga, T. Nakanishi, A. Arakaki, D. Niwa, and H. Iida, “Synthesis of magnetic nanoparticles and their application to bioassays,” *Anal. Bioanal. Chem.*, vol. 384, pp. 593–600, 2006.
[355] K. Chen, H. Lyu, S. Hao, G. Luo, S. Zhang, and J. Chen, “Separation of phenolic compounds with modified adsorption resin from aqueous phase products of hydrothermal liquefaction of rice straw,” *Bioresour. Technol.*, vol. 182, pp. 160–168, 2015.
[356] C. Long, A. Li, H. Wu, and Q. Zhang, “Adsorption of naphthalene onto macroporous and hypercrosslinked polymeric adsorbent: Effect of pore structure of adsorbents on thermodynamic and kinetic properties,” *Colloids Surfaces A Physicochem. Eng. Asp.*, vol. 333, no. 1–3, pp. 150–155, 2009.
[357] O. Moradi and G. Sharma, “Emerging novel polymeric adsorbents for removing dyes from wastewater: A comprehensive review and comparison with other adsorbents,” *Environ. Res.*, p. 111534, 2021.
[358] H. N. M. E. Mahmud, A. K. O. Huq, and R. Yahya, “Polymer-based adsorbent for heavy metals removal from aqueous solution,” in *IOP Conference Series: Materials Science and Engineering*, 2017, vol. 206, no. 1, doi: 10.1088/1757-899X/206/1/012100.
[359] V. Popova, E. Dmitrienko, and A. Chubarov, “Magnetic Nanocomposites and Imprinted Polymers for Biomedical Applications of Nucleic Acids,” *Magnetochemistry*, vol. 9, no. 1, p. 12, 2022.
[360] Y. Li, L. Huang, W. He, Y. Chen, and B. Lou, “Preparation of functionalized magnetic Fe3O4@Au@polydopamine nanocomposites and their application for copper(II) removal,” *Polymers (Basel).*, vol. 10, no. 6, 2018, doi: 10.3390/polym10060570.
[361] A. K. Das *et al.*, “Green Synthesis of Unsaturated Fatty Acid Mediated Magnetite Nanoparticles and Their Structural and Magnetic Studies,” *Magnetochemistry*, vol. 8, no. 12, 2022, doi: 10.3390/magnetochemistry8120174.
[362] P. B. Shete, R. M. Patil, B. M. Tiwale, and S. H. Pawar, “Water dispersible oleic acid-coated Fe3O4 nanoparticles for biomedical applications,” *J. Magn. Magn. Mater.*, vol. 377, pp. 406–410, 2015, doi: 10.1016/j.jmmm.2014.10.137.
[363] S. Wang, L. Huang, Y. Zhang, L. Li, and X. Lu, “A mini-review on the modeling of volatile organic compound adsorption in activated carbons: Equilibrium, dynamics, and heat effects,” *Chinese J. Chem. Eng.*, vol. 31, pp. 153–163, 2021, doi: https://doi.org/10.1016/j.cjche.2020.11.018.
[364] A. Malek and S. Farooq, “Comparison of Isotherm Models for Hydrocarbon Adsorption on Activated Carbon,” *AIChE J.*, vol. 42, no. 11, pp. 3191–3201, 1996, doi: 10.1002/aic.690421120.
[365] M. Peng, A. V Nguyen, J. Wang, and R. Miller, “A critical review of the model fitting quality and parameter stability of equilibrium adsorption

models," *Adv. Colloid Interface Sci.*, vol. 262, pp. 50–68, 2018, doi: https://doi.org/10.1016/j.cis.2018.10.001.
[366] A. E. Kojo, W. Cho, and C. Park, "Mildly oxidized porous covalent triazine frameworks with rapid and high adsorption capability for aqueous organic micropollutants," *J. Ind. Eng. Chem.*, vol. 116, pp. 250–256, 2022, doi: https://doi.org/10.1016/j.jiec.2022.09.015.
[367] H. Li *et al.*, "Synthesis of porous dimethoxypillar[5]arene knitted β-cyclodextrin copolymers for efficient adsorption of organic micropollutants," *Carbohydr. Polym.*, vol. 310, p. 120719, 2023, doi: https://doi.org/10.1016/j.carbpol.2023.120719.
[368] R. Chen *et al.*, "Microporous melamine-formaldehyde networks loaded on rice husks for dynamic removal of organic micropollutants," *Environ. Pollut.*, vol. 322, p. 121200, 2023, doi: https://doi.org/10.1016/j.envpol.2023.121200.
[369] M. Fatih Dilekoglu and M. Yapici, "Adsorption of naproxen pharmaceutical micropollutant from aqueous solutions on superior activated carbon synthesized from sheep manure: Kinetics, thermodynamics, and mechanism," *J. Mol. Liq.*, vol. 381, p. 121839, 2023, doi: https://doi.org/10.1016/j.molliq.2023.121839.
[370] J. H. Chun, S. K. Jeon, N. Y. Kim, and J. Y. Chun, "The phase-shift method for determining Langmuir and Temkin adsorption isotherms of over-potentially deposited hydrogen for the cathodic H2 evolution reaction at the poly-Pt/H2SO4 aqueous electrolyte interface," *Int. J. Hydrogen Energy*, vol. 30, no. 13, pp. 1423–1436, 2005, doi: https://doi.org/10.1016/j.ijhydene.2004.12.005.
[371] H. Brunhoferova, S. Venditti, and J. Hansen, "Characterization of unconventional sand-based substrates for adsorption of micropollutants in nature-based systems," *J. Environ. Manage.*, vol. 318, p. 115593, 2022, doi: https://doi.org/10.1016/j.jenvman.2022.115593.
[372] A. Haghtalab, M. Nabipoor, and S. Farzad, "Kinetic modeling of the Fischer–Tropsch synthesis in a slurry phase bubble column reactor using Langmuir–Freundlich isotherm," *Fuel Process. Technol.*, vol. 104, pp. 73–79, 2012, doi: https://doi.org/10.1016/j.fuproc.2011.07.005.
[373] Y. El Ouardi, V. Lenoble, C. Branger, K. Laatikainen, B. Angeletti, and A. Ouammou, "Enhancing clay adsorption properties: A comparison between chemical and combined chemical/thermal treatments," *Groundw. Sustain. Dev.*, vol. 12, p. 100544, 2021, doi: https://doi.org/10.1016/j.gsd.2020.100544.
[374] X. Zhou, R. Maimaitiniyazi, and Y. Wang, "Some consideration triggered by misquotation of Temkin model and the derivation of its correct form," *Arab. J. Chem.*, vol. 15, no. 11, p. 104267, 2022, doi: https://doi.org/10.1016/j.arabjc.2022.104267.
[375] T. S. van Erp and J. A. Martens, "A standardization for BET fitting of adsorption isotherms," *Microporous Mesoporous Mater.*, vol. 145, no. 1, pp. 188–193, 2011, doi: https://doi.org/10.1016/j.micromeso.2011.05.022.
[376] F. Gritti and G. Guiochon, "Band splitting in overloaded isocratic elution chromatography: III. Modeling of adsorbate–adsorbate interactions by a two-component extension of a BET kinetic isotherm model," *J. Chromatogr. A*, vol. 1028, no. 1, pp. 121–137, 2004, doi: https://doi.org/10.1016/j.chroma.2003.11.088.

[377] Y. Tan and J. H. O'Haver, "Use of the BET adsorption isotherm equation to examine styrene adsolubilization by nonionic surfactants at the water–silica interface," *J. Colloid Interface Sci.*, vol. 279, no. 2, pp. 289–295, 2004, doi: https://doi.org/10.1016/j.jcis.2004.06.101.
[378] S. Nimesh, "1 - Nanotechnology: an introduction," in *Woodhead Publishing Series in Biomedicine*, S. B. T.-G. T. Nimesh, Ed. Woodhead Publishing, 2013, pp. 1–12.
[379] A. K. Adya and E. Canetta, "Chapter 14 - Nanotechnology and Its Applications to Animal Biotechnology," A. S. Verma and A. B. T.-A. B. Singh, Eds. San Diego: Academic Press, 2014, pp. 247–263.
[380] R. Zhao, J. Xiang, B. Wang, L. Chen, and S. Tan, "Recent advances in the development of noble metal NPs for cancer therapy," *Bioinorg. Chem. Appl.*, vol. 2022, 2022.
[381] N. Toropov and T. Vartanyan, "1.03 - Noble Metal Nanoparticles: Synthesis and Optical Properties☆," D. L. Andrews, R. H. Lipson, and T. B. T.-C. N. and N. (Second E. Nann, Eds. Oxford: Academic Press, 2019, pp. 61–88.
[382] Y.-C. Yeh, B. Creran, and V. M. Rotello, "Gold nanoparticles: preparation, properties, and applications in bionanotechnology," *Nanoscale*, vol. 4, no. 6, pp. 1871–1880, 2012.
[383] A. E. F. Oliveira, A. C. Pereira, M. A. C. Resende, and L. F. Ferreira, "Gold Nanoparticles: A Didactic Step-by-Step of the Synthesis Using the Turkevich Method, Mechanisms, and Characterizations," *Analytica*, vol. 4, no. 2. pp. 250–263, 2023, doi: 10.3390/analytica4020020.
[384] M. H. Magnusson, K. Deppert, J.-O. Malm, J.-O. Bovin, and L. Samuelson, "Size-selected gold nanoparticles by aerosol technology," *Nanostructured Mater.*, vol. 12, no. 1–4, pp. 45–48, 1999.
[385] D. C. Tien *et al.*, "Novel technique for preparing a nano-silver water suspension by the arc-discharge method," *Rev. Adv. mater. sci*, vol. 18, no. 8, pp. 752–758, 2008.
[386] M. Shariq *et al.*, "Successful Synthesis of Gold Nanoparticles through Ultrasonic Spray Pyrolysis from a Gold(III) Nitrate Precursor and Their Interaction with a High Electron Beam," *ChemistryOpen*, vol. 7, no. 7, pp. 533–542, Jul. 2018, doi: https://doi.org/10.1002/open.201800101.
[387] R. F. Elsupikhe, K. Shameli, M. B. Ahmad, N. A. Ibrahim, and N. Zainudin, "Green sonochemical synthesis of silver nanoparticles at varying concentrations of κ-carrageenan," *Nanoscale Res. Lett.*, vol. 10, no. 1, p. 302, 2015, doi: 10.1186/s11671-015-0916-1.
[388] M. Tsuji, M. Hashimoto, Y. Nishizawa, M. Kubokawa, and T. Tsuji, "Microwave-Assisted Synthesis of Metallic Nanostructures in Solution," *Chem. – A Eur. J.*, vol. 11, no. 2, pp. 440–452, Jan. 2005, doi: https://doi.org/10.1002/chem.200400417.
[389] K. Shameli *et al.*, "Green synthesis of silver/montmorillonite/chitosan bionanocomposites using the UV irradiation method and evaluation of antibacterial activity," *Int. J. Nanomedicine*, vol. 5, no. null, pp. 875–887, Oct. 2010, doi: 10.2147/IJN.S13632.
[390] K. M. M. Abou El-Nour, A. Eftaiha, A. Al-Warthan, and R. A. A. Ammar, "Synthesis and applications of silver nanoparticles," *Arab. J. Chem.*, vol. 3, no. 3, pp. 135–140, 2010, doi: https://doi.org/10.1016/j.arabjc.2010.04.008.
[391] C. Daruich De Souza, B. Ribeiro Nogueira, and M. E. C. M. Rostelato, "Review of the methodologies used in the synthesis gold nanoparticles by

chemical reduction," *J. Alloys Compd.*, vol. 798, pp. 714–740, 2019, doi: https://doi.org/10.1016/j.jallcom.2019.05.153.
[392] M. Iqbal *et al.*, "Preparation of gold nanoparticles and determination of their particles size via different methods," *Mater. Res. Bull.*, vol. 79, pp. 97–104, 2016, doi: https://doi.org/10.1016/j.materresbull.2015.12.026.
[393] S. J. Amina and B. Guo, "A review on the synthesis and functionalization of gold nanoparticles as a drug delivery vehicle," *Int. J. Nanomedicine*, pp. 9823–9857, 2020.
[394] T. K. Sau and C. J. Murphy, "Room Temperature, High-Yield Synthesis of Multiple Shapes of Gold Nanoparticles in Aqueous Solution," *J. Am. Chem. Soc.*, vol. 126, no. 28, pp. 8648–8649, Jul. 2004, doi: 10.1021/ja047846d.
[395] M. T. Reetz and W. Helbig, "Size-selective synthesis of nanostructured transition metal clusters," *J. Am. Chem. Soc.*, vol. 116, no. 16, pp. 7401–7402, 1994.
[396] M. Brust, M. Walker, D. Bethell, D. J. Schiffrin, and R. Whyman, "Synthesis of thiol-derivatised gold nanoparticles in a two-phase Liquid–Liquid system," *J. Chem. Soc. Chem. Commun.*, no. 7, pp. 801–802, 1994, doi: 10.1039/C39940000801.
[397] P. Sahu and B. L. V Prasad, "Time and Temperature Effects on the Digestive Ripening of Gold Nanoparticles: Is There a Crossover from Digestive Ripening to Ostwald Ripening?," *Langmuir*, vol. 30, no. 34, pp. 10143–10150, Sep. 2014, doi: 10.1021/la500914j.
[398] M. Noruzi, D. Zare, K. Khoshnevisan, and D. Davoodi, "Rapid green synthesis of gold nanoparticles using Rosa hybrida petal extract at room temperature," *Spectrochim. Acta Part A Mol. Biomol. Spectrosc.*, vol. 79, no. 5, pp. 1461–1465, Sep. 2011, doi: 10.1016/j.saa.2011.05.001.
[399] R. Herizchi, E. Abbasi, M. Milani, and A. Akbarzadeh, "Current methods for synthesis of gold nanoparticles," *Artif. Cells, Nanomedicine, Biotechnol.*, vol. 44, no. 2, pp. 596–602, Feb. 2016, doi: 10.3109/21691401.2014.971807.
[400] L. C. Moraes *et al.*, "High diversity of microalgae as a tool for the synthesis of different silver nanoparticles: A species-specific green synthesis," *Colloid Interface Sci. Commun.*, vol. 42, p. 100420, 2021, doi: https://doi.org/10.1016/j.colcom.2021.100420.
[401] M. Shakibaie *et al.*, "Green synthesis of gold nanoparticles by the marine microalga Tetraselmis suecica," *Biotechnol. Appl. Biochem.*, vol. 57, no. 2, pp. 71–75, 2010.
[402] E. Basiratnia, A. Einali, O. Azizian-Shermeh, E. Mollashahi, and A. Ghasemi, "Biological Synthesis of Gold Nanoparticles from Suspensions of Green Microalga Dunaliella salina and Their Antibacterial Potential," *Bionanoscience*, vol. 11, no. 4, pp. 977–988, 2021, doi: 10.1007/s12668-021-00897-4.
[403] S. Swaminathan, S. Murugesan, S. Damodarkumar, R. Dhamotharan, and S. Bhuvaneshwari, "Synthesis and characterization of gold nanoparticles from alga acanthophora specifera (VAHL) boergesen," *Int. J. Nanosci. Nanotechnol*, vol. 2, pp. 85–94, 2011.
[404] P. Rajasulochana, P. Krishnamoorthy, and R. Dhamotharan, "Potential application of Kappaphycus alvarezii in agricultural and pharmaceutical industry," *J. Chem. Pharm. Res*, vol. 4, no. 1, pp. 33–37, 2012.
[405] G. Singaravelu, J. S. Arockiamary, V. G. Kumar, and K. Govindaraju, "A novel extracellular synthesis of monodisperse gold nanoparticles using

marine alga, Sargassum wightii Greville," *Colloids surfaces B Biointerfaces*, vol. 57, no. 1, pp. 97–101, 2007.
[406] T. S. Dhas, V. G. Kumar, L. S. Abraham, V. Karthick, and K. Govindaraju, "Sargassum myriocystum mediated biosynthesis of gold nanoparticles," *Spectrochim. Acta Part A Mol. Biomol. Spectrosc.*, vol. 99, pp. 97–101, 2012.
[407] F. A. A. Rajathi, C. Parthiban, V. G. Kumar, and P. Anantharaman, "Biosynthesis of antibacterial gold nanoparticles using brown alga, Stoechospermum marginatum (kützing)," *Spectrochim. Acta Part A Mol. Biomol. Spectrosc.*, vol. 99, pp. 166–173, 2012.
[408] G. Ghodake and D. S. Lee, "Biological synthesis of gold nanoparticles using the aqueous extract of the brown algae Laminaria japonica," *J. Nanoelectron. Optoelectron.*, vol. 6, no. 3, pp. 268–271, 2011.
[409] M. Benita, Z. Dubinsky, and D. Iluz, "Padina pavonica: Morphology and calcification functions and mechanism," *Am. J. Plant Sci.*, vol. 9, no. 6, pp. 1156–1168, 2018.
[410] K. KERZABI-KANOUN *et al.*, "Antioxidant Activity of Brown Seaweed (Padina pavonica (L.) Extracts From the Algerian Mediterranean Coast," *J. Nat. Prod. Res. Appl.*, vol. 1, pp. 54–62, Dec. 2021, doi: 10.46325/jnpra.v1i02.15.
[411] H. B. KESKİNKAYA *et al.*, "HPLC-UV analysis of phenolic compounds and biological activities of Padina pavonica and Zanardinia typus marine macroalgae species," *Turk. J. Botany*, vol. 47, no. 3, pp. 231–243, 2023.
[412] G. Isaac and R. E. Renitta, "Brown algae mediated synthesis,characterization of gold nano particles using padina pavonica and their antibacterial activity against human pathogens," vol. 8, pp. 31–40, Jan. 2015.
[413] A. F. Erulaş, M. Şaylan, S. Topal, B. T. Zaman, E. G. Bakırdere, and S. Bakırdere, "A new microextraction method for trace nickel determination in green tea samples: Solventless dispersion based dispersive liquid-liquid microextraction combined with slotted quartz tube- flame atomic absorption spectrophotometry," *J. Food Compos. Anal.*, vol. 94, 2020, doi: 10.1016/j.jfca.2020.103623.
[414] Z. Tekin, N. E. Karlıdağ, N. Özdoğan, E. S. Koçoğlu, and S. Bakırdere, "Dispersive solid phase extraction based on reduced graphene oxide modified Fe3O4 nanocomposite for trace determination of parabens in rock, soil, moss, seaweed, feces, and water samples from Horseshoe and Faure Islands," *J. Hazard. Mater.*, vol. 426, p. 127819, Mar. 2022, doi: 10.1016/J.JHAZMAT.2021.127819.
[415] N. B. Turan, H. S. Erkan, D. S. Chormey, A. Cağlak, S. Bakirdere, and G. O. Engin, "Feasibility Studies on the Effect of Natural Plant Compounds on Sludge Characteristics in a Batch-Type Aerobic Reactor and N-butyryl-L Homoserine Lactone," *Anal. Lett.*, vol. 53, no. 15, pp. 2431–2444, 2020.
[416] I. Langmuir, "The adsorption of gases on plane surfaces of glass, mica and platinum.," *J. Am. Chem. Soc.*, vol. 40, no. 9, pp. 1361–1403, 1918.
[417] G. Onkal Engin, B. Muftuoglu, and E. Senturk, "Dynamic biosorption characteristics and mechanisms of dried activated sludge and Spirulina platensis for the removal of Cu2+ ions from aqueous solutions," *Desalin. Water Treat.*, vol. 47, no. 1–3, pp. 310–321, 2012.
[418] H.-A. Tayebi, Z. Dalirandeh, A. Shokuhi Rad, A. Mirabi, and E. Binaeian, "Synthesis of polyaniline/Fe3O4 magnetic nanoparticles for removal of

reactive red 198 from textile waste water: kinetic, isotherm, and thermodynamic studies," *Desalin. Water Treat.*, vol. 57, no. 47, pp. 22551–22563, 2016.
[419] K. V. Kumar and S. Sivanesan, "Isotherm parameters for basic dyes onto activated carbon: Comparison of linear and non-linear method," *J. Hazard. Mater.*, vol. 129, no. 1–3, pp. 147–150, 2006.
[420] Organization for Economic Co-operation and Development (OECD), "OECD Guidelines for the Testing of Chemicals, Section 2, Test No. 202: Daphnia sp. Acute Immobilisation Test," 2004. doi: https://doi.org/10.1787/9789264069947-en.
[421] M. May Chan, Y. Tong Szeto, S. Cheon Pak, and W. Kalle, "In vivo genoprotective effect against UV irradiation by red grapes (Vitis vinifera L.) juice," *J. Funct. Foods*, vol. 107, p. 105630, 2023, doi: https://doi.org/10.1016/j.jff.2023.105630.
[422] S. Dadfarnia and A. M. Haji-Shabani, "5 Choice of Solvent in Liquid-Phase Microextraction," in *Miniaturization in sample preparation*, De Gruyter Open Poland, 2014, pp. 253–275.
[423] J. M. Kokosa, "Selecting an extraction solvent for a greener liquid phase microextraction (LPME) mode-based analytical method," *TrAC Trends Anal. Chem.*, vol. 118, pp. 238–247, Sep. 2019, doi: 10.1016/j.trac.2019.05.012.
[424] A. Zgoła-Grześkowiak and T. Grześkowiak, "Dispersive liquid-liquid microextraction," *TrAC Trends Anal. Chem.*, vol. 30, no. 9, pp. 1382–1399, 2011.
[425] O. T. K. Nguyen, H. T. Pha, H. D. Khoa, D. C. Nguyen, and N. T. H. Tam, "Copper Ferrite Superparamagnetic Nanoparticle-Catalyzed Cross-coupling Reaction to Form Diindolylmethane (DIM): Effect of Experimental Parameters," *Bull. Chem. React. Eng. Catal.*, vol. 15, no. 3, pp. 631–640, 2020.
[426] A. Banerjee and A. Ray, "13 - A survey of adsorption process parameter optimization related to degradation of environmental pollutants," in *Intelligent Data-Centric Systems*, S. Bhattacharyya, N. K. Mondal, J. Platos, V. Snášel, and P. B. T.-I. E. D. M. for P. M. Krömer, Eds. Academic Press, 2021, pp. 289–309.
[427] H. Zavvar Mousavi and S. R. Seyedi, "Kinetic and equilibrium studies on the removal of Pb (II) from aqueous solution using nettle ash," *J. Chil. Chem. Soc.*, vol. 55, no. 3, pp. 307–311, 2010.
[428] B. E. Reed and M. R. Matsumoto, "Modeling cadmium adsorption by activated carbon using the Langmuir and Freundlich isotherm expressions," *Sep. Sci. Technol.*, vol. 28, no. 13–14, pp. 2179–2195, 1993.
[429] K. Ezeh, I. Ogbu, K. Akpomie, N. Ojukwu, and J. Ibe, "Utilizing the sorption capacity of local Nigerian sawdust for attenuation of heavy metals from solution: isotherm, kinetic, and thermodynamic investigations," *Pac. J. Sci. Technol*, vol. 18, pp. 251–264, 2017.
[430] D. Baruah, M. Goswami, R. N. S. Yadav, A. Yadav, and A. M. Das, "Biogenic synthesis of gold nanoparticles and their application in photocatalytic degradation of toxic dyes," *J. Photochem. Photobiol. B Biol.*, vol. 186, pp. 51–58, 2018, doi: https://doi.org/10.1016/j.jphotobiol.2018.07.002.
[431] S. Ahmed, Annu, S. Ikram, and S. Yudha S., "Biosynthesis of gold

nanoparticles: A green approach," *J. Photochem. Photobiol. B Biol.*, vol. 161, pp. 141–153, 2016, doi: https://doi.org/10.1016/j.jphotobiol.2016.04.034.
[432] N. Stănciuc and G. Râpeanu, "13 - Kinetics of Phytochemicals Degradation During Thermal Processing of Fruits Beverages," A. M. Grumezescu and A. M. B. T.-N.-A. B. Holban, Eds. Woodhead Publishing, 2019, pp. 407–440.
[433] S. L. Smitha, D. Philip, and K. G. Gopchandran, "Green synthesis of gold nanoparticles using Cinnamomum zeylanicum leaf broth," *Spectrochim. Acta Part A Mol. Biomol. Spectrosc.*, vol. 74, no. 3, pp. 735–739, 2009.
[434] A. Akouibaa, R. Masrour, A. Jabar, M. Benhamou, M. Ouarch, and A. Derouiche, "Study of the optical and thermoplasmonics properties of gold nanoparticle embedded in Al2O3 matrix," *Plasmonics*, vol. 17, no. 3, pp. 1157–1169, 2022.
[435] Z. Masoudyfar and S. Elhami, "Surface plasmon resonance of gold nanoparticles as a colorimetric sensor for indirect detection of Cefixime," *Spectrochim. Acta Part A Mol. Biomol. Spectrosc.*, vol. 211, pp. 234–238, 2019, doi: https://doi.org/10.1016/j.saa.2018.12.007.
[436] A. Moores and F. Goettmann, "The plasmon band in noble metal nanoparticles: an introduction to theory and applications," *New J. Chem.*, vol. 30, no. 8, pp. 1121–1132, 2006, doi: 10.1039/B604038C.
[437] M. Hassellöv, J. W. Readman, J. F. Ranville, and K. Tiede, "Nanoparticle analysis and characterization methodologies in environmental risk assessment of engineered nanoparticles," *Ecotoxicology*, vol. 17, no. 5, pp. 344–361, 2008, doi: 10.1007/s10646-008-0225-x.
[438] S. C. Capaldi Arruda, A. L. Diniz Silva, R. Moretto Galazzi, R. Antunes Azevedo, and M. A. Zezzi Arruda, "Nanoparticles applied to plant science: A review," *Talanta*, vol. 131, pp. 693–705, 2015, doi: https://doi.org/10.1016/j.talanta.2014.08.050.
[439] C. E. A. Botteon *et al.*, "Biosynthesis and characterization of gold nanoparticles using Brazilian red propolis and evaluation of its antimicrobial and anticancer activities," *Sci. Rep.*, vol. 11, no. 1, p. 1974, 2021, doi: 10.1038/s41598-021-81281-w.
[440] S. Ghosh *et al.*, "Gnidia glauca flower extract mediated synthesis of gold nanoparticles and evaluation of its chemocatalytic potential," *J. Nanobiotechnology*, vol. 10, no. 1, p. 17, 2012, doi: 10.1186/1477-3155-10-17.
[441] D. Philip, "Rapid green synthesis of spherical gold nanoparticles using Mangifera indica leaf," *Spectrochim. Acta Part A Mol. Biomol. Spectrosc.*, vol. 77, no. 4, pp. 807–810, 2010, doi: https://doi.org/10.1016/j.saa.2010.08.008.
[442] W. Wang, X. Ding, Q. Xu, J. Wang, L. Wang, and X. Lou, "Zeta-potential data reliability of gold nanoparticle biomolecular conjugates and its application in sensitive quantification of surface absorbed protein," *Colloids Surfaces B Biointerfaces*, vol. 148, pp. 541–548, 2016, doi: https://doi.org/10.1016/j.colsurfb.2016.09.021.
[443] M. A. Ali, T. Salaheldin, M. M. Gihan, M. T. Islam, and I. I. Omara, "Detection of E. Coli O157:H7 in Feed Samples Using Gold Nanoparticles Sensor," *Int. J. Curr. Microbiol. App. Sci.*, vol. 3, pp. 697–708, Jan. 2014.
[444] M. A. AHMED, S. A. FARHAN, R. M. DADOOSH, and A. M. N. JASSİM, "Biosynthetic Gold Nanoparticles as Sensitive and Selective Colorimetric

Method for Mercury Ions," *J. Turkish Chem. Soc. Sect. A Chem.*, vol. 10, no. 4, pp. 877–886.
[445] V. Pellegri, G. Gorbi, and A. Buschini, "Comet Assay on Daphnia magna in eco-genotoxicity testing," *Aquat. Toxicol.*, vol. 155, pp. 261–268, 2014, doi: https://doi.org/10.1016/j.aquatox.2014.07.002.
[446] V. Pellegri, G. Gorbi, and A. Buschini, "DNA damage detection by Comet Assay on Daphnia magna: Application in freshwater biomonitoring," *Sci. Total Environ.*, vol. 705, p. 135780, 2020, doi: https://doi.org/10.1016/j.scitotenv.2019.135780.
[447] M. Lavorgna, C. Russo, B. D'Abrosca, A. Parrella, and M. Isidori, "Toxicity and genotoxicity of the quaternary ammonium compound benzalkonium chloride (BAC) using Daphnia magna and Ceriodaphnia dubia as model systems," *Environ. Pollut.*, vol. 210, pp. 34–39, 2016, doi: https://doi.org/10.1016/j.envpol.2015.11.042.
[448] E. Galdiero *et al.*, "Integrated analysis of the ecotoxicological and genotoxic effects of the antimicrobial peptide melittin on Daphnia magna and Pseudokirchneriella subcapitata," *Environ. Pollut.*, vol. 203, pp. 145–152, 2015, doi: https://doi.org/10.1016/j.envpol.2015.03.046.
[449] A. Parrella, M. Lavorgna, E. Criscuolo, C. Russo, and M. Isidori, "Eco-genotoxicity of six anticancer drugs using comet assay in daphnids," *J. Hazard. Mater.*, vol. 286, pp. 573–580, 2015, doi: https://doi.org/10.1016/j.jhazmat.2015.01.012.
[450] J. E. Havel, "Cladocera," G. E. B. T.-E. of I. W. Likens, Ed. Oxford: Academic Press, 2009, pp. 611–622.
[451] European Council, "Commission directive 93/67/EEC of 20 July 1993 laying down the principles for assessment of risks to man and the environment of substances notified in accordance with council directive 67/548/EEC," *Off J Eur Commun*, vol. 227, pp. 1–3, 1993.
[452] N. B. Mohd Zanuri, M. G. Bentley, and G. S. Caldwell, "Assessing the impact of diclofenac, ibuprofen and sildenafil citrate (Viagra®) on the fertilisation biology of broadcast spawning marine invertebrates," *Mar. Environ. Res.*, vol. 127, pp. 126–136, 2017, doi: https://doi.org/10.1016/j.marenvres.2017.04.005.
[453] S. Kamiloglu, G. Sari, T. Ozdal, and E. Capanoglu, "Guidelines for cell viability assays," *Food Front.*, vol. 1, no. 3, pp. 332–349, 2020.
[454] T. L. Riss *et al.*, "Cell viability assays," *Assay Guid. Man. [Internet]*, 2016.
[455] M. Nikzamir, A. Akbarzadeh, and Y. Panahi, "An overview on nanoparticles used in biomedicine and their cytotoxicity," *J. Drug Deliv. Sci. Technol.*, vol. 61, p. 102316, 2021.
[456] A. Kroll, M. H. Pillukat, D. Hahn, and J. Schnekenburger, "Current in vitro methods in nanoparticle risk assessment: limitations and challenges," *Eur. J. Pharm. Biopharm.*, vol. 72, no. 2, pp. 370–377, 2009.
[457] E. Grela, J. Kozłowska, and A. Grabowiecka, "Current methodology of MTT assay in bacteria–A review," *Acta Histochem.*, vol. 120, no. 4, pp. 303–311, 2018.
[458] Y. J. Oh and J. Hong, "Application of the MTT-based colorimetric method for evaluating bacterial growth using different solvent systems," *Lwt*, vol. 153, p. 112565, 2022.
[459] R. Bala *et al.*, "In-vitro cytotoxicity of nickel oxide nanoparticles against L-6 cell-lines: MMP, MTT and ROS studies," *Environ. Res.*, vol. 215, p.

114257, 2022.
[460] K. Sak, “Cytotoxicity of dietary flavonoids on different human cancer types,” *Pharmacogn. Rev.*, vol. 8, no. 16, p. 122, 2014.

PUBLICATIONS FROM THE THESIS

Conference Papers

1. B.T. Zaman, G. Dalgıç Bozyiğit, E.S. Koçoğlu, B. Kartoğlu, E.S. Aydın, A. Girgin, T. Borahan, S. Oflu, Y. Kılınç, S. Bakırdere "Simultaneous Determination of 29 Endocrine Disruptor Compounds-Pesticides in Rock, Soil, Water, Moss and Feces Samples from Antarctica Using Simple and Effective Fine Droplet Formation Based Spray Assisted Liquid Phase Microextraction Prior to Gas Chromatography-Mass Spectrometry", 4th International Environmental Chemistry Congress (4th Envirochem 2022), 30 October-2 November 2022, Antalya, Türkiye.

Papers

1. B.T. Zaman, G. Dalgıç Bozyiğit, E.S. Koçoğlu, B. Kartoğlu, E.S. Aydın, A. Girgin, T. Borahan, S. Oflu, Y. Kılınç, E.G. Bakırdere, S. Bakırdere, "Implementation of simple and effective fine droplet formation-based spray-assisted liquid phase microextraction for the simultaneous determination of twenty-nine endocrine disruptor compounds and pesticides in rock, soil, water, moss, and feces samples from antarctica using gas chromatography-mass spectrometry", *Environ Sci Pollut Res*, vol. 31, p.10920-10933, 2024, DOI: 10.1007/s11356-023-31750-8.

Projects

1.119Z846, Horseshoe Adasındaki Çevresel Örneklerde Organik/İnorganik Kirleticilerin, Değerli Metallerin ve Radyoaktif Elementlerin Önderiştirme Yöntemleri ile Birleştirilmiş Kromatografik ve Spektroskopik Yöntemler Kullanılarak Yüksek Doğruluk ve Duyarlılıkta Tayinleri, 1001 - Research, Scholarship, ARDEB, KBAG - Chemistry Biology Research Support Group, Project Participation/Departure Dates: 15.04.2020 - 15.03.2023, Project Start/End Dates: 15.03.2020 - 15.03.2023.